Chem. Rev. **2003,** *103,* 1793–1873

Conceptual Density Functional Theory

P. Geerlings,*,[†] F. De Proft,[†] and W. Langenaeker[‡]

Eenheid Algemene Chemie, Faculteit Wetenschappen, Vrije Universiteit Brussel (VUB), Pleinlaan 2, 1050 Brussels, Belgium, and Department of Molecular Design and Chemoinformatics, Janssen Pharmaceutica NV, Turnhoutseweg 30, B-2340 Beerse, Belgium

Received April 2, 2002

Contents

I. Introduction: Conceptual vs Fundamental and Computational Aspects of DFT

It is an understatement to say that the density functional theory (DFT) has strongly influenced the evolution of quantum chemistry during the past 15 years; the term "revolutionalized" is perhaps more appropriate. Based on the famous Hohenberg and Kohn theorems,[1] DFT provided a sound basis for the development of computational strategies for obtaining information about the energetics, structure, and properties of (atoms and) molecules at much lower costs than traditional ab initio wave function techniques. Evidence "par excellence" is the publication of Koch and Holthausen's book, *Chemist's Guide to Density Functional Theory*,[2] in 2000, offering an overview of the performance of DFT in the computation of a variety of molecular properties as a guide for the practicing, not necessarily quantum, chemist. In this sense, DFT played a decisive role in the evolution of quantum chemistry from a highly specialized domain, concentrating, "faute de mieux", on small systems, to part of a toolbox to which also different types of spectroscopy belong today, for use by the practicing organic chemist, inorganic chemist, materials chemist, and biochemist, thus serving a much broader scientific community.

The award of the Nobel Prize for Chemistry in 1998 to one, if not *the* protagonist of (ab initio) wave function quantum chemistry, Professor J. A. Pople,[3] and the founding father of DFT, Professor Walter Kohn,[4] is the highest recognition of both the impact of quantum chemistry in present-day chemical research and the role played by DFT in this evolution. When looking at the "story of DFT", the basic idea that the electron density, $\rho(\boldsymbol{r})$, at each point $\boldsymbol{r}$ determines the ground-state properties of an atomic, molecular, ... system goes back to the early work of

---

* Corresponding author (telephone +32.2.629.33.14; fax +32.2.629.33.17; E-mail pgeerlin@vub.ac.be).

[†] Vrije Universiteit Brussel.

[‡] Janssen Pharmaceutica NV.

10.1021/cr990029p CCC: $44.00

P. Geerlings (b. 1949) is full Professor at the Free University of Brussels (Vrije Universiteit Brussel), where he obtained his Ph.D. and Habilitation, heading a research group involved in conceptual and computational DFT with applications in organic, inorganic, and biochemistry. He is the author or coauthor of nearly 200 publications in international journals or book chapters. In recent years, he has organized several meetings around DFT, and in 2003, he will be the chair of the Xth International Congress on the Applications of DFT in Chemistry and Physics, to be held in Brussels (September 7–12, 2003). Besides research, P. Geerlings has always strongly been involved in teaching, among others the Freshman General Chemistry course in the Faculty of Science. During the period 1996–2000, he has been the Vice Rector for Educational Affairs of his University.

W. Langenaeker (b. 1967) obtained his Ph.D. at the Free University of Brussels (Vrije Universiteit Brussel) under the guidance of P. Geerlings. He became a Postdoctoral Research Fellow of the Fund for Scientific Research–Flanders in this group and was Postdoctoral Research Associate with Professor R. G. Parr at the University of North Carolina in Chapel Hill in 1997. He has authored or coauthored more than 40 research papers in international journals and book chapters on conceptual DFT and computational quantum chemistry. In 1999, he joined Johnson & Johnson Pharmaceutical Research and Development (at that time the Janssen Research Foundation), where at present he has the rank of senior scientist, being involved in research in theoretical medicinal chemistry, molecular design, and chemoinformatics.

F. De Proft (b. 1969) has been an Assistant Professor at the Free University of Brussels (Vrije Universiteit Brussel) since 1999, affiliated with P. Geerlings' research group. He obtained his Ph.D. at this institution in 1995. During the period 1995–1999, he was a postdoctoral fellow at the Fund for Scientific Research–Flanders (Belgium) and a postdoc in the group of Professor R. G. Parr at the University of North Carolina in Chapel Hill. He is the author or coauthor of more than 80 research publications, mainly on conceptual DFT. His present work involves the development and/or interpretative use of DFT-based reactivity descriptors.

Thomas,[5] Fermi,[6] Dirac,[7] and Von Weizäcker[8] in the late 1920s and 1930s on the free electron gas.

An important step toward the use of DFT in the study of molecules and the solid state was taken by Slater in the 1950s in his X_α method,[9−11] where use was made of a simple, one-parameter approximate exchange correlation functional, written in the form of an exchange-only functional. DFT became a full-fledged theory only after the formulation of the Hohenberg and Kohn theorems in 1964.

Introducing orbitals into the picture, as was done in the Kohn−Sham formalism,[12,13] then paved the way to a computational breakthrough. The introduction, around 1995, of DFT via the Kohn−Sham formalism in Pople's GAUSSIAN software package,[14] the most popular and "broadest" wave function package in use at that time and also now, undoubtedly further promoted DFT as a computationally attractive alternative to wave function techniques such as Hartree−Fock,[15] Møller−Plesset,[16] configuration interaction,[17] coupled cluster theory,[18] and many others (for a comprehensive account, see refs 19−22).

DFT as a theory and tool for calculating molecular energetics and properties has been termed by Parr and Yang "computational DFT".[23] Together with what could be called "fundamental DFT" (say, N and v representability problems, time-dependent DFT, etc.), both aspects are now abundantly documented in the literature: plentiful books, review papers, and special issues of international journals are available, a selection of which can be found in refs 24−55.

On the other hand, grossly in parallel, and to a large extent independent of this evolution, a second (or third) branch of DFT has developed since the late 1970s and early 1980s, called "conceptual DFT" by its protagonist, R. G. Parr.[23] Based on the idea that the electron density is the fundamental quantity for describing atomic and molecular ground states, Parr and co-workers, and later on a large community of chemically orientated theoreticians, were able to give sharp definitions for chemical concepts which were already known and had been in use for many years in various branches of chemistry (electronegativity being the most prominent example), thus affording their calculation and quantitative use.

This step initiated the formulation of a theory of chemical reactivity which has gained increasing attention in the literature in the past decade. A breakthrough in the dissemination of this approach was the publication in 1989 of Parr and Yang's *Density Functional Theory of Atoms and Molecules*,[27] which not only promoted "conceptual DFT" but, certainly due to its inspiring style, attracted the attention of many chemists to DFT as a whole. Numerous, in fact most, applications have been published since the book's appearance. Although some smaller review papers in the field of conceptual DFT were published in the second half of the 1990s and in the beginning of this century[23,49,50,52,56−62] (refs 60−62 appeared when this review was under revision), a large review of this field, concentrating on both concepts and applications, was, in our opinion, timely. To avoid any confusion, it should be noted that the term "conceptual DFT" does not imply that the other branches of DFT mentioned above did not contribute to the development of concepts within DFT. "Conceptual DFT" concentrates on the extraction of chemically relevant concepts and principles from DFT.

This review tries to combine a clear description of concepts and principles and a critical evaluation of their applications. Moreover, a near completeness of the bibliography of the field was the goal. Obviously (cf. the list of references), this prevents an in-depth discussion of all papers, so, certainly for applications, only a selection of some key papers is discussed in detail.

Although the two branches (conceptual and computational) of DFT introduced so far have, until now, been presented separately, a clear link exists between them: the electronic chemical potential. We therefore start with a short section on the fundamental and computational aspects, in which the electronic chemical potential is introduced (section II). Section III concentrates on the introduction of the concepts (III.A), their calculation (III.B), and the principles (III.C) in which they are often used. In section IV, an overview of applications is presented, with regard to atoms and functional groups (IV.A), molecular properties (IV.B), and chemical reactivity (IV.C), ending with applications on clusters and catalysis (IV.D).

II. Fundamental and Computational Aspects of DFT

A. The Basics of DFT: The Hohenberg−Kohn Theorems

The first Hohenberg−Kohn (HK) theorem[1] states that the electron density, $\rho(\boldsymbol{r})$, determines the external (i.e., due to the nuclei) potential, $v(\boldsymbol{r})$. $\rho(\boldsymbol{r})$ determines N, the total number of electrons, via its normalization,

$$\int \rho(\boldsymbol{r})\, \mathrm{d}\boldsymbol{r} = N \tag{1}$$

and N and $v(\boldsymbol{r})$ determine the molecular Hamiltonian, H_{op}, written in the Born−Oppenheimer approximation, neglecting relativistic effects, as (atomic units are used throughout)

$$H_{\mathrm{op}} = -\sum_{i}^{N}\frac{1}{2}\nabla_i^2 - \sum_{A}^{n}\sum_{i}^{N}\frac{Z_A}{r_{iA}} + \sum_{i<j}^{N}\sum_{j}^{N}\frac{1}{r_{ij}} + \sum_{B<A}^{n}\sum_{A}^{n}\frac{Z_A Z_B}{R_{AB}} \tag{2}$$

Here, summations over i and j run over electrons, and summations over A and B run over nuclei; r_{ij}, r_{iA}, and R_{AB} denote electron−electron, electron−nuclei, and internuclear distances. Since H_{op} determines the energy of the system via Schrödinger's equation,

$$H_{\mathrm{op}}\Psi = E\Psi \tag{3}$$

Ψ being the electronic wave function, $\rho(\boldsymbol{r})$ ultimately determines the system's energy and all other ground-state electronic properties. Scheme 1 clearly shows that, consequently, E is a functional of ρ:

Scheme 1. Interdependence of Basic Variables in the Hohenberg−Kohn Theorem[1,4]

$$\begin{tikzcd}
\rho(\boldsymbol{r}) \arrow[r] \arrow[dr] & v(\boldsymbol{r}) \arrow[r] & H_{op} \arrow[r] & E \\
& N \arrow[ur] & &
\end{tikzcd}$$

$$E = E_v[\rho] \tag{4}$$

The index "v" has been written to make explicit the dependence on v.

The ingenious proof (for an intuitive approach, see Wilson cited in a paper by Lowdin[65]) of this famous theorem is, quoting Parr and Yang, "disarmingly simple",[66] and its influence (cf. section I) has been immense. A pictoral representation might be useful in the remaining part of this review (Scheme 2).

Scheme 2. Visualization of the First Hohenberg−Kohn Theorem

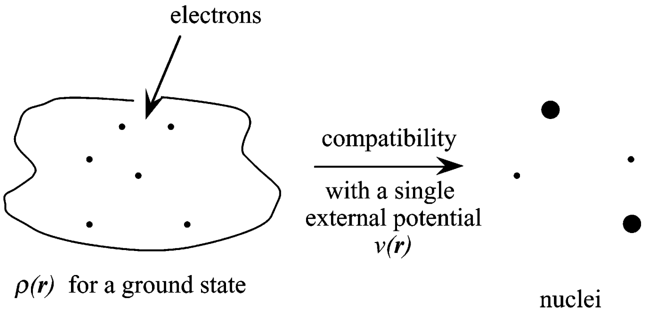

Suppose one gives to an observer a visualization of the function $\rho(\boldsymbol{r})$, telling him/her that this function corresponds to the ground-state electron density of an atom or a molecule. The first HK theorem then states that this function corresponds to a unique number of electrons N (via eq 1) and constellation of nuclei (number, charge, position).

The second HK theorem provides a variational ansatz for obtaining ρ: search for the $\rho(\boldsymbol{r})$ minimizing E.

For the optimal $\rho(\boldsymbol{r})$, the energy E does not change upon variation of $\rho(\boldsymbol{r})$, provided that $\rho(\boldsymbol{r})$ integrates at all times to N (eq 1):

$$\delta(E - \mu\rho(\boldsymbol{r})) = 0 \tag{5}$$

where μ is the corresponding Lagrangian multiplier.

One finally obtains

$$\nu(\boldsymbol{r}) + \frac{\delta F_{\mathrm{HK}}}{\delta \rho(\boldsymbol{r})} = \mu \tag{6}$$

where F_{HK} is the Hohenberg–Kohn functional containing the electronic kinetic energy functional, $T[\rho]$, and the electron–electron interaction functional, $V_{\mathrm{ee}}[\rho]$:

$$E_\nu[\rho] = \int \rho(\boldsymbol{r})\nu(\boldsymbol{r})\, \mathrm{d}\boldsymbol{r} + F_{\mathrm{HK}}[\rho] \tag{7}$$

with

$$F_{\mathrm{HK}}[\rho] = T[\rho] + V_{\mathrm{ee}}[\rho] \tag{8}$$

The Euler–Lagrange equation (6) is the DFT analogue of Schrödinger's time-independent equation (3). As the Lagrangian multiplier μ in eq 6 does not depend on $\boldsymbol{r}$, the $\rho(\boldsymbol{r})$ that is sought for should make the left-hand side of eq 6 r-independent. The functionals $T[\rho]$ and $V_{\mathrm{ee}}[\rho]$, which are not known either completely or partly, remain problems.

Coming back to Scheme 1, as $\rho(\boldsymbol{r})$ determines ν and N, and so H_{op}, it determines in fact all properties of the system considered, including excited-state properties.

The application of the HK theorem to a subdomain of a system has been studied in detail in an important paper by Riess and Münch,[67] who showed that the ground-state particle density, $\rho_\Omega(\boldsymbol{r})$, of a finite but otherwise arbitrary subdomain Ω uniquely determines all ground-state properties in Ω, in any other subdomain Ω', and in the total domain of the bounded system.

In an in-depth investigation of the question of transferability of the distribution of charge over an atom in a molecule within the context of Bader's atoms-in-molecules approach,[68] Becker and Bader[69] showed that it is a corollary of Riess and Münch's proof that, if the density over a given atom or any portion with a nonvanishing measure thereof is identical in two molecules 1 and 2 [$\rho_{1\Omega}(\boldsymbol{r}) = \rho_{2\Omega}(\boldsymbol{r})$], then the electron density functions $\rho_1(\boldsymbol{r})$ and $\rho_2(\boldsymbol{r})$ are identical in total space.

Very recently, Mezey generalized these results, dropping the boundedness conditions, and proved that any finite domain of the ground-state electron density fully determines the ground state of the entire, boundary-less molecular system (the "holographic electron density theorem").[70,71] The importance of (local) similarity of electron densities is thus clearly accentuated and will be treated in section III.B.5.

B. DFT as a Tool for Calculating Atomic and Molecular Properties: The Kohn–Sham Equations

The practical treatment of eq 6 was provided by Kohn and Sham,[12] who ingeniously turned it into a form showing high analogy with the Hartree equations.[72] This aspect later facilitated its implementation in existing wave-function-based software packages such as Gaussian[14] (cf. section I). This was achieved by introducing orbitals into the picture in such a way that the kinetic energy could be computed simply with good accuracy. They started from an N-electron non-interacting reference system with the following Hamiltonian [note that in the remaining part of this review, atomic units will be used, unless stated otherwise]:

$$H_{\mathrm{ref}} = -\sum_i^N \frac{1}{2}\nabla_i^{\,2} + \sum_i^N \nu_i(\boldsymbol{r}) = \sum_i h_{\mathrm{ref},\,i} \tag{9}$$

with

$$h_{\mathrm{ref},i} = -\frac{1}{2}\nabla_i^{\,2} + \nu_i(\boldsymbol{r}) \tag{10}$$

excluding electron–electron interactions, showing the same electron density as the exact electron density, $\rho(\boldsymbol{r})$, of the real interacting system. Introducing the orbitals Ψ_i, eigenfunctions of the one-electron operator (eq 10), all physically acceptable densities of the non-interacting system can be written as

$$\rho_{\mathrm{s}} = \sum_i^N |\Psi_i|^2 \tag{11}$$

where the summation runs over the N lowest eigenstates of h_{ref}. Harriman has shown, by explicit construction, that any non-negative, normalized density (i.e., all physically acceptable densities) can be written as a sum of the squares of an arbitrary number of orthonormal orbitals.[73] The Hohenberg–Kohn functional, F_{HK},[8] can be written as

$$F_{\mathrm{HK}}[\rho] = T_{\mathrm{s}}[\rho] + J[\rho] + E_{\mathrm{xc}}[\rho] \tag{12}$$

Here, T_{s} represents the kinetic energy functional of the reference system given by

$$T_{\mathrm{s}}[\rho] = \sum_i^N \left\langle \Psi_i \middle| -\frac{1}{2}\nabla^2 \middle| \Psi_i \right\rangle \tag{13}$$

$J[\rho]$ representing the classical Coulombic interaction energy,

$$J[\rho] = \frac{1}{2}\int\int \frac{\rho(\boldsymbol{r})\rho(\boldsymbol{r}')}{|\boldsymbol{r} - \boldsymbol{r}'|}\, \mathrm{d}\boldsymbol{r}\, \mathrm{d}\boldsymbol{r}' \tag{14}$$

and the remaining energy components being assembled in the $E_{\mathrm{xc}}[\rho]$ functional: the exchange correlation energy, containing the difference between the exact kinetic energy and T_{s}, the nonclassical part of $V_{\mathrm{ee}}[\rho]$, and the self-interaction correction to eq 14.

Combining eqs 6, 12, 13, and 14, the Euler equation (6) can be written as follows: [Note that all derivatives with respect to $\rho(\boldsymbol{r})$ are to be computed for a fixed total number of electrons N of the system. To simplify the notation, this constraint is not explicitly written for these types of derivatives in the remaining part of the review.]

$$\mu = \nu_{\mathrm{eff}}(\boldsymbol{r}) + \frac{\delta T_{\mathrm{s}}}{\delta \rho} \tag{15}$$

where an effective potential has been introduced,

$$\begin{aligned} \nu_{\mathrm{eff}}(\boldsymbol{r}) &= \nu(\boldsymbol{r}) + \frac{\delta J}{\delta \rho} + \frac{\delta E_{\mathrm{xc}}}{\delta \rho} \\ &= \nu(\boldsymbol{r}) + \int \frac{\rho(\boldsymbol{r})}{|\boldsymbol{r}-\boldsymbol{r}'|}\,\mathrm{d}\boldsymbol{r}' + \nu_{xc}(\boldsymbol{r}) \end{aligned} \tag{16}$$

containing the exchange correlation potential, $\nu_{\mathrm{xc}}(\boldsymbol{r})$, defined as

$$\nu_{\mathrm{xc}} = \frac{\delta E_{\mathrm{xc}}}{\delta \rho(\boldsymbol{r})} \tag{17}$$

Equation 15, coupled to the normalization condition (eq 1), is exactly the equation one obtains by considering a non-interacting N-electron system, with electrons being subjected to an external potential, $\nu_{\mathrm{eff}}(\boldsymbol{r})$. So, for a given $\nu_{\mathrm{eff}}(\boldsymbol{r})$, one obtains $\rho(\boldsymbol{r})$, making the right-hand side of eq 15 independent of $\boldsymbol{r}$, as

$$\rho(\boldsymbol{r}) = \int \sum_i^N |\Psi_i(\mathbf{x})|^2\,\mathrm{d}\sigma \tag{18}$$

x denotes the four vector-containing space and spin variables, and the integration is performed over the spin variable σ.

The molecular orbitals Ψ_i should moreover satisfy the one-electron equations,

$$\left(-\frac{1}{2}\nabla^2 + \nu_{\mathrm{eff}}(\boldsymbol{r})\right)\Psi_i = \epsilon_i \Psi_i \tag{19}$$

This result is regained within a variational context when looking for those orbitals minimizing the energy functional (eq 7), subject to orthonormality conditions,

$$\int \Psi_i^*(\mathbf{x})\Psi_j(\mathbf{x})\,\mathrm{d}\mathbf{x} = \delta_{ij} \tag{20}$$

The Kohn–Sham equations (eq 19) are one-electron equations, just as the Hartree or Hartree–Fock equations, to be solved iteratively. The price to be paid for the incorporation of electron correlation is the appearance of the exchange correlation potential, ν_{xc}, the form of which is unknown and for which no systematic strategy for improvement is available. The spectacular results from recent years in this search for the “holy grail” by Becke, Perdew, Lee, Parr, Handy, Scuseria, and many others will not be detailed in this review (for a review and an inspiring perspective, see refs 74 and 75). Nevertheless, it should be stressed that today density functional theory, cast in the Kohn–Sham formalism, provides a computational tool with an astonishing quality/cost ratio, as abundantly illustrated in the aforementioned book by Koch and Holthausen.[2]

This aspect should be stressed in this review as many, if not most, of the applications discussed in section IV were conducted on the basis of DFT computational methods (summarized in Scheme 3). The present authors were in the initial phase of their investigations of DFT concepts using essentially wave function techniques. Indeed, in the early 1990s, the assessment of DFT methods had not yet been performed up to the level of their wave function counterparts, creating uncertainty related to testing concepts via techniques that had not been tested themselves sufficiently.

Scheme 3. Conceptual DFT at Work

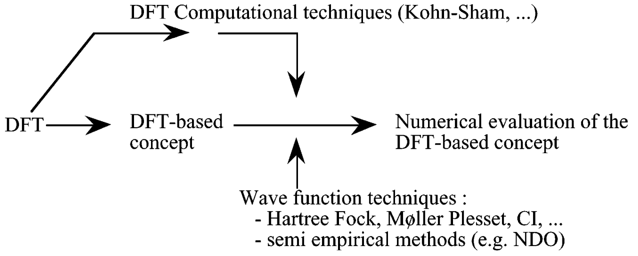

This situation changed dramatically in recent years, as is demonstrated by the extensive tests available now for probably the most popular ν_{xc}, the B3LYP functional.[76,77] Its performance in combination with various basis sets has been extensively tested, among others by the present authors, for molecular geometries,[78] vibrational frequencies,[79] ionization energies and electron affinities,[80−82] dipole and quadrupole moments,[83,84] atomic charges,[83] infrared intensities,[83] and magnetic properties (e.g., chemical shifts[85]).

C. Electronic Chemical Potential and Electronegativity: Bridging Computational and Conceptual DFT

The cornerstone of conceptual DFT was laid in a landmark paper by Parr and co-workers[86] concentrating on the interpretation of the Lagrangian multiplier μ in the Euler equation (6).

It was recognized that μ could be written as the partial derivative of the system's energy with respect to the number of electrons at fixed external potential $\nu(\boldsymbol{r})$:

$$\mu = \left(\frac{\partial E}{\partial N}\right)_{\nu(\boldsymbol{r})} \tag{21}$$

To get some feeling for its physical significance, thus establishing a firm basis for section III, we consider the energy change, dE, of an atomic or molecular system when passing from one ground state to another. As the energy is a functional of the number of electrons and the external potential $\nu(\boldsymbol{r})$ (cf. Scheme 1) [the discussion of N-differentiability is postponed to III.B.1; note that N and $\nu(\boldsymbol{r})$ determine perturbations as occurring in a chemical reaction], we can write the following expression:

$$\mathrm{d}E = \left(\frac{\partial E}{\partial N}\right)_{\nu(\boldsymbol{r})} \mathrm{d}N + \int \left(\frac{\partial E}{\partial \nu(\boldsymbol{r})}\right)_N \delta\nu(\boldsymbol{r})\,\mathrm{d}\boldsymbol{r} \tag{22}$$

On the other hand, E is a functional of $\rho(\boldsymbol{r})$, leading to

$$\mathrm{d}E = \int \left(\frac{\delta E}{\delta \rho(\boldsymbol{r})}\right)_{\nu(\boldsymbol{r})} \delta\rho(\boldsymbol{r})\,\mathrm{d}\boldsymbol{r} \tag{23}$$

where the functional derivative $(\delta E/\delta\rho(\boldsymbol{r}))_{\nu(\boldsymbol{r})}$ is introduced.

In view of the Euler equation (15), it is seen that the Lagrangian multiplier μ can be written as

$$\mu = \left(\frac{\delta E}{\delta \rho(\boldsymbol{r})}\right)_{\nu} \tag{24}$$

Combining eqs 22 and 24, one obtains

$$\mathrm{d}E_{\nu} = \int \mu \delta\rho(\boldsymbol{r})\,\mathrm{d}\boldsymbol{r} = \mu \int \delta\rho(\boldsymbol{r})\,\mathrm{d}\boldsymbol{r} = \mu\,\mathrm{d}N \tag{25}$$

where it has been explicity indicated that the variation in $\rho(\boldsymbol{r})$ is for a given ν. Comparison of the first term in eq 22, the only term surviving at fixed ν, and eq 25 yields eq 21.

On the other hand, it follows from simple wave function perturbation theory (see, e.g., ref 21) that the first-order correction $\mathrm{d}E^{(1)}$ to the ground-state energy due to a change in external potential, written as a one-electron perturbation

$$V = \sum_i \delta\nu(\boldsymbol{r}_i) \tag{26}$$

at fixed number of electrons gives

$$\mathrm{d}E_N^{(1)} = \int \Psi^{(\mathrm{O})*}\delta V \Psi^{(\mathrm{O})}\,\mathrm{d}\mathbf{x}^N = \int \rho(\boldsymbol{r})\delta\nu(\boldsymbol{r})\,\mathrm{d}\boldsymbol{r} \tag{27}$$

$\Psi^{(\mathrm{O})}$ denoting the unperturbed wave function.

Comparing eq 27 with the second term of eq 22 yields

$$\rho(\boldsymbol{r}) = \left(\frac{\delta E}{\delta \nu(\boldsymbol{r})}\right)_N \tag{28}$$

upon which the identification of the two first derivatives of E with respect to N and ν is accomplished.[87]

In the early 1960s, Iczkowski and Margrave[88] showed, on the basis of experimental atomic ionization energies and electron affinities, that the energy E of an atom could reasonably well be represented by a polynomial in n (number of electrons (N) minus the nuclear charge (Z)) around $n = 0$:

$$E = E(N) = an^4 + bn^3 + cn^2 + dn; \quad n = N - Z \tag{29}$$

Assuming continuity and differentiability of E,[89,90] the slope at $n = 0$, $-(\partial E/\partial n)_{n=0}$, is easily seen to be a measure of the electronegativity, χ, of the atom. Iczkowski and Margrave proposed to define the electronegativity as this derivative, so that

$$\chi = -\left(\frac{\partial E}{\partial N}\right) \tag{30}$$

for fixed nuclear charge.

Because the cubic and quartic terms in eq 29 were negligible, Mulliken's definition,[91]

$$\chi = \frac{1}{2}(I + A) \tag{31}$$

where I and A are the first ionization energy and electron affinity, respectively, was regained as a particular case of eq 30, strengthening its proposal. Note that the idea that electronegativity is a chemical potential originates with Gyftopoulos and Hatsopoulos.[92]

Combining eqs 30, 31, and 21, generalizing the fixed nuclear charge constraint to fixed external potential constraint, the Lagrangian multiplier μ of the Euler equation is now identified with a longstanding chemical concept, introduced in 1932 by Pauling.[93] This concept, used in combination with Pauling's scale (later on refined[94−96]), was to be of immense importance in nearly all branches of chemistry (for reviews, see refs 97−102).

A remarkable feature emerges: the linking of the chemical potential concept to the fundamental equation of density functional theory, bridging conceptual and computational DFT. The "sharp" definition of χ and, moreover, its form affords its calculation via electronic structure methods. Note the analogy with the thermodynamic chemical potential of a component i in a macroscopic system at temperature T and pressure P:

$$\mu_i = \left(\frac{\partial G}{\partial n_i}\right)_{P,\,T,\,n_j(j\neq i)} \tag{32}$$

where n_j denotes the number of moles of the jth component.[103]

In an extensive review and influential paper in 1996, three protagonists of DFT, Kohn, Parr, and Becke,[74] stressed this analogy, stating that the $\mu = (\partial E/\partial N)_{\nu}$ result "contains considerable chemistry. μ characterizes the escaping tendency of electrons from the equilibrium system. Systems (e.g. atoms or molecules) coming together must attain at equilibrium a common chemical potential. This chemical potential is none other than the negative of the electronegativity concept of classical structural chemistry."

Nevertheless, eq 21 was criticized, among others by Bader et al.,[104] on the assumption that N in a closed quantum mechanical system is a continuously variable property of the system. In section III.B.1, this problem will be readdressed. Anyway, its use is, in the writers' opinion, quite natural when focusing on atoms in molecules instead of isolated atoms (or molecules). These "parts" can indeed be considered as open systems, permitting electron transfer; moreover, their electron number does not necessarily change by integer values.[89]

The link between conceptual and computational DFT being established, we concentrate in the next section on the congeners of electronegativity forming a complete family of "DFT-based reactivity descriptors".

III. DFT-Based Concepts and Principles

A. General Scheme: Nalewajski's Charge Sensitivity Analysis

The introduction of electronegativity as a DFT reactivity descriptor can be traced back to the consideration of the response of a system (atom, molecule, etc.) when it is perturbed by a change in its number of electrons at a fixed external potential. It immediately demands attention for its counterpart

Scheme 4. Energy Derivatives and Response Functions in the Canonical Ensemble, $\delta^n E/\partial^m N \delta^{m'} \nu(\boldsymbol{r})$ ($n \leq 3$)[a]

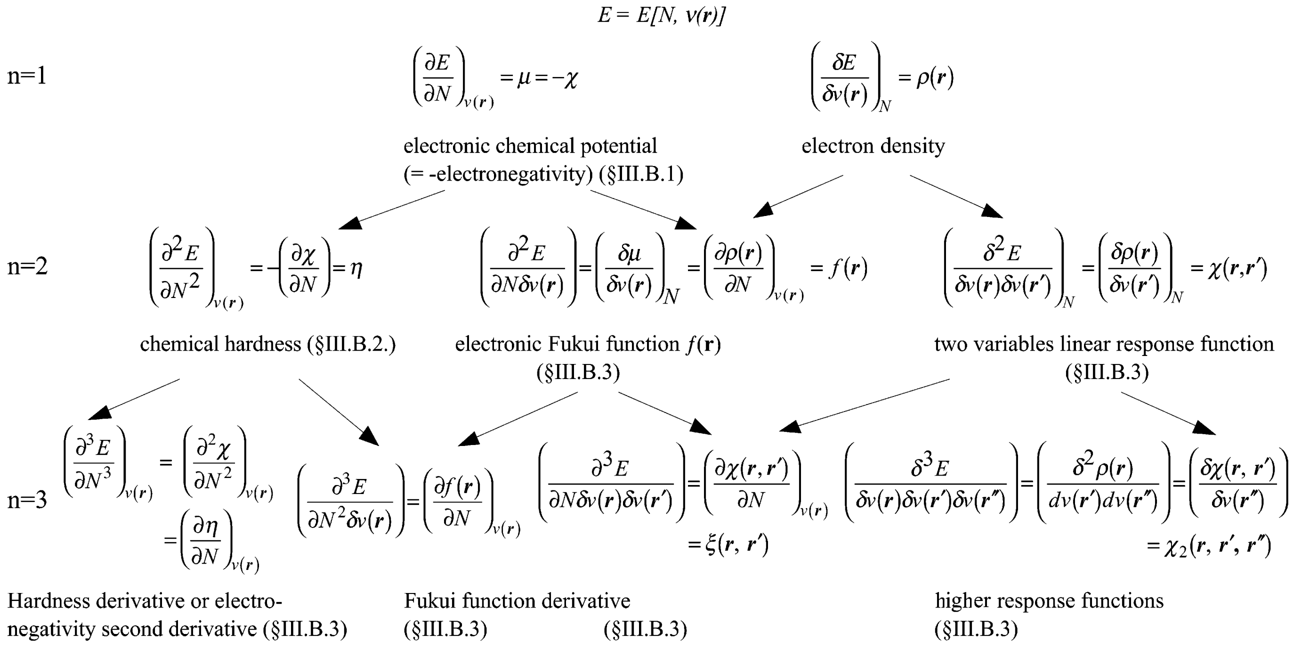

[a] Also included are definitions and/or identification and indication of the section where each equation is discussed in detail.

(cf. eq 24), $(\delta E/\delta \nu(\boldsymbol{r}))_N$, which, through eq 28, was easily seen to be the electron density function $\rho(\boldsymbol{r})$ itself, indicating again the primary role of the electron density function.

Assuming further (functional) differentiability of E with respect to N and $\nu(\boldsymbol{r})$ (vide infra), a series of response functions emerge, as shown in Scheme 4, which will be discussed in the remaining paragraphs of this section.

Note that we consider working first in the 0 K limit (for generalizations to finite temperature ensembles, see ref 105) and second within the Canonical ensemble ($E = E[N,\nu(\boldsymbol{r}),T]$). It will be seen that other choices are possible and that changing the variables is easily performed by using the Legendre transformation technique.[106,107]

Scheme 4 shows all derivatives $(\delta^n E/\partial^m N \delta^{m'} \nu(\boldsymbol{r}))$ up to third order ($n = 3$), together with the identification or definition of the corresponding response function ($n \geq 2$) and the section in which they will be treated. Where of interest, Maxwell relationships will be used to yield alternative definitions.

In a natural way, two types of quantities emerge in the first-order derivatives: a global quantity, χ, being a characteristic of the system as a whole, and a local quantity, $\rho(\boldsymbol{r})$, the value of which changes from point to point. In the second derivatives, a kernel $\chi(\boldsymbol{r},\boldsymbol{r}')$ appears for the first time, representing the response of a local quantity at a given point $\boldsymbol{r}$ to a perturbation at a point $\boldsymbol{r}'$. This trend of increasing "locality" to the right-hand side of the scheme is continued in the third-order derivatives, in which at the right-most position variations of $\rho(\boldsymbol{r})$ in response to simultaneous external perturbations, $\nu(\boldsymbol{r}')$ and $\nu(\boldsymbol{r}'')$, are shown. "Complete" global quantities obviously only emerge at the left-most position, with higher order derivatives of the electronegativity or hardness with respect to the number of electrons.

Within the context of the finite temperature ensemble description in DFT, the functional Ω (the grand potential), defined as

$$\Omega = E - N\mu \quad \text{or} \quad = E - \mu(N - N_0) \qquad (33)$$

(where N_0 is the reference number of electrons), plays a fundamental role, with natural variables μ, $\nu(\boldsymbol{r})$, and T.

At a given temperature T, the following hierarchy of response functions, $(\delta^n \Omega/\partial^m \mu \delta^{m'} \nu(\boldsymbol{r}))$, limited to second order, was summarized by Chermette[50] (Scheme 5). It will be seen in section III.B that the response functions with $n = 2$ correspond or are related to the inverse of the response functions with $n = 2$ in Scheme 4. The grand potential Ω will be of great use in discussing the HSAB principle in section III.C, where open subsystems exchanging electrons should be considered.

The consideration of other ensembles, $F[N,\rho]$ and $R[\mu,\rho]$, with associated Legendre transformations,[108,109]

$$F[N,\rho] = E - \int \rho(\boldsymbol{r})\nu(\boldsymbol{r})\,\mathrm{d}\boldsymbol{r} \quad \text{(isomorphic ensemble)} \qquad (34)$$

$$R[\mu,\rho] = E - \mu N - \int \rho(\boldsymbol{r})\nu(\boldsymbol{r})\,\mathrm{d}\boldsymbol{r} \quad \text{(grand isomorphic ensemble)} \qquad (35)$$

will be postponed until the introduction of the shape function, $\sigma(\boldsymbol{r})$, in section III.B.5, yielding an altered isomorphic ensemble:[110]

$$F[N,\sigma] = E - N\int \sigma(\boldsymbol{r})\nu(\boldsymbol{r})\,\mathrm{d}\boldsymbol{r} \qquad (36)$$

Finally, note that instead of Taylor expansions in, for instance, the canonical ensemble $E = E[N,\nu(\boldsymbol{r})]$, functional expansions have been introduced by Parr.

Scheme 5. Grand Potential Derivatives and Response Functions in the Grand Canonical Ensemble, $\delta^n\Omega/\partial^m\mu\delta^{m'}v(\mathbf{r})$ (with $n \leq 2$)[a]

$$\Omega = \Omega[\mu, v(\mathbf{r})]$$

$$\begin{tikzcd}
n=1 & & \left(\frac{\partial\Omega}{\partial\mu}\right)_{v(\mathbf{r})} = -N \arrow[dl] \arrow[dr] & & \left(\frac{\partial\Omega}{\delta v(\mathbf{r})}\right)_N = \rho(\mathbf{r}) \arrow[dl] \arrow[dr] & \\
n=2 & \left(\frac{\partial^2\Omega}{\partial\mu^2}\right)_{v(\mathbf{r})} = -\left(\frac{\partial N}{\partial\mu}\right)_{v(\mathbf{r})} = S & & \left(\frac{\partial^2\Omega}{\partial\mu\delta v(\mathbf{r})}\right) = \left(\frac{\partial\rho(\mathbf{r})}{\partial\mu}\right)_{v(\mathbf{r})} = s(\mathbf{r}) & & \left(\frac{\delta^2\Omega}{\delta v(\mathbf{r})\delta v(\mathbf{r}')}\right)_N = -s(\mathbf{r}, \mathbf{r}') \\
 & \text{global softness} & & \text{local softness} & & \text{softness kernel} \\
 & (\S\text{III.B.2}) & & (\S\text{III.B.3}) & & (\S\text{III.B.3})
\end{tikzcd}$$

[a] Also included are definitions and/or identification and indication of the section where each equation is discussed in detail.

B. Concepts and Their Calculation

1. Electronegativity and the Electronic Chemical Potential

The identification of the Lagrangian multiplier μ in eq 6 with the negative of the electronegativity χ,[86]

$$\mu = -\chi = -\left(\frac{\partial E}{\partial N}\right)_v \tag{37}$$

offers a way to calculate electronegativity values for atoms, functional groups, clusters, and molecules. In this sense, it was an important step forward, as there was no systematic way of evaluating electronegativities for all species of the above-mentioned type with the existing scales by Pauling[93,95,96] and the panoply of scales presented after his 1932 landmark paper by Gordy,[111] Allred and Rochow,[112] Sanderson,[113] and others (for a review, see ref 114).

A spin-polarized extension of eq 37 has been put forward by Ghosh and Ghanty:[115]

$$\chi_\alpha = -\left(\frac{\partial E}{\partial N_\alpha}\right)_{v,N_\beta} \qquad \chi_\beta = -\left(\frac{\partial E}{\partial N_\beta}\right)_{v,N_\alpha} \tag{38}$$

where N_α and N_β stand for the number of α and β spin electrons, respectively.

Fundamental problems, however, still arise when implementing these sharp definitions, particularly the question of whether E is differentiable with respect to N (necessarily an integer for isolated atoms, molecules, etc.).

This problem obviously is not only pesent in the evaluation of the electronegativity but is omnipresent in all higher and mixed N-derivatives of the energy as hardness, Fukui function, etc. (sections III.B.2, III.B.3, etc.). The issues to be discussed in this section are of equal importance when considering these quantities. Note that the fundamental problem of the integer N values (see the remark in section II.C, together with the open or closed character of the system) is not present when concentrating on an atom in an atoms-in-molecules context,[68] where it is natural to think in terms of partially charged atoms that are capable of varying their electron number in a continuous way.

In a seminal contribution (for a perspective, see ref 90), Perdew et al.[89] discussed the fractional particle number and derivative discontinuity issues when extending the Hohenberg–Kohn theorem by an ensemble approach. Fractional electron numbers may arise as a time average in an open system, e.g., for an atom X free to exchange electrons with atom Y. These authors proved that, within this context, the energy vs N curve is a series of straight line segments and that “the curve E versus N itself is continuous but its derivative $\mu = \partial E/\partial N$ has possible discontinuities at integral values of N. When applied to a single atom of integral nuclear charge Z, μ equals $-I$ for $Z - 1 < N < Z$ and $-A$ for $Z < N < Z + 1$.”[89]

The chemical potential jumps by a constant as N increases by an integer value. For a finite system with a nonzero energy gap, $\mu(N)$ is therefore a step function with constant values between the discontinuities (jumps) at integral N values. (This problem has been treated in-depth in textbooks by Dreizler and Gross[30] and by Parr and Yang[27] and in Chermette’s[50] review.) An early in-depth discussion can be found in the article by Lieb.[116]

$(\partial E/\partial N)_v$ may thus have different values when evaluated to the left or to the right of a given integer N value. The resulting quantities (electronegativity via eq 37) correspond to the response of the energy of the system to electrophilic ($dN < 0$) or nucleophilic ($dN > 0$) perturbations, respectively.

It has been correctly pointed out by Chermette[50] that these aspects are more often included in second-derivative-type reactivity descriptors (hardness) and in local descriptors such as the Fukui function and local softness (superscript + and −) than in the case of the first derivative, the electronegativity.

Note that the definition of hardness by Parr and Pearson, as will be seen in subsequent discussion (section II.B.2, eq 57), does not include any hint to left or right derivative, taking the curvature of an $E = E(N)$ curve at the neutral atom. In the present discussion on electronegativity, the distinction will be made whenever appropriate.

An alternative to the use of an ensemble is to use a continuous N variable, as Janak did[117] (vide infra). The consistency between both approaches has been pointed out by Casida.[118]

The larger part of the work in the literature on electronegativity has been carried out within the finite difference approach, in which the electronegativity is calculated as the average of the left- and right-hand-side derivatives:

$$\chi^- = E(N = N_0 - 1) - E(N = N_0) = I \quad (39)$$

$$\chi^+ = E(N = N_0) - E(N = N_0 + 1) = A \quad (40)$$

$$\chi = \frac{1}{2}(\chi^+ + \chi^-) = \frac{1}{2}(I + A) \quad (41)$$

where I and A are the ionization energy and electron affinity of the N_0-electron system (neutral or charged) studied.

This technique is equivalent to the use of the Mulliken formula (eq 31) and has been applied to study the electronegativity of atoms, functional groups, molecules, etc. Equation 41 also allows comparison with experiment on the basis of vertical (cf. the demand of fixed ν in eq 37) ionization energies and electron affinities, and tables of χ (and η; see section III.B.2) values for atoms, monatomic ions, and molecules have been compiled, among others by Pearson.[119−122]

Extensive comparison of "experimental" and high-level theoretical finite difference electronegativities (and hardness, see section III.B.2) have been published by the present authors for a series of 22 atoms and monatomic ions yielding almost perfect correlations with experiment both for χ and η at the B3LYP/6-311++G(3df,2p) level[80] (with standard deviations of the order of 0.20 eV for χ and 0.08 eV for η).

As an approximation to eq 41, the ionization energy and electron affinity can be replaced by the HOMO and LUMO energy, respectively, using Koopmans' theorem,[123] within a Hartree−Fock scheme, yielding

$$\chi = \frac{1}{2}(\epsilon_{\text{HOMO}} + \epsilon_{\text{LUMO}}) \quad (42)$$

This approximation might be of some use when large systems are considered: the evaluation of eq 41 necessitates three calculations. Also, in the case of systems leading to metastable $N_0 + 1$ electron systems (typically anions), the problem of negative electron affinities is sometimes avoided via eq 42 (for reviews about the electronic structure of metastable anions and the use of DFT to calculate temporary anion states, see refs 124−126). (An interesting study by Datta indicates that, for isolated atoms, a doubly negatively charged ion will always be unstable.[127a] For a recent review on multiply charged anions in the gas phase, see ref 127b.) Pearson stated that if only ionization leads to a stable system, a good working equation for μ is obtained by

$$\mu = -I \quad (43)$$

putting EA = 0.[122]

An alternative is the use of Janak's theorem[117] (see also Slater's contribution[128]): in his continuous N extension of Kohn−Sham theory, it can be proven that

$$\frac{\partial E}{\partial n_i} = \epsilon_i \quad (44)$$

where n_i is the occupation number of the ith orbital, providing a meaning for the eigenvalues ϵ_i of the Kohn−Sham equation (19). This approach is present in some of the following studies.

For the calculation of atomic (including ionic) electronegativities, indeed a variety of techniques has been presented and already reviewed extensively.

In the late 1980s, Bartolotti used both transition-state and non-transition-state methods in combination with non-spin-polarized and spin-polarized Kohn−Sham theory.[129] Alonso and Balbas used simple DFT, varying from Thomas−Fermi via Thomas−Fermi−Dirac to von Weizsäcker type models,[130] and Gazquez, Vela, and Galvan reviewed the Kohn−Sham formalism.[131] Sen, Böhm, and Schmidt reviewed calculations using the Slater transition state and the transition operator concepts.[132] Studies on molecular electronegativities were, for a long time, carried out mainly in the context of Sanderson's electronegativity equalization method (see section III.B.2), where this quantity is obtained as a "byproduct" of the atomic charges and, as such, is mostly studied in less detail (vide infra).

Studies using the $(I + A)/2$ expression are appearing in the literature from the early 1990s, however hampered by the calculation of the $E[N = N_0 + 1]$ value.

In analogy with the techniques for the calculation of gradients, analytical methods have been developed to calculate energy derivatives with respect to N, leading to coupled perturbed Hartree−Fock equations,[133] by Komorowski and co-workers.[134]

In a coupled perturbed Hartree−Fock approach, Komorowski derived explicit expressions for the hardness (vide infra). Starting from the diagonal matrix **n** containing the MO occupations, its derivative with respect to N is the diagonal matrix of the MO Fukui function indices:

$$\mathbf{f} = \left(\frac{\partial \mathbf{n}}{\partial N}\right) \quad (45)$$

Combined with the matrix **e**, defined as

$$\mathbf{e} = \left(\frac{\partial E}{\partial \mathbf{n}}\right) \quad (46)$$

it yields χ via the equation

$$\chi = -\text{tr}\ \mathbf{f}\ \mathbf{e} \quad (47)$$

With the requirement of an integer population of molecular orbitals, eq 47 leads to

$$\chi^+ = -\epsilon_{\text{LUMO}} \quad (48)$$

and

$$\chi^- = -\epsilon_{\text{HOMO}} \quad (49)$$

for the right- and left-hand-side derivatives.

Coming back to the basic formula eq 37, fundamental criticism has been raised by Allen on the assumption that $\chi = -\mu$ [with $\mu = (\partial E/\partial N)_\nu$].[135−139] He proposed an average valence electron ionization energy as an electronegativity measure:

$$\chi_{\text{spec}} = -\sum_i n_i e_i / \sum_i n_i \qquad (50)$$

where the summations run over all valence orbitals with occupation number n_i. Liu and Parr[140] showed that this expression is a special case of a more general equation,

$$\chi = \sum_i \chi_i f_i \qquad (51)$$

where χ_i stands for an orbital electronegativity, a concept introduced in the early 1960s by Hinze and Jaffé:[141]

$$\chi_i = -\left(\frac{\partial E}{\partial n_i}\right)_{\nu, n_j (j \neq i)} \qquad (52)$$

the f_i values being defined as

$$f_i = \left(\frac{\partial n_i}{\partial N}\right)_{\nu} \qquad (53)$$

representing an orbital resolution of the Fukui function (see section III.B.3).

In the case that a given change in the total number of electrons, dN, is equally partitioned among all valence electrons, eq 50 in recovered.

In this sense, χ_{spec} should be viewed as an average electronegativity measure. The existence of fundamental differences between Pauling-type scales and the absolute scale has been made clear in a comment by R. G. Pearson,[142] stressing the point that the absolute electronegativity scale in fact does not conform to the Pauling definition of electronegativity as a property of an atom in a molecule, but that its essential idea reflects the tendency of attracting and holding electrons: there is no reason to restrict this to combined atoms.

As stated above, the concept of orbital electronegativity goes back to work done in the early 1960s by Hinze and Jaffé,[141,143−146] specifying the possibility of different electronegativity values for an atom, depending on its valence state, as recognized by Mulliken[91] in his original definition of an absolute electronegativity scale. In this sense, the electronegativity concept is complicated by the introduction of the orbital characteristics; on the other hand, it reflects in a more realistic way the electronegativity dependence on the surroundings. Obviously, within an EEM approach (see section III.C.1) and allowing nonintegral occupation numbers, the same feature is accounted for.

Komorowski,[147−149] on the other hand, also presented a "chemical approximation" in which the chemical electronegativity, $\bar{\chi}$, of an atom can be considered as an average of the function $\chi(q)$ over a suitable range of charge:

$$\bar{\chi} = \langle \chi(q) \rangle \qquad (54)$$

An analogous definition is presented for the hardness. When eq 54 is evaluated between $q = -e$ and $q = +e$, $\bar{\chi}$ yields the Mulliken electronegativity, $\chi = (I + A)/2$, for an atom just as

$$\bar{\eta} = \langle \eta(q) \rangle \qquad (55)$$

yields

$$\eta = \frac{1}{2}(I - A) \qquad (56)$$

As is obvious from the preceding part, a lot of "electronegativity" data are present in the literature. Extreme care should be taken when comparing values obtained with different methodologies [finite difference Koopmans-type approximation (eq 42); analytical derivatives (eq 47)], sometimes combined with the injection of experimental data (essentially ionization energies and electron affinities), yielding in some cases values which are quoted as "experimental".

As was already the case in the pre-DFT, purely "experimental" or "empirical" area, involving the Pauling, Mulliken, Gordy, et al. scales, the adage "when making comparisons between electronegativity values of two species never use values belonging to different scales" is still valid.

Even if a consensus is reached about the definition of eq 37 (which is not completely the case yet, as illustrated in this section), it may take some time to see a convergence of the computational techniques, possibly mixed with high-precision experimental data (e.g., electron affinities). Numerical data on χ will essentially be reserved for the application section (section IV.A). A comparison of various techniques will be given in the next section in the more involved case of the hardness, the second derivative of the energy, based on a careful study by Komorowski and Balawender.[150,151]

2. Global Hardness and Softness

The concepts of chemical hardness and softness were introduced in the early 1960s by Pearson, in connection with the study of generalized Lewis acid−base reactions,

$$\mathrm{A} + :\mathrm{B} \rightleftarrows \mathrm{A{-}B}$$

where A is a Lewis acid or electron pair acceptor and B is a Lewis base or electron pair donor.[152] It was known that there was no simple order of acid and base strengths that would be valid to order the interaction strengths between A and B as measured by the reaction enthalpy. On the basis of a variety of experimental data, Pearson[152−156] (for reviews and early history, see refs 122, 155−157) presented a classification of Lewis acids in two groups (a and b, below), starting from the classification of the donor atoms of the Lewis bases in terms of increasing electronegativity:

$$\mathrm{As} < \mathrm{P} < \mathrm{Se} < \mathrm{S} \sim \mathrm{I} \sim \mathrm{C} < \mathrm{Br} < \mathrm{Cl} < \mathrm{N} < \mathrm{O} < \mathrm{F}$$

The criterion used was that Lewis acids of class a would form stabler complexes with donor atoms to the right of the series, whereas those of class b would preferably interact with the donor atoms to the left. The acids classified on this basis in class a mostly had the acceptor atoms positively charged, leading to a small volume (H^+, Li^+, Na^+, Mg^{2+}, etc.), whereas class b acids carried acceptor atoms with low positive charge and greater volume (Cs^+, Cu^+). This classification turns out to be essentially polarizability-based, leading to the classification of the bases as "hard" (low polarizability; NH_3, H_2O, F^-, etc.) or "soft" (high polarizability; H^-, R^-, R_2S, etc.).

On this basis, Pearson formulated his hard and soft acids and bases (HSAB) principle, which will be discussed in detail in section III.C.2: hard acids preferably interact with hard bases, and soft acids with soft bases. The *Journal of Chemical Education* paper by Pearson further clarified the concepts[158] (this paper was in 1986 already a Citation Classic, cited almost 500 times[159]) which gradually entered and now have a firm place in modern textbooks of inorganic chemistry[160−163] (for an interesting perspective, see also ref 164). Its recognition, also based on the theoretical approaches described in section III.C.2, is witnessed by a recent *Tetrahedron* report by an experimental organic chemist, S. Woodward, on its elusive role in selective catalysis and synthesis.[165]

Nevertheless, the classification of a new acid or base is not always so obvious, and the insertion of a compound on a hardness or softness scale may lead to vivid discussions. The lack of a sharp definition, just as was the case with Pauling's electronegativity, is again causing this difficulty.

Therefore, the paper by Parr and Pearson,[163] identifying the hardness as the second derivative of the energy with respect to the number of electrons at fixed external potential, is crucial. Similar to the identification of χ as $-(\partial E/\partial N)_\nu$, it offers a sharp definition enabling the calculation of this quantity and its confrontation with experiment:

$$\eta = \frac{1}{2}\left(\frac{\partial^2 E}{\partial N^2}\right)_\nu \tag{57}$$

[Note that in some texts the arbitrary factor $^1/_2$ is omitted.] This indicates that hardness can also be written as

$$\eta = \frac{1}{2}\left(\frac{\partial \mu}{\partial N}\right)_\nu \tag{58}$$

showing that hardness is the resistance of the chemical potential to changes in the number of electrons.

Using the finite difference approximation, we obtain eq 56, indicating that it is one-half of the reaction energy for the disproportionation reaction

$$M + M \rightleftharpoons M^+ + M^-$$

Equation 56 directly offers the construction of tables of "experimental" hardnesses via the (vertical) ionization and electron affinity values[119−121] and comparison with theoretical values.

The identification of the "absolute" hardness of DFT, $(\partial^2 E/\partial N^2)_\nu/2$, with the chemical hardness arising in Pearson's HSAB principle has been criticized by Reed.[166,167]

This author presents an operational chemical hardness based on reaction enthalpies of metathesis reactions,

$$AB + A'B' \rightleftharpoons AB' + A'B$$

obtained from published heats of formation.

Although some of the points raised by these authors are worth consideration, just as in the case of the electronegativity identification by Allen in section III.B.1, the overwhelming series of results presented up to now in the literature (see the application in section IV) gives additional support to the adequacy and elegancy in the identification of $(\partial E/\partial N)_\nu$ and $(\partial^2 E/\partial N^2)_\nu$.

Before turning to the calculation of the hardness, its relationship to other atomic or molecular properties should be clarified. First, global softness, S, was introduced as the reciprocal of the hardness by

$$S = \frac{1}{2\eta} = \left(\frac{\partial N}{\partial \mu}\right)_{\nu(\mathbf{r})} \tag{59}$$

Within the spirit of the hardness−polarizability link introduced in Pearson's original and defining approach to the introduction of the HSAB principles, it is not surprising at all that softness should be a measure of polarizability. Various studies relating atomic polarizability and softness, to be discussed in section IV.A, confirm this view.

A deeper insight into the physical or chemical significance of the hardness and its relation to the electronegativity for an atom or group embedded in a molecule can be gained when writing a series expansion of E around N_0 (typically the neutral system) at fixed external potential (for an excellent paper on this topic, see Politzer and co-wokers[168]):

$$E(N) = E(N_0) + \alpha(N - N_0) + \beta(N - N_0)^2 + \gamma(N - N_0)^3 + \ldots \tag{60}$$

where the coefficients α, β, and γ can be written as

$$\alpha = \left(\frac{\partial E}{\partial N}\right)_\nu = -\chi \tag{61}$$

$$\beta = \frac{1}{2}\left(\frac{\partial^2 E}{\partial N^2}\right)_\nu = \eta \tag{62}$$

$$\gamma = \frac{1}{6}\left(\frac{\partial^3 E}{\partial N^3}\right)_\nu = \frac{1}{3}\left(\frac{\partial \eta}{\partial N}\right)\nu \tag{63}$$

Differentiating eq 60 with respect to N, one obtains

$$-\chi(N) = -\chi(N_0) + 2\beta(N - N_0) + \ldots \tag{64}$$

or

$$\chi(N) = \chi(N_0) - 2\eta(N - N_0) + \ldots \tag{65}$$

indicating that the hardness modulates the electronegativity of an atom, group, etc., according to the charge of the system: increasing the number of electrons in a system decreases its electronegativity, its tendency to attract electrons from a partner, and vice versa, as intuitively expected.

This simple result accounts for Sanderson's principle of electronegativity equalization, as announced in section III.B.1 and discussed in detail in section III.C.1.

Politzer highlighted the role of the coefficient β (related to η) in eqs 64 and 65: it is a measure of the responsiveness of, e.g., an atom's electronegativity to a gain or loss of electronic charge. In fact, Huheey suggested that the coefficient of the charge ($N - N_0$) in eqs 64 and 65 (which at that time had not yet been identified as the hardness) is related inversely to the atom's ability to "retain" electronic charge once the charge has been acquired.[169-171] This charge capacity, designated by κ,

$$\left(\frac{\partial^2 E}{\partial N^2}\right)_{N_0} = \frac{1}{\kappa} \tag{66}$$

is thus the inverse of η,

$$2\eta = \frac{1}{\kappa} \tag{67}$$

This equation, of course, identifies the charge capacity with the softness (eq 59): $\kappa = S$. It seems intuitively reasonable that this charge capacity e.g., of an atom or group is intimitately related to the polarizability of the atom or group.

An early review on the role of the concept of charge capacity in chemistry can be found in the 1992 paper by Politzer et al.[168] Its relation to its role in acidity and basicity will be discussed in detail in section IV.C.3.

As for electronegativity, many calculations have been carried out in the finite difference method[56] or an approximation to it,

$$\eta = \frac{1}{2}(\epsilon_{\mathrm{LUMO}} - \epsilon_{\mathrm{HOMO}}) \tag{68}$$

indicating that hardness is related to the energy "gap" between occupied and unoccupied orbitals (Figure 1). [Discontinuity problems similar to those described for the electronegativity in section III.B.1 are then encountered. In this context, Komorowski's approach should be mentioned[147,148] to take as the hardness the average of the neutral and negatively charged atom or the neutral and positively charged atom respectively for acidic and basic hardness. Alternatively, Chattaraj, Cedillo, and Parr proposed that, in analogy with eqs 39 and 40, three different types of hardness kernels[172] should exist corresponding to three types of hardness for electrophilic, nucleophilic, and radical attack.] Equations 42 and 68 clearly offer a nice interpretation of χ and η in terms of a frozen orbitals approach (for a detailed analysis, see p 38 of ref 157).

Most studies reported in the literature are based on the finite difference approximation. For atoms, Kohn–Sham calculations have been presented by Gazquez et al.,[173] among others.

An important aspect, differing from the electronegativity calculation, is the recognition that hardness is obtained when minimizing the functional

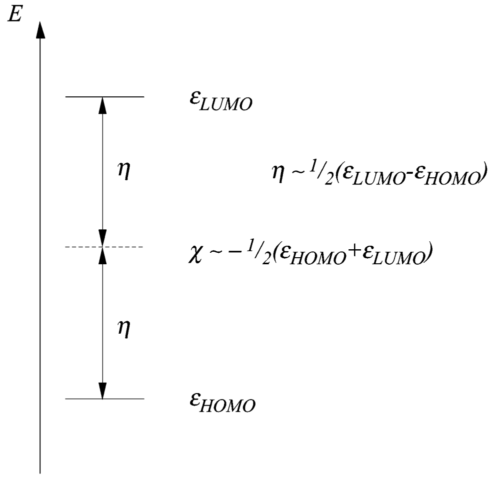

Figure 1. χ and η in a molecular orbital context.

$$\eta[g] = \int\int g(\mathbf{r})\eta(\mathbf{r},\mathbf{r}')g(\mathbf{r}')\,\mathrm{d}\mathbf{r}\,\mathrm{d}\mathbf{r}' \tag{69}$$

as will be discussed in more detail in section III.B.3. Here, $\eta(\mathbf{r},\mathbf{r}')$ is the hardness kernel and $g(\mathbf{r})$ is constrained to integrate to 1.[172]

Minimizing $\eta[g]$ yields $g(\mathbf{r}) = f(\mathbf{r})$, the electronic Fukui function, with $\eta[f] = \eta$. Work along these lines has been performed by De Proft, Liu, Parr, and Geerlings.[174,175] In the latter study on atoms, it was shown that a simple approximation for the hardness kernel,

$$\eta(\mathbf{r},\mathbf{r}') = \frac{1}{|\mathbf{r} - \mathbf{r}'|} + C \tag{70}$$

yields good results when compared with experimental hardness for both main- and transition-group elements (Figure 2) (also cf. section III.B.3). Extreme care should be taken when comparing hardness values of different species using different scales or methodologies.

An important step has been taken by Komorowski and Balawender[150] considering the above-mentioned coupled perturbed Hartree–Fock approach to the hardness evaluation, obtaining as a final result

$$\eta^{\pm} = \frac{1}{4} J_{\mathrm{FMO}} + \sum_{i}^{\mathrm{vir}} \sum_{j}^{\mathrm{occ}} U_{ij}^{\pm}[2(i, j/\mathrm{FMO}, \mathrm{FMO}) - (i, \mathrm{FMO}/j, \mathrm{FMO})] \tag{71}$$

where the two electron integrals (ij/kl) are defined as usual. FMO denotes a frontier molecular orbital leading, according to its choice as HOMO or LUMO, to η^- or η^+ values, respectively. The elements of the $\mathbf{U}$ matrix connect the N derivatives of the LCAO coefficients, $C_{\lambda i}$, and the unperturbed coefficients,

$$\left(\frac{\partial \mathbf{C}}{\partial N}\right)_{\nu(\mathbf{r})} = \mathbf{CU} \tag{72}$$

In Table 1, we give Komorowski and Balawender's values of η^+, η^-, and their averages and compare them with the results of the more frequently used

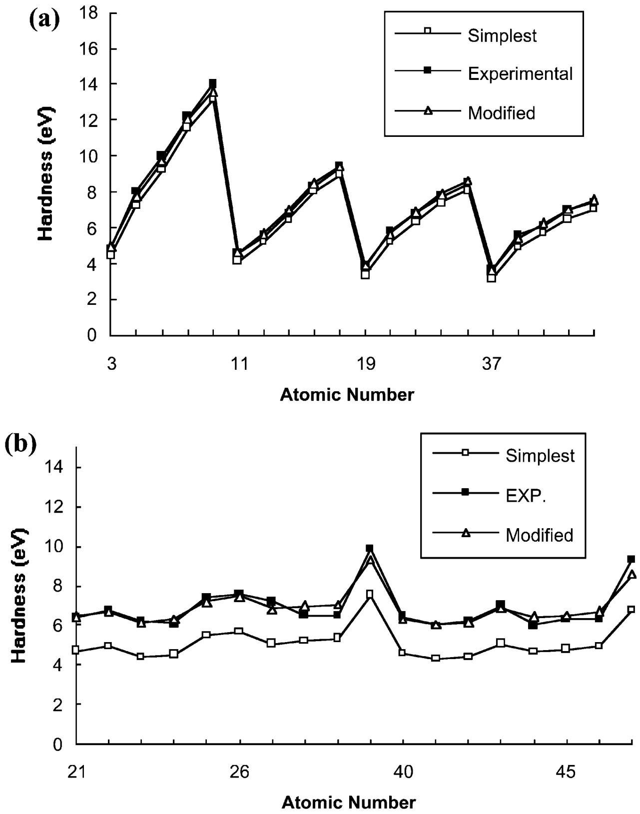

Figure 2. (a) Experimental and theoretical atomic hardnesses for main group elements. Plotted are the experimental data and data obtained using eq 70 with $C = 0$ (simplest) and $C = 0.499$ eV (modified). (b) Experimental and theoretical atomic hardnesses for transition elements. Plotted are the experimental data and data obtained using eq 70 with $C = 0$ (simplest) and $C = 1.759$ eV (modified). Reprinted with permission from ref 174. Copyright 1997 American Chemical Society.

working equations (56). This table illustrates the problematics in the definition/evaluation of energy vs N derivatives, already addressed in the case of electronegativity (cf. section III.B.1).

It was found that both the η^+ and η^- values were substantially smaller than both the finite difference and orbital gap values. Within this much smaller range, trends of decreasing hardness are recovered when passing in analogous compounds from first to second row and when passing from cationic via neutral to anionic species. The smaller values were attributed to the presence of the second term in eq 71, which is an orbital relaxation term and is always negative. The first term is identical to one proposed earlier by Komorowski and co-workers[134,151] and yields, upon the introduction of the Pariser approximation[176] for Coulomb integrals

$$J = \int\int \frac{\phi_1^*(\boldsymbol{r}_1)\phi_2^*(\boldsymbol{r}_2)\phi_1(\boldsymbol{r}_2)\phi_2(\boldsymbol{r}_2)}{|\boldsymbol{r}_1 - \boldsymbol{r}_2|}\, d\boldsymbol{r}_1\, d\boldsymbol{r}_2 \approx I - A \tag{73}$$

originally proposed for atoms, a proportionality between η and $I-A$ which is recovered in the finite difference approximation (eq 56).

Table 1. Molecular Hardnesses (eV) As Calculated by Different Methods[a]

molecule	$(I - A)/2$	$(\epsilon_L - \epsilon_H)/2$	$(\eta^+ + \eta^-)/2$	η^+	η^-
BCl_3	6.537	7.294	1.566	1.561	1.570
BF_3	10.242	11.677	2.202	2.162	2.243
BH_3	7.192	7.973	2.285	2.041	2.530
C_2H_2	7.610	8.509	2.088	1.983	2.192
C_2H_4	6.549	7.569	1.864	1.820	1.909
C_2H_6	9.501	9.943	1.649	1.428	1.871
CF_3^-	4.944	5.735	2.143	1.878	2.408
CF_3^+	9.576	11.388	2.466	2.516	2.416
CH_3^-	5.700	6.501	1.916	1.706	2.126
CH_3^+	8.021	9.071	2.574	2.256	2.892
CN^-	8.149	9.198	2.272	2.102	2.442
CNO^-	8.386	9.336	1.974	1.984	1.964
H_2O	7.443	9.098	2.122	2.066	2.177
H_2S	6.856	7.573	2.028	1.828	2.227
NCO^-	8.386	9.336	2.068	2.049	2.087
NH_2^-	5.958	7.098	2.060	1.918	2.202
NH_3	7.237	8.308	2.143	1.797	2.489
NH_4^+	12.021	12.851	2.150	1.735	2.566
PH_2^-	5.352	5.906	1.793	1.659	1.928
PH_3	5.746	6.331	1.900	1.733	2.068
PH_4^+	10.025	10.464	1.920	1.673	2.167
OH^-	6.761	8.176	2.441	2.345	2.537
HS^-	6.347	7.159	1.967	1.851	2.083
SO_2	6.224	7.012	2.012	1.977	2.046
SO_3	7.004	8.192	1.955	1.938	1.973
CO	8.579	9.715	2.684	2.373	2.994
H_2CO	6.299	7.908	2.066	2.073	2.060
SCN^-	6.780	7.619	1.638	1.503	1.772

[a] See text. Data from ref 150.

The exchange integrals K in an MO basis, on the other hand, are written as

$$K = \int\int \frac{\phi_1^*(\boldsymbol{r}_1)\phi_2^*(\boldsymbol{r}_2)\phi_1(\boldsymbol{r}_2)\phi_2(\boldsymbol{r}_1)}{|\boldsymbol{r}_1 - \boldsymbol{r}_2|}\, d\boldsymbol{r}_1\, d\boldsymbol{r}_2 \tag{74}$$

The use of a simplified methodology involving only FMO Coulomb and exchange integrals has been advocated by de Giambiagi et al.[177,178] and Julg.[179]

An evaluation of the molecular hardness based upon the computation of an MO-resolved hardness tensor has been presented by Russo and co-workers.[180]

In this approach, the elements η_{ij} of the matrix η,

$$\eta_{ij} = \frac{\partial^2 E}{\partial n_i n_j} \tag{75}$$

are written using Janak's theorem (eq 44)[117] for fractional occupations as

$$\eta_{ij} = \frac{\partial \epsilon_i}{\partial n_j} \tag{76}$$

Next, a finite difference approach is used to compute them as

$$\eta_{ij} = [\epsilon_i(n_j - \Delta n_j) - \epsilon_i(n_j)]/\Delta n_j \tag{77}$$

with $\Delta n_j = n_j - n_j^0$ the change in number of electrons, which can be either positive or negative.

Inverting the η matrix yields the softness matrix, $\mathbf{S}$, whose elements S_{ij} are used in an additive scheme to yield the total softness S and, from it, the total hardness:

$$\eta = \frac{1}{S} = \frac{1}{\sum_i \sum_j s_{ij}} \tag{78}$$

The results for a series of small molecules (HCN, HSiN, N_2H_2, HCP, and O_3H^+) indicate, at first sight, strong deviations between the HOMO−LUMO band gap value and the η value obtained via the procedure described above; introducing a factor of 2 (cf. eq 57) brings the values relatively close to each other.

The evaluation of hardness in an atoms-in-molecules context (AIM) was reviewed by Nalewajski;[181] as further detailed in section III.B.3, the method is based on the construction of a hardness tensor in an atomic resolution, where the matrix elements η_{ij} are evaluated as will be explained here.

As in the MO ansatz described above, the global hardness is then obtained via the softness matrix, obtained after inverting η, summing its diagonal elements, and inverting the total softness calculated in that way:

$$\eta_{ij} \rightarrow \eta \rightarrow \sigma = \eta^{-1} \rightarrow \sum_i \sigma_{ii} = S \rightarrow \eta = \frac{1}{S} \tag{79}$$

An alternative and direct evaluation of the atomic softness matrix, which can be considered as a generalization of the atom−atom polarizability matrix in Hückel theory,[182] has been proposed by Cioslowski and Martinov.[183]

It should be noted that hardness can also be obtained in the framework of the electronegativtity equalization as described in detail by Baekelandt, Mortier, and Schoonheydt.[184]

The concept of hardness of an atom in a molecule was also addressed by these and the present authors by investigating the effect of deformation of the electron cloud on the chemical hardness of atoms (mimicked by placing fractions of positive and negative charges upon ionization onto neighboring atoms and evaluating an AIM ionization energy or electron affinity). The results generally point in the direction of increasing hardness of atoms with respect to the isolated atoms.[185]

We end this section with a discussion of a reactivity index combining electronegativity and hardness: the electrophilicity index, recently introduced by Parr, Von Szentpaly, and Liu.[186,187] These authors commence by referring to a study by Maynard and coworkers on ligand-binding phenomena in biochemical systems (cf. section IV.C.2-f) involving partial charge transfer,[188] where $\chi^2{}_A/\eta_A$ was first suggested as the capacity of an electrophile to stabilize a covalent (soft) interaction. They then addressed the question of to what extent partial electron transfer between an electron donor and an electron acceptor contributes to the lowering of the total binding energy in the case of maximal flow of electrons (note the difference with the electron affinity measuring the capability of an electron acceptor to accept precisely one electron). Using a model of an electrophilic ligand immersed in an idealized zero-temperature free electron sea of zero chemical potential, the saturation point of the ligand for electron inflow was characterized by putting

$$\Delta E/\Delta N = 0 \tag{80}$$

For ΔE, the energy change to second order at fixed external potential was taken,

$$\Delta E = \mu \Delta N + \frac{1}{2}\eta \Delta N^2 \tag{81}$$

where μ and η are the chemical potential and hardness of the ligand, respectively.

If the electron sea provides enough electrons, the ligand is saturated when (combining eqs 80 and 81)

$$\Delta N_{\max} = -\frac{\mu}{\eta} \tag{82}$$

which yields a stabilization energy,

$$\Delta E = -\frac{\mu^2}{2\eta} \tag{83}$$

which is always negative as $\eta > 0$. The quantity $\mu^2/2\eta$, abbreviated as ω, was considered to be a measure of the electrophilicity of the ligand:

$$\omega = \frac{\mu^2}{2\eta} \tag{84}$$

Using the parabolic model for the $E_\nu = E_\nu(N)$ curve (eq 29), one easily obtains

$$\Delta N_{\max} = N_{\max} - N_0 = \frac{1}{2}\frac{I + A}{I - A} \tag{85}$$

and

$$\omega = \frac{(I + A)^2}{8(I - A)} \tag{86}$$

The A dependence of ω is intuitively expected; however, I makes the difference between ω and EA ($\omega \sim A$ if $I = 0$), as there should be one as A reflects the capability of accepting only one electron from the environment, whereas ω is related to a maximal electron flow.

Parr, Von Szentpaly, and Liu[186] calculated ω values from experimental I and A data for 55 neutral atoms and 45 small polyatomic molecules, the resulting ω vs A plot illustrating the correlation (Figure 3).

ω values for some selected functional groups (CH_3, NH_2, CF_3, CCl_3, CBr_3, CHO, COOH, CN) mostly parallel group electronegativity values with, e.g., $\omega(CF_3) > \omega(CCl_3) > \omega(CBr_3)$, the ratio of the square of μ and η apparently not being able to reverse some electronegativity trends.

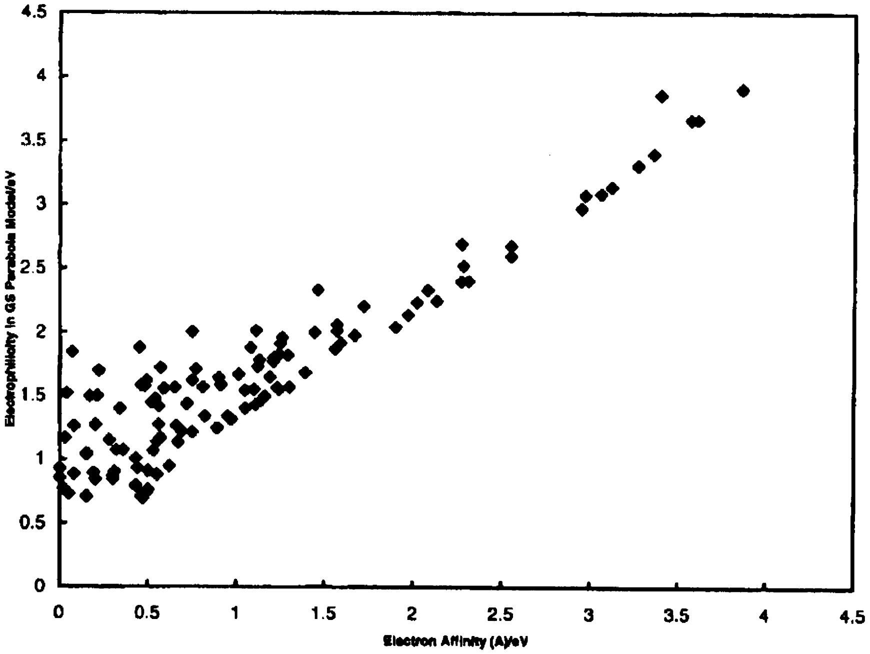

Figure 3. Correlation between electrophilicity ω and electron affinity A for 54 atoms and 55 simple molecules. Reprinted with permission from ref 186. Copyright 1999 American Chemical Society.

Note, however, that ω(F) (8.44) > ω(Br) (7.28) ≫ ω(I) (6.92) > ω(Cl) (6.66 eV), where the interplay between μ and η changes the electronegativity order, F > Cl > Br > I, however putting Cl with lowest electrophilicity.

3. The Electronic Fukui Function, Local Softness, and Softness Kernel

The electronic Fukui function $f(\boldsymbol{r})$, already presented in Scheme 4, was introduced by Parr and Yang[189,190] as a generalization of Fukui's frontier MO concept[191−193] and plays a key role in linking frontier MO theory and the HSAB principle.[194]

It can be interpreted (cf. the use of Maxwell's relation in this scheme) either as the change of the electron density $\rho(\boldsymbol{r})$ at each point $\boldsymbol{r}$ when the total number of electrons is changed or as the sensitivity of a system's chemical potential to an external perturbation at a particular point $\boldsymbol{r}$,

$$f(\boldsymbol{r}) = \left(\frac{\partial\rho(\boldsymbol{r})}{\partial N}\right)_{\nu} = \left(\frac{\delta\mu}{\delta\nu(\boldsymbol{r})}\right)_{N} \tag{87}$$

The latter point of view, by far the most prominent in the literature, faces the N-discontinuity problem of atoms and molecules,[89,90] leading to the introduction[189] of both right- and left-hand-side derivatives, both to be considered at a given number of electrons, $N = N_0$:

$$f^{+}(\boldsymbol{r}) = \left(\frac{\partial\rho(\boldsymbol{r})}{\partial N}\right)^{+}_{\nu(\boldsymbol{r})} \tag{88}$$

for a nucleophilic attack provoking an electron increase in the system, and

$$f^{-}(\boldsymbol{r}) = \left(\frac{\partial\rho(\boldsymbol{r})}{\partial N}\right)^{-}_{\nu(\boldsymbol{r})} \tag{89}$$

for an electrophilic attack provoking an electron decrease in the system.

The properties of the Fukui function have been reviewed by Ayers and Levy:[190] besides normalization and asymptotic decay, the cusp condition for the density[195] implies that the Fukui function should also satisfy it.[196]

The essential role of the Fukui function in DFT has recently been re-emphasized by Ayers and Parr,[197] stressing the point that the FF minimizes the hardness functional $\eta[\rho_{N_0},\Delta\rho_{+1}]$, where $\Delta\rho_{+1}$ stands for the density distribution of the added electron subject to the constraint that $\Delta\rho_{+1}$ integrates to 1.

The importance of Fukui's FMO concept in modern chemistry can hardly be overestimated and is nicely summarized in Kato's perspective,[193] where it is said that Fukui's 1952 papers may be regarded as a bridge connecting the two stages of chemical reactivity description in the 20th century. The first stage is the electronic theory of organic chemistry, generalized by Coulson and Longuet-Higgins, based on quantum mechanics. The second stage is the establishment of symmetry rules for the MOs in predicting the course of a reaction (i.e., FMO theory and Woodward−Hoffmann rules). "Fukui's paper proposed a reactivity index for interpreting the orientation effect in a chemical reaction, the main subject of the electronic theory of organic chemistry, and was the starting point of the second stage after the concept of frontier orbitals was first introduced and it became the key ingredient in the further development of the theory." [193]

The electronic Fukui function now generalizes this important concept.

Although, in principle, the neutral or N_0-electron system's electron density contains all information needed for the evaluation of the Fukui function, most studies in the literature have been carried out in the so-called finite difference method, approximating

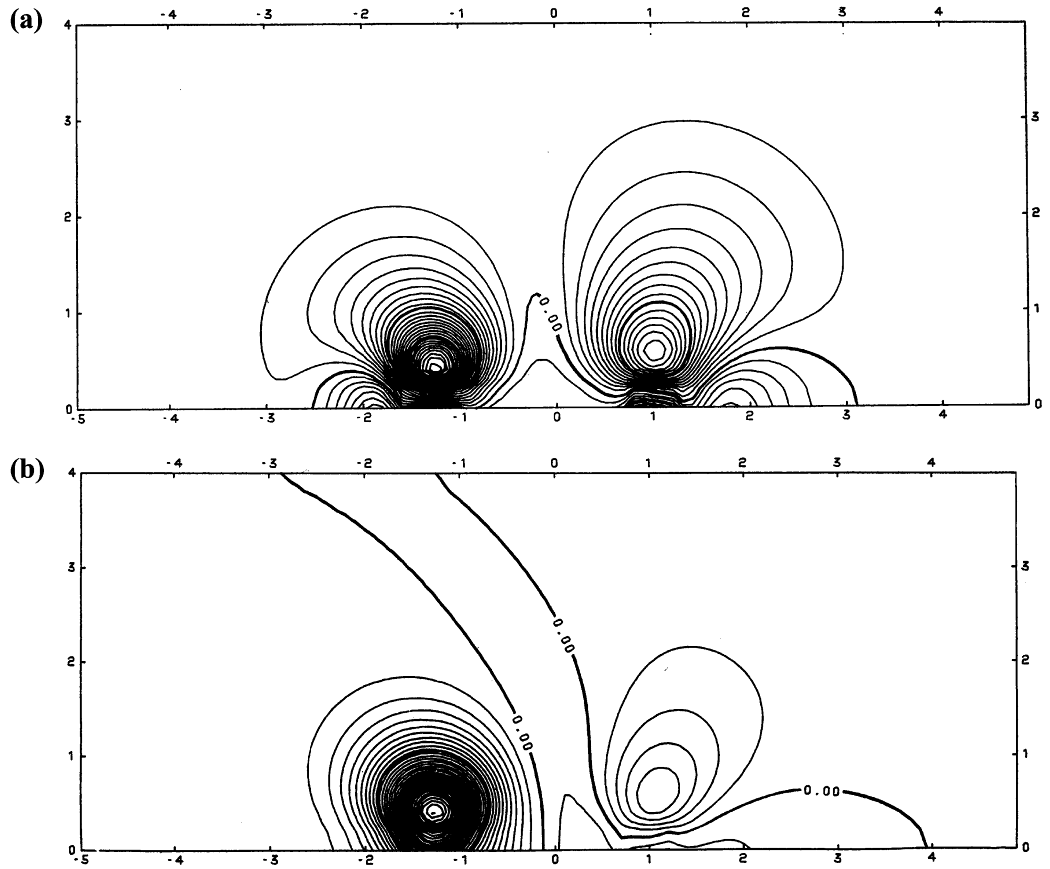

Figure 4. Parr's early local softness plots for H_2CO in the plane perpendicular to the molecular plane: nucleophilic vs electrophilic reaction sites on H_2CO, as indicated by $s^+(\mathbf{r})$ and $s^-(\mathbf{r})$, respectively. Reprinted with permission from ref 199. Copyright 1988 Elsevier Science.

$$f^+(\mathbf{r}) \quad \text{as} \quad f^+(\mathbf{r}) \approx \rho_{N_0+1}(\mathbf{r}) - \rho_{N_0}(\mathbf{r}) \tag{90}$$

and

$$f^-(\mathbf{r}) \quad \text{as} \quad f^-(\mathbf{r}) \approx \rho_{N_0}(\mathbf{r}) - \rho_{N_{0-1}}(\mathbf{r}) \tag{91}$$

which is, in many cases, seriously hampered by the possibility of metastable anions.[124-126]

A third function describing radical attack, $f^0(\mathbf{r})$, is then obtained as the arithmetic average of $f^+(\mathbf{r})$ and $f^-(\mathbf{r})$.

Note that, when a frozen approach is used when studying the $N_0 \pm 1$ situations (e.g., describing them with the orbitals of the N_0 system), $f^+(\mathbf{r})$ reduces to $\rho_{\mathrm{LUMO}}(\mathbf{r})$ and $f^-(\mathbf{r})$ to $\rho_{\mathrm{HOMO}}(\mathbf{r})$, indicating that Fukui's frontier orbital densities can be considered as approximations to the function named in his honor.[192] Note also that Yang, Parr, and Pucci showed that f^+ and f^- are directly related to the appropriate FMOs[198] and that $f^+(\mathbf{r})$ for an M-electron system may be written as

$$f^+(\mathbf{r}) = |\Psi_{\mathrm{LUMO}}(\mathbf{r})|^2 + \sum_{i=1}^{M} \frac{\partial}{\partial N}|\Psi_i(\mathbf{r})|^2 \tag{92}$$

and $f^-(\mathbf{r})$ as

$$f^-(\mathbf{r}) = |\Psi_{\mathrm{HOMO}}(\mathbf{r})|^2 + \sum_{i=1}^{M-1} \frac{\partial}{\partial N}|\Psi_i(\mathbf{r})|^2 \tag{93}$$

in the context of Janak's extension of Kohn–Sham theory.[117]

The earliest numerical calculations on Fukui functions were reported by Lee, Yang, and Parr[199] (Figure 4), concentrating on the plots of the local softness derived from it (vide infra) for H_2CO, SCN^-, and CO, followed by studies by Mendez et al.[200,201] and Geerlings et al.[202-205] Particular attention to the (3D) visualization of the Fukui function has been given by Flurchick and Bartolotti.[206] When taken in comparative perspective, it was shown by the latter authors that appreciable differences exist between the HOMO (or LUMO) density and the Fukui function. Moreover, the suggestion by Gambiagi et al.[207,208] that $f(\mathbf{r})$ is closely related to the Laplacian of the charge density,[209,210] of fundamental importance in Bader's atoms-in-molecules theory,[68] turned out to be not true. The influence of correlation on the Fukui function was investigated by Langenaeker et al. in the case of the $f^-(\mathbf{r})$ function of ambident nucleophiles (NO_2^-, CH_2CHO^-, and SCN^-), which showed less important effects than expected. These studies at a moderate level (CISD; 6-31++G**)[211] were later completed by B3LYP-DFT and QCISD calculations[212] using Dunning's augmented correlation-consistent basis sets,[213,214] revealing for SCN^- a slightly enhanced selectivity for the S-terminus in the case of the DFT calculations, the QCISD and CISD results being highly similar.

In recent years, intensive research has been conducted on the development of methods avoiding the rather cumbersome finite difference method, which moreover bears sources of errors.

A gradient approximation has been developed by Chattaraj et al.[196] and Pacios et al.,[215,216] proposing an expansion,

$$f(\boldsymbol{r}) = \frac{\rho(\boldsymbol{r})}{N}[1 + \alpha\Phi(\boldsymbol{r},\rho(\boldsymbol{r}),\nabla\rho,\nabla^2\rho,...)] \qquad (94)$$

which was written as

$$f(\boldsymbol{r}) = \frac{\rho(\boldsymbol{r})}{N} + \frac{\alpha}{N}\rho_0^{-2/3}\left\{\left[\left(\frac{\rho}{\rho_0}\right)^{2/3} - 1\right]\nabla^2\rho - \frac{2}{3}\left(\frac{\rho_0}{\rho}\right)^{2/3}\frac{\nabla\rho_0\cdot\nabla\rho}{\rho}\right\} \qquad (95)$$

where ρ_0 is the density at the nucleus, α being a parameter which can be determined, e.g., from ρ_0. This technique, which was exclusively used for atoms hitherto, yields a single Fukui function, not distinguishing between $f^+(\boldsymbol{r})$ and $f^-(\boldsymbol{r})$.

The results of the radial distribution of the Fukui function, $4\pi r^2 f(r)$, for Li, N, and F are similar to those obtained by Gazquez, Vela, and Galvan[217] using a finite difference approach within a spin-polarized formalism; they show a slow decay for electropositive atoms and a faster one for electronegative atoms.

De Proft et al.[175] implemented the variational principle for chemical hardness formulated by Chattaraj, Cedillo, and Parr,[172] stating that the global hardness and the Fukui function can be obtained simultaneously by minimizing the functional (69), where $\eta(\boldsymbol{r},\boldsymbol{r}')$ is the hardness kernel (see section III.B.4) and where $g(\boldsymbol{r})$ is constrained to integrate to 1. Whereas the gradient extension method does not distinguish between $f^+(\boldsymbol{r})$ and $f^-(\boldsymbol{r})$, these functions may be obtained in the variational approach by using the one-sided hardness kernel, $\eta^+(\boldsymbol{r},\boldsymbol{r}')$ or $\eta^-(\boldsymbol{r},\boldsymbol{r}')$.

The extremal functional of eq 69 can be shown to be the Fukui function, the functional $\eta[g=f]$ leading to the global hardness. As stated by Ayers and Levy,[190] the variational method may be the method of choice in the future, but the accurate determination of the hardness kernel remains a problem. This conclusion also emerges in a natural way from the recent in-depth and generalizing study by Ayers and Parr on variational principles for describing chemical reactions: the Fukui function appears as the function minimizing the hardness functional.[197]

Introducing the approximation

$$\eta(\boldsymbol{r},\boldsymbol{r}') \approx \frac{1}{|\boldsymbol{r} - \boldsymbol{r}'|} \qquad (96)$$

leads to the hardness expression

$$\eta = \int\int \frac{f(\boldsymbol{r})\, f(\boldsymbol{r}')}{|\boldsymbol{r} - \boldsymbol{r}'|}\, \mathrm{d}\boldsymbol{r}\, \mathrm{d}\boldsymbol{r}' \qquad (97)$$

Using a linear combination of atomic Fukui functions, the condensed form of this methodology was shown to yield results in line with the sensitivity analysis approach formulated by Nalewajski and was also used by Mortier.

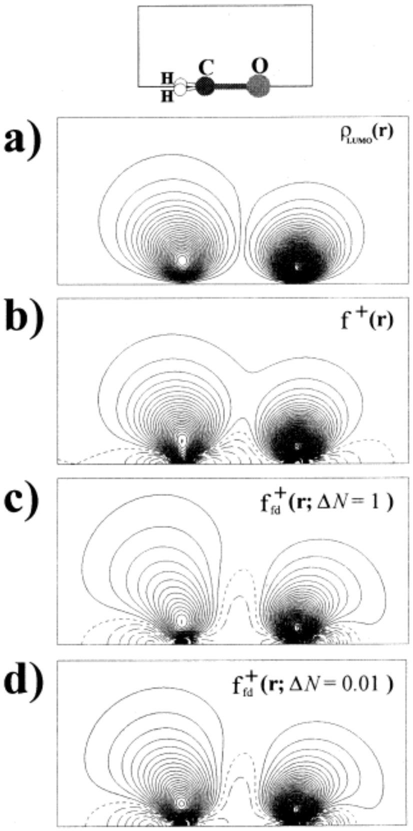

Figure 5. f^+ contour diagram for H_2CO in a plane perpendicular to the molecular plane containing the CO bond. Drawn are the differential $f^+(\boldsymbol{r})$, the finite diffence $f^+(\boldsymbol{r})$ corresponding to $\Delta N = 1$ and $\Delta N = 0.01$, and the LUMO density. Reprinted with permission from ref 218. Copyright 1999 American Chemical Society.

Nalewajski et al. showed that the Fukui function can be obtained from a single Kohn–Sham calculation.[218] It is determined by adding to the rigid, frontier orbital term (see also eqs 92 and 93) the density relaxation contribution, which is determined by differentiation of the Kohn–Sham equations with respect to N:

$$f(\boldsymbol{r}) = f^{\mathrm{F}}(\boldsymbol{r}) + f^{\mathrm{R}}(\boldsymbol{r}) \qquad (98)$$

Here, f^{F} is the frontier term corresponding to the "frozen" shape of orbitals, and f^{R} corresponds to orbital relaxation.

Neglecting the exchange correlation term in the N derivative, contour maps of the Fukui function f^+ for H_2CO obtained in this analytical way (differential Fukui Function) are compared in Figure 5 with the finite difference results obtained with two different ΔN values, the usual $|\Delta N| = 1$ case and a smaller value (0.01), and with the LUMO density corresponding to the first term in eq 95. It is seen that, as compared to the LUMO density (antibonding π* orbital), the orbital relaxation mixes the frontier orbital with the other occupied MOs including σ orbitals, a feature present in both the finite difference and differential methods. In Figure 6, a more detailed comparison between these two methods is given, along a line parallel to the CO bond in the planes of Figure 5. It is clearly seen that the differential method approaches the finite difference results upon decreasing ΔN. This trend is confirmed in other cases.[217]

Russo et al.[219] also presented an atoms-in-molecules variant of his MO approach, based on Mayer's

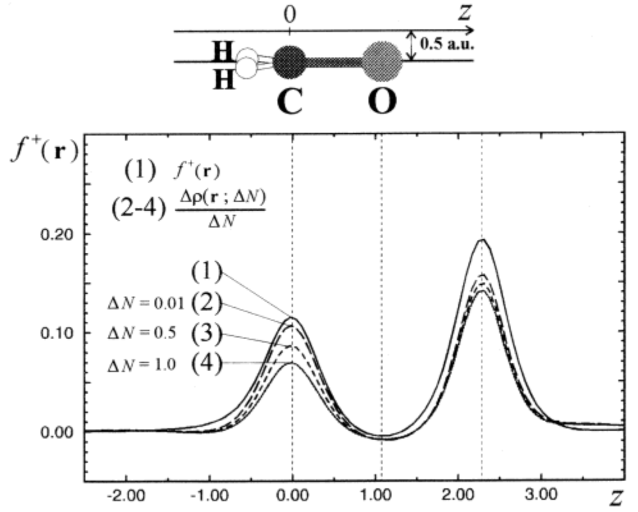

Figure 6. Comparison between the finite difference and differential f^+ results for H_2CO along a line parallel to the CO bond in the plane of the figure. Curve 1 is the differential result; curves 2, 3, and 4 represent the finite difference results with $\Delta N = 0.01$, 0.5, and 1.0, respectively. Reprinted with permission from ref 218. Copyright 1999 American Chemical Society.

bond order indices and atomic valences.[220,221] A similar approach was followed by Grigorov et al., using the thermal extension of DFT,[222,223] and by Liu.[224] Landmark papers on the atoms-in-molecules approach were written by Nalewajski et al., who introduced these concepts in the late 1980s and early 1990s[225,226] (for reviews, see refs 227−229). It is one of the most elaborated and documented techniques to obtain information about Fukui functions and local softness at the atomic level. It is, in fact, part of a general analysis on intermolecular interactions in the hardness/softness context. Depending on the resolution involved, specified by a given partitioning of the system in the physical space, one defines the electron density distribution $\rho(\boldsymbol{r})$ (local resolution), the population of atoms in molecules (N_A, N_B, etc.; AIM resolution), the populations attributed to larger molecular fragments (e.g., groups; N_X, N_Y, N_Z, etc.; group resolution), or the total number of electrons ($N = \int\rho(\boldsymbol{r})\,d\boldsymbol{r} = \sum_A N_A = \sum_X N_X$; global resolution). An interesting intermediate resolution is situated at the MO level.[230,231]

In the AIM resolution, a semiempirical ansatz is used to construct the elements of the atom−atom hardness matrix, η_{AB}, using the finite difference formula, $\eta_A = (I_A - A_A)/2$ (eq 56), for the diagonal elements and the Ohno formula,[232,233]

$$\eta_{AB} = 1/\sqrt{\alpha_{AB}^2 + R_{AB}^2} \tag{99}$$

for the off-diagonal elements, R_{AB} being the interatomic distance, α_{AB} being defined as

$$\frac{2}{(\eta_A + \eta_B)} \tag{100}$$

Note that Balawender and Komorowski[150] presented a coupled perturbed Hartree−Fock scheme (for a comprehensive account of the CPHF methods, see ref 133) in a MO basis to obtain first-order correction terms to the orbital frozen Fukui function.

The matrix of the derivative MO coefficients $(\partial\mathbf{C}/\partial N)_{\nu(\boldsymbol{r})}$ is written in terms of the unperturbed MOs as eq 72, where **U** is determined via a coupled perturbed Hartree−Fock scheme.

Retaining integer occupation numbers for the MOs requires

$$\begin{aligned} f^+ = \left(\frac{\partial n_i}{\partial N}\right)^+ &= 0 \qquad i \neq \text{LUMO} \\ &= 1 \qquad i = \text{LUMO} \end{aligned} \tag{101}$$

$$\begin{aligned} f^- = \left(\frac{\partial n_i}{\partial N}\right)^- &= 0 \qquad i \neq \text{HOMO} \\ &= 1 \qquad i = \text{HOMO} \end{aligned} \tag{102}$$

The correlation between atomic Fukui function indices obtained in this way and the finite difference approximation turns out to be remarkably good in a series of diatomics.

Russo and co-workers presented[52,219] a method based on the diagonalization of the hardness matrix in a valence MO basis, $n_{ij} = \partial\epsilon_i/\partial n_j$, yielding orbital Fukui functions, the Kohn−Sham eigenvalues ϵ_i being evaluated on the basis of Janak's theorem.[117]

Senet[234,235] proposed a different methodology based on the knowledge of the linear response function $\chi(\boldsymbol{r},\boldsymbol{r}')$, offering also a generalization to higher order Fukui functions,

$$\left(\frac{\partial^n f(\boldsymbol{r})}{\partial N^{\,n}}\right)_{\nu(\boldsymbol{r})} = \left(\frac{\partial^{n+1}\rho(\boldsymbol{r})}{\partial N^{\,n+1}}\right)_{\nu(\boldsymbol{r})} \tag{103}$$

for which, however, no numerical results have been reported yet.

Preceding Nalewajski's AIM approach, a condensed form of the Fukui function was introduced in 1986 by Yang and Mortier,[236] based on the idea of integrating the Fukui function over atomic regions, similar to the procedure followed in population analysis techniques.[237] Combined with the finite difference approximation, this yields working equations of the type

$$f_A^+ = q_A(N+1) - q_A(N) \equiv q_{A,N_0+1} - q_{A,N_0} \tag{104}$$

$$f_A^- = q_A(N) - q_A(N-1) \equiv q_{A,N_0+1} - q_{A,N_0-1} \tag{105}$$

where $q_A(N)$ denotes the electronic population of atom A of the reference system, more carefully denoted as q_{A,N_0}. The simplification of eq 103 in the frozen orbital approach has been considered by Contreras et al.[238]

Obviously, the q_A values will be sensitive both to the level of the calculation of the electron density function $\rho(\boldsymbol{r})$ which is differentiated and to the partitioning scheme. As such, the inclusion of correlation effects in the Hartree−Fock-based wave function-type calculations is crucial, as is the choice of the exchange correlation functional in DFT methods (cf. the change in the number of electron pairs when passing from N_0 to $N_0 + 1$ or $N_0 - 1$).

The partitioning scheme encompasses the panoply of techniques in population analysis, varying from Mulliken,[239] over CHELPG[240] and natural population analysis,[241] to Cioslowski's atomic polar tensor (APT)-based formalism[242−244] and Bader's atoms-in-molecules picture.[68] Comprehensive studies, including also the effect of the atomic orbital basis set, have been performed by Martin, De Proft, and Geerlings,[56,212,245] Chermette and co-workers,[246] Arumozhiraja and Kolandaivel,[247] and Cioslowski et al.[243] Taking QCISD[248,249] results as a reference, Geerlings showed that B3LYP and especially B3PW91 perform very well, better than Hartree−Fock and MP2 in combination with NPA or Bader's analysis, APT being computationally demanding for larger systems, since dipole moment derivatives are involved.[242] It is the authors' experience that problems of basis set dependence of atomic populations are often transferred to condensed Fukui functions. Basis set and population analysis sensitivity are still prominent in the condensed FF values, as also noticed by Arumozhiraja and Kolandaivel.[247] Chermette, on the other hand, used a numerical integration scheme derived by Becke,[250] dividing the three-dimensional space into weighted atomic subregions. In an extensive study on maleimide, a gratifying stability of the f_A values was found for various combinations of exchange correlation functionals, basis sets, and also for the numerical parameters defining the grid.

Most studies hitherto concentrated on condensed Fukui functions for closed-shell molecules; studies exclusively devoted to open-shell molecules are scarce. Misra and Sannigrahi,[251] in a study of small radicals, found this effect of spin contamination on the finite difference Fukui function to be small. In a recent study,[252] the DFT-B3LYP approach was preferred to the use of UHF wave functions, as the latter are appreciably spin-contaminated in many cases. Chandra and Nguyen were the first to use Fukui functions to study reactions involving the attack of radicals on nonradical systems (in the case of olefins)[253] (see section IV.C.2-d). Kar and Sannigrahi, on the other hand,[252] used f^0 and s^0 values in the study of radical reactions, concentrating on the stereoselectivity of radical−radical interactions, invoking a HSAB-type (section III.C.3) argument that sites of maximal f^0 should interact.

When working at the local level, eqs 104 and 105 sometimes lead to negative Fukui functions which, at first sight, may seem contra-intuitive. However, although this problem has been investigated in detail by Roy et al.,[254,255] no definitive answer has been given yet to the question of whether negative values are physically acceptable or are artifacts. In the case of the condensed Fukui function, Fuentealba et al.[256] presented a series of arguments for a positive definite condensed Fukui function based on an analysis of the finite difference expressions, eqs 104 and 105. Possible origins of negative Fukui functions have been attributed by Roy et al. to relaxation effects and improper charge partitioning techniques. A thorough study on the nature of the Mulliken-based condensed Fukui function indices indicates that, analytically, nothing can be predicted about the sign of the condensed Fukui function indices.[257]

These authors promoted Hirshfeld's stockholder partitioning technique,[258,259] later discussed by Maslen and Spackman[260] as a partitioning technique superior to others (although it was remarked that there are sites having negative values).

This technique has also been recently used by the authors[261] in view of the recent information theory-based proof by Parr and Nalewajski, which showed that when maximal conservation of the information content of isolated atoms is imposed upon molecule formation, the stockholder partitioning of the electron density is recovered.[262] It was seen that Hirshfeld charges can be condensed as a valuable tool to calculate Fukui function indices.

Moreover, Ayers[263] showed that Hirshfeld charges also yield maximally transferable AIMs, pointing out that the strict partitioning of a molecule into atomic regions is generally inconsistent with the requirement of maximum transferability.

Nalewajski and Korchowiec[229,264−266] extended the Fukui function concept to a two-reactant description of the chemical reaction. A finite difference approach to both diagonal and off-diagonal Fukui functions in local and AIM resolutions was presented, considering these functions as components of the charge-transfer Fukui function, $f^{\mathrm{CT}}(\boldsymbol{r})$:

$$f^{\mathrm{CT}}(\boldsymbol{r}) = \left(\frac{\partial \rho(\boldsymbol{r})}{\partial N_{\mathrm{CT}}}\right) \qquad (106)$$

where

$$\mathrm{d}N_{\mathrm{CT}} = \mathrm{d}N_{\mathrm{A}} = -\mathrm{d}N_{\mathrm{B}} \qquad (107)$$

and

$$f^{\mathrm{CT}}(\boldsymbol{r}) = \{f_{\mathrm{AA}}(\boldsymbol{r}) - f_{\mathrm{BA}}(\boldsymbol{r})\} + \{f_{\mathrm{AB}}(\boldsymbol{r}) - f_{\mathrm{BB}}(\boldsymbol{r})\} \qquad (108)$$

with

$$f_{\mathrm{AA}}(\boldsymbol{r}) = \left(\frac{\partial \rho_{\mathrm{A}}(\boldsymbol{r})}{\partial N_{\mathrm{A}}}\right) \qquad f_{\mathrm{AB}}(\boldsymbol{r}) = \left(\frac{\partial \rho_{\mathrm{A}}(\boldsymbol{r})}{\partial N_{\mathrm{B}}}\right) \qquad (109)$$

In a case study on the reaction of a methyl radical with ethylene, it was concluded that the reorganization of electron density due to charge transfer is proportional to the sum of forward (AB) and backward (BA) $f^{\mathrm{CT}}(\boldsymbol{r})$, involving both diagonal and off-diagonal Fukui functions.

The Fukui function clearly contains relative information about different regions in a given molecule. When comparing different regions in different molecules, the local softness turns out to be more interesting (for a review, see ref 49).

This quantity $s(\boldsymbol{r})$ was introduced in 1985 by Yang and Parr as[267]

$$s(\boldsymbol{r}) = \left(\frac{\partial \rho(\boldsymbol{r})}{\partial \mu}\right)_{\nu(\boldsymbol{r})} \qquad (110)$$

as a local analogue of the total softness S, which can be written as

$$S = \left(\frac{\partial N}{\partial \mu}\right)_{\nu(\boldsymbol{r})} \tag{111}$$

By applying the chain rule, $s(\boldsymbol{r})$ can be written as the product of the total softness and the Fukui function,

$$s(\boldsymbol{r}) = \left(\frac{\partial \rho(\boldsymbol{r})}{\partial \mu}\right)_{\nu} = \left(\frac{\partial \rho(\boldsymbol{r})}{\partial N}\right)_{\nu}\left(\frac{\partial N}{\partial \mu}\right)_{\nu} = Sf(\boldsymbol{r}) \tag{112}$$

indicating that $f(\boldsymbol{r})$ redistributes the global softness among the different parts of the molecule and that $s(\boldsymbol{r})$ integrates to S:

$$\int s(\boldsymbol{r})\, \mathrm{d}\boldsymbol{r} = \int Sf(\boldsymbol{r})\, \mathrm{d}\boldsymbol{r} = S\int f(\boldsymbol{r})\, \mathrm{d}\boldsymbol{r} = S \tag{113}$$

The predictive power for intermolecular reactivity sequences of the local softness clearly emerges from consideration of eq 110, showing that $f(\boldsymbol{r})$ and $s(\boldsymbol{r})$ contain the same information on the relative site reactivity within a single molecule, but that $s(\boldsymbol{r})$, in view of the information about the total molecular softness, is more suited for intermolecular reactivity sequences.

It is interesting to note that the concepts of hardness and Fukui function (and thus also the local softness) can be extended to the theory of metals.[267] It was shown by Yang and Parr that, at $T = 0$,

$$\frac{1}{\eta} = g(\epsilon_{\mathrm{F}}) \tag{114}$$

and

$$f(\boldsymbol{r}) = \frac{g(\epsilon_{\mathrm{F}},\boldsymbol{r})}{g(\epsilon_{\mathrm{F}})} \tag{115}$$

where $g(\epsilon_{\mathrm{F}})$ and $g(\epsilon_{\mathrm{F}},\boldsymbol{r})$ are the density of states and the local density of states at the Fermi level, respectively. $g(\epsilon)$ and $g(\epsilon,\boldsymbol{r})$ are defined respectively as[267,268]

$$g(\epsilon) = \sum_i \delta(\epsilon_i - \epsilon) \tag{116}$$

$$g(\epsilon,\boldsymbol{r}) = \sum_i |\Psi_i(\boldsymbol{r})|^2 \delta(\epsilon_i - \epsilon) \tag{117}$$

Methodological issues for the calculation of $s(\boldsymbol{r})$ can be brought back to those of $f(\boldsymbol{r})$ and S in view of eq 112, and we refer to section III.B.3.

In fact, relatively few softness plots have been shown in the literature, their discussion being almost always devoted to the intramolecular reactivity sequences, for which $f(\boldsymbol{r})$ can serve as well. Direct applications are mostly reported in a condensed form completely equivalent to the condensed Fukui function equations, e.g., in the finite difference approach:

$$s_{\mathrm{A}}^{+} = s_{\mathrm{A}}(N+1) - s_{\mathrm{A}}(N) \equiv s_{\mathrm{A},N_0+1} - s_{\mathrm{A},N_0} \tag{118}$$

$$s_{\mathrm{A}}^{-} = s_{\mathrm{A}}(N) - s_{\mathrm{A}}(N-1) \equiv s_{\mathrm{A},N_0} - s_{\mathrm{A},N_0-1} \tag{119}$$

A variety of techniques described for the Fukui function have been used to calculate them. Recently, a new approach was presented by Russo et al., obtaining AIM softnesses[218] from Mayer's atomic valences.[219,220]

In recent years, to cope with the problem of negative Fukui functions, Roy et al. introduced a relative nucleophilicity and a relative electrophilicity index defined as follows in atomic resolution.[269,270] For an atom k, one writes

s_k^-/s_k^+ (relative nucleophilicity) and
s_k^+/s_k^- (relative electrophilicity)

It was argued that the individual values of s_k^+ and s_k^- might be influenced by basis set limitations and thus insufficiently take into account electron correlation effects.

Derivatives of the Fukui function or local softness were scarcely considered in the literature. Parr, Contreras, and co-workers[271,272] introduced $(\partial f/\partial N)_\nu$, $(\partial f/\partial \mu)_\nu$, and $(\partial s/\partial N)_\nu$.

One can expect, as argued by Fuentealba and Cedillo,[273] that, e.g., a quantity of the type $\partial f(\boldsymbol{r})/\partial N$ should be small. (It is exactly zero in the approximation $f(\boldsymbol{r}) = 1/N\rho(\boldsymbol{r})$ used as the first order in the gradient expansion.)

Of larger direct importance may be the variation of the FF under an external perturbation, for which some model calculations in the case of the H atom perturbed by a proton or an electric field have been reported by the same authors.[273]

It should finally be noticed that Mermin[105] formulated a finite temperature version of DFT in which density and temperature define everything, even for nonhomogeneous systems. In the grand canonical ensemble, global and local softness are related to density and number fluctuations,[267]

$$S = \beta[\langle N^2\rangle - \langle N\rangle\langle N\rangle] \tag{120}$$

$$s(\boldsymbol{r}) = \beta[\langle N\rho(\boldsymbol{r})\rangle - \langle N\rangle\langle \rho(\boldsymbol{r})\rangle] \tag{121}$$

with $\beta = 1/kT$ and where "$\langle\ \rangle$" indicate averages over the grand canonical ensemble.

Using the finite temperature version of DFT, Galvan et al.[274] were able to establish an interesting and promising relationship between the local softness, $s(\boldsymbol{r})$, and the conductance in the context of scanning tunneling microscopy (STM) images,[275,276] stressing the possibility of obtaining experimental local softnesses for surfaces.

We finally consider the softness kernel, $s(\boldsymbol{r},\boldsymbol{r}')$, introduced by Berkowitz and Parr[277] and defined as

$$s(\boldsymbol{r},\boldsymbol{r}') = -\frac{\delta \rho(\boldsymbol{r}')}{\delta u(\boldsymbol{r})} = -\frac{\delta \rho(\boldsymbol{r})}{\delta u(\boldsymbol{r}')} \tag{122}$$

Here, $u(\boldsymbol{r})$ is the modified potential,

$$u(\boldsymbol{r}) = \nu(\boldsymbol{r}) - \mu = -\frac{\delta F[\rho]}{\delta \rho} \tag{123}$$

Upon integration of $s(\boldsymbol{r},\boldsymbol{r}')$, we obtain a quantity, $t(\boldsymbol{r})$,

$$t(\boldsymbol{r}) = \int s(\boldsymbol{r},\boldsymbol{r}')\, \mathrm{d}\boldsymbol{r}' \tag{124}$$

which can be identified[189,277] as

$$t(\mathbf{r}) = Sf(\mathbf{r}) = s(\mathbf{r}) \tag{125}$$

and which couples the conventional linear response function $(\delta\rho(\mathbf{r})/\delta\nu(\mathbf{r}'))_N = \chi_1(\mathbf{r},\mathbf{r}')$ in Scheme 4 to the softness kernel:

$$\left(\frac{\delta\rho(\mathbf{r})}{\delta\nu(\mathbf{r}')}\right)_N = -s(\mathbf{r},\mathbf{r}') + \frac{s(\mathbf{r})s(\mathbf{r}')}{S} \tag{126}$$

In the same spirit as eq 121, it has been shown that the following fluctuation formula holds for the softness kernel:

$$s(\mathbf{r},\mathbf{r}') = \frac{1}{kT}[\langle\rho(\mathbf{r})\rho(\mathbf{r}')\rangle - \langle\rho(\mathbf{r})\rangle\langle\rho(\mathbf{r}')\rangle] \tag{127}$$

The corresponding hardness kernel, $\eta(\mathbf{r},\mathbf{r}')$, defined as (vide infra)

$$\eta(\mathbf{r},\mathbf{r}') = \frac{\delta^2 F[\rho]}{\delta\rho(\mathbf{r})\delta\rho(\mathbf{r}')} \tag{128}$$

yields a reciprocity relation between $\eta(\mathbf{r},\mathbf{r}')$ and $s(\mathbf{r},\mathbf{r}')$, in the sense that

$$\int s(\mathbf{r},\mathbf{r}')\eta(\mathbf{r}',\mathbf{r}'')\,\mathrm{d}\mathbf{r}' = \delta(\mathbf{r} - \mathbf{r}'') \tag{129}$$

Senet[234,235] showed that Fukui functions can be related to the linear response function $\chi_1(\mathbf{r},\mathbf{r}')$ through the following equation:

$$\int \chi_1(\mathbf{r},\mathbf{r}')\eta(\mathbf{r}',\mathbf{r}'')\,\mathrm{d}\mathbf{r}' = f(\mathbf{r}) - \delta(\mathbf{r} - \mathbf{r}'') \tag{130}$$

Approximate expressions for the calculation of the linear response function have been derived by Fuentealba,[278] yielding, however, constant local hardness $\eta(\mathbf{r})$ (see section III.B.4)

Higher order response functions have been proposed in the literature by Senet[234,235] and by Fuentealba and Parr[271,273,279] with complete computational schemes up to nth order. Numerical results, already present for the first-order derivative of η with respect to N (third-order energy derivative),[271] are still scarce. It will be interesting to see whether, in the near future, practical calculation schemes will be developed and what the order of magnitude of these quantities will be determining their role in chemical reactivity. The demand for visualization of these quantities will also present a challenge. Recent results by Toro-Labbé and co-workers for the hardness derivatives of HCXYH (X, Y = O, S) and their hydrogen-bonded dimers indicated low γ values.[280] On the other hand, in a functional expansion[281] study of the total energy, Parr and Liu[282] gave arguments for a second-order truncation, stating that it is quite natural to assume that third-order quantities of the type $\delta^3 F/\delta\rho(\mathbf{r})\delta\rho(\mathbf{r}')\delta\rho(\mathbf{r}'')$ would be small and that the quantities entering second-order formulas for chemical charges are “tried and true” ingredients of simple theories.

4. Local Hardness and Hardness Kernel

The search for a local counterpart of η, the local hardness[283] for which in this review the symbol $\eta(\mathbf{r})$ will be used throughout, turns out to be much more complicated than the search for the global−local softness relationship discussed in section III.B.3, which resulted in an expression (eq 113) indicating that the Fukui function distributes the global softness among the various parts of the system.

The search for a local counterpart of the hardness begins by considering

$$\eta(\mathbf{r}) = \left(\frac{\delta\mu}{\delta\rho(\mathbf{r})}\right)_\nu \tag{131}$$

Note that this quantity also appears in a natural way when the chain rule is applied to the global hardness:

$$\eta = \frac{1}{2}\left(\frac{\partial^2 E}{\partial N^2}\right)_\nu = \frac{1}{2}\left(\frac{\partial\mu}{\partial \mathrm{N}}\right)_\nu = \frac{1}{2}\int\left(\frac{\delta\mu}{\delta\rho(\mathbf{r})}\right)_\nu\left(\frac{\delta\rho(\mathbf{r})}{\delta N}\right)_\nu \mathrm{d}\mathbf{r}$$
$$= \frac{1}{2}\int \eta(\mathbf{r})\, f(\mathbf{r})\,\mathrm{d}\mathbf{r} \tag{132}$$

An explicit expression for $\eta(\mathbf{r})$ can be obtained by starting from the Euler equation (6) and multiplying it by a composite function $\lambda(\rho(\mathbf{r}))$,[284] integrating to N:

$$\int \lambda(\rho(\mathbf{r}))\,\mathrm{d}\mathbf{r} = N \tag{133}$$

yielding

$$N\mu = \int \nu(\mathbf{r})\lambda(\rho(\mathbf{r}))\,\mathrm{d}\mathbf{r} + \int \frac{\delta F_{\mathrm{HK}}}{\delta\rho(\mathbf{r})}\lambda(\rho(\mathbf{r}))\,\mathrm{d}\mathbf{r} \tag{134}$$

Taking the functional derivative with respect to $\rho(\mathbf{r})$ at fixed ν yields, after some algebra,

$$\left(\frac{\delta\mu}{\delta\rho}\right)_\nu = \frac{1}{N}\left(\left(\frac{\partial\lambda(\rho(\mathbf{r}))}{\partial\rho(\mathbf{r})}\right) - 1\right)\mu + \frac{1}{N}\int \frac{\delta^2 F_{\mathrm{HK}}}{\delta\rho(\mathbf{r})\delta\rho(\mathbf{r}')}\lambda(\rho(\mathbf{r}'))\,\mathrm{d}\mathbf{r}' \tag{135}$$

If one forces the local hardness into an expression of type

$$\left(\frac{\delta\mu}{\delta\rho}\right)_\nu = \frac{1}{N}\int \frac{\delta^2 F_{\mathrm{HK}}}{\delta\rho(\mathbf{r})\delta\rho(\mathbf{r}')}\lambda(\rho(\mathbf{r}'))\,\mathrm{d}\mathbf{r}' \tag{136}$$

which is desirable if a simple relationship with the second functional derivative of the Hohenberg−Kohn functional is the goal, then an additional constraint for the composite function $\lambda(\rho(\mathbf{r}))$ appears:[285]

$$\left(\frac{\partial\lambda(\rho(\mathbf{r}))}{\partial\rho}\right)_\nu = 1 \tag{137}$$

As the hardness kernel is defined as shown in eq 128,[189,283] the expression for local hardness then becomes

$$\eta_\lambda(\mathbf{r}) = \frac{1}{N}\int \eta(\mathbf{r},\mathbf{r}')\lambda(\rho(\mathbf{r}'))\,\mathrm{d}\mathbf{r}' \tag{138}$$

The ambiguity in the definition of the local hardness was discussed by Ghosh,[286] Harbola, Chattaraj, and Parr,[284,287] Geerlings et al.,[285] and Gazquez.[173] Restricting λ to functions of the first degree in ρ, the following possibilities emerge:

$$\lambda(\rho(\boldsymbol{r})) = \rho(\boldsymbol{r}) \qquad \text{yielding}$$
$$\eta_D(\boldsymbol{r}) = \frac{1}{N}\int \eta(\boldsymbol{r},\boldsymbol{r}')\rho(\boldsymbol{r}')\, d\boldsymbol{r}' \quad (139)$$

$$\lambda(\rho(\boldsymbol{r})) = Nf(\boldsymbol{r}) \qquad \text{yielding}$$
$$\eta_D(\boldsymbol{r}) = \int \eta(\boldsymbol{r},\boldsymbol{r}')f(\boldsymbol{r}')\, d\boldsymbol{r}' \quad (140)$$

The latter case yields, however,[284,285]

$$\eta_F(\boldsymbol{r}) = \eta \quad (141)$$

i.e., a local hardness equal to the global hardness at every point in space. At first sight, this form is less appropriate as (quoting Pearson[121]), "unlike the chemical potential there is nothing in the concept of hardness which prevents it from having different values in the different parts of the molecule". The choice leading to $\eta(\boldsymbol{r}) = \eta$ leads to the question of whether we could not do without the local hardness in DFT or if another quantity should be considered to play this role. On the other hand, the result leads to an increased emphasis on local softness and attributes a smaller role to local hardness.

Parr and Yang[23] stated that the $(\delta^2 F/\delta\rho(\boldsymbol{r})\delta\rho(\boldsymbol{r}'))$ functional derivative, the hardness kernel $\eta(\boldsymbol{r},\boldsymbol{r}')$, is of utmost importance, as can be expected from the second functional derivative of the universal Hohenberg−Kohn functional with respect to $\rho(\boldsymbol{r})$, the basic DFT quantity. It appears in a natural way when the chain rule is applied to the global hardness:

$$\eta = \frac{1}{2}\left(\frac{\partial^2 E}{\partial N^2}\right)_\nu = \frac{1}{2}\int\int \frac{\delta^2 F_{HK}}{\delta\rho(\boldsymbol{r})\delta\rho(\boldsymbol{r}')} f(\boldsymbol{r})f(\boldsymbol{r}')\, d\boldsymbol{r}\, d\boldsymbol{r}' \quad (142)$$

It was shown[288] that, starting from the Thomas−Fermi−Dirac approach and taking into account the exponential fall-off of the density in the outer regions (see also ref 285), $\eta_D(\boldsymbol{r})$ can be approximated as

$$\eta_D(\boldsymbol{r}) \approx -\frac{1}{2N} V_{el}(\boldsymbol{r}) \quad (143)$$

$V_{el}(\boldsymbol{r})$ being the electronic part of the molecular electrostatic potential[289] [for applications of these working equations, see section IV.C.3].

It should be clear that, as opposed to the local softness $s(\boldsymbol{r})$, $\eta(\boldsymbol{r})$ as seen in eq 132 does not integrate to its global counterpart. Only upon multiplication by the electronic Fukui function is η recovered upon integration. This prompted an introduction of a hardness density,[285]

$$h(\boldsymbol{r}) = \eta_\lambda(\boldsymbol{r})f(\boldsymbol{r}) \quad (144)$$

yielding, in the TFD approximation mentioned above, the following working equations

$$h_D(\boldsymbol{r}) \approx -\frac{1}{4N} V_{el}(\boldsymbol{r})f(\boldsymbol{r}) \quad (145)$$

$$h_F(\boldsymbol{r}) \approx \frac{1}{4N}\left(\frac{\partial V_{el}(\boldsymbol{r})}{\partial N}\right)_{\nu(\boldsymbol{r})} \rho(\boldsymbol{r}) \quad (146)$$

Local hardness in the form $\eta_D(\boldsymbol{r})$ appears in a natural way in the hardness functional,

$$H[\rho] = \int \rho(\boldsymbol{r})\frac{\delta F[\rho]}{\delta\rho(\boldsymbol{r})}\, d\boldsymbol{r} - F[\rho] \quad (147)$$

introduced by Parr and Gazquez,[290] for which at all orders

$$\frac{\delta H[\rho]}{\delta\rho} = N\eta_D(\boldsymbol{r}) \quad (148)$$

Let us finally come back to the hardness kernel $\eta(\boldsymbol{r},\boldsymbol{r}')$. It can be seen that the softness kernel $s(\boldsymbol{r},\boldsymbol{r}')$ and $\eta(\boldsymbol{r},\boldsymbol{r}')$ are reciprocals in the sense that

$$\int s(\boldsymbol{r},\boldsymbol{r}')\eta(\boldsymbol{r}',\boldsymbol{r}'')\, d\boldsymbol{r}' = \delta(\boldsymbol{r} - \boldsymbol{r}'') \quad (149)$$

Using eqs 124 and 125 and the local hardness expression η_D, one finds

$$\begin{aligned}\int s(\boldsymbol{r})\eta_D(\boldsymbol{r})\, d\boldsymbol{r} &= \int s(\boldsymbol{r},\boldsymbol{r}')\, d\boldsymbol{r}' \frac{1}{N}\int \eta(\boldsymbol{r},\boldsymbol{r}'')\rho(\boldsymbol{r}'')\, d\boldsymbol{r}''\, d\boldsymbol{r} \\ &= \int \rho(\boldsymbol{r}'')\, d\boldsymbol{r}''\, d\boldsymbol{r}' \frac{1}{N}\int s(\boldsymbol{r},\boldsymbol{r}')\eta(\boldsymbol{r},\boldsymbol{r}'')\, d\boldsymbol{r} \\ &= \frac{1}{N}\int \rho(\boldsymbol{r}'')\, d\boldsymbol{r}''\, d\boldsymbol{r}'\delta(\boldsymbol{r} - \boldsymbol{r}'') \\ &= \frac{1}{N}\int \rho(\boldsymbol{r})\, d\boldsymbol{r} = 1 \end{aligned} \quad (150)$$

indicating that $s(\boldsymbol{r})$ and $\eta_D(\boldsymbol{r})$ are reciprocals, in the sense that

$$\int s(\boldsymbol{r})\eta_D(\boldsymbol{r})\, d\boldsymbol{r} = 1 \quad (151)$$

The explicit form of the hardness kernel, in view of its importance, has gained widespread interest in the literature: Liu, De Proft, and Parr for example,[174] proposed for the expression

$$\eta(\boldsymbol{r},\boldsymbol{r}') = \frac{1}{|\boldsymbol{r} - \boldsymbol{r}'|} + R(\boldsymbol{r},\boldsymbol{r}') \quad (152)$$

various approximation for $R(\boldsymbol{r},\boldsymbol{r}')$, the $1/|\boldsymbol{r} - \boldsymbol{r}'|$ arising from the classical Coulombic part in the Hohenberg−Kohn universal density functional. Various approaches to $R(\boldsymbol{r},\boldsymbol{r}')$ were presented to take into account the kinetic energy, exchange, and correlation parts.

An extensive search for the modelization of the hardness kernel at the AIM level (cf. section III.B.3) has been carried out by Nalewajski, Mortier, and others.[184,226,230,231,291−295]

5. The Molecular Shape Function—Similarity

The molecular shape function, or shape factor $\sigma(\boldsymbol{r})$, introduced by Parr and Bartolotti,[296] is defined as

$$\sigma(\boldsymbol{r}) = \frac{\rho(\boldsymbol{r})}{N} \quad (153)$$

It characterizes the shape of the electron distribution and carries relative information about this electron distribution. Just as the electronic Fukui function redistributes the (total) softness over the various parts of the molecule (eq 112), $\sigma(\mathbf{r})$ redistributes the total number of electrons.

$$\rho(\mathbf{r}) = N\sigma(\mathbf{r}) \tag{154}$$

Just as $f(\mathbf{r})$, $\sigma(\mathbf{r})$ is normalized to 1:

$$\int \sigma(\mathbf{r})\, \mathrm{d}\mathbf{r} = 1 \tag{155}$$

N and $\sigma(\mathbf{r})$ are independent variables, forming the basis of the so-called isomorphic ensemble.[297] (Recently, however Ayers argued that, for a finite Coulombic system, $\sigma(\mathbf{r})$ determines both $v(\mathbf{r})$ (as $\rho(\mathbf{r})$ does) and N.[298])

Baekelandt, Cedillo, and Parr[299,300] showed that the hardness in the canonical ensemble, η_v (the η expression, eq 57, used in this review hitherto), and its counterpart in the isomorphic ensemble, η_σ, are related via the following equation:

$$\eta_v = \eta_\sigma + \int \left(\frac{\delta\mu}{\delta\sigma(\mathbf{r})}\right)_N \left(\frac{\partial\sigma(\mathbf{r})}{\partial N}\right)_v \mathrm{d}\mathbf{r} \tag{156}$$

where it is easily seen that

$$\left(\frac{\partial\sigma(\mathbf{r})}{\partial N}\right)_N = \frac{1}{N}(f(\mathbf{r}) - \sigma(\mathbf{r})) \tag{157}$$

a fluctuation term involving the deviation of the Fukui function from the average electron density per electron.

The $(\delta\mu/\delta\sigma(\mathbf{r}))_N$ index was identified as a nuclear/geometrical reactivity index related to local hardness (cf. section III.B.4):

$$\eta_v = \int h(\mathbf{r}) f(\mathbf{r})\, \mathrm{d}\mathbf{r} \qquad \eta_\sigma = \int h(\mathbf{r})\sigma(\mathbf{r})\, \mathrm{d}\mathbf{r} \tag{158}$$

with

$$h(\mathbf{r}) = \frac{1}{N}\left(\frac{\delta\mu}{\delta\sigma(\mathbf{r})}\right)_N \tag{159}$$

De Proft, Liu, and Parr provided an alternative definition for the local hardness in this ensemble.[301]

De Proft and Geerlings[302] concentrated on the electronegativity analogue of eq 156,

$$\chi_v = \chi_\sigma + \int \left(\frac{\delta E}{\delta\sigma(\mathbf{r})}\right)_N \left(\frac{d\sigma(\mathbf{r})}{dN}\right)_v \mathrm{d}\mathbf{r} \tag{160}$$

pointing out that the electronegativity conventionally used, χ_v, can be seen as a term representing the energy versus N variation at fixed shape and a contribution due to the variation of the energy with the shape factor at a fixed number of electrons modulated by a fluctuation term. The quantity $(\delta E/\delta\sigma(\mathbf{r}))_N$ can be put on equal footing with the first-order response functions in Scheme 4 $(\delta E/\delta v(\mathbf{r}))_N$ $(= \rho(\mathbf{r}))$ and $(\partial E/\partial N)_v$ $(= -\chi)$.

A possible way to model changes in the shape factor is to substitute a particular orbital, Ψ_i, in the density expression by a different one, Ψ_j. Working within a Hartree–Fock scheme and using a Koopmans type of approximation, one gets

$$\left(\frac{\Delta E}{\Delta\sigma(\mathbf{r})}\right)_N \approx \frac{\epsilon_j - \epsilon_i}{|\Psi_j(\mathbf{r})|^2 - |\Psi_i(\mathbf{r})|^2} N \tag{161}$$

$$\rho = \sum_i n_i |\varphi_i|^2 \tag{162}$$

Identifying Ψ_i and Ψ_j with Ψ_{HOMO} and Ψ_{LUMO}, and using the approximation of eq 68 for the hardness, we obtain

$$\left(\frac{\Delta E}{\Delta\sigma(\mathbf{r})}\right)_N \approx N \frac{\eta}{|\Psi_{\mathrm{LUMO}}(\mathbf{r})|^2 - |\Psi_{\mathrm{HOMO}}(\mathbf{r})|^2} \tag{163}$$

indicating that polarizable systems (η large, α small; cf. section IV.A) show a higher tendency to change their shape factor. A similar conclusion was reached by Fuentealba.[303]

We finally mention that Chan and Handy[304] introduced the shape factor for subsystems, with density $\rho_i(\mathbf{r})$ satisfying the relation

$$\rho(\mathbf{r}) = \sum_i^m \rho_i(\mathbf{r}) \tag{164}$$

with

$$\rho_i(\mathbf{r}) = n_i \sigma_i(\mathbf{r}) \tag{165}$$

n_i being the subsystem's occupation numbers, the total number of subsystems being m. The concept of electronic chemical potential was extended to the shape chemical potential of the subsystem i,

$$\mu_i = \left(\frac{\partial E}{\partial n_i}\right)_{n_j, \sigma_i} \tag{166}$$

the indices indicating that the occupation numbers of all subsystems different from i and the shape functions of all subsystems are held fixed. It was proven that, as opposed to μ (eq 37), the μ_i values in eq 166 do not equalize between subsystems, the advantage being that this property characterizes the electron-attracting/-donating power of any given density fragment rather than that of the system as a whole.

The importance of the shape factor is also stressed in a recent contribution by Gal,[305] considering differentiation of density functionals $A[\rho]$ conserving the normalization of the density. In this work, functional derivatives of $A[\rho]$ with respect to ρ are written as a sum of functional derivatives with respect to ρ at fixed shape factor σ, "$\delta_\sigma\rho$", and fixed N, "$\delta_N\rho$", respectively:

$$\frac{\delta A[\rho]}{\delta\rho(\mathbf{r})} = \frac{\delta A[\rho]}{\delta_\sigma\rho(\mathbf{r})} + \frac{\delta A[\rho]}{\delta_N\rho(\mathbf{r})} \tag{167}$$

The shape factor $\sigma(\mathbf{r})$ plays a decisive role when comparing charge distributions and reactivity between molecules. In this context, the concept of "similarity" of charge distributions has received considerable attention in the past two decades, under the impetus of R. Carbo and co-workers (for reviews see, for example, refs 306–309).

Several similarity indices have been proposed for the quantum molecular similarity (QMS) between two molecules, A and B, of which the simplest form is written as[310]

$$Z^{\rho}_{AB} = \frac{\int \rho_A(\boldsymbol{r})\rho_B(\boldsymbol{r})\,d\boldsymbol{r}}{[\int \rho^2_A(\boldsymbol{r})\,d\boldsymbol{r} \int \rho^2_B(\boldsymbol{r})\,d\boldsymbol{r}]^{1/2}} \tag{168}$$

Introducing the shape factor $\sigma(\boldsymbol{r})$ via eq 154, this expression simplifies to

$$Z^{\rho}_{AB} = \frac{\int \sigma_A(\boldsymbol{r})\sigma_B(\boldsymbol{r})\,d\boldsymbol{r}}{[\int \sigma^2_A(\boldsymbol{r})\,d\boldsymbol{r} \int \sigma^2_B(\boldsymbol{r})\,d\boldsymbol{r}]^{1/2}} \tag{169}$$

indicating that the similarity index depends only on the shape of the density distribution and not on its extent. The latter feature emerges in the so-called Hodgkin–Richards[311] index,

$$H^{\rho}_{AB} = \frac{2\int \rho_A(\boldsymbol{r})\rho_B(\boldsymbol{r})\,d\boldsymbol{r}}{\int \rho^2_A(\boldsymbol{r})\,d\boldsymbol{r} + \int \rho^2_B(\boldsymbol{r})\,d\boldsymbol{r}} \tag{170}$$

which, upon introduction of the shape factor, reduces to

$$H^{\rho}_{AB} = \frac{2N_AN_B\int \sigma_A(\boldsymbol{r})\sigma_B(\boldsymbol{r})\,d\boldsymbol{r}}{N^2_A\int \sigma^2_A(\boldsymbol{r})\,d\boldsymbol{r} + N^2_B\int \sigma^2_B(\boldsymbol{r})\,d\boldsymbol{r}} \tag{171}$$

which cannot be simplified for the number of electrons of the molecules A and B (N_A, N_B). Both the shape and the extent (via N) of the charge distribution are accounted for in the final expression.

To yield a more reactivity-related similarity index, Boon et al.[312] proposed to replace the electron density in eq 168 by the local softness, $s(\boldsymbol{r})$, yielding a Carbo-type index:

$$Z^{s}_{AB} = \frac{\int s_A(\boldsymbol{r})s_B(\boldsymbol{r})\,d\boldsymbol{r}}{[\int s^2_A(\boldsymbol{r})\,d\boldsymbol{r} \int s^2_B(\boldsymbol{r})\,d\boldsymbol{r}]^{1/2}} \tag{172}$$

Exploiting the analogy between $\sigma(\boldsymbol{r})$ and $f(\boldsymbol{r})$ (redistribution of the total number of electrons or the total softness among various parts of space), eq 172 yields

$$Z^{s}_{AB} = \frac{\int f_A(\boldsymbol{r})f_B(\boldsymbol{r})\,d\boldsymbol{r}}{[\int f^2_A(\boldsymbol{r})\,d\boldsymbol{r} \int f^2_B(\boldsymbol{r})\,d\boldsymbol{r}]^{1/2}} \tag{173}$$

This expression, in analogy with eq 169, depends only on the Fukui function of the molecules A and B, but not on their total softnesses, S_A and S_B. The Hodgkin–Richards analogue of Z^S_{AB} still combines this information:

$$H^{S}_{AB} = \frac{2S_AS_B\int f_A(\boldsymbol{r})f_B(\boldsymbol{r})\,d\boldsymbol{r}}{S^2_A\int f^2_A(\boldsymbol{r})\,d\boldsymbol{r} + S^2_B\int f^2_B(\boldsymbol{r})\,d\boldsymbol{r}} \tag{174}$$

The quality of these various quantum similarity descriptors has been studied systematically for a series of peptide isosteres.[312,313] Isosteric replacement of a peptide bond, –CO–NH–, has indeed been an attractive strategy for circumventing the well-known susceptibility of peptide bonds to hydrolysis.[314,315] In the model system CH_3–CO–NH–CH_3, the –CO–NH– moiety has been replaced by –CH=H–, –CF=CH– (*Z* and *E* isomers), –CH_2–CH_2–, –CH_2–S–, –CO–CH_2–, –CH_2–NH–, –CCl=CH–, etc., and the merits of the various analogues have been investigated.

In the first series of results obtained via numerical integration of $\int\rho_A(\boldsymbol{r})\rho_B(\boldsymbol{r})\,d\boldsymbol{r}$ and $\int s_A(\boldsymbol{r})s_B(\boldsymbol{r})\,d\boldsymbol{r}$, the problem of the dependence of these integrals on the relative orientation and position (besides conformational aspects) was avoided by aligning the central bonds of the isosteres and bringing the centers of the central bond to coincidence. For the softness similarity, the (*Z*)-fluorinated alkene structure shows the higher resemblance with the amide bond, due to the similarity in polarity with the carbonyl group, in agreement with the experimental results[316,317] on the potential use of C=C–F as a peptidomimetic.

In a later study,[313] the problems of relative orientation and position were circumvented by introducing the autocorrelation function,[318,319] first introduced in molecular modeling and quantitative structure–activity relationship studies by Moreau and Broto,[320,321] and a principal component analysis,[322,323] moreover bringing butanone to the forefront, rather than the (*Z*)-fluoroalkene structure.

6. The Nuclear Fukui Function and Its Derivatives

As seen in section III.B.3, the electronic Fukui function comprises the response of a system's electron density function $\rho(\boldsymbol{r})$ to a perturbation of its total number of electrons N at a fixed external potential. As such, it is part of the tree of response functions in the canonical ensemble with the energy functional $E = E[N,\nu(\boldsymbol{r})]$.

The question of what would be the response of the nuclei (i.e., their position) to a perturbation in the total number of electrons is both intriguing and highly important from a chemical point of view: chemical reactions indeed involve changes in nuclear configurations, and the relationship between changes in electron density and changes in nuclear configuration was looked at extensively by Nakatsuji in the mid-1970s,[324–326] referring to the early work by Berlin.[327]

A treatment in complete analogy with the previous paragraphs, however, leads to serious difficulties, as a response kernel is needed to convert electron density changes in external potential changes.[299,328] Cohen et al.[329,330] circumvented this problem by introducing the nuclear Fukui function $\boldsymbol{\Phi}_\alpha$,

$$\boldsymbol{\Phi}_\alpha = \left(\frac{\partial \mathbf{F}_\alpha}{\partial N}\right)_\nu \tag{175}$$

where $\mathbf{F}_\alpha$ is the force acting on the nucleus α, $\mathbf{\Phi}_\alpha$ measuring its change when the number of electrons is varied. This function does not measure the actual response of the external potential to changes in N, but rather the magnitude of the onset of the perturbation (force inducing the displacement), and as such is rewarding and reflects the electron-cloud preceding idea present in "chemical thinking" on reactions.[331]

Using a Maxwell-type relation, as in Schemes 4 and 5, Baekelandt[332] showed that $\mathbf{\Phi}_\alpha$ also represents the change of the electronic chemical potential upon nuclear displacement $\mathbf{R}_\alpha$:

$$\mathbf{\Phi}_\alpha = \left(\frac{\partial \mathbf{F}_\alpha}{\partial N}\right)_\nu = \left(\frac{\partial^2 E}{\partial \mathbf{R}_\alpha \partial N}\right)_\nu = \frac{\partial}{\partial \mathbf{R}_\alpha}\left(\frac{\partial E}{\partial N}\right)_\nu = \left(\frac{\partial \mu}{\partial \mathbf{R}_\alpha}\right)_N \tag{176}$$

In this way, a scheme in analogy with Scheme 4 can be constructed starting from an $E = E[N,\mathbf{R}_\alpha]$ relationship, the corresponding first-order response functions being

$$\left(\frac{\partial E}{\partial \mathbf{R}_\alpha}\right)_N = -\mathbf{F}_\alpha \tag{177}$$

and

$$\left(\frac{\partial E}{\partial N}\right)_{\mathbf{R}_\alpha} = \mu \tag{178}$$

the charge of the nuclei being fixed.

Only a relatively small number of studies have been devoted to the NFF until now; the first numerical results were reported only in 1998,[110] obtained using a finite difference approach (vide infra) for a series of diatomic molecules. In recent work by Balawender and Geerlings, an analytical approach was developed[333] in analogy with Komorowski and Balawender's coupled Hartree–Fock approach to the electronic Fukui function,[150] previously applied in the study of aromaticity (vide infra).[334]

The results were compared with those of the finite field approach for both $(\partial \mathbf{F}_\alpha/\partial N)_\nu$ and $(\partial \mu/\partial \mathbf{R}_\alpha)_\nu$. A reasoning along the lines described in section III.B.2 for the analytical evaluation of η yields, after some tedious matrix algebra, the expression

$$\mathbf{\Phi}_\alpha = -\mathrm{tr}\ \mathbf{F}^\alpha(\mathbf{f} + \mathbf{U}^N\mathbf{n} - \mathbf{n}\mathbf{U}^N) + \mathrm{tr}\ \mathbf{S}^\alpha(\mathbf{G}^N\mathbf{n} + \mathbf{F}(\mathbf{f} + \mathbf{U}^N\mathbf{n} - \mathbf{n}\mathbf{U}^N)) \tag{179}$$

where the matrix $\mathbf{f}$ represents the derivative of the MO occupation numbers when the total number of electrons is unchanged. $\mathbf{U}^N$ is defined as in eq 72. $\mathbf{F}^\alpha$ and $\mathbf{S}^\alpha$ are core and skeleton derivatives.[133] In the case of $\mathbf{S}^\alpha$, e.g., this becomes

$$\mathbf{S}^\alpha = \mathbf{C}^+\left(\frac{\partial \mathbf{S}^{\mathrm{AO}}}{\partial \mathbf{R}_\alpha}\right)\mathbf{C} \tag{180}$$

where $\mathbf{C}$ is defined as in eq 72, and $\mathbf{S}^{\mathrm{AO}}$ denotes the matrix of the overlap integrals in the atomic basis. The $\mathbf{G}^N$ matrix arises from the differentiation of the two-electron part of the energy.

Table 2. Analytical Values of the Left Nuclear Fukui Function (NFF "l"), Gradient of the Cation, and the HOMO Energy for a Series of Diatomic Molecules[a]

molecule	NFF "l"	HOMO	gradient cation
AlCl	0.03625	0.04251	0.04277
AlF	0.04315	0.04469	0.04487
AlH	0.01437	0.01559	0.01129
BCl	0.05628	0.06623	0.07571
BeO	−0.09816	−0.08233	−0.11307
BF	0.04559	0.07005	0.07182
BH	0.01171	0.01550	0.01689
Cl_2	0.05106	0.05548	0.05865
ClF	0.05145	0.07275	0.05410
CO	0.04578	0.06747	0.04114
CS	−0.12344		−0.10465
F_2	0.09626	0.11894	0.12771
H_2	−0.16247	−0.16336	−0.14694
HCl	−0.01470	−0.01194	−0.02144
HF	−0.05530	−0.05540	−0.08623
Li_2	−0.00816	−0.00998	−0.00831
LiCl	−0.03680	−0.03219	−0.03683
LiF	−0.05649	−0.05545	−0.06650
LiH	−0.02747	−0.02904	−0.02947
N_2	−0.04472	−0.05363	−0.04167
PN	−0.13527	−0.11459	−0.06227
SiO	0.00110	0.01599	−0.06770
SiS	−0.07833		−0.08475

[a] Data from ref 60. All values are in au. Blank entries correspond to cases where the highest occupied molecular orbitals change their ordering upon increasing bond length.

The solution of the $\mathbf{U}^N$ matrix elements is obtained via the coupled perturbed Hartree–Fock equations for a single-configuration, closed-shell system.[133]

It turns out that the correlation coefficient between analytical and finite difference NFF is remarkably high, both for the finite difference approach to

$$\left(\frac{\partial \mathbf{F}_\alpha}{\partial N}\right)_\nu: \quad \mathbf{\Phi}_\alpha^+ = \mathbf{F}_\alpha(N+1) - \mathbf{F}_\alpha(N) = -\nabla_\alpha E(N+1) \tag{181}$$

and for

$$\left(\frac{\partial \mu}{\partial \mathbf{R}_\alpha}\right)_N: \quad \mathbf{\Phi}_\alpha^+ = \nabla_\alpha \mu = -\nabla_\alpha e_{\mathrm{LUMO}} \tag{182}$$

In the former expression, μ has been approximated by the FMO energy. The corresponding equations for the left-side derivative are

$$\mathbf{\Phi}_\alpha^- = -\nabla_\alpha E(N-1) \quad \text{and} \quad \mathbf{\Phi}_\alpha^- = -\nabla_\alpha e_{\mathrm{HOMO}} \tag{183}$$

As an example, we give in Table 2 the values of the analytical NFF, $\nabla_\alpha E(N-1)$, and $\nabla_\alpha e_{\mathrm{HOMO}}$ and show in Figure 7a the correlation between the two numerical approaches and in Figure 7b the correlation between the analytical approach and $\nabla_\alpha e_{\mathrm{HOMO}}$. Molecules in the upper right quadrant show, in both approaches, bond contraction upon ionization, whereas those in the lower left quadrant show bond elongation.

The analytical results can be interpreted in terms of the Hellman–Feynman theorem[335,336] for the force $\mathbf{F}_\alpha$ acting on nucleus α:

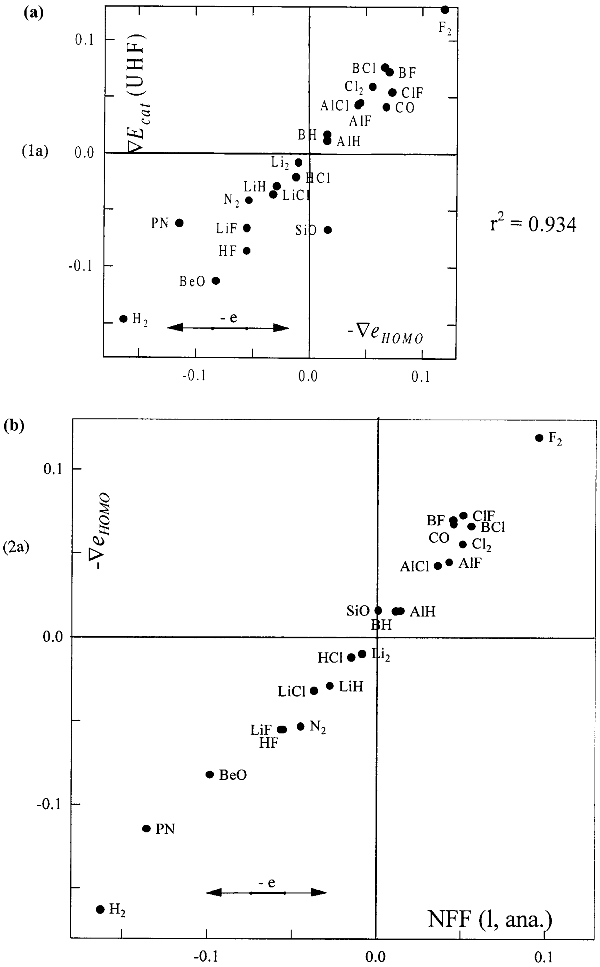

Figure 7. (a) Correlation between $\nabla E(N-1)$ and ∇e_{HOMO} for a series of selected diatomic molecules. All values are in au. (b) Correlation between the analytical left nuclear Fukui function and $-\nabla e_{\mathrm{HOMO}}$. All values are in au. Negative values of the quantities considered are associated with bond elongation upon ionization, as shown in the lower left quadrant.

$$\mathbf{F}_\alpha = -\int \frac{\rho(\boldsymbol{r})}{\boldsymbol{r}_\alpha^3}\boldsymbol{r}_\alpha \, d\boldsymbol{r} + \sum_{\beta\neq\alpha} \frac{Z_\beta Z_\alpha \mathbf{R}_{\alpha\beta}}{\mathbf{R}_{\alpha\beta}{}^3} \tag{184}$$

with $\boldsymbol{r}_\alpha = \boldsymbol{r} - \mathbf{R}_\alpha$ and $\mathbf{R}_{\alpha\beta} = \mathbf{R}_\beta - \mathbf{R}_\alpha$, indicating that $\rho(\boldsymbol{r})$ completely determines the electronic contribution of this force and that here the functional relationship between $\mathbf{F}_\alpha$ and ρ is known.

Introducing Wang and Peng's binding function F_{B},[337] which is in fact the virial of the forces acting on the nuclei to keep them fixed in the molecule,

$$F_{\mathrm{B}} = -\sum_\alpha \mathbf{R}_\alpha \cdot \mathbf{F}_\alpha \tag{185}$$

one obtains, by combining eqs 184 and 185,

$$F_{\mathrm{B}} = \int f(\boldsymbol{r}) \left(\sum_\alpha - \frac{\mathbf{R}_\alpha \boldsymbol{r}_\alpha}{\boldsymbol{r}_\alpha^3} Z_\alpha \right) d\boldsymbol{r} - \sum_{\beta\neq\alpha}\sum_\alpha \frac{Z_\alpha Z_\beta}{R_{\alpha\beta}}$$
$$= \int \rho(\boldsymbol{r})\, f(\boldsymbol{r})\, d\boldsymbol{r} - \sum_{\alpha\neq\beta}\sum \frac{Z_\alpha Z_\beta}{R_{\alpha\beta}} \tag{186}$$

where $f_\nu(\boldsymbol{r})$ is Berlin's function.[327] Clearly, a pile-up of electron density in regions where $f_\nu(\boldsymbol{r}) > 0$ increases F_{B}; i.e., it tends to "shrink" the molecule (forces acting into the molecule). Deriving the binding function at fixed external potential yields an expression in which electronic the Fukui function appears:

$$\left(\frac{\partial F_\beta}{\partial N}\right)_\nu = \int f(\boldsymbol{r})\, f_\nu(\boldsymbol{r})\, d\boldsymbol{r} \tag{187}$$

The change in binding function upon variation of N at fixed ν can be written in terms of the electronic Fukui function (local resolution) or the nuclear Fukui function (atomic resolution):

$$dF_{\mathrm{B}} = \int f(\boldsymbol{r})\, f_\nu(\boldsymbol{r})\, d\boldsymbol{r}\, dN = -\sum_\alpha \mathbf{R}_\alpha \cdot \mathbf{\Phi}_\alpha\, dN \tag{188}$$

It then follows that, to have $dF_{\mathrm{B}} > 0$ upon changing N, either the nuclear Fukui function (vector) multiplied by dN should represent a force acting into the molecule or the electronic Fukui function should be positive in the binding region for $dN > 0$ or in the antibinding region for $dN < 0$. The discussion illustrates how, in local resolution, the electronic Fukui function, combined with Berlin's function, governs the onset of this nuclear displacement, translated, when passing to atomic resolution, in the scalar product of the nuclear Fukui function and the nuclear position vector.

An application of this methodology was recently presented in a study on the direction of the Jahn–Teller distortions in $C_6H_6^-$, BH_3^+, CH_4^+, SiH_4^+, and $C_3H_6^+$.[338]

In analogy with the basic local electronic reactivity descriptors, the Fukui function $f(\boldsymbol{r})$ and the local softness $s(\boldsymbol{r})$, written as N and μ derivatives of $\rho(\boldsymbol{r})$, Cohen et al.[329,330] completed the nuclear reactivity picture by introducing, as a counterpart to $\mathbf{\Phi}_\alpha$, $(\partial \mathbf{F}_\alpha/\partial N)_\nu$, the nuclear softness $\boldsymbol{\sigma}_\alpha$, a vectorial quantity defined as

$$\boldsymbol{\sigma}_\alpha = \left(\frac{\partial \mathbf{F}_\alpha}{\partial \mu}\right)_\nu \tag{189}$$

This quantity can easily be converted to the product of the total softness and the nuclear Fukui function:

$$\boldsymbol{\sigma}_\alpha = \left(\frac{\partial \mathbf{F}_\alpha}{\partial \mu}\right)_\nu = \left(\frac{\partial \mathbf{F}_\alpha}{\partial N}\right)_\nu \left(\frac{\partial N}{\partial \mu}\right)_\nu = \mathbf{\Phi}_\alpha S \tag{190}$$

As the nuclear Fukui function is equal to the Hellman–Feynman force due to the electronic Fukui function,

$$\mathbf{F}_\alpha = -Z_\alpha \int \frac{f(\boldsymbol{r})(\boldsymbol{r} - \mathbf{R}_\alpha)}{|\boldsymbol{r} - \mathbf{R}_\alpha|^3}\, d\boldsymbol{r} \tag{191}$$

the relationship between total and local softness (eq 112) immediately shows that nuclear softness is the electrostatic force due to the electronic local softness $s(\boldsymbol{r})$:

$$\boldsymbol{\sigma}_\alpha = -Z_\alpha \int \frac{s(\boldsymbol{r})(\boldsymbol{r} - \mathbf{R}_\alpha)}{|\boldsymbol{r} - \mathbf{R}_\alpha|^3}\, \mathrm{d}\boldsymbol{r} \tag{192}$$

Only a single numerical study on $\boldsymbol{\sigma}_\alpha$ was performed hitherto,[110] its evaluation being straightforward via eq 190 and the computational techniques mentioned in section III.B.2 and the present pargraph. No in-depth discussion on trends of this quantity in diatomic and polyatomic molecules is available yet.

The kernel corresponding to $\boldsymbol{\sigma}_\alpha$, denoted here as $\boldsymbol{\sigma}_\alpha(\boldsymbol{r})$, was introduced as

$$\boldsymbol{\sigma}_\alpha(\boldsymbol{r}) = -Z_\alpha \int \frac{s(\boldsymbol{r},\boldsymbol{r}')(\boldsymbol{r}' - \mathbf{R}_\alpha)}{|\boldsymbol{r}' - \mathbf{R}_\alpha|^3}\, \mathrm{d}\boldsymbol{r}' \tag{193}$$

obeying

$$\boldsymbol{\sigma}_\alpha = \int \boldsymbol{\sigma}_\alpha(\boldsymbol{r})\, \mathrm{d}\boldsymbol{r} \tag{194}$$

in analogy with the electronic softness kernel $s(\boldsymbol{r},\boldsymbol{r}')$ (eqs 124 and 125), yielding $s(\boldsymbol{r})$ upon integration over $\boldsymbol{r}'$.

Recently, the question of higher order derivatives of $\mathbf{F}_\alpha$ with respect to N has been considered. The second-order derivative, termed nuclear stiffness,

$$\left(\frac{\partial^2 \mathbf{F}_\alpha}{\partial N^2}\right)_\nu = \left(\frac{\partial \boldsymbol{\Phi}_\alpha}{\partial N}\right)_\nu = \mathbf{G}_\alpha \tag{195}$$

has been studied by Ordon and Komorowski,[339] which is easily seen (cf. eqs 58 and 176) to be equal to $(\partial\eta/\partial\mathbf{R}_\alpha)_N$, i.e., the variation of molecular hardness with changing geometry. The numerical results for a series of diatomics show that, when converted to internal coordinates, G is mostly (though not exclusively) negative, indicating a decrease in hardness upon elongation of the bond, in agreement with AIM models developed by Nalewajski and Korchowiec[340] (cf. the dependence of the hardness matrix elements (section III.B.4) η_{ij} on the internuclear distance R_{ij}: $\eta_{ij} \sim 1/R_{ij}$). Further work, directly related to the maximum hardness principle, is needed to settle this problem.

Very recently, compact expressions for all higher order derivatives of the nuclear Fukui function with respect to N within the four Legendre transformed ensembles of DFT (cf. section III.A) have been derived by Chamorro, Contreras, and Fuentealba.[341]

We end this section with reference to recent work by Ayers and Parr.[342,343] Whereas, conventionally, variational principles helping to explain chemical reactivity were formulated in terms of the electron density (see ref 197 for a detailed discussion, also referring to the fundamental role of the Hohenberg–Kohn theorem[1]), they used similar methods to explore the effect of changing the external potential, yielding among others stability (Ξ) and lability (Λ).

Within the same spirit, their recent work, on the Grochala–Albrecht–Hoffmann bond length rule,[344] which states that

$$R_+ + R_- - R_{\mathrm{gs}} - R_{\mathrm{es}} \approx 0 \tag{196}$$

where R_+, R_-, R_{gs}, and R_{es} are the lengths of some bond for the cation, anion, singlet ground state, and first triplet excited state of a molecule, respectively, should also be mentioned.[345]

7. Spin-Polarized Generalizations

Within the context of spin-polarized DFT,[346−348] the role of $\rho(\boldsymbol{r})$ as the basic variable is shared by either $\rho_\alpha(\boldsymbol{r})$ and $\rho_\beta(\boldsymbol{r})$ (the electron densities of α and β spin electrons) or $\rho(\boldsymbol{r})$ itself and $\rho_{\mathrm{s}}(\boldsymbol{r})$, with

$$\rho(\boldsymbol{r}) = \rho_\alpha(\boldsymbol{r}) + \rho_\beta(\boldsymbol{r}) \tag{197}$$

$$\rho_{\mathrm{s}}(\boldsymbol{r}) = \rho_\alpha(\boldsymbol{r}) - \rho_\beta(\boldsymbol{r}) \tag{198}$$

$\rho(\boldsymbol{r})$ being the total charge density and $\rho_{\mathrm{s}}(\boldsymbol{r})$ the spin density.

Note, however, that Capelle and Vignale have shown that, in spin density functional theory, the effective and external potentials are not uniquely defined by the spin densities only.[349]

Normalization conditions to be fulfilled are

$$N_\alpha = \int \rho_\alpha(\boldsymbol{r})\, \mathrm{d}\boldsymbol{r} \qquad \left(\text{or} \int \rho(\boldsymbol{r})\, \mathrm{d}\boldsymbol{r} = N\right) \tag{199}$$

$$N_\beta = \int \rho_\beta(\boldsymbol{r})\, \mathrm{d}\boldsymbol{r} \tag{200}$$

$$\int \rho_{\mathrm{s}}(\boldsymbol{r})\, \mathrm{d}\boldsymbol{r} = N_\alpha - N_\beta = N_{\mathrm{s}} \tag{201}$$

where N_α and N_β denote the total number of α and β spin electrons and N_{s} is the spin number.

The extension of DFT to the spin-polarized case is necessary to describe many-electron systems in the presence of a magnetic field. Moreover, in the limit of $\mathbf{B} \rightarrow 0$, the formalism leads to a suitable DFT description of the electronic structure of atoms, molecules with a spin-polarized ground state without an external magnetic field (say, atoms and molecules having an odd number of electrons).

So, it was not unexpected that the extension of the DFT-based reactivity descriptors discussed in the previous paragraphs was treated quite soon after their introduction in the late 1970s and early 1980s. Galvan, Gazquez, and Vela introduced the spin density analogue of the Fukui function in ref 350 and completed the picture of DFT reactivity descriptors in the spin-polarized approach in a detailed analysis in ref 351. Considering the general case of a system in the presence of an external potential $\nu(\boldsymbol{r})$ and an external magnetic field $\mathbf{B}$ in the z direction, the total energy can be written as (cf. eq 7)

$$E[\rho,\rho_{\mathrm{s}},\nu,\mathbf{B}] = E[\rho,\rho_{\mathrm{s}}] + \int \rho(\boldsymbol{r})\nu(\boldsymbol{r})\, \mathrm{d}\boldsymbol{r} - \mu_{\mathrm{B}} \int \mathbf{B}(\boldsymbol{r})\rho_{\mathrm{s}}(\boldsymbol{r})\, \mathrm{d}\boldsymbol{r} \tag{202}$$

where μ_{B} is the Bohr magneton.

As ρ and ρ_{s} are independent functions, independent minimization procedures have to be carried out, taking into account the variation of the energy with respect to both of them. Imposing the normalization conditions and introducing two Lagrange multipliers μ_{N} and μ_{S}, one obtains (cf. eq 6)

$$\mu_N = \left(\frac{\delta E}{\delta \rho(\boldsymbol{r})}\right)_{\rho_s,\nu,\mathbf{B}} = \nu(\boldsymbol{r}) + \frac{\delta F}{\delta \rho(\boldsymbol{r})} \quad (203)$$

and

$$\mu_s = \left(\frac{\delta E}{\delta \rho_s(\boldsymbol{r})}\right)_{\rho,\nu,\mathbf{B}} = -\mu_B \mathbf{B}(\boldsymbol{r}) + \frac{\delta F}{\delta \rho_s(\boldsymbol{r})} \quad (204)$$

A procedure in analogy with the one described in section II.C yields the following identification of μ_N and μ_S:

$$\mu_N = \left(\frac{\partial E}{\partial N}\right)_{N_s,\nu,\mathbf{B}} \quad (205)$$

$$\mu_S = \left(\frac{\partial E}{\partial N_S}\right)_{N,\nu,\mathbf{B}} \quad (206)$$

The first of these relations is the equivalent of the electronic chemical potential in the spin-restricted case, except for the fact that the derivative is taken at a fixed N_S value. The second Lagrangian multiplier, μ_S, can be identified as the "spin potential", as it measures the tendency of a system to change its spin polarization. (Note that, in analogy to eq 37, the discontinuity in the $(\partial E/\partial N_S)$ function has received attention by Galvan and Vargas[352a] and by Vargas, Galvan, and Vela in a study on the relation between singlet−triplet gaps in halocarbenes and spin potentials.[352b])

In an analogous way, the corresponding expressions for hardness and Fukui functions may be written:

$$\eta_{NN} = \left(\frac{\partial \mu_N}{\partial N}\right)_{N_s,\nu,\mathbf{B}} \quad (207)$$

$$\eta_{NS} = \left(\frac{\partial \mu_N}{\partial N_S}\right)_{N,\nu,\mathbf{B}} = \left(\frac{\partial \mu_S}{\partial N}\right)_{N_s,\nu,\mathbf{B}} = \eta_{SN} \quad (208)$$

$$\eta_{SS} = \left(\frac{\partial \mu_S}{\partial N_S}\right)_{N,\nu,\mathbf{B}} \quad (209)$$

$$f_{NN}(\boldsymbol{r}) = \left(\frac{\partial \rho(\boldsymbol{r})}{\partial N}\right)_{N_s,\nu,\mathbf{B}} \quad (210)$$

$$f_{SN}(\boldsymbol{r}) = \left(\frac{\partial \rho_s(\boldsymbol{r})}{\partial N}\right)_{N_s,\nu,\mathbf{B}} \quad (211)$$

$$f_{NS}(\boldsymbol{r}) = \left(\frac{\partial \rho(\boldsymbol{r})}{\partial N_s}\right)_{N,\nu,\mathbf{B}} \qquad f_{SS}(\boldsymbol{r}) = \left(\frac{\partial \rho_s(\boldsymbol{r})}{\partial N_s}\right)_{N,\nu,\mathbf{B}} \quad (212)$$

Whereas η_{NN} is the equivalent of the hardness in the spin-restricted case (except for the condition of fixed N_s), η_{SN} and η_{NS} contain new information: the variation of the chemical potential with respect to changes in spin number or the variation in spin potential with respect to changes in the total number of electrons. η_{SS}, the spin hardness, is the second derivative of the energy with respect to the spin number. Analogous interpretations can be given to the four types of Fukui functions, f_{NN}, f_{SN}, f_{NS}, and f_{SS}, which can be used to probe the reactivity of various sites of a molecule. Within a Kohn−Sham formalism, a FMO approach was presented to obtain working equations for all the quantities defined above (which are the extensions/analogues of eqs 68, 90, and 91 and the comments in section III.B.3).

Numerical values for the spin potential for atoms from $Z = 3$ to $Z = 54$ were obtained by Galvan and Vargas[353] within the framework of the spin-polarized Kohn−Sham theory. The quantity shows periodic behavior, such as electronegativity or ionization potential. The structure of the curve μ_S^+ vs Z, for example, shows peaks corresponding to atoms with half-filled shells (alkali atoms, nitrogen family, chromium, etc.). In general, μ_S measures the tendency of a system to change its multiplicity. The same authors later used the Fukui function $f_{NS}^-(\boldsymbol{r})$ to rationalize the stability of half-filled shells.[352a] In analogy with the treatment of local softness for Fukui functions in refs 350 and 351, Garza and Robles[354] investigated the extension of the local hardness concept to the spin-polarized case.

Finally, and in advance of the section on the electronegativity equalization method (section III.C.1), we mention that Cioslowski and Martinov[355] analyzed the individual spin contributions to electron flow in molecules in a spin-resolved version of the electronegativity equalization method.

Also, Ghanty and Ghosh[115] used a spin-polarized generalization of the concept of electronegativity equalization in the study of bond formation, using however ρ_α and ρ_β as basic variables, which seems, in our view, less appropriate from the chemist's point of view than ρ and ρ_s.

8. Solvent Effects

Until quite recently, all studies on electronegativity, hardness, Fukui functions, local softness, etc. were performed in the gas phase. However, it is generally known that the properties of molecules may differ considerably between the gas phase and solution.[356,357] Two main techniques were developed in recent decades to include solvent effects on a variety of properties: continuum models and discrete solvent models. In continuum models,[358] the solvent is treated as a continuum, with a uniform dielectric constant ϵ, surrounding a solute molecule which is placed in a cavity. The variety of approaches differ in the way the cavity and the reaction field are defined, the simplest being the Onsager reaction field model.[359] The second type of reaction field methods is the polarized continuum model (PCM), proposed by Tomasi and co-workers,[358,360,361] later refined in the self-consistent isodensity polarized continuum model (SCI−PCM).[362,363] In this method, the electron density minimizing the energy, including the effect of solvation, is determined. This result, however, is dependent on the cavity, which is in turn determined by the electron density. The effect of the solvent is thus taken into account self-consistently, offering a complete coupling of the cavity and the electron density.

Lipinski and Komorowski[364] were the first to evaluate solvent effects on the electronegativity and hardness of bonded atoms in a homogeneous polar medium using a virtual charge model. It was observed that the hardness of ions decreases with increasing solvent polarizability, whereas the electronegativity index decreases for cations and increases for anions. Molecular χ and η indices, however, showed minor dependencies on the solvent polarity. Qualitatively, the conclusions agree with the work of Pearson,[365] who studied changes in ionization energy and electron affinities due to hydration. The electronegativity of neutral molecules does not change in water, while their hardness decreases. Anions become poorer electron donors (hence more electronegative), whereas cations become poorer electron acceptors (hence less electronegative).

Safi et al.[366] were the first to use the continuum approach to study the influence of solvent on group electronegativity and hardness values of CH_2F, CH_2Cl, CH_3, CH_3-CH_2, and $C(CH_3)_3$, previously computed by De Proft et al. (vide infra, section IV.A), and concluded that the groups become less electronegative and less hard with increasing dielectric constant.

The values were used in a study by the same group on the acidity of alkyl-substituted alcohols,[366] the basicity of amines,[367] and the solvent effect on the thermodynamic and kinetic aspects of the $X^- + CH_3Y \rightarrow Y^- + CH_3X$ S_N2 reaction.[368]

A comparable approach, but concentrating on the Fukui function, was followed by Sivanesan et al.[369] in studying the influence of solvation in H_2O on formaldehyde, methanol, acetone, and formamide, leading to the conclusion that a simultaneous enhancement of reactivity for both the electrophilic and the nucleophilic nature of the constituent atoms is not found, though the potential for electrophilic and nucleophilic attack increases when passing from the gas phase to an aqueous medium.

Similar approaches have been followed by Perez, Contreras, and co-workers,[370,371] using a continuum approach to study the solvation energy from the linear response function.[371] In detailed studies, they treated the solvent influence on the isomerization reaction of MCN (M = H, Li, Na),[372] and they discussed the difference between gas- and solution-phase reactivity of the acetaldehyde enolate (vide infra, section IV.C.2-b).[373] Very recently, these same authors studied the continuum solvent effect on the electrophilicity index recently proposed by Parr, Von Szentpaly, and Liu[186] (eq 84). They found a clear relationship between the change in electrophilicity index and the solvation energy within the context of reaction field theory. In an interesting study on a series of 18 common electrophiles, representing a wide diversity in structure and bonding properties, solvation was seen to enhance the electrophilic power of neutral electrophilic ligands but to attenuate this power in charged and ionic electrophiles.[374]

Recently, the first steps toward the exploration of noncontinuum models have been taken by Balawender, Safi, and Geerlings,[375,376] adopting Gordon's effective fragment potential model, including the effect of discrete solvent molecules.[377,378] Each solvent is considered explicitly by adding one-electron terms directly to the ab initio Hamiltonian,

$$H_{\mathrm{TOT}} = H_{\mathrm{AR}} + V \tag{213}$$

where H_{AR} is the ab initio Hamiltonian describing the "active region" of the system (solute and any solvent molecules that directly participate in a bond-making or -breaking process); the perturbation term V is composed of three one-electron terms representing the potential due to the solvent (fragment) molecules, corresponding to electrostatic, polarization, and exchange repulsion/charge-transfer interactions between the solvent molecules and the electrons and nuclei in the active region. In a case study on NH_3, it has been shown[375] that the HOMO−LUMO gap and electrophilic hardness increase with addition of water molecules: the saturation point for solvation of ammonia was located around a cluster with 16 molecules of water.

In a study on diatomic and small polyatomic molecules, use was made of the binding function (cf. section III.B.6) for monitoring the solvation of the molecule using a 30-solvent-molecules surrounding.[376]

9. Time Evolution of Reactivity Indices

The time dependency of the electron density is governed by the time-dependent Kohn−Sham equations, being at the basis of time-dependent density functional theory (TDDFT), a promising approach for the computation of excitation energies (the current status of affairs in this vigorously evolving field of DFT is reviewed in ref *2*).

Studies involving the time evolution of the DFT-based concepts, reactivity indices, and principles have been relatively scarce. The majority of contributions (essentially concentrating on atoms) has been provided by Chattaraj and co-workers, within the framework of quantum fluid DFT, involving the solution of a generalized nonlinear Schrödinger equation.[379−384] Applications included the dynamical response of He in an intense laser field,[379] N in an external field and colliding with a proton,[380,381] Be in both its ground and excited states colliding with a proton and with an α particle,[382,383] and He in its ground and excited states interacting with monochromatic and bichromatic laser pulses of different intensities.[384] Both the dynamics of concepts such as electronegativity, covalent radius, hardness, polarizability, electrophilicity, and its inverse, nucleophilicity, and the principles, such as the electronegativity equalization principle and the maximum hardness and miminum polarizability principle, have been studied. The time evolution of both the electronegativity and the covalent radius provided a method to divide the interaction of two colliding particles into three steps, i.e., approach, encounter, and departure. When the time dependence of the global hardness was investigated, it appeared to be a manifestation of a dynamical version of the maximum hardness principle: the global hardness gets maximized in the encounter regime.[383] This was also confirmed for excited states. Moreover, the local hardness was found to be the highest in regions of accumulated electron density, implying indeed the applicability of this concept for charge-controlled reactions. In addition, the principle of minimum polarizability was also confirmed within this framework, as was the maximum entropy principle. This maximization of the entropy happens during the encounter process, indicating that the charge transfer occurring due to the collision is a favorable process.

A recent and very promising study involving time dependence of DFT-based reactivity descriptors was conducted by Vuilleumier and Sprik.[385] They investigated the electronic structure of both a hard and a soft ion (Na^+ and Ag^+, respectively) in aqueous solution using Car−Parinello molecular dynamics.[386] The response properties calculated were the global hardness together with the electronic and nuclear Fukui functions. For the hard cation, the HOMO was found to remain buried in the valence bands of the solvent, whereas for the soft cation, this orbital mixed with the lone pair orbitals of the four coordinating water molecules; this observation could serve as a means of distinguishing between hard and soft species and was put forward as a conjecture, meriting further investigation.

C. Principles

1. Sanderson's Electronegativity Equalization Principle

The electronegativity equalization principle originally formulated by Sanderson[113,387−391] has formed the basis for a number of attractive computational schemes. Sanderson postulated that, upon molecule formation, the electronegativities of the constituent atoms $\{\chi_A^0\}$ become equal, yielding a molecular (Sanderson) electronegativity χ_M which is postulated to be the geometric mean of the original electronegativity of the atoms (the symbol S instead of χ being used in Sanderson's work),

$$\chi_M = (\chi_A^0\,\chi_B^0\,\chi_C^0\,...)^{1/(m+n+p+\cdots)} \tag{214}$$

where m, n, and p are the numbers of atoms of a given element (A, B, C, etc.).

In this way, partial atomic charges q_i can be obtained starting from isolated atom electronegativities; comparing the χ_M for NaF (2.01) as obtained from the isolated atom values (0.70 for Na and 5.75 for F), the χ difference for F is 3.74. Assuming 90% ionicity of the NaF bond and a linear relationship between χ and q, the difference in χ when passing from F to F^- is $3.74 \times 0.9 = 4.16$, and that on going from Na to Na^+ is 1.46. Later, these $\Delta\chi$ values were put in a general equation of the type $\Delta\chi_i = 1.56\,\chi_i^{1/2}$, affording charge calculation for atoms of different elements.

A serious drawback of the method was that all atoms of the same element adopt the same atomic charge within a molecule.

Huheey[169−171] was one of the first, aside from Sanderson, to use the idea of electronegativity equalization to obtain molecular charge distributions, using the idea of a charge-dependent electronegativity:

$$\chi = a + b\delta \tag{215}$$

where χ was written as a linear function of the partial charge δ on an atom,[169] b being termed a charge coefficient.

In the diatomic AB case, one obtains

$$\delta_A = \frac{a_B - a_A}{b_A + b_B} \tag{216}$$

which was used by Huheey to study the inductive effect of alkyl groups.[171] (See section IV.C.3-c for a recent approach along these lines.)

Using the symbols χ and η and eq 65, one obtains an actualized version,

$$\Delta N_A = N_A - N_A^0 = \frac{\chi_A^0 - \chi_B^0}{2(\eta_A^0 + \eta_B^0)} \tag{217}$$

illustrating that the direction of charge transfer is dictated by the difference in electronegativities of the isolated atoms χ_A^0 and χ_B^0 ($=\chi_A(N_{A_0})$ and $\chi_B(N_{A_0})$, modulated however by their hardnesses.

Although the introduction of the concept of a molecular electronegativity was intuitively appealing and computationally attractive, it raised questions about the compatibility of this scale with Pauling's definition.[392] Nevertheless, the method received relatively little attention in the literature until the late 1970s, when a solid proof of the electronegativity equalization principle was initially given by Donnelly and Parr[393] and later on by Politzer and Weinstein.[394]

Parr, in fact, demonstrated the constancy of the chemical potential (minus the electronegativity) over the system considered and proved also that the electronegativities or chemical potentials of the natural orbitals of a molecule in the ground state are equal.[393]

Politzer and Weinstein proved, independent of any particular theoretical framework, that the electronegativities of all arbitrary portions of the total number of electrons, not necessarily grouped into orbitals or atoms, are the same for molecules in the ground state.[394] Parr and Bartolotti, on the other hand, offered theoretical and numerical support for the geometric mean postulate, on the basis of an exponentially decaying energy and thus also exponentially decaying electronic chemical potential:[395]

$$E_A = A_A \exp[-\gamma_A(N - Z)] + B_A \tag{218}$$

or

$$\mu_A = \mu_A^0 \exp[-\gamma_A(N - Z)] \tag{219}$$

where A_A, B_A, and γ_A are constants for a given atom type.

For a more detailed analysis, including electrostatic (external potential) effects, we refer to Nalewajski's work,[396] indicating that increasing deviation is expected from eq 217 when both interaction partners become harder. Note that, in this approach, the relationship between μ, I, and A changes:

$$\mu = \frac{IA}{I - A}\ln\left(\frac{I}{A}\right) \tag{220}$$

For an alternative approach, see Ohwada.[397] This author derived the following equation for the chemical potential of a polyatomic molecule:

$$\mu_{\mathrm{mol}} = \frac{\sum_{X} \mu_{\mathrm{X}}^{0}/\langle \eta_{\mathrm{X}} \rangle}{\sum_{X} 1/\langle \eta_{X} \rangle} \tag{221}$$

i.e., the chemical potential is the statistical mean of the chemical potential of the constituent atoms weighted by the inverse of what Ohwada introduced as their apparent chemical hardnesses $\langle \eta_{\mathrm{X}} \rangle$. Based on two different approximations for the latter, he obtained chemical potentials for a large series of tri-, tetra-, and polyatomic molecules.

An alternative to the geometric mean has been discussed by Wilson and Ichikawa.[398] Based on the observation that the ratio of η and χ, γ is relatively constant over the majority of the elements,[399] the equalization of electronegativity (vide infra) yields a χ_{M} which in the case of a diatomic molecule is written as

$$\chi_{\mathrm{M}} = \left(\frac{\chi_1^0 \chi_2^0}{\chi_1^0 + \chi_2^0} \right) \tag{222}$$

described by Nalewajski as the harmonic mean.[399]

The generalized harmonic mean for polyatomic molecules can then be written as

$$\chi_{\mathrm{M}}^{-1} = n \left(\sum_{i=1}^{n} \frac{1}{\chi_i^0} \right) \tag{223}$$

Analysis of molecular charge distributions obtained with Sanderson's χ scale and the geometric mean on one hand, and scales correlating linearly with Sanderson's scale and using the harmonic mean on the other hand, suggests that the proportionality between χ and η is implicit in Sanderson electronegativities.

The above-described concepts incited a lot of research to exploit the principle for obtaining molecular charge distributions with relatively little computational effort. (For reviews, see ref 101.)

Gasteiger and Marsili were among the first to conduct studies on the partial equalization of orbital electronegativity (PEOE),[400] yielding a rapid calculation of atomic charges in σ-bonded and nonconjugated π systems, coping with the problem of identical charges for atoms of the same element by performing an iterative scheme on each bond to evaluate the charge shift. [For its extension to conjugated π systems, see ref 401.] Nalewajski et al.[396,402] showed that it was convenient to discuss the electronegativity equalization during bond formation in terms of the AIM model, taking into account both the electron-transfer and external potential effects.

An important step was taken by Mortier and coworkers, who in 1985–1986 established an electronegativity equalization method (EEM). (For reviews, see refs 184, 403, and 404, which also contain a comprehensive account of the pre-1985 work of Huheey, Ponec, Reed, and Sanderson.) This ansatz can be summarized as follows.[294,405–409]

Starting from isolated atom electronegativities $\{\chi_{\mathrm{A}}^0\}$ and hardnesses $\{\eta_{\mathrm{A}}^0\}$, the following expression is written for the AIM electronegativity:

$$\chi_{\mathrm{A}} = (\chi_{\mathrm{A}}^0 + \Delta\chi_{\mathrm{A}}) + 2(\eta_{\mathrm{A}}^0 + \Delta\eta_{\mathrm{A}})q_{\mathrm{A}} + k \sum_{B \neq A} \frac{q_{\mathrm{B}}}{R_{\mathrm{AB}}} \tag{224}$$

where $\Delta\chi_{\mathrm{A}}$ and $\Delta\eta_{\mathrm{A}}$ are terms to correct the isolated atoms' values (vide infra). A sound theoretical basis has been given in refs 407 and 408 for the initial empirical approach.[405] The final term (in which k comprises the constant $1/4\pi\epsilon_0$ and an energy conversion factor) accounts for the external potential. This equation was derived by writing the molecular electron density as a sum of spherical atom contributions,

$$\rho_{\mathrm{mol}}(\boldsymbol{r}) = \sum_{A} \rho_{\mathrm{A}}^{\mathrm{mol}}(\boldsymbol{r}) \tag{225}$$

splitting the energy into intra- and inter-atomic contributions and expanding the intra-atomic term in a Taylor series around the spatially confined neutral atom energies analogous to the isolated neutral atom in eq 60. The first- and second-order coefficients in this expansion, μ_{A}^* and η_{A}^*, can then be written as

$$\begin{aligned} \mu_{\mathrm{A}}^* &= \mu_{\mathrm{A}}^0 + \Delta\mu_{\mathrm{A}} \\ \eta_{\mathrm{A}}^* &= \eta_{\mathrm{A}}^0 + \Delta\eta_{\mathrm{A}} \end{aligned} \tag{226}$$

where $\Delta\mu_{\mathrm{A}}$ and $\Delta\eta_{\mathrm{A}}$ are correction terms for the changes in size and shape of the atom in the molecule, as compared to the isolated atom values (μ_{A}^0 and η_{A}^0).

Writing

$$\chi_{\mathrm{A}} = \chi_{\mathrm{B}} = \chi_{\mathrm{C}} = ... \bar{\chi} \tag{227}$$

where $\bar{\chi}$ is the average molecular electronegativity, yields n simultaneous equations for an n-atomic molecule. Along with the constraint on the charge,

$$\sum_{i=1}^{n} q_i = Q \tag{228}$$

where Q is the total charge of the molecule, this system of $n + 1$ linear equations yields all atomic charges (n) and the average molecular electronegativity $\bar{\chi}$.

In matrix form, one has

$$\begin{pmatrix} q_{\mathrm{A}} \\ q_{\mathrm{B}} \\ \vdots \\ q_n \\ -\bar{\chi} \end{pmatrix} = \begin{pmatrix} 2\eta_{\mathrm{A}}^* & k/R_{\mathrm{AB}} & \cdots & k/R_{\mathrm{A}n} & 1 \\ k/R_{\mathrm{BA}} & 2\eta_{\mathrm{B}}^* & \cdots & k/R_{\mathrm{B}n} & 1 \\ \vdots & \vdots & \vdots & \vdots & \vdots \\ k/R_{n\mathrm{A}} & k/R_{n\mathrm{B}} & \cdots & 2\eta_n^* & 1 \\ 1 & 1 & \cdots & 1 & 0 \end{pmatrix} \begin{pmatrix} -\chi_{\mathrm{A}}^* \\ -\chi_{\mathrm{B}}^* \\ \vdots \\ -\chi_n^* \\ Q \end{pmatrix} \tag{229}$$

Evaluation of the $\Delta\chi_A$, $\Delta\eta_A$ values is done by calibration of ab initio (Hartree–Fock STO-3G) and EEM charges for H, C, N, O, Al, Si, and P.

Note that the charges thus obtained are dependent on both connectivity and geometry, which is not the case in the simple Huheey approach (eq 216), neglecting the external potential term.

The method of full equalization of orbital electronegativity (FEOE) has been extented to the solid state, where charges and external potential are generated in a self-consistent way using Ewald's method for determining the Madelung potential.[408]

An advantage of this formalism is that other fundamental DFT properties, such as hardness, softness, Fukui function, and local softness, can be obtained similarly in a straightforward and transparent calculation;[404] it is, for example, easily seen that the Fukui function in atomic resolution and the hardness can be obtained by a similar matrix equation:

$$\begin{pmatrix} f_A \\ f_B \\ \vdots \\ f_n \\ -\eta \end{pmatrix} = \begin{pmatrix} 2\eta_A^* & k/R_{AB} & \cdots & k/R_{An} & 1 \\ k/R_{BA} & 2\eta_B^* & \cdots & k/R_{Bn} & 1 \\ \vdots & \vdots & \vdots & \vdots & \vdots \\ k/R_{nA} & k/R_{nB} & \cdots & 2\eta_n^* & 1 \\ 1 & 1 & \cdots & 1 & 0 \end{pmatrix}^{-1} \begin{pmatrix} 0 \\ 0 \\ \vdots \\ 0 \\ 1 \end{pmatrix} \qquad (230)$$

from which local and global softness can be obtained immediately via eqs 59 and 112.

In the 1990s, several other EEM-type formalisms were presented. A charge-constrained electronic structure calculation allows a rigorous analysis of electron flow and electronegativity equalization in the process of bond formation, including a spin-resolved analysis (cf. section III.B.7) by Cioslowski et al.,[355,410,411] in the form of a charge equilibration method (Qeq) by Rappé and Goddard,[412] as the atom–bond electronegativity equalization method (ABEEM) by Yang and Wang,[413−418] and the chemical potential equalization method by York and Yang[419,420] and by Itskowitz and Berkowitz[421] among others, further refining the evaluation of the χ_A^* and η_A^* values (dependency on neighboring atoms).

Further variants were presented by No and Sheraga[422−424] (extension of PEOE) for polypeptides and proteines), and some beautiful models (mostly concentrating on small molecules) were presented by Ghosh, Ghanty, and Parr[115,425−428] and Von Szentpaly,[429] for which, however, not many applications have appeared in recent years. Our group formulated a nonempirical electronegativity equalization scheme, starting from a first-order expression of the electronegativity of an atom in a molecule, based on the change, upon molecule formation, of the number of electrons, and the external potential:[430]

$$\chi_A = \chi_A^0 + 2\eta_A^0 q_A + \sum_i Z_{B_i}^{\text{eff}} \left(\frac{\partial V_A^{\text{el},0}(R_{BA})}{\partial N} \right)_{N_A \neq N_A{}^0} \qquad (231)$$

Here, $Z_{B_i}^{\text{eff}}$ is the effective nuclear charge of atom B_i as experienced by A, and $V_A^{\text{el},0}$ is the electronic part of the electrostatic potential of an isolated atom A at a distance R_{BA}. Z^{eff} is obtained as

$$Z_B^{\text{eff}} = \left[Z_B^0 - \int_0^{r_{\text{min,out}}} D(r)\,\mathrm{d}r\right] \mathrm{e}^{-\lambda_{\text{out}}(R_{AB} - r_{\text{min,out}})} \qquad (232)$$

where Z_B^0 is the nuclear charge of B, $r_{\text{min,out}}$ the outermost minimum in the radial distribution function of B, and λ_{out} the falloff parameter of the electron density of B in the valence region ($r > r_{\text{min,out}}$). The resulting charge distributions and molecular electronegativities for diatomics and small polyatomics showed a fair correlation with a variety of other, parametrized, techniques mentioned in this section.

The exact inclusion of the external potential contribution in an EEM context was discussed by Nalewajski[396] (also described in Parr and Yang's book[27]) and by Berkowitz,[431] leading to the following ΔN equation (extending eq 217):

$$\Delta N = \frac{(\mu_B^0 - \mu_A^0) + \int f_B(\boldsymbol{r})\Delta\nu_B(\boldsymbol{r})\,\mathrm{d}\boldsymbol{r} - \int f_A(\boldsymbol{r})\Delta\nu_A(\boldsymbol{r})\,\mathrm{d}\boldsymbol{r}}{2(\eta_A + \eta_B)} \qquad (233)$$

The second and third terms in the numerator are potential-dependent terms, moderating the chemical difference in driving the charge transfer.

An extension of the EEM concept to functional groups and to amino acid residues,[432] based on parameter-free calculations of group[433] and residue[434] electronegativities and hardnesses, was presented by the present authors.[430,434]

We present the method developed by York and Yang in some more detail, as some other methods can be seen as particular cases derived from it, its essential advantages being the expansion of the energy around the molecular ground state instead of the neutral atom ground state and the use of both functions when studying the density response to perturbations of applied fields or other molecules. Considering the effect of a perturbation $\delta\nu(\boldsymbol{r})$ on the ground state, a second-order expansion of $E[\rho_0 + \delta\rho, \nu_0 + \delta\nu]$ leads to the following Euler equation for the perturbed system,

$$\Delta\mu = \mu - \mu_0 = \int \left[\frac{\delta^2 F}{\delta\rho(\boldsymbol{r})\delta\rho(\boldsymbol{r}')} \right] \delta\rho(\boldsymbol{r}')\,\mathrm{d}\boldsymbol{r}' + \delta\nu(\boldsymbol{r}) \qquad (234)$$

involving the second-order density derivative of the Hohenberg–Kohn functional, which is the equation on which the method is based. Introducing a finite basis for $\delta\rho(\boldsymbol{r})$,

$$\delta\rho(\boldsymbol{r}) = \sum_\lambda c_\lambda \varphi_\lambda(\boldsymbol{r}) \qquad (235)$$

a matrix equation for $\Delta\mu$ is obtained.

The results provide a linear response framework for describing the redistribution of electrons upon perturbation by an applied field and the foundation for a model including polarization and charge transfer in molecular interactions.

The FEOE methods by Mortier, Rappé, and Goddard are, in fact, particular cases of this more general formalism, putting density basis functions as δ functions about the atomic positions (Mortier), or if atom-centered ns Slater-type orbitals are used, as basis functions. On the other hand, in Cioslowski's approach, much more effort is put into properly defining the atomic character of the basis functions.

The ABEEM method by Z. Z. Yang and co-workers, which has received considerable interest in recent years, was designed for the study of large organic molecules. Extending Mortier's density decomposition as a sum over atoms contributions, it also includes bond contributions,

$$\rho_M(\boldsymbol{r}) = \sum_A \rho_A(\boldsymbol{r}) + \sum_G \sum_H \rho_{GH}(\boldsymbol{r}) \tag{236}$$

where ρ_{GH} denotes the electron density allocated to the G−H bond region. The summation over A extends over all atoms of the molecule, and the one over G and H extends over all bonds. On the basis of this equation, an EEM principle is formulated both for atoms and bonds:

$$\chi_A = \chi_B = ... = \chi_{G-H} = \chi_{H-J} = ... = \bar{\chi}_{\text{molecule}} \tag{237}$$

Originally, the theory was formulated for σ bonds; it was later extended to π bonds[418] and to the incorporation of lone pairs.[415] A correlation between ab initio STO-3G and ABEEM charges for the polypeptide $C_{32}N_9O_6H_{99}$ yielded a regression equation with an R value of 0.9950, passing almost perfectly through the origin.[418]

A means for obtaining linear response functions (atom/atom, atom/bond, bond/bond) and the Fukui function was generalized recently[416] and offers a promising technique for non-ab initio DFT reactivity descriptors for very large molecules, the elements however still restricted to H, C, N, and O.

It should be mentioned that some authors have been focusing on equalization of other properties.

We mentioned before that Nalewajski[399] and Wilson and Ichikawa[398] wrote a harmonic mean for the averaged electronegativity based on substantial evidence that χ^0 and η^0 are proportional, where the proportionality factor could be universal:

$$\eta^0 = \gamma\chi^0 \tag{238}$$

Parr and Bartolotti obtained a γ value of 2.15 ± 0.59 for 32 atoms;[395] Datta obtained 1.58 ± 0.37 for a series of radicals.[435]

By inserting eq 237 into eq 222, an expression for an equilibrated hardness is obtained.

$$\eta_M = n\left(\sum_i \frac{1}{\eta_i^0}\right)^{-1} \tag{239}$$

In fact, in 1986, Datta formulated the idea of an equalization of atomic hardness, more precisely to their geometric mean:[436,437]

$$\eta_M = \left(\prod_i^n \eta_i^0\right)^{1/n} \tag{240}$$

Note that the proportionality between η and χ, noticed by Yang, Lee, and Ghosh[438] and by Nalewajski,[399] brought Yang et al. in 1985 to the conclusion that there should be a simple relationship between molecular softness and the softness of the constituent atoms:[438]

$$S = \frac{1}{n}\sum_{i=1}^n S_i \tag{241}$$

These findings should be considered in the context of the ongoing discussion on an unambiguous definition of local hardness (cf. section III.B.4), where in several of the most detailed papers[284,285] one of the possibilities put forward is simply to write (cf. eq 141)

$$\eta(\boldsymbol{r}) = \eta \tag{242}$$

i.e., to equalize local and global hardness, eliminating local hardness from the DFT scene. Pearson's comment,[113] cited in section III.B.4, expresses a feeling that certainly reflects the chemical intuition of many researchers in the field. The story goes on.

2. Pearson's Hard and Soft Acids and Bases Principle

a. The Global Level. As described in section III.B.2, Pearson formulated his HSAB principle on the basis of experimental data guided by chemical intention without a sharp definition of hardness and softness. The introduction, by Parr and Pearson, of the definition of hardness as the second derivative of the energy of an atomic or molecular system with respect to the number of electrons paved the way to a proof of the principle.

In fact, in 1991, two proofs were given by Chattaraj, Lee, and Parr.[439] In the first proof, the interaction process between an acid A and a base B is dissected into two steps: a charge-transfer process, resulting in a common chemical potential at a fixed external potential, and a reshuffling process at a fixed chemical potential.

Opposing tendencies for S_A vs S_B for a given $\mu_B - \mu_A$ in the two steps were reconciled by a compromise:

$$S_A = S_B \tag{243}$$

i.e., the HSAB principle. Note S_A and S_B are softnesses either before or after electron transfer; the N dependence of η (or S) is known to be weak.[271] It is easily seen, on the basis of eqs 217, 60, and 61, that the energy change in the charge-transfer step yields the following expression:

$$\Delta E = -\frac{(\mu_B^0 - \mu_A^0)^2}{4(\eta_A^0 + \eta_B^0)} \tag{244}$$

illustrating once more the interplay between electronegativity and hardness.

In the second proof, the minimum softness/maximum hardness principle, proven in the same *J. Am. Chem. Soc.* issue by Parr and Chattaraj[440] (see section III.C.3), is invoked in a qualitative treatment.

Nalewajski[396] introduced the first-order perturbation contribution of the external potential due to the partner of a given atom in a molecule. Starting from a full second-order expansion of the energy of an atom A in a molecule, as a function of N_A and Z_A, he obtained the following generalization of the expression for the electron flow between the two atoms A and B:

$$\Delta N = -\frac{\mu_B^0 - \mu_A^0}{2(\eta_A^0 + \eta_B^0)} \rightarrow$$

$$\Delta N = \frac{1}{2(\eta_A^0 + \eta_B^0)}[\mu_B^0 - \mu_A^0 + 2(\alpha_B \Delta Z_B - \alpha_A \Delta Z_A)] \quad (245)$$

Here, the core charge of an atom in a molecule, ΔZ_x, is essential to account for the fact that, in the A–B complex, outer electrons of an atom are in the presence of both atomic cores (contraction of atomic density contribution). α_A is equal to $(\partial\mu_A/\partial Z_A)_{N_A}/2$.

Using this expression, the first-order stabilization energy becomes

$$\begin{aligned}\Delta E &= (\mu_A^0 - \mu_B^0)\Delta N + \nu_A^0 \Delta Z_A + \nu_B^0 \Delta Z_B \\ &= -\frac{(\mu_B^0 - \mu_A^0)}{2(\eta_A^0 + \eta_B^0)} + \\ &\quad \frac{(\mu_A^0 - \mu_B^0)(\alpha_B \Delta Z_B - \alpha_A \Delta Z_A)}{\eta_A^0 + \eta_B^0} + \\ &\quad (\nu_A^0 \Delta Z_A + \nu_B^0 \Delta Z_B)\end{aligned} \quad (246)$$

From now on, the superscript "0" will be dropped to simplify the notation if expressions obviously involve isolated atom properties. It is argued that the second term will, in general, be small due to cancellation effects; the first (Huheey–Parr–Pearson) term is then identified as the one explaining the soft–soft complex, whereas the hard–hard interactions yield an important last term. In the case of soft–hard interactions, both terms are small.

In the second proof, one casts eq 244 into the form

$$\Delta E = \Delta\Omega_A + \Delta\Omega_B \quad (247)$$

introducing the grand potentials (cf. eq 33) Ω_A and Ω_B of the interacting systems as the natural "thermodynamic" quantity for an atom, functional group, or any other subunit of the molecule due to their "open" nature. $\Delta\Omega_A$ is given as

$$\Delta\Omega_A = -\frac{(\mu_A - \mu_B)^2}{4}\frac{\eta_A}{(\eta_A + \eta_B)^2} \quad (248)$$

with an analogous expression for $\Delta\Omega_B$.

For a given $\mu_A - \mu_B$ and η_B, minimization of $\Delta\Omega_A$ with respect to η_A yields

$$\eta_A = \eta_B \quad (249)$$

The same result is obtained when $\Delta\Omega_B$ is minimized with respect to η_B, for a given η_A. The calculation shows that one again recovers the HSAB principle. Equation 249 moreover implies that, under these conditions,

$$\Delta\Omega_A = \Delta\Omega_B \quad (250)$$

indicating that Ω_A and Ω_B separately like to be as negative as possible. For a recent extension of this proof to cases including external potential charges, see ref 441.

Gazquez[173,442] elaborated on this work, deriving an alternative proof that provides additional support for a better understanding of the HSAB principle. The basic equation involves the separation of the core and "effective" valence electron density,[290]

$$\rho(\mathbf{r}) = \rho_C(\mathbf{r}) + N_e f(\mathbf{r}) \quad (251)$$

where N_e is the effective number of valence electrons, $f(\mathbf{r})$ the Fukui function, supposed to be determined only by the valence electrons, and $\rho_C(\mathbf{r})$ the core electron density. The total number of core electrons N_C is equal to $N - N_e$.

Up to second order, Gazquez found

$$E[\rho] = \mu N_e - \frac{1}{2}\eta N_e^2 + E_{core}[\rho] \quad (252)$$

where E_{core} represents the core contribution to the total electronic energy. Equation 252 was then used for A, B, and AB to write the interaction energy between A and B as

$$\Delta E_{AB} = E_{AB} - E_A - E_B + E_{AB}^{NN} \quad (253)$$

where E_{AB}^{NN} is the nuclear–nuclear repulsion energy.

Invoking the EEM principle (see section III.C.1), μ_{AB} was written as

$$\mu_{AB} = \frac{\mu_A S_A + \mu_B S_B}{S_A + S_B} \quad (254)$$

Furthermore, invoking softness additivity,[226,438] as was also done by Parr in his first proof,

$$S_{AB} = k(S_A + S_B) \quad (255)$$

k being a proportionality constant, a rather complex expression for ΔE_{AB} was obtained.

Setting

$$\frac{\partial \Delta E_{AB}}{\partial S_B} = 0 \quad (256)$$

for a given S_A and all other variables fixed, the expression

$$S_B = S_A \frac{1 + \sqrt{y}}{y - 1} \quad (257)$$

was obtained, where y is an expression involving k, μ_A, μ_B, S_A, $N_{e,A}$, $N_{e,B}$, and $N_{e,AB}$. Inspection shows that

y should be close to 4, indicating

$$S_B \approx S_A \tag{258}$$

regaining the HSAB principle.

The three proofs follow a different methodology and sometimes differ in details, e.g., in the contribution from changes in the external potential (for a detailed discussion, see the last paragraph in Gazquez's 1997 paper[442]). Combined, however, they give abundant qualitative and quantitative arguments in favor of the HSAB principle, indicating however that, when going to numerical applications, the approximations involved should always be kept in mind.

In practice, much use is made of the working equation put forward by Gazquez and co-workers,[443,444] writing ΔE_{AB} as

$$\Delta E_{AB} = \Delta E_{AB,\nu} + \Delta E_{AB,\mu} \tag{259}$$

with

$$\Delta E_{AB,\nu} \approx -\frac{1}{2}\frac{(\mu_A - \mu_B)^2}{S_A + S_B} S_A S_B \qquad \left(= -\frac{1}{2}\frac{(\mu_A - \mu_B)^2}{\eta_A + \eta_B}\right) \tag{260}$$

$$\Delta E_{AB,\mu} \approx -\frac{1}{2}\frac{\lambda}{S_A + S_B} \tag{261}$$

where Parr's dissection in two steps is kept: the first term $\Delta E_{AB,\nu}$ expressing the gain in energy upon equalizing chemical potentials at fixed external potential, and the second term $\Delta E_{AB,\mu}$ being identified as the rearrangement term at fixed chemical potential. λ is a constant involving the effective number of valence electrons in the interaction and the proportionality constant k between S_{AB} and $S_A + S_B$ (eq 255).

In the preceding discussion, we considered the HSAB principle at the global level, i.e., neglecting the local characteristics of the interacting partners. In the next section, it will be seen that extensions to various levels of locality were presented and used. (For a review, see ref 445.)

b. The Local Level. Mendez and Gazquez proposed a semilocal version of the working equation (259), for the cases in which a system A interacts with B via its kth atom, thus transforming eqs 259−261 into

$$\Delta E_{AB,k} \approx -\frac{1}{2}\frac{(\mu_A - \mu_B)^2}{S_A f_{Ak} + S_B} S_A S_B f_{Ak} - \frac{1}{2}\frac{\lambda}{S_A f_{Ak} + S_B} \tag{262}$$

where the authors introduced the condensed Fukui function f_{Ak} for atom k in the acid A. Within the context of the grand potential approach, they transformed eq 248 into

$$\Delta\Omega_{Ak} \approx -\frac{1}{2}\frac{(\mu_A - \mu_B)^2}{(S_A + S_B)^2} S_B^2 S_A f_{Ak} \tag{263}$$

and similarly,

$$\Delta\Omega_{Bl} \approx -\frac{1}{2}\frac{(\mu_A - \mu_B)^2}{(S_A + S_B)^2} S_A^2 S_B f_{Bl} \tag{264}$$

if the interaction occurs via atom l of the base B.

Minimizing $\Delta\Omega_{Ak}$ with respect to S_A for a given $\mu_A - \mu_B$, S_B, and f_{Ak} leads to

$$f_{Ak} = f_{Bl} \tag{265}$$

However, since it was found at another stage of the analysis that $S_A = S_B$ guarantees the minimization of $\Delta\Omega_{Ak}$ with respect to S_A at fixed $\mu_B - \mu_A$ and S_B (and analogously for $\Delta\Omega_{Bl}$), it was concluded that the interaction sites may be characterized by the condition

$$s_{Ak} = s_{Bl} \tag{266}$$

It should be mentioned that the equation is, in fact, a particular case of the general expression in which S_A may or may not be equal to S_B and f_{Ak} may or may not be equal to f_{Bl}, but

$$S_A f_{Ak} = S_B f_{Bl} \tag{267}$$

and therefore

$$s_{Ak} = s_{Bl} \tag{268}$$

Geerlings et al.[446] obtained eq 268 directly by assuming from the start a direct interaction between atom k of A and atom l of B. Calculating $\Delta\Omega_{Ak}$ and $\Delta\Omega_{Bl}$ yields the expressions

$$\Delta\Omega_{Ak} \approx -\frac{1}{2}\frac{\mu_B - \mu_A}{(s_{Ak} + s_{Bl})^2} s_{Ak} s_{Bl}^2 \tag{269}$$

$$\Delta\Omega_{Bl} \approx -\frac{1}{2}\frac{(\mu_B - \mu_A)^2}{(s_{Ak} + s_{Bl})^2} s_{Bl} s_{Ak}^2 \tag{270}$$

Minimizing $\Delta\Omega_{Ak}$ with respect to s_{Ak} at fixed $\mu_B - \mu_A$ and s_{Bl} directly yields the demand (eq 268).

The minimization of $\Delta\Omega_{Bl}$ with respect to s_{Bl} at fixed $\mu_B - \mu_A$ and s_{Ak} yields exactly the same requirement. The total stabilization energy ΔE is obtained as

$$\Delta E = -\frac{1}{2}(\mu_A - \mu_B)^2 \frac{s_{Ak}\, s_{Bl}}{s_{Ak} + s_{Bl}} \tag{271}$$

which generalizes eq 260.

The softness-matching criterion in the case of multiple sites of interaction has been cast in the form of the minimization of a quadratic form by Geerlings et al.,[446] here denoted as Σ (and later applied by these authors, Nguyen and Chandra, and others, vide infra):

$$\Sigma = (s_{Ak} - s_{Bl})^2 + (s_{Ak'} - s_{Bl'})^2 \tag{272}$$

where k and k' are sites of reactivity on A, and l and l' are sites of reactivity on B.

This expression is extremely suitable for studing cycloaddition reactions (softness matching at a local−

local approach[445]). In the case of a single interaction site at one of the partners, say A

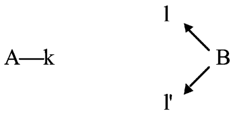

(e.g., free radical addition to olefins and [2 + 1] cycloadditions between isocyanide and (heteronuclear) dipolarophiles[253,447,448]), it was proposed to look at the difference between

$$|s_{\mathrm{A}k} - s_{\mathrm{B}l}| \qquad \text{and} \qquad |s_{\mathrm{A}k} - s_{\mathrm{B}l'}|$$

Cases studied in the literature involve the cycloaddition of HNC to simple dipolarophiles, where it has been assumed in all cases that local softness values are positive, as they usually are. For an in-depth discussion on the positiveness of the Fukui function, being equal to the local softness divided by the total softness (eq 112), the latter value being always positive, see also section III.B.3.

Ponti[449] generalized this approach by explicitly calculating the difference between grand potential changes, neglecting the charge reshuffling term. In the case of one interacting site k at one of the partners A, the most favorable interaction site turns out to be governed by the smallest local softness, $s_{\mathrm{B}l} < s_{\mathrm{B}l'}$, irrespective of the softness of the atom k on A. The cases considered in refs 253 and 447 were shown to give the same regioselectivity as that obtained with the Ponti criterion, $s_{\mathrm{B}l} + s_{\mathrm{B}l'} < 2s_{\mathrm{A}k}$. In the case of two interacting sites on each reaction partner, our choice has again been justified. Indeed, other criteria of the local softness-matching type,

$$\Delta s_k = (|s_{\mathrm{A}k} - s_{\mathrm{B}l}|^n + |s_{\mathrm{A}k} - s_{\mathrm{B}l'}|^n)^{1/n} \qquad n = \pm 1, \pm 2, \ldots \quad (273)$$

may be presented, the cases' arithmetic mean ($n = 1$) and harmonic mean ($n = -1$) being not less or more reasonable than the root-mean-square mean ($n = 2$) used in ref 446. However, it was shown by Ponti that the choice $n = 2$ shows complete equivalence with the criterion of separate minimization of grand potential invoked as the "figure of merit" in Ponti's study. Further discussion of the results as such will be given in section IV.C.2.

On the basis of an energy perturbation method, Li and Evans[194,450] presented a slightly different formulation, indicating that, for a hard reaction, the site of minimal Fukui function is preferred, whereas for a soft reaction, the site of maximal Fukui function is preferred. Nevertheless, when this argument is analyzed in detail, the proximity of low or high softness values for hard or soft interactions, as advocated by Gazquez and Mendez, also emerges from this paper.

One of the most extensive softness calculations reported to date was done by Galvan and co-workers.[451] Using total energy pseudopotential calculations,[452] the local softness function s($\boldsymbol{r}$) of Charybdotoxin was studied. This 37-residue polypeptide has been extensively used in site-directed mutagenesis experiments as a template to deduce models for the external pore appearance of K^+ channels. In the analysis of $s^+(\boldsymbol{r})$ and $s^-(\boldsymbol{r})$ (and its complement, the MEP), regions of the size of amino acids were considered in a HSAB discussion, at the local level, this order of magnitude being appropriate to correlate with site-directed mutagenesis experiments.

Another beautiful application of the HSAB at the local level is the study by Galvan, Dal Pino, and Joannopolous on the Si system. By using probe atoms of different softness (Ga and Si), softer regions in the cluster were seen to interact preferably with the softer atom (Ga).[453] These authors also analyzed the process of impurity segregation at grain boundaries as a chemical reaction between the impurity and the interface. The HSAB principle at the local level was used to predict the most probable site for impurity accumulation. A soft impurity atom will preferably attack the softer surface, having a larger $s^+(r)$ value. A detailed investigation was performed on a germanium grain boundary[454] and yielded results in accordance with the HSAB principle. Matching of the softness values of arsenic and gallium leads to the conclusion that arsenic atoms must segregate at the grain boundary considered, as opposed to gallium.

It should be noted that Nalewajski et al.,[455] in the context of semiempirical charge sensitivity analysis at atomic resolution, presented a regional softness-matching criterion in terms of a maximum complementarity rule, looking for the largest difference between the softness of the basic and acceptor atoms of each newly formed bond. Further work is necessary to reconcile with the results cited above this alternative view, formulated in a two-reactant approach.

Coming back to the interaction energy evaluation proposed by Gazquez and Mendez,[173,443] an important issue to be discussed remains the λ quantity in the reshuffling term at constant chemical potential. In their initial study on the regioselectivity of enolate alkylation,[444] a λ value of 0.5 was used without further justification. This value was also considered by Geerlings et al.[456] in a more quantitative study on this topic, with explicit softness evaluation of the alkylating agent and the solvent effect, thus working in a global–local approach[445] for the interaction energy. In the study by Mendez, Tamariz, and Geerlings[457] on 1,3 dipolar cycloaddition reactions, the dependence of the total interaction energy, evaluated at a local (dipole)–global (dipolarophile) level, on λ indicates that regioselectivity in the reactions between benzonitrile oxide and vinyl *p*-nitrobenzoate and 1-acetylvinyl *p*-nitrobenzoate is predicted correctly as long as $\lambda > 0.2$.

The problem of adequately quantifying λ, involved in a term in the interaction energy which may become dominant in the case of weak interactions, was studied recently by Pal and co-workers.[458,459] Pal and Chandrakumar[458] stated that λ, being the product of an effective number of valence electrons and the proportionality constant k in eq 246, could be related to the change in electron densities of the system before and after the interaction process. This quantity can then, for system A, be written as

$$\lambda_A = \sum_{i}^{M} N_{A,i}^{eq} - \sum_{i}^{M} N_{A,i}^{0} \tag{274}$$

where the summation over i runs over all M atoms of A participating in the interaction, and the superscripts “eq” and “0” refer to the molecule AB and the isolated atom A, respectively. N denotes the number of electrons.

Analogously, one has

$$\lambda_B = \sum_{j=1}^{M} N_{B,j}^{eq} - \sum_{j=1}^{M} N_{B,j}^{0} \tag{275}$$

As obviously $\lambda_A = -\lambda_B$, the λ value for the interaction has been recovered in this way. In the case of interactions of small molecules (N_2, CO_2, CO) with Li, Na, and K zeolites, studied using Mulliken’s population analysis [3-21G(d, p) vs 6-31G(d,p)], λ values of the order of 0.1 or 0.05 were obtained, depending on the basis set. In a study on the interaction of DNA base pairs, values of the order of 0.01 were obtained.[459] Note that, in ref 459, multiple site effects were included by summing equations such as eq 262 over all possible interacting subsystems. As the quantity obtained via eqs 274 and 275 is highly method dependent, further work needs to be done to settle this point.

A very recent and important critical study by Chattaraj[460] should be mentioned at the end of this HSAB section, pointing out, as intuitively expected, that the Fukui function is not the proper descriptor for hard−hard interactions because, in the Klopman terminology,[461] they are not frontier controlled. In early studies reported by our group, e.g., on the electrophilic substitution on benzene, it was stressed that, for hard reactants, the local softness or, equivalently, the Fukui function is not an adequate descriptor and local hardness should be preferred, albeit that an unambiguous definition is lacking. Chattaraj concludes that the Fukui function is predominant in predictive power only in soft−soft interactions, where the covalent term in the interaction energy, written by Parr and Yang[27] as

$$\Delta E_{cov} = -\frac{(\mu_B^0 - \mu_A^0 + \int f_B(\boldsymbol{r})\Delta\nu_B(\boldsymbol{r})\,d\boldsymbol{r} - \int f_A(\boldsymbol{r})\Delta\nu_A(\boldsymbol{r})\,d\boldsymbol{r})^2}{4(\eta_A^0 + \eta_B^0)} \tag{276}$$

dominates; hard−soft interactions are generally small.[462] For hard−hard interactions, one faces the challenge of the local hardness definition, albeit that the approximation of eq 143 was successful (see section IV.C.3). A local version of the Coulombic-type interactions, as suggested by Chattaraj, may always be invoked:

$$F_{ij}^{AB} \approx \frac{q_i^A q_j^B}{r_{ij}} \tag{277}$$

where F_{ij}^{AB} is the interaction force between atoms i and j of A and B, respectively, q_i^A and q_i^B being their net charges and r_{ij} their inter-atomic distance. As such, minimum Fukui function conditions may complement the maximum net charge conditions.

In the next sections, the maximum hardness principle will be discussed, one of its immediate applications and/or support being the directionality of reactions. However, this aspect can obviously also be treated in a HSAB context, the applications being relatively scarce in recent literature. Pearson’s book[157] advocated a better understanding of the HSAB principle in terms of the exchange reaction

$$AB + CD \rightarrow AC + BD$$

rather than the binary complex formation,

$$A + B \rightarrow AB$$

Recent numerical data by Chattaraj and co-workers[463] on the interaction of soft (Ag^+) and hard (HF) acids with NH_3 and PH_3 support this view. The exchange reaction

$$[Ag(NH_3)]^+ + FH\text{- - -}PH_3 \rightarrow FH\text{- - -}NH_3 + [Ag(PH_3)]^+$$

which has been shown to be exothermic, reflects the higher tendency of the harder base (NH_3) to bind to the harder acid (HF) and of the softer base (PH_3) to bind to the softer acid (Ag^+).

3. The Maximum Hardness Principle

Pearson formulated his principle of maximum hardness (MHP) in 1987, under the form that “there seems to be a rule of nature that molecules arrange themselves to be as hard as possible”.[158] (For an extensive review on various aspects of chemical hardness by Pearson himself, see refs 157, 464, and 465.)

A series of studies by Parr, Zhou, and co-workers[466−470] on the relationship between absolute and, later, relative hardness and aromaticity of hydrocarbons supported this idea (see also section IV.B.3 on aromaticity), and in 1991, a formal proof of the principle of maximum hardness was given by Parr and Chattaraj.[440] The proof is based on a combination of the fluctuation dissipation theorem from statistical mechanics and density functional theory. It will not be treated here in detail, as different texts already extensively comment on it.[157,465,466] A point of utmost interest to be mentioned here, however, is that the proof relies on the constancy of both the external and chemical potentials, ν and μ, a severe restriction which will put heavy constraints on the applicability of the principle, or serious question marks on results obtained when one or two of these constraints are relaxed (vide infra). The validity of the proof has been questioned by Sebastian,[471a] who however later reported errors in his numerical counterexamples.[471b] In 2000, Ayers and Parr[197] presented conclusive evidence for the validity of the original Parr−Chattaraj proof.[440]

Another approach was followed by Liu and Parr.[282] Using functional expansion methods, they obtained, up to second order, the following expression for $E[N,\nu]$:

$$E[N,\nu] = N\mu - \frac{1}{2}N^2\eta + \int \nu(\mathbf{r})[\rho(\mathbf{r}) - Nf(\mathbf{r})]\,\mathrm{d}\mathbf{r} - \frac{1}{2}\int\int \rho(\mathbf{r})\rho(\mathbf{r}')\omega(\mathbf{r},\mathbf{r}')\,\mathrm{d}\mathbf{r}\,\mathrm{d}\mathbf{r}' \tag{278}$$

connecting the total energy, the chemical potential μ, the hardness η, the Fukui function $f(\mathbf{r})$, and the response function $\omega(\mathbf{r},\mathbf{r}')$ in the canonical ensemble. Neglecting the contribution from the last two local terms, one finds, at fixed N, μ, and ν, that the larger the hardness, the lower the energy (note the minus sign in front of the second term, not present in a typical Taylor expansion). In view of the restrictions, and as one does not know the relationship between the unconstrained variables during a variational process for the global hardness, the authors do not consider the equation as "the final statement" but rather as offering a favorable viewpoint.

Early numerical tests by Pearson and Palke[472] on NH_3 and ethane (comparison of η values at equilibrium geometry and upon distortions along symmetry coordinates) indicated that the molecular point groups are, indeed, determined by maximal hardness, equilibrium bond angles and distances being determined by the electrostatic Hellmann−Feynman theorems: non-totally symmetric distortions yield maximal η at the equilibrium geometry, whereas for totally symmetric distortions, no maximum is found. Similar studies were performed early by Chattaraj and coworkers[473] on PH_3, for which the results found were similar to those found for NH_3 in ref 472, and on the internal rotation in $H_3X{-}YH_3$ (X, Y = C, Si), B_2H_6, and C_2H_4, which were seen to obey the maximum hardness principle[474] with minimum hardness values at the high-energy conformer.

These authors also compared in ref 473 the isomers HCN and HNC and found a higher hardness for the stabler isomer (HCN), the μ values, however, not being identical. Investigation of seven isomers of Si_2H_2 led to analogous conclusions, indicating that the constraints of fixed chemical and external potentials associated with the original proof may be relaxed. In the period from 1992 to 1993, the directionality of inorganic reactions[475] and the stability of metallic clusters (Li_n, $n = 2{-}67$)[476] were also found to obey the MHP, the former study joining previous, more intuitive work by Pearson.

In fact, in his textbook, Huheey already came to the conclusion that "we are therefore led to believe that, at least in these examples, the presumably electrostatic energy of the hard−hard interaction is the major driving force" (ref 160, p 320). We note that, in the cluster study, again the external potential is not a constant and the chemical potential is only "on the average" a constant. Chandra[477] pointed out that there is a linear relationship between hardness and bond order, and in a study on ethane, it was seen that the hardness is maximum when the molecule was in the staggered conformation.

Datta et al.[475,478] used empirical and semiempirical η values, together with experimental $\Delta H°$ values, to study exchange reactions,

$$AB + CD \rightarrow AC + BD$$

In general, it turns out that exchange reactions evolve in a direction so as to generate the hardest possible species, an example being the Pauling−Pearson paradox[160] for

$$LiI + CsF \rightarrow LiF + CsI$$

(exothermic reaction with failure of Pauling's bond energy equation[95]). A study by Ghanty and Ghosh[479] on exchange reactions of the above-mentioned type based on ΔH and $\Delta\alpha^{1/3}$ [the cube root of the change of dipole polarizability between the products and the reagents, taken as a measure of softness (see, e.g., section IV.A)] is to be mentioned: in the 13 cases studied, a negative ΔH was always accompanied by a lowering of the average value of $\alpha^{1/3}$, indicating that products were always harder than reactants. These results are in line with earlier work by Datta et al.,[475,478] who found that, in exchange reactions, the average hardness of the products is higher than that of the reactants and that the direction of the reaction is so as to produce the hardest possible species.

This problem has more recently (1997) been reconsidered by Gazquez,[480] who applied the methodology described in section III.C.2-a to a bond formation process. In this contribution, he succeeded in writing the ΔE_μ term in eq 259 in terms of the hardness of the reactants:

$$\Delta E_{AB,\mu} = -\frac{1}{2}N_e^2\frac{\eta_A^0\eta_B^0}{\eta_A^0 + \eta_B^0} \tag{279}$$

N_e being the effective number of valence electrons involved. He came to the conclusion that, in general, the reaction energy is negative when the sum of the hardness of the products is larger than that of the reactants.

Very recently, Hohm[481] studied atomization reactions,

$$A_mB_n \rightarrow mA + nB \tag{280}$$

and considered the change in dipole polarizability,

$$\Delta\alpha = \sum_i \nu_i\alpha_i \tag{281}$$

ν_i being the stoichiometric coefficients, taken to be negative for the reactants. The cube-root version of eq 281 was also considered:

$$\Delta\alpha_{CR} = \sum_i \nu_i\alpha_i^{1/3} \tag{282}$$

and confronted with the atomization energies D^{at} taken from the literature.

A linear relationship was found:

$$D^{at} = A + B\Delta\alpha \tag{283}$$

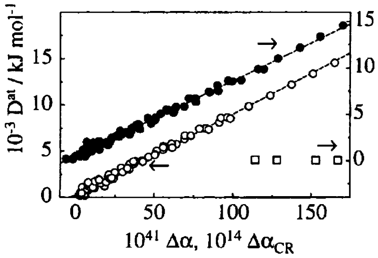

Figure 8. Plot of the atomization energy D^{at} (10^3 kJ/mol) vs Δα (●), right scale, and $\Delta\alpha_{CR}$ (○), left scale, for the atomization reaction (280) for a series of nonconjugated compounds. The data points □ are $\Delta\alpha_{CR}$ for a series of alkali metal diatomic molecules and refer to the scale on the right-hand side. The units for the Δα and $\Delta\alpha_{CR}$ values are $C^2\ m^2\ J^{-1}$ and $(C^2\ m^2\ J^{-1})^{-1/3}$, respectively. Reprinted with permission from ref 481. Copyright 2000 American Chemical Society.

Correlation coefficients r of 0.9963 (Δα) and 0.9968 ($\Delta\alpha_{CR}$) were found for a series of ±90 molecules, the correlation being worse when conjugated systems were included. $\Delta\alpha_{CR}$ values are invariably positive, whereas for Δα some exceptions (homonuclear diatomics) are found. B is positive, indicating that higher atomization energies are found when Δα is larger, i.e., for larger differences between the molecules' hardness and that of their constituent atoms. Figure 8 shows the correlation between D^{at} and Δα and $\Delta\alpha_{CR}$ for a series of more than 80 nonconjugated compounds.

Datta was the first to point out an interesting corollary of the MHP, namely that the transition state (TS) of a reaction should have a minimum hardness value as compared to other points along the reaction path.[482] He reported the first hardness profiles: the inversion of ammonia and the intramolecular proton transfer in malonaldehyde, calculated at the semiempirical MNDO level.

Evidence for his thesis results from these plots: η reaches a minimum at the TS (it was checked that the change in μ along the reaction path is small in the second case, μ however reaching a maximum in the first case).

Gazquez, Martinez, and Mendez[483] studied hardness variations upon elongation of homonuclear diatomics, writing the energy evolution at a fixed chemical potential of an N-electron system as (cf. the demand for fixed μ)

$$\Delta E_{\mu} \approx -\frac{1}{2}N^2\Delta\eta \qquad (284)$$

indicating that when a system evolves toward a state of greater hardness under conditions of fixed chemical potential, its stability increases ($\Delta E < 0$). Numerical calculations of the R dependence of μ and η showed that the changes in η are considerably larger than those in μ and that ΔE is, indeed, roughly proportional to $\Delta\eta$, implying that increasing hardness is accompanied by greater stability.

In recent years, many studies have appeared in which an application/validation of the maximum hardness principle, besides the directionality of a reaction, was sought, concentrating mainly on MHP in internal rotation and isomerization processes. An overview of this vast literature is presented below without going into detail: some selected, representative examples are discussed in section IV.C, where studies by Toro Labbé and co-workers are the focus.

- internal rotations (nitrous acid and hydrogen persulfide;[484-486] HO−NS, HS−NO, HS−NS, FO−NO, HO−OH, and HO−OF;[485-487] HS−OH;[487] HSSH[488])
- cis−trans isomerization (HN=NH),[489a] including the effect of solvent[489b]
- intramolecular rearangements (HNC → HCN; HClO → HOCl; HONS → HSNO; H_2SO → HSOH; H_2SiO → HSiOH; F_2S_2 → FSSF; H_3PO → H_2POH; H_3AsO → H_2AsOH; CH_2SH_2 → CH_3SH)[490]
- vibrations in NH_3 and H_2S[491]
- double-proton-transfer reactions in HCXXH- - -HXXCH (X = O, S)[491]
- keto−enol tautomerism in acetyl derivatives CH_3COX [X = H, OH, CH_3, OCH_3, NH_2, $N(CH_3)_2$, OCHO, F, Cl, Br][492]

Kar and Scheiner studied 1,2-hydrogen shift reactions in molecules of the type HAB (AB = CN, SiN, BO, AlO, BS, AlS, BeF) and HAB^+ (AB = CO, SiO, CS, N_2)[493] and extended their study to open-shell HAB → HBA isomerizations (HNO, HSO).[494]

Russo and collaborators studied the isomerizations of HCN, HSiN, N_2H_2, HCP, and O_3H^+ using their technique of the MO-resolved hardness tensor described in section III.B.2,[180] the protonation of CH_2SO,[495] and the isomerization of HNO and ClNO.[496]

Kolandaivel studied isomers of XC(O)OX′ (X, X′ = F, Cl), C_2H_3NO (nitrosoetylene), C_2H_2, and HCNC and hydrogen-bonding complexes HF- - -HCN, HF- - -HCl, and CH_3OH- - -H_2O;[497] later they extended their study to a series of 18 molecules showing "positional and geometrical" isomerism.[498]

Ghanty and Ghosh studied the influence of bond distortion or external changes on the hardness of HF, H_2O, and NH_3[499] and the internal rotation in formamide and thioformamide,[500] and in the isomerization reaction HAB → HBA (AB = BO, AlO, GaO, BS, AlS, CN, CO^-, CS^-, SiO^-, SiS^-).[479]

Studies by our group concentrated on cycloadditions of HNC[448] and CO and CS to acetylenes.[501,502] Studies by M. T. Nguyen treated the 1,3-cycloadditions of R−N=S[503] and the 1,3 dipolar cycloadditions to phosphorus-containing dipolarophiles.[504] Studies by Chandra focused on internal rotation in ethane[505] and substituted methyl radicals ($XCH^{\bullet}_2$; X = BH_2, CH_3, NH_2, OH)[506] and the 1,3 dipolar cycloaddition of fulminic acid to acetylene.[507]

It should be noted that, in some of the abovementioned papers, the maximum hardness principle was studied under the form of a minimal softness−minimal polarizability principle: indeed, for many systems, hardness calculations often yield problems in the finite difference approximation (eq 56), whereas polarizability calculations can now routinely be performed e.g., in the finite field approach.[508] As polarizability (often the cube root is used) for atomic and molecular systems shows a proportionality with softness (see section IV.A), the use of a minimum softness−minimum polarizability criterion is a useful alternative to the MHP.

The whole of these studies can be summarized as follows: in many but not all cases, the hardness profile shows a minimum, situated sometimes (but mostly not) at the TS, giving support to the MHP, although the demand for fixed μ and ν was fulfilled in practically no case studied. Neverthless, some cases give serious deviations, which are mostly ascribed by the authors to deviations from the fixed μ and ν.

As a whole, the situation for the MHP is still less clear-cut than for the EEM (cf. section III.C.1), which is now widely accepted. It is also less convincing than the HSAB principle, for which nevertheless the proof(s) was (were) shown to contain a number of approximations/pitfalls (cf. III.B.1).

Inspection of all published material shows that the demand for fixed ν and μ is (obviously) never fulfilled. The crucial question then becomes, Which deviations from the ideal situation are allowed in order to have the MHP working? Only if some insight is gained in this issue may a predictive power be attributed to the MHP; otherwise, the phase of “testing” may be extended further and will become too long for practical purposes. Note that, very recently, M. Solà and co-workers showed that, in the favorable case of non-totally symmetric vibrations (the B_2 normal mode of pyridine at 1304.4 cm^{-1}), where μ and $\nu(\boldsymbol{r})$ stay approximately constant, neither the MHP nor the MPP is obeyed.[509]

Also very recently, Chandra and Uchimaru[510] addressed this question using the finite difference approach to the hardness, written as

$$\eta = \frac{1}{2}(E_{N-1} + E_{N+1} - 2E_N) \tag{285}$$

They considered $\partial\eta/\partial q$, q being the reaction coordinate, as an “operational hardness profile”. It is easily seen that $\partial\eta/\partial q$ goes to an extremum at the TS, when

$$\left(\frac{\partial E_{N-1}}{\partial q}\right)_{\mathrm{TS}} = -\left(\frac{\partial E_{N+1}}{\partial q}\right)_{\mathrm{TS}} \tag{286}$$

or when both energy derivatives are zero, which is the case when the $(N-1)$- and $(N+1)$-electron systems have extrema at the TS. For a symmetrical reaction profile, this is obviously the case, leading to the conclusion that operational hardness profiles along the reaction coordinate have an extremum at the symmetric point (e.g., the D_{3h} TS for the inversion of NH_3). (See also ref 511 for a discussion on the effect of symmetry on the hardness profile.) From the numerical data in the literature (e.g., refs 479, 482, 491, and 500), it is seen that the extremum should be a minimum, which was shown to depend on the difference in curvature of the $N-1$ and $N+1$ systems at the TS.

A similar approach for the chemical potential indicates that the operational chemical potential, $(E_{N+1} - E_{N-1})/2$, also goes through an extremum at the TS, indicating that the MHP can hold even when neither μ nor ν remains constant if the energy profiles for the $(N-1)$- and $(N+1)$-electron systems satisfy certain conditions.

A detailed analysis of the operational hardness profile for an unsymmetrical reaction coordinate (isomerization of HCN to HNC) shows that the point of lowest hardness does not necessarily correspond to the TS. Considering the CH_3 radical case in detail (where a minimum hardness value along the reaction coordinate of inversion is found when the energy reaches its minimum value), the authors finally question whether the observations made in the literature for symmetric reaction profiles can be considered as tests of the MHP. They consider this a natural conclusion, since the MHP requirements (fixed μ and ν) cannot be satisfied all along the reaction coordinate of a chemical process. Further research is certainly needed in the case of reactions in which orbital control is predominant. It would be interesting to link the orbital picture with the orbital-free hardness concept, introducing the phase factor[512] in the analysis. A first example in this direction was recently given by Chattaraj and co-workers[513] on the electrocyclic transformation between butadiene and cyclobutene. On the basis of polarizability calculations of the conrotatory and disrotatory TS, a higher hardness value was found for the symmetry-allowed conrotatory mode, in agreement with the Woodward−Hoffmann rules.[514]

An interesting concept within the MHP context is the activation hardness $\Delta\eta^{\ddagger}$, introduced by Zhou and Parr[515] as the difference between the hardness of reactants and TS:

$$\Delta\eta^{\ddagger} = \eta_{\mathrm{R}} - \eta_{\mathrm{TS}} \tag{287}$$

Studying the (kinetically controlled) orientation of electrophilic aromatic substitution,[516] the faster reaction, or the preferred orientation, was found to be accompanied by the smaller activation hardness, as obtained via simple Huckel MO theory.

A complementary study by Amic and Trinajstic on nucleophilic aromatic substitution (flavylium salts) confirmed the $\Delta\eta^{\ddagger}$ capability.[517]

Ray and Rastogi applied a similar methodology to study the cycloaddition of even linear polyenes and obtained perfect matching for both the thermal and photochemical reactions with the Woodward−Hoffman rules.[518] Similar successes were obtained in the case of sigmatropic shifts.[519]

An indirect way to use the activation hardness was followed by the present authors and M. T. Nguyen in studies on regioselectivity in which the identity of the reactants for two regioisomeric TS implies that only the hardness values of the two TS have to be considered. This technique was successful in discussing cycloadditions,[448,501−504] yielding results that were complementary to those of, e.g., (local) softness matching (cf. section III.C.2).

We finally note that Toro Labbé and co-workers extensively used the activation hardness concept in the study of rotational isomerization processes,[484,487] the cis−trans isomerization of diimide,[489] and the double-proton-transfer reaction in $(HCX{-}XH)_2$.[491]

To end this section, the remarkable and beautiful analogy between chemical and physical hardness and the corresponding maximum hardness principles[520,521] (for reviews, see refs 465, 522, and 523) should be mentioned. Only a very brief account of this work will be given, the subject of this review being chemically orientated.

The chemical hardness definition eqs 57 and 58 should be compared with the classical thermodynamic equation,

$$\left(\frac{\partial \mu_0}{\partial N}\right)_{V,T} = \frac{V}{\kappa} \tag{288}$$

in which μ_0 is the ordinary chemical potential and N the number of moles. The compressibility κ can clearly be placed on equal footing with the chemical softness and can be considered as a measure of the physical or mechanical softness. Parr has shown[524] that, for various crystalline solids, $\kappa^{-1}V_0$ (V_0 being the molar volume) is proportional to the crystal hardness as measured by Moh's scale[525] and other comparable scales.[523] Recent details on the use of electronic structure calculations in predicting physical hardness can, for instance, be found in contributions by Louie and Cohen.[526,527] It therefore seems reasonable to call $\kappa^{-1}V_0$, having the dimensions of energy, the "physical hardness". Whereas chemical hardness is a measure of resistance to changes in the electron distribution of a system, physical hardness measures the resistance to change of the nuclear positions of the system. Along the lines followed in the maximum (chemical) hardness proof by Parr and Chattaraj,[440] one expects the resistance to be the largest at the equilibrium state of a condensed system, recovering a principle of maximum physical hardness,[520,521] often written in terms of a maximum value for BV_0, B being the bulk modulus.

In the fundamental concepts and principles sections treated previously in this paper, some applications were highlighted when we considered them as being directly relevant as an illustration, irrespective of the nature of the substrate(s).

In the Applications section (section IV), however, a detailed discussion will be given of applications classified according to the structures involved and their interactions: atoms, functional groups, molecules, different types of reactions, etc.

IV. Applications

A. Atoms and Functional Groups

In this section, the computation and application of the above-mentioned DFT-based chemical concepts for atoms and functional groups will be reviewed. As discussed in section II.C, the contribution by Parr and co-workers opened the gate to nonempirical evaluations of these quantities, for which basically three approaches can be adopted. In the first approach, one derives analytically the energy functional $E[\rho]$ with respect to the number of electrons using some kind of approximate exchange correlation functional. In the second approach, the finite difference approximation described in general in section III.B, one calculates the energy of the system (atom, functional group, or molecule) for different numbers of electrons at fixed nuclear configurations; this approach has, until now, by far been the most adopted. In the third strategy, the so-called chemical approximation, one evaluates the property using empirical correlations (that can, however, be based for some part on first-principles derivations) with other more traditional chemical concepts. In the case of electronegativity, however, one would end up again in the period before the late 1970s. As stated in the Introduction, Pauling defined the electronegativity as "the power of an atom in a molecule to attract electrons to itself",[93-95] and many definitions have been developed since then, each one providing a set of values for the elements, and all showing some degree of relation and correlation. A review of the most important atomic and group electronegativity scales can be found in the contribution of Mullay.[114] Recently, Murphy, Meek, Allred, and Allen formulated nine rules, which an appropriate electronegativity scale should obey.[528] Some of these guidelines are that it should be a free atom definition, expressed as an energy per electron, and it must have a "quantum mechanically viable definition", i.e., it should be compatible with quantum chemical concepts such as quantum numbers, energy levels, and shell structure. These and other rules were applied to the Pauling electronegativity scale in this contribution; the scale was found to violate more than half of the criteria put forward by these authors.

Bartolotti, Gadre, and Parr made use of Slater's transition-state concept within X_α theory and obtained an expression for the electronegativity in terms of the X_α Lagrange multipliers.[529] As such, they obtained electronegativities for 54 main group elements of the Periodic Table, which were in good agreement with other electronegativity scales. Similar calculations were reported by Sen et al. for rare earth atoms, made using relativistic X_α theory.[530] The work of Bartolotti, Gadre, and Parr was extended by Robles and Bartolotti to the use of spin-polarized density functional theory,[531] in combination with the X_α and Gunnarson−Lundqvist exchange correlation functional[532] and a transition-state process involving the change from $N - \delta$ to $N + \delta$ electrons. The number of atoms studied was extended to 86, and ionization energies, electron affinities, and hardnesses were also evaluated. Gazquez and Ortiz proposed a Taylor series expansion of the energy of an atomic system in the charge around the value of the neutral atom (cf. eq 60):[533]

$$E(Z,q) = E(Z,0) + q\left(\frac{\partial E}{\partial q}\right)_{Z,q=0} + \frac{q^2}{2!}\left(\frac{\partial^2 E}{\partial q^2}\right)_{Z,q=0} + ... \tag{289}$$

Truncating after second order and identifying the first- and second-order derivatives as the electronegativity and hardness,

$$E(Z,q) = E(Z,0) + q\chi + q^2\eta \tag{290}$$

they correlated the relaxed first-order derivative and the unrelaxed second-order derivative from X_α and hyper Hartree−Fock theory with the frontier orbital energies and the self-repulsion integral of the atomic highest occupied orbital. Remark, however, that this is a non-N-representable theory.[534] Relaxational effects were included in the second-order derivative by the application of a simple screening model, leading to the following expression for the isolated atom hardness:

$$\eta = \frac{1}{4}\langle r^{-1}\rangle_i \tag{291}$$

of which the evaluation requires only one calculation and where i is the index of the frontier orbital. This expression was used, together with the X_α expression of the electronegativity, $\chi = -\epsilon_i$, and a simple expression for the electronegativity of an atom in a molecule,[219] to calculate molecular electronegativities for some diatomic and polyatomic molecules, which were shown to be in good agreement with other estimates. These estimates were taken from ref 535 and calculated using Sanderson's geometric mean principle[113] with Mulliken electronegativities, based on the experimental first ionization energy and electron affinity.

Teller's theorem states that chemical binding between atoms does not exist in systems described by Thomas−Fermi and Thomas−Fermi−Dirac theory.[536,537] Upon observation that the chemical potential within Thomas-Fermi theory is zero and that it is a constant within Thomas−Fermi−Dirac theory, Alonso and Balbas calculated electronegativities for atoms and ions, starting from the energy density functional containing a Weiszacker type of kinetic energy functional and the local Dirac and Wigner formula for exchange and correlation, respectively.[130] They concluded that electronegativities obtained in this way show more or less the same trends as those calculated by more accurate models; the range of values spanned, however, was found to be more reduced. In this sense, they found that the key problem here is the treatment of the kinetic energy functional: a local treatment of $T[\rho]$ is not satisfactory, and the inhomogeneity of the electron density has to be included to get qualitatively useful and correct results. Sen calculated transition-state method electronegativities using spin-unrestricted X_α theory for several atomic Rydberg states.[538] (A more detailed account of the use of DFT-based reactivity descriptors for excited states is given in section IV.C.1.) For the atoms Li, Be, and B, it appears that a large decrease in the electronegativity is encountered when going from the ground state to the first excited state. In a study of the geometric mean principle for electronegativity equalization, Parr and Bartolotti found that the necessary condition for this principle to hold was the use of valence-state atomic energies that decay exponentially with increasing number of electrons (cf. section III.B.1).[395] On the basis of the experimental ionization energy and electron affinity for 34 neutral atoms, the experimental decay factor was found to be 2.15 ± 0.59. Finite difference electronegativies and hardness derived from experimental ionization energies and electron affinities for a large series of atoms, radicals, and molecules were published by Pearson.[119,120,539] Liu and Parr obtained electronegativities and hardnesses of atomic orbitals in different states of ionization using spin-restricted X_α theory.[140]

The atomic radius has been an important concept in many definitions of atomic electronegativities. This can be witnessed from the early works of Gordy[111] and Allred and Rochow,[112] defining the atomic electronegativity as the electrostatic potential and force respectively felt by the valence electron at a distance r away from the nucleus, r here being the atomic radius. The Sanderson electronegativity S also contains the atomic radius, i.e., $S \sim Z/r^3$.[113] Within the context of Thomas−Fermi−Dirac theory, Politzer, Parr, and Murphy investigated the points in space where the chemical potential equals the total electrostatic potential of the atom.[540] These points correspond to regions in space where

$$\frac{\delta T_s}{\delta \rho} + v_{xc} = 0 \tag{292}$$

Within the TFD model, eq 292 yields an equation in which the only unknown is ρ, and this was found to be satisfied for $\rho(r) = 0.00872$. This approach, later called the uniform density criterion,[541] thus justifies the approach adopted by Gordy.[111] The atomic radii obtained in this way, moreover, were found to show a good correlation with the single-bond covalent radius. This approach was generalized later by Harbola, Lee, and Parr for the hardness.[542] They showed that the atomic hardness can be expressed as the electrostatic potential due to the Fukui function at the covalent radius, which in turn can be obtained by the electrostatic potential of the positive and negative ions. On the basis of the DFT definition of the electronegativity and a simple bond charge model proposed by Pasternak,[543] Ray, Samuels, and Parr[535] showed a proportionality between $(I - A)^{-1}$ for atoms and the internuclear distance in homonuclear diatomic molecules before $I - A$ was identified as an approximation to the chemical hardness. Arulmozhiraja and Kolandaivel found a proportionality between the hardness and both the force constants and binding energies for diatomic molecules; they moreover stated that the hardness is a better indicator of chemical stability of molecules than the chemical potential.[247] As already stated, Gazquez and Ortiz derived a relationship between the chemical hardness and $\langle r^{-1}\rangle$. Komorowski stated that the van der Waals radii and not the covalent radii yield more realistic values for the hardness; the covalent radii were declared to be "inappropriate".[148,544] Moreover, the best correlation with the Parr and Pearson absolute hardness values was found for ionic radii derived from refractivity data. In Komorowski's work (cf. section IV.C.3-c), also the concepts of acidic and basic hardness were introduced, corresponding to the cases where electrons are added and subtracted from the system, respectively. Calculations were reported for atoms and free ions. Komorowski also derived an expression for the hardness in the so-called "electrodynamical model", providing a simple relationship between hardness and size.[148] This relationship is not unexpected, since in Pearson's original classification, hard species have, in general, been associated with small-size entities.

Much work has also been performed in the so-called "chemical approximation" to the hardness. When an atom is considered to be a metallic conducting sphere of radius r, the second-order derivative of its energy with respect to its charge, the hardness, is given by

$$\eta = (4\pi\epsilon_0 r)^{-1} \tag{293}$$

in the case where the radius is considered to be a constant and not a function of the charge on the sphere. The electric capacity of the sphere σ can then immediately be identified with the softness.[148] The concept of hardness has, indeed, long been related to the inverse of charge capacity, the ability of the atom in a molecule to absorb electronic charge, as described in section III.B.2.[169−171] Politzer, Murray, and Grice noticed that, as the neutral atom electronegativity increased, the charge capacity decreased.[545]

As the relationship between the polarizability and global softness is often used, some more attention will now be devoted to the rationalization of this proportionality.

Politzer was the first to put forward a relationship between the polarizability and the softness.[546] Vela and Gazquez used a local approximation to the softness kernel to derive an expression for the linear response function in terms of local and global components that are proportional to the Fukui function and global softness.[547] Indeed, the softness kernel in their work was approximated as

$$s(\boldsymbol{r},\boldsymbol{r}') \approx S f(\boldsymbol{r})\delta(\boldsymbol{r} - \boldsymbol{r}') \tag{294}$$

so that, using the Berkowitz−Parr relation[277] (eq 126), the linear response function becomes

$$\left[\frac{\delta\rho(\boldsymbol{r})}{\delta\nu(\boldsymbol{r}')}\right]_N = S f(\boldsymbol{r})(f(\boldsymbol{r}') - \delta(\boldsymbol{r} - \boldsymbol{r}')) \tag{295}$$

The energy change up to second order in $d\nu$ can thus be written as

$$\mathrm{d}E = \int \rho(\boldsymbol{r})\delta\nu(\boldsymbol{r})\,\mathrm{d}\boldsymbol{r} + \frac{1}{2}S\left[\left(\int f(\boldsymbol{r})\delta\nu(\boldsymbol{r})\,\mathrm{d}\boldsymbol{r}\right)^2 - \int f(\boldsymbol{r})(\delta\nu(\boldsymbol{r}))^2\,\mathrm{d}\boldsymbol{r}\right] \tag{296}$$

When the static dipole polarizabilities are considered, the change in external potential is given by

$$\delta\nu(\boldsymbol{r}) = \boldsymbol{r}\cdot\xi \tag{297}$$

where ξ represents a uniform field of unit amplitude. The second-order correction to the energy in this case is given by

$$E^{(2)} = -\frac{1}{2}\xi\cdot\alpha\cdot\xi \tag{298}$$

Here, α denotes the polarizability tensor.

One finally ends up with

$$\alpha = -S\left\lfloor\left(\int \boldsymbol{r} f(\boldsymbol{r})\,\mathrm{d}\boldsymbol{r}\right)^2 - \int \boldsymbol{r}\boldsymbol{r} f(\boldsymbol{r})\,\mathrm{d}\boldsymbol{r}\right\rfloor \tag{299}$$

For an atomic system, this equation can be further simplified to

$$\alpha = S\int r^2 \cos^2\theta\, f(r)\,\mathrm{d}r \tag{300}$$

indicating, indeed, that the polarizability is proportional to the global softness of the system.

A plot of the experimental polarizability of a series of neutral atoms vs the finite difference approximation to the softness, $1/(I - A)$, revealed a linear relationship. Vela and Gazquez also analyzed the case where the static perturbation corresponds to a point charge Q located as some position R far away. After some algebraic manipulation, the exact asymptotic expression for the induction energy or charge-induced dipole interaction was recovered, strengthening the conclusions of their work.

Equation 300 can be rewritten as

$$\alpha = \int r^2 \cos^2\theta\, s(r)\,\mathrm{d}r \tag{301}$$

suggesting a relationship between the local softness and local polarizability. It was pleasing to note that the local polarizability plots of Stott and Zaremba[548] and the atomic Fukui functions are similar.

In the framework of molecules absorbed in cages, Langenaeker, De Proft, Tielens, and Geerlings derived similar expressions,[549] also relating softness and polarizability. The proposed approximation to the softness kernel and similar equations were used by Perez, Contreras, and Aizman to obtain solvatation energies from the linear response function.[371] They showed an inverse linear relationship between the solvatation energies of the monatomic ions Li^+, Na^+, K^+, Rb^+, F^-, Cl^-, Br^-, and I^- and their softnesses.

Correlations between the polarizability and S^3 were also presented on a less rigorous basis by various authors. For atomic systems, Nagle demonstrated a proportionality between the softness and $(\alpha/n)^{1/3}$, where n represents the number of valence electrons.[550] Ghanty and Ghosh found, on an empirical basis, that the softness linearly correlates with $\alpha^{1/3}$ for a number of atoms and sodium clusters.[551] In a study of the relationship between the atomic softness and the electric dipole polarizability, Fuentealba and Reyes concluded that, in the case of both atoms and ions with one or two valence electrons, a good relationship exists between the latter property and the third power of the softness.[552] Note, however, that they claim that a general correlation between the polarizability and the softness cannot be expected because of the number of valence electrons, which varies along the Periodic Table. On the basis of the classical equations for the energy needed to charge a conducting sphere and its polarizability, Hati and Datta derived the following relationship between the hardness and the polarizability:[553]

$$\eta = \frac{1}{2}\left(\frac{C}{\alpha}\right)^{1/3} \tag{302}$$

where the value of C yields the closest reproduction of the experimental hardnesses. Further and more recent evidence for this cubic relationship was provided by Simón-Manso and Fuentealba within a local density approximation for the local softness. Their finding was supported by calculations on s-, p-, and d-block atoms, diatomics, and hydrocarbon molecules.[554]

Starting from the general expression of the frequency-dependent polarizability $\alpha(\omega)$, and after introducing some simplifications, Ghanty and Ghosh obtained the following simplified expression for the atomic polarizability:[555]

$$\alpha = k_\alpha \int \rho_{\mathrm{HOMO}}(r) r^3 \, \mathrm{d}r = k_\alpha \langle r^3 \rangle_{\mathrm{HOMO}} \quad (303)$$

where k_α is an empirical constant. Moreover, they derived an expression for the hardness as the ratio of two expectation values, i.e.,

$$\eta = k_\eta \frac{\langle r^3 \rangle_{\mathrm{HOMO}}}{\langle r^2 \rangle_{\mathrm{HOMO}}} \quad (304)$$

which, naively, can be identified with $\langle r \rangle$. Since there has also been a proposal for an inverse relationship between the electronegativity and the cube root of the polarizability, Ghanty and Ghosh[555] also proposed that

$$\chi = k_\chi (\langle r^3 \rangle_{\mathrm{HOMO}})^{1/3} \quad (305)$$

The empirical constants k_α, k_η, and k_χ were subsequently determined by minimizing the standard deviation between the experimental and calculated values of the different atomic quantities considered. Several other approaches along these lines were proposed by these authors for the calculation of the atomic and ionic hardnesses, polarizabilities, and covalent radii.[110,556-558]

A different starting point was taken by Fricke, who observed that there is a linear relationship between the atomic polarizability and the ionization energy.[559] Politzer et al. confirmed this finding for the so-called "average local ionization energy" evaluated on the atomic radius, defined as the sphere encompassing 98% of the total electron density, suggesting that the latter could be used as a measure for the local polarizability $\alpha(\mathbf{r})$.[545] This average local ionization energy is defined as

$$\bar{I}(\mathbf{r}) = \sum_i \frac{\rho_i(\mathbf{r}) |\epsilon_i|}{\rho(\mathbf{r})} \quad (306)$$

where $\rho_i(\mathbf{r})$ and ϵ_i are the electron density and the orbital energy of the ith molecular orbital. This index has been interpreted as the average energy needed to remove an electron from a point $\mathbf{r}$ in space and was shown, when plotted on the molecular surface, to be a good indicator of reactivity toward electrophiles. Moreover, this index was also shown to exhibit the atomic shell structure (vide infra).[545,560]

The local temperature $T(\mathbf{r})$ was introduced in a natural way by Ghosh, Berkowitz, and Parr.[561] Writing the kinetic energy in terms of a local function $t(\mathbf{r})$, the local counterpart of the energy expression,

$$E = \frac{3}{2} nkT \quad (307)$$

leads to a local temperature $T(\mathbf{r})$ as two-thirds of the Kohn–Sham kinetic energy per electron at each point in space:[561]

$$E_{\mathrm{kin}} = \int t(\mathbf{r}) \, \mathrm{d}\mathbf{r} = \frac{3}{2} \int \rho(\mathbf{r}) kT(\mathbf{r}) \, \mathrm{d}\mathbf{r} \quad (308)$$

where k is Boltzmann's constant.

A problem in its definition, however, arises due to the ambiguity in the definition of $t(\mathbf{r})$: any amount of $\nabla^2 \rho(\mathbf{r})$ (or any amount of ∇^2 of any function with vanishing gradient as $r \to \infty$ by virtue of Green's theorem) can be added without altering the value of E_{kin}. Nagy, Parr, and Liu[562] argued that the definition

$$\frac{3}{2} \rho(\mathbf{r}) kT(\mathbf{r}) = \frac{1}{8} \sum_i \frac{\nabla \rho_i \cdot \nabla \rho_i}{\rho_i} \quad (309)$$

where ρ_i is the density of Kohn–Sham orbital i, is the most appropriate one. Moreover, they showed that $T(\mathbf{r})$ for atoms exhibits behavior similar to that of Politzer's average local ionization energy. Gal and Nagy computed $T(\mathbf{r})$ for molecules and confirmed this similarity in behavior.[563]

Senet showed that hardnesses of atoms and molecules can be derived from the screened interaction energy of the electrons in the frontier molecular orbitals.[564] Along the same lines, Liu, De Proft, and Parr used eq 70 in the calculation of atomic hardnesses for 54 neutral atoms, including both main group and transition elements.[174] It was, as mentioned in section III.B.2 as an example of the practical calculation of atomic hardnesses, concluded that a very simple model for the hardness kernel (eq 70), where only the Coulombic part was included and C is a constant, yielded good results for the hardness when compared with the experimental finite difference results.

Atomic hardnesses have also been computed by Liu and Parr from the functional expansion approach truncated at second order, for which some arguments were provided (vide supra, section III.B.3); this approach immediately recovers the principle of maximum hardness.[282]

Until now, attention was focused only on the first- and second-order derivatives of the atomic and molecular energy with respect to the number of electrons. Fuentealba and Parr were the first to obtain (section III.B.3) numerical values for the change in the chemical hardness with respect to the number of electrons for a large number of atoms and ions[271] (eq 63).

However, as was also stated in the paper introducing this derivative, "it is highly desirable that any extension of the theory to include third order should imply only slight modifications of the formula for μ and η, or rather only small changes in their numerical values", implying that γ should be small. On the basis of the following formula for the variation of the energy E with respect to the number of electrons N,

$$E(N) = \frac{aN + bN^2}{1 + cN} \quad (310)$$

it was found that the new values of μ and η differed only slightly from the usual finite difference ones; moreover, in comparison to these values, γ was found to be small and to vary regurarly thoughout the Periodic Table.

So far, the emphasis has been on global atomic DFT-based reactivity descriptors; local atomic descriptors, however, have also been the subject of numerous studies, especially the derivative in eq 28, the central quantity from DFT, the electron density $\rho(\boldsymbol{r})$. In this overview, of course, we will not cover all electron density and shell structure studies in the chemical literature. The atomic electron density has been studied exhaustively in the literature; in most cases, these studies are devoted to the shell structure. This shell structure is revealed by many functions of the electron density.[565-577] The spherically averaged electron density is a piecewise, exponentially decreasing function of the distance r from the nucleus for atoms in their ground states and shows one unique maximum located at the nucleus.[578] The rate of this exponential decrease changes at certain intervals or points, which were shown to coincide with the minima in the radial density distribution function $D(r)$, defined as

$$D(r) = 4\pi r^2 \rho(r) \tag{311}$$

In the case of a first-row atom (Li, Be, etc.), the single minimum can be used in the construction of a boundary surface between the atomic core and valence regions. For atoms having a principal quantum number larger than 2, two or more minima are found, and it was arugued by Parr and Politzer that, in those cases, the outermost minimum should be used to separate core and valence regions.[579] When the radial density distribution function is integrated between two successive minima, the number of electrons contained in that shell is obtained. The shell structure of atoms has been obtained by a large number of people, and the effect of electron correlation on it has been established. Politzer also observed that the shell structure is also present in the so-called average local electrostatic potential function $V(r)/\rho(r)$, defined as the ratio of the electrostatic potential and the electron density; $V(r)/\rho(r)$ has a maximum at each point where $D(r)$ has a minimum.[575,576] This function was studied in more detail by Sen et al., who, among other studies, established the core-valence separation of the atoms Li through Ac and related it to the average local hardness density.[577] Moreover, the effect of electron correlation on the shell structure, as exhibited by this function, was also studied.[580]

Atomic Fukui functions were studied by Chattaraj, Cedillo, and Parr and were expressed by an LDA approximation and a gradient correction, including only one single parameter (eq 95), determined from atomic Fukui function moments.[196] It was claimed that the main basic features of $f(r)$ should be largely independent of the set of α values used. The radial distribution function plots of the Fukui function $4\pi r^2 f(r)$ for the atoms Li, N, and F were found to be similar to those published by Gazquez et al.: the decay is slow for electropositive atoms and faster for electronegative atoms. Moreover, this function was used in combination with eq 69 (with $g(\boldsymbol{r}) = f(\boldsymbol{r})$) and a Thomas−Fermi−Dirac−Weizsäcker functional, including a local Wigner functional for correlation, to calculate atomic hardnesses for the first- and second-row atoms. Reasonable agreement with the experimental finite difference values was observed, except for the elements possessing half-filled shells. Moreover, since the hardness has been derived as the electrostatic potential due to the Fukui function at the covalent radius, the analytical expression of the Fukui function was also used to determine this radius. These estimates compared well with other estimates from the literature. Finally, the atomic cusp condition for the Fukui function was derived as

$$\lim_{r \to 0} \frac{\boldsymbol{r} \cdot \nabla f}{f} = -2Z \tag{312}$$

where Z is the nuclear charge.

In two subsequent papers, Pacios et al. studied this gradient expansion of the Fukui function using atomic HF wave functions as mentioned in section III.B.3.[215,216] Furthermore, the influence of the variation of α on the atomic hardnesses, obtained by the same methodology used by Parr et al., was studied in more detail, where it was found that small variations in this parameter lead to large variations in η. Moreover, an analysis was presented of the shell structure as obtained from the gradient correction.

Vargas and Galvan used the spin-polarized Fukui function, in combination with the charge redistribution between states of different multiplicities, in the rationalization of the stability of half-filled shells.[352]

Chattaraj and Sengupta[581] have studied the relationship between the possible chaotic dynamics of Rydberg atoms in an external field and the dynamical properties of hardness and polarizability.

Electronegativities and hardnesses have also been calculated for functional groups. In the past, however, a lot of attention has been devoted to obtaining substituent electronegativities, and many scales have been proposed. Among the most important ones, we mention Well's scale,[582] based on bond vibrational data, the inductive parameter ι proposed by Inamoto and Masuda,[583-586] and the scales proposed by Huheey,[160,587] Mullay,[588] Sanderson,[391] and Bratsch,[589] all based on electronegativity equalization schemes. Mariott, Reynolds, Taft, and Topsom[590] obtained the electronegativity of a group G as the Mulliken population of the hydrogen atom in the H−G molecule. Boyd and Edgecombe evaluated group electronegativities from the topological properties of the electron densities in these compounds.[591,592] Very recently, Suresh and Koga obtained group electronegativities by considering H_3C-EXYZ compounds, where the position and value of the MEP bond critical point at the CE bond is brought into relation with the electronegativity of the EXYZ group.[593] Sen, Böhm, and Schmidt calculated molecular-orbital-based electronegativities within semiempirical CNDO theory, using the transition operator method.[132] Reed and Allen reported substituent electronegativities based on the so-called bond polarity index, a quantum-mechanical measure of the one-electron energy difference between two adjacent atoms in a molecule.[594] Bergman and Hinze obtained orbital electronegativities depending on both the hybridization and partial charge on the atom, using atomic and ionic spectroscopic data. These data were used, in combination with an electronegativity equalization scheme involving two bond-forming orbitals, to obtain atomic partial charges in molecules. Moreover, this concept was extended to group electronegativities, which were then used in the rationalization of bond lengths, NMR chemical shifts, and proton affinities.[146] Molecular fragment electronegativities were also obtained by Korchowiec and Nalewajski on the basis of a MNDO calculation scheme, with the inclusion of a contribution from the environment. In combination with the calculated Fukui function indices, these electronegativities were shown to be very useful in the reproduction of known substituent effects.[595] De Proft, Langenaeker, and Geerlings were the first to obtain intrinsic group electronegativities, hardnesses, and softnesses for 30 groups frequently encountered in organic molecules, using the finite difference formulas (cf. sections III.B.1 and III.B.2).[433] In the finite difference approach, the functional groups were considered as the corresponding radicals, with the geometry the group usually adopts in molecules. The obtained electronegativities were found to correlate well with most other scales and with the ^{13}C ipso-ortho coupling constants in monosubstituted benzenes. The trends for the group hardnesses were rationalized using the hardness of the central atom of the group. Moreover, a good correlation was found with the experimental finite difference hardnesses of the corresponding radicals; the correlation with the hardnesses obtained by Bergman and Hinze was less satisfactory. Recently, the series was extended to functional groups containing Sn, their values proving to be excellent for use in the correlation with ^{119}Sn chemical shifts.[596] Komorowski, Lipinski, and Pyka obtained inherent functional group electronegativities and hardnesses, derived from both the explicit calculation of bonded fragment electronegativities and Mulliken charges.[134] Moreover, it was stated that the obtained group electronegativities cannot be correlated directly with Hammett substituent constants, without taking the hardness into account.

Chemical potentials and hardnesses for open-shell radicals were also obtained by Pal and Roy using the radical optimized geometries and a finite difference approximation at the Hartree–Fock level.[597] These values were then used to obtain the hardness sequence of the corresponding anions, as proposed by Pearson. Kneisler and Zhou showed the existence of a Hammett-like equation for the chemical hardness of the HOMO–LUMO gap.[598]

From the whole of the studies considered in this section, it can be concluded that DFT has, indeed, provided a mathematical framework for the introduction of previously empirically defined chemical concepts, offering their nonempirical evaluation for atoms and functional groups.

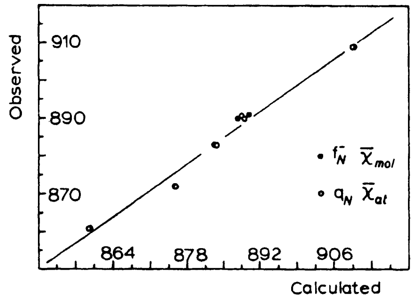

Figure 9. Correlation between the observed gas-phase basicities (kJ/mol) and those calculated using a two-parameter linear model, including f_N^- (the Fukui function on the basic center) and $\bar{\chi}_{mol}$ (the average effective molecular electronegativity, as determined by the EEM method), or q_N (the atomic charge on the basic center) and $\bar{\chi}_{at}$, (the average molecular Sanderson electronegativity). Reprinted with permission from ref 236. Copyright 1986 American Chemical Society.

B. Molecular Properties

1. Dipole Moment, Hardness, Softness, and Related Properties

In this section, we will focus on global molecular properties. Properties considered either are introduced within the framework of DFT, such as the global hardness, global softness, and electrophilicity, or are traditionally known molecular properties such as the molecular polarizability, electronegativity, and dipole moment, calculated however in a conceptual DFT context using some form of the electronegativity equalization method (section III.C.1).

The major advantage of the latter category is the fact that the properties are rapidly calculated, thus making the world of very large molecules and/or large numbers of molecules accessible to computational chemistry describing electronical effects or characteristics. The bigger part of the published applications is situated in the field of large molecules, e.g., those of pharmaceutical interest, since practically all commercial modeling software includes some form of the Gasteiger–Marsili algorithm[400,401] for atomic charge calculation, and catalysis, which will be discussed in a separate section (section IV.D). Despite the existence of a number of software packages (academic[599] as well as commercial[600]), only a limited number of studies involving small molecules have been published. An extremely interesting property, in this context, is the molecular dipole moment. Apart from some fundamental studies,[420,601,602] no applications as such have been reported yet.

A nice example of the study of a more traditionally known molecular property can be found in the early work of Yang and Mortier.[236] They demonstrated that the variation of the gas-phase basicity of amines (see also below) can be analyzed using both a global and a local descriptor. A nice correlation of calculated gas-phase basicities with experimental values was obtained using a model containing the equalized effective electronegativity (Figure 9).

A second example of the application of a DFT-based algorithm (EEM), in this case in combination with a property (hardness) that was also introduced within the DFT framework, can be found in recent work by Zhang and Yang.[417] They used the ABEEM method[413] in a study regarding the reactivity of maleic anhydride and β-propiolactone with respect to different nucleophiles. They examined the reactivity of different sites within one molecule (both compounds are ambident electrophiles), an aspect of reactivity studies that will be discussed in more detail below, not only by using local descriptors for the compounds' behavior toward nucleophilic attack, but also, more importantly for this section, by considering the global molecular properties of the reaction partner. Experimentally, it was found that hard nucleophiles react with hard electrophiles and soft nucleophiles with soft sites in the two compounds considered. On the basis of the global hardness values of a series of nucleophiles calculated using the ABEEM, in combination with a local reactivity descriptor, the experimental results could be reproduced completely.

Further examples of the use of DFT-based molecular properties (in this case, however, not calculated using an EEM-like procedure) can be found in numerous papers describing (simple) organic and inorganic reactions and a series of quantitative structure−activity relationship studies.[119,120,603−609] We will discuss two studies regarding compounds showing bioactivity, thus demonstrating not only the usefulness of these properties to reproduce or even predict experimentally determined (re)activity data, but also the ability to give us a better insight into the actual processes involved in the interactions or reactions considered.

First, we will consider the study of a structure−activity relationship (SAR) for a series of compounds showing some specific bioactivity.[610] This study focuses on the understanding of the interaction between a drug and an enzyme in the actual drug−enzyme complex. This interaction can be associated with the characteristics of a compound related to its "intrinsic" reactivity, expressed in terms of absolute hardness and absolute electronegativity. Using these properties, thus focusing on the actual mechanism (see below) responsible for the bioactivity of the compounds, a relationship between bioactivity and different complementary reactivity descriptors was determined. Semiempirical calculations were used in combination with eqs 43 and 66 to determine the hardness and electronegativity values for a series of quinolines, 1,8-naphtheridines, and polychlorinated dibenzo-p-dioxines and biphenyls. The quinolines and 1,8-naphtheridines show antibacterial activity through the inhibition of DNA gyrase by means of reversible (covalent) binding in the α-subunit of the enzyme.[611] The dioxins and biphenyls, on the other hand, show activity as xenobiotics by means of noncovalent binding to the arylhydrocarbon receptor (AhR).[612,613] When establishing the SAR, or in this case the property−activity relationship (PAR), the η−χ activity diagrams, with η and χ as coordinates of biological activity, as shown in Figure 10, were used.

In this way, the compounds showing high xenobiotic activity are found to be hard, a result perfectly in line with the fact that a noncovalent, electrostatic interaction is involved in the mode of action (cf. section IV.C.1). In the case of the antibacterials, the hardness could not discriminate between active and nonactive compounds, whereas the electronegativity could (see Figure 10). In contrast to the case of the hardness-controlled activity, electrostatic interactions are clearly not predominant here. This implies that the process of charge transfer between the two interacting compounds plays an important role. As the amount of charge transfer is partially determined by the electronegativity (see also below), the importance of this quantity in this case study can thus be rationalized. The electronegativity is not, however, the only quantity that plays a role in this context, as will be demonstrated in the next and final example of the use of molecular properties originating within the DFT framework.

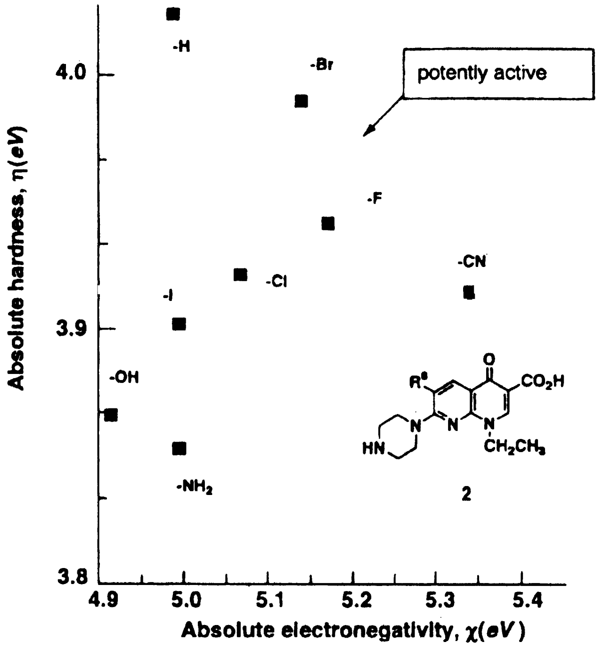

Figure 10. Plot of an absolute hardness−absolute electronegativity activity diagram for quinoline antibacterials. Reprinted with permission from ref 610. Copyright 1998 Pharmaceutical Society of Japan.

This example involves a recent study by Maynard et al.[188] using a new molecular property, electrophilicity[186] (eq 84), in this case, expressed in terms of two known descriptors, as introduced in section III.B.2. Again, this is an example of a well-known chemical concept, finding a clear definition in DFT in such a way that it can be quantified. This electrophilicity index is expressed in terms of η and χ (see eq 84), quantifying the capacity of an electrophile to promote a covalent (soft) reaction. The case study is part of an investigation involving the search for a new strategy in the development of anti-human immunodeficiency virus (anti-HIV) drugs, which is extremely important because of the emergence of protease and reverse transcriptase drug-resistant HIV strains. The antiviral activity of a specific series of drugs was found to be related to the covalent modification of zinc finger Cys thiolates of the nucleocapsid protein p7 (NCp7). In this covalent interaction, the thiolates act as nucleophiles, with the specific characteristic that they are substantially softer nucleophiles than other metal chelators in

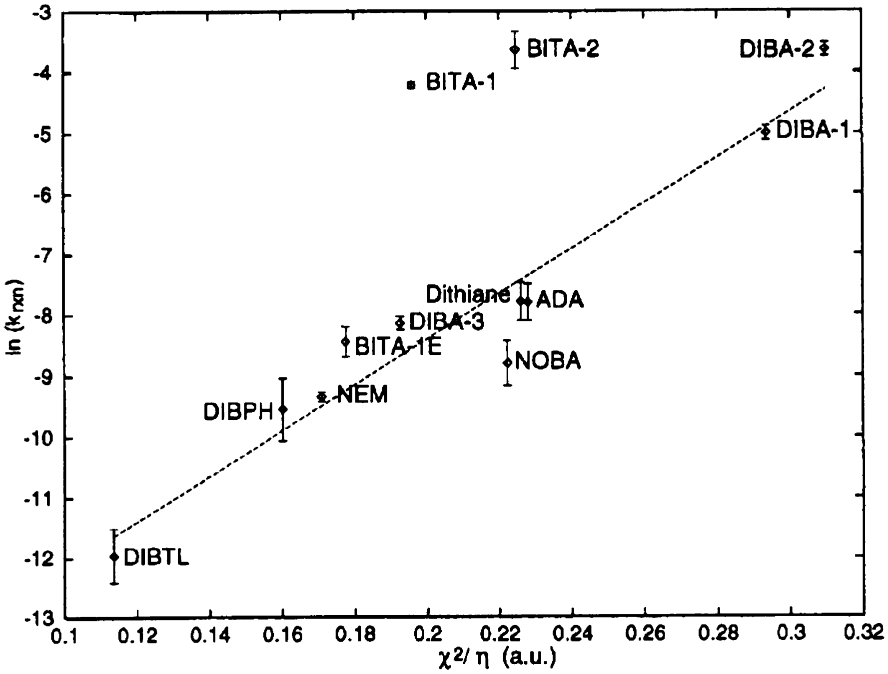

Figure 11. Correlation between the observed NCp7 reaction rates and the ligand capacity to promote a covalent (soft) reaction, χ^2/η (in au). Reprinted with permission from ref 188. Copyright 1998 National Academy of Science.

general, thus leading to the presumption that electrophiles that promote soft reactions will show higher activity. These electrophiles should have a high electrophilicity value. To verify this, a number of global DFT-related reactivity descriptors were calculated for a series of electrophiles. An excellent linear correlation of the electrophilicity with the logarithm of the observed reaction rate constants was found (Figure 11), whereas the global softness itself correlated only qualitatively with the reaction rates. On the other hand, a nice correlation with the calculated electronegativity was observed, implying that a large χ value is probably essential to drive the reaction (see also above).

2. Conformation

Molecular properties of the type mentioned in section IV.B.1 can also play a role in the study of the conformational behavior of a compound. As was discussed in section III.C.3, a system will evolve to a configuration of maximum hardness according to the MHP. The inverse relationship between hardness, η, and the polarizability, α, led to the formulation of the minimum polarizability principle (MPP). As both principles are valid only under certain restriction, i.e., fixed electronical chemical potential and external potential, Chattaraj et al.[486] made a clear distinction between two cases when studying the distortions of ammonia (see also section III.C.3). On one hand, they considered the asymmetric distortions, which do comply with the restriction, and on the other hand, they considered symmetrical distortions for which the MHP does not hold. All distortions were situated along the directions specified by vibrational symmetry. The profiles for η, α, and the energy E for the asymmetrical distortion both in bond length, ΔR, and in bond angle, $\Delta\theta$, are given in Figure 12.

In both cases, the polarizability is minimal for the equilibrium geometry, i.e., minimal E. Furthermore, the hardness shows a maximum at the same point. This could be expected on the basis of the mirror image relationship between η and α. It clearly demonstrates the validity of both the MHP and the MPP in the context of molecular vibrations.

In the case of the totally symmetrical oscillation, the hardness was found to increase monotonically when the nuclei approached each other, a finding that was also reported earlier by Pearson and Palke.[472] At the same time, the polarizability was found to decrease as expected.

3. Aromaticity

Zhou, Parr, and Garst put forward the absolute and relative hardness as a measure of aromaticity.[467,468] This proposition was based on the fact that both hardness and aromaticity are measures of high stability and low reactivity. Aromaticity is a key concept in chemistry, associated with the cyclic delocalization of electrons, resulting in an extra stabilization in the case of aromatic compounds and destabilization in the case of antiaromatic compounds.[614−617] Many criterea have been put forward to measure aromaticity, which can be roughly divided into four categories: energetic, geometric, magnetic, and criteria based on reactivity. Very recently, a detailed account including an impressive number of references was given in a special issue of *Chemical Reviews* on aromaticity,[618] containing a more thorough presentation of conceptual and computational DFT in the study of aromaticity.[59]

As stated in the Introduction, the HOMO−LUMO or band gap can be seen as an approximation to the global hardness of the system. In the 1960s and 1970s, antiaromatic compounds were characterized as compounds with a small band gap.[619−627] Fowler argued, however, that the band gap cannot be considered to be a general criterion for the aromaticity or kinetic stability, because it decreases to a limiting

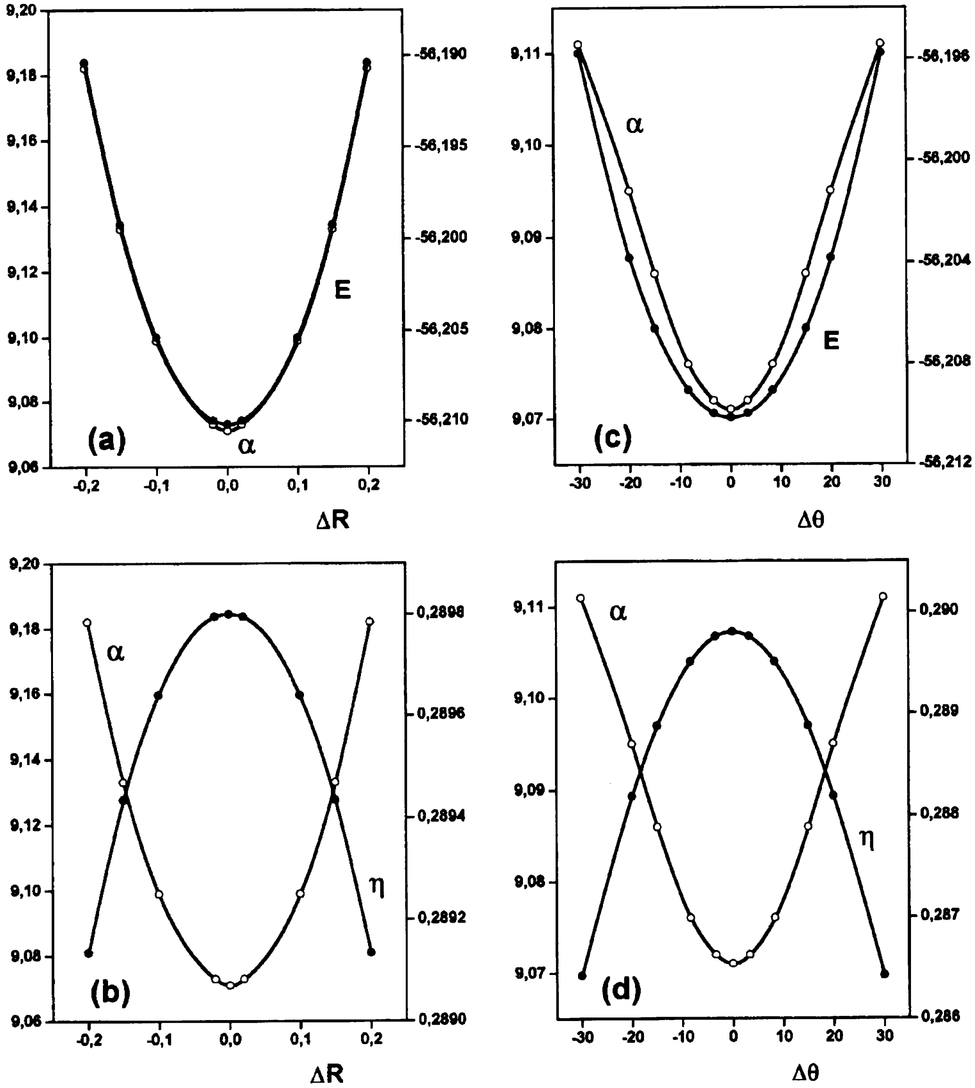

Figure 12. Asymmetric distortions in ammonia. (a) Profiles of the energy and polarizability and (b) profiles of the hardness and polarizability for a distortion in the N−H bond distance. (c) Profiles of the energy and polarizability and (d) profiles of the hardness and polarizability for a distortion in the H−N−H bond angle. All values are in au. The values for the polarizability are on the left axis and correspond to open circles. Reprinted with permission from ref 486. Copyright 1999 American Chemical Society.

value with increasing size of the molecule, whether it is or is not more or less aromatic or kinetically stable.[628] As such, Aihara introduced the HOMO−LUMO separation multiplied by the number of conjugated atoms to measure the kinetic stability.[629−632]

MNDO hardnesses were obtained by Zhou and Navangul for a series of 14 benzenoid hydrocarbons and were shown to be a good indicator of their aromaticity.[633] Moreover, the hardness criterion was also used by these authors in the prediction of the aromaticity of kekulene, coronene, and the corannulene tetraanion.[470] The aromaticity of organometallic compounds was studied using the hardness by Chamizo, Morgado, and Sosa.[634] Bird studied the absolute hardness as a criterion for the aromaticity of various heterocyclic rings.[635] In this work, it was revealed that the correlation of the aromaticity, as measured by hardness, and the Hückel resonance energies per π electron broke down when heteroaromatic compounds were included, as was confirmed by a related study by Bean. Calculation of the hardness, however, using a chemical approximation containing molecular refractivity data, as put forward by Komorowski (cf. section IV.A), yielded nice correlations with resonance energies and the so-called Bird index of aromaticity, based on bond orders.[149,544]

Roy, Choho, De Proft, and Geerlings studied the reactivity of acetaldehyde and some aromatic aldehydes toward nucleophilic attack and, among others, evaluated the intermolecular reactivity trends using DFT-based reactivity descriptors and the concept of aromaticity.[636] They showed a good correlation between the intrinsic hardness, computed as the global hardness of the system multiplied by its volume and corresponding to the local hardness of the corresponding homogeneous system with the same global hardness, and the aromaticity. In a subsequent paper, Balawender, De Proft, Geerlings, and Komorowski showed that the HOMO−LUMO gap correlates with the aromaticity of a series of five-membered heterocycles, as measured by the magnetic susceptibility exaltation. They, however, introduced the change of the molecular valence when the number of electrons in the system is increased as a new index of aromaticity, free from the choice of a reference structure.[334]

As stated in section IV.A, a relationship was shown to exist between the global softness and the polarizability. Since softness, in turn, is inversely related to hardness, which measures aromaticity, a relationship between aromaticity and polarizability can also be expected. Lazeretti and Tossell proposed to use the average polarizability of the system as an indicator of aromaticity.[637] The π contribution to the in-plane polarizability, divided by the number of endocyclic bonds, was put forward by Bulgarevich as a measure of aromaticity.[638] The same author also proposed to use the ratio of the longitudinal polarizability of the formal single and double bonds in the Lewis structure of the compound.[638] Archibong and Thakkar suggest using the excess of in-plane polarizability over out-of-plane polarizability,[639,640] whereas Millifiori and Alparone put forward the exaltation of the molecular dipole polarizability over mean polarizability, determined using atomic or group polarizabilities.[641] Katritzky et al. concluded, on the basis of statistical analysis, that the polarizability as a measure of aromaticity captures a mixture of classical and magnetic aromaticity.[642]

Next to the hardness, several other DFT-based concepts have been involved in the determination of the aromaticity of compounds. The topological features of the central quantity of DFT, the electron density,[68] have been used in many studies to quantify aromaticity. A detailed account can be found in ref 468. For a series of polyaromatic hydrocarbons, Howard and Krygowski correlated the electron density, the Laplacian of the density, and the ellipticity of the charge density at the ring critical points with the aromaticity,[643] as measured by their harmonic oscillator model of aromaticity (HOMA) index,[644−646] on the basis of geometric arguments. Moreover, the topological features of the π electron density were found to correlate almost equally well with HOMA and the nucleus-independent chemical shifts (NICS), introduced by Schleyer et al.[647]

This feature also emerges from a recent report by Van Lier, De Proft, Fowler, and Geerlings, where local and global aromaticity patterns in cylindrical fullerenes, obtained by extending C_{60} along the C_5, C_3, and C_2 axes, were investigated. For the (5,5), (9,0), and (8,2) series, structures were examined that varied in size between C_{70} and C_{152}.[648]

Next to the electron density itself, some properties related to it have also been used to probe the aromaticity. Murray, Abu-Awwad, and Politzer used the average local ionization energy and the electrostatic potential on the molecular surface for a series of polyaromatic hydrocarbons.[649,650] Chesnut and Bartolotti[651] described the aromaticity of a series of substituted five-membered cyclopentatienyl compounds using the electron localization function (ELF), which is defined for a single-determinant Hartree−Fock or Kohn−Sham wave function as[652−654]

$$\mathrm{ELF} = \frac{1}{1 + (D/D_{\mathrm{h}})^2} \tag{313}$$

where

$$D = \frac{1}{2}\sum_i |\nabla\psi_i|^2 - \frac{1}{8}\frac{|\nabla\rho|^2}{\rho} \tag{314}$$

and

$$D_{\mathrm{h}} = \frac{3}{10}(3\pi^2)^{2/3}\rho^{5/3} \tag{315}$$

In previous works, it has been shown that this function, developed by Savin, Silvi, and co-workers, can be interpreted as a local measure of the Pauli repulsion between the electrons as a result of the exclusion principle.[653,654] This function, moreover, allows the definition of molecular regions of basins that can be associated with different electron pairs. Chesnut and Bartolloti discovered that the basin populations of the formal single bonds in these compounds correlated very well with the homonuclear homodesmotic stabilization energies. As stated in section III.B.4, the local hardness is related to the molecular electrostatic potential. Since the global hardness is claimed to be a measure of aromaticity, one can suppose that the local hardness through the electrostatic potential is so, too. Murray, Seminario, and Politzer have used the ratio of the electrostatic potential minimum along a CC double bond and the minimum in ethylene to probe the aromaticity.[649] Suresh and Gadre[655] have revisited Clar's aromatic sextet rule[656,657] using the electrostatic potential topography for a series of cyclic polybenzenoid hydrocarbons. The electrostatic potential topography was shown to provide insight into the aromaticity of these compounds: the average values of the electrostatic potential at the individual rings and for the whole molecule were shown to correlate with the local aromaticity values reported by Li and Jiang[658] and the hardness values reported by Parr and Zhou,[468] respectively.

It is thus clear that many DFT-based chemical concepts can play an important role in probing the aromaticity of compounds. This adds up to the powerful density functionals developed in the past 15 years, making high-quality predictions of more classical aromaticity criterea, based on magnetic, energetic, and geometric properties, accessible.

C. Reactivity

1. Introduction

Chemists prefer to describe reactions in terms of the properties of isolated systems, chosen to yield information on the behavior of a given reactant under perturbation by another reactant. In the literature, these reactivity descriptors or response functions (cf. Scheme 4) are mostly used to describe the onset of the reactions (kinetics), although they also often are invoked when exploring thermodynamic aspects (stability).

The studies reported in this section are all, to some extent, based on the use of the HSAB principle (cf. section III.C.2). However, it is not evident that both thermodynamically and kinetically controlled reactions can be described by using one and the same set of reactivity descriptors.

If we look, for instance, at the general form of an acid−base reaction between two reactants A and B, involved in the formation of a transition state (A−B)*,

$$A + B \rightarrow (A{-}B)^* \rightarrow \text{products}$$

the rate constant, *k*, can be calculated from the energy of A, B, and (A−B)*, i.e., the activation energy. The reactivity descriptors, introduced earlier, describe some characteristics of the isolated reactants. This implies that they are relevant only with respect to the initial interaction between the acid and the base. This type of information can be related to the reactivity only if the transition state still shows a high resemblance to the reactants; in other words, the reactants are responsible for only a relatively small perturbation of one another. Such a reaction is said to have an early transition state. No information whatsoever about the reaction products is used. This implies that the reactivity indices primarily describe kinetically controlled reactions.[659,660] When this is not the case, one could argue that not enough information is encapsulated in the earlier introduced reactivity descriptors to describe deterministically the transformation from reactants to products.

On the other hand, it can be argued that there may be a correlation between the rate constant of a reaction (kinetic property) and the equilibrium constant (thermodynamic property). This correlation can be rationalized in the following way. The rate of a reaction is a function of the energy of the transition state: the more stable the transition state, the lower the activation energy and the faster the reaction. As, for a series of similar reactions, the ratio of the energy necessary to reach a particular (but common) point on the respective reaction path curves is proportional to the ratio of the activation energies, a lower activation energy automatically implies stabler products. This is known as the noncrossing rule.[461] The reactivity descriptors thus can be expected to provide some information about the thermodynamic aspects for a series of similar reactions, again as long as the transition state is reactant-like.

Once the applicability of the reactivity descriptors is established, a second consideration has to be made. The HSAB principle is based on the distinction between hard−hard interaction and soft−soft interaction.[460,461] Considering the original classification of the acids and bases on the basis of properties such as the polarizability and the charge, the hard−hard interaction can be expected to be electrostatic in nature, whereas the soft−soft interaction is primarily covalent in nature. This is completely in line with the close relationships between the molecular electrostatic potential and the hardness, and between the frontier molecular orbitals characteristics and the softness, discussed in sections III.B.2, III.B.3, and III.B.4.

It was demonstrated, for example, in the ABEEM study by Zhang and Yang[417] reported above, and in the landmark paper by Lee, Yang, and Parr[199] in which the Fukui function was introduced, that some molecules can be involved in different kinds of interactions, hard−hard interaction as well as soft−soft interaction, depending on the characteristics of the reaction partner (vide infra). Klopman et al.[661] made this distinction between interactions of a substrate with hard and with soft electrophiles. It was shown that the reaction potential map (RPM) of SCN$^-$ with a hard electrophile differs only slightly from the MEP. If a comparison is made between the RPM of SCN$^-$ with a soft electrophile and the Fukui function f^- for SCN$^-$, an overall agreement is observed. In other cases, both types of interactions can play a role in one and the same reaction. A nice example of this can be found in the electrophilic aromatic substitution on monosubstituted benzenes. This reaction “has a special significance in being the area where much of organic reaction mechanism theory, and in particular the electronic effects of substituents, was developed”.[662] The most common reaction scheme for this reaction involves an addition followed by an elimination (Scheme 6), for which the reaction profile is schematized in Figure 13.

In the first step of the reaction, a nonspecific coordination between the two reactants, known as a π complex, occurs. This type of complex, in which the coordination partner of the π system is often a cation,

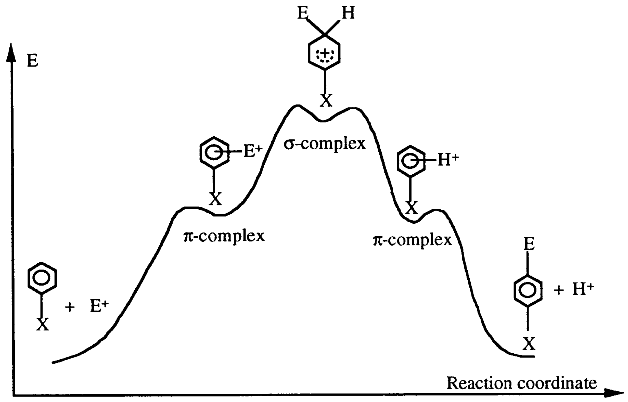

Figure 13. Addition−elimination energy profile of an electrophilic aromatic substitution.

Scheme 6. Reaction Mechanism of Electrophilic Aromatic Substitution for Which the Reaction Profile Is Shown in Figure 13

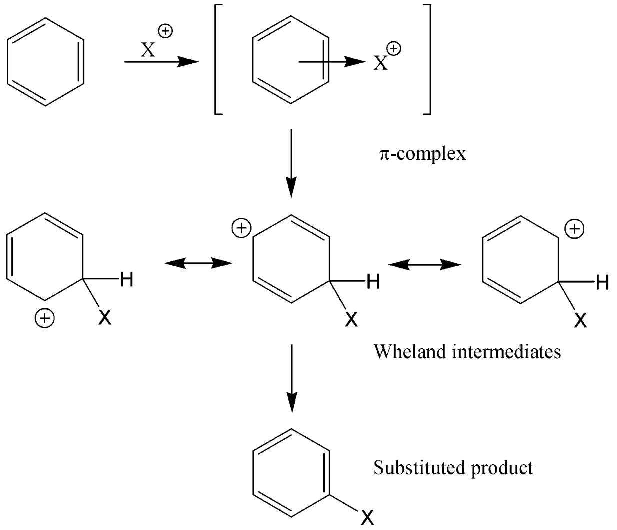

Table 3. Condensed Fukui Functions f_C^-, $f_C^-(\pi)$, and $f_C^-(\sigma)$ for PhX for Ortho, Meta, and Para Positions[a]

	f_C^-			$f_C^-(\pi)$			$f_C^-(\sigma)$		
X	ortho	meta	para	ortho	meta	para	ortho	meta	para
F	0.0472	0.0260	0.0926	0.1088	0.0895	0.2641	−0.0616	−0.0635	−0.1715
NH_2	0.0713	−0.0012	0.0715	0.0137	0.0213	0.1827	−0.0654	−0.0225	−0.1112
OH	0.0580	0.0189	0.0797	0.1213	0.0744	0.2185	−0.0634	−0.0555	−0.1389
O^-	0.1232	−0.0294	0.1070	0.2147	−0.0185	0.2621	−0.0914	−0.0109	−0.1552
$CHCH_2$	0.0464	0.0145	0.0614	0.1019	0.0532	0.1726	−0.0555	−0.0387	−0.1113
CHO	0.0753	0.1033	−0.0289	0.2069	0.2908	−0.0611	−0.1316	−0.1875	0.0322
CN	0.0403	0.0211	0.1003	0.0875	0.0784	0.2832	−0.0472	−0.0573	−0.1829
NO_2	0.1003	0.0910	−0.0146	0.2483	0.2606	−0.0374	−0.1480	−0.1696	0.0228
NH_3^+	0.0310	0.0431	0.1494	0.0499	0.1329	0.4036	−0.0189	−0.0899	−0.2542

[a] Data from ref 203. All values are in au.

is very often described in terms of electrostatics,[663] which allows us to expect a nice correlation between the reactivity of these aromatic systems and some hardness-related descriptors (vide infra). In a second step, a σ complex (Wheland intermediate) that contains some information about the actual bonds that will be formed can be distinguished. As this interaction involves the initial part of the formation of covalent bonds, a correlation with the softness-related quantities can be expected. This descriptor will thus be very useful in rationalizing and predicting site selectivity (vide infra). In combination with the well-known fact that the vast majority of electrophilic aromatic substitution reactions proceed under kinetic control,[664] the HSAB-related descriptors can be expected to give a complete description of both the rate- and product-determining step in this reaction.

2. Comparison of Intramolecular Reactivity Sequences

In this section, we present an overview of different studies of intramolecular reactivity sequences using the Fukui function, in its integrated and nonintegrated forms, and some approximations to the local hardness. Note that this approach is completely equivalent to the case of the local softness in view of eq 112, the softness S being a global molecular quantity. We start from electrophilic reactions on substituted aromatic systems (monosubstituted benzenes, substituted anilines and phenols) and then study ambident nucleophiles (enolates) and pass via nucleophilic additions at α,β-unsaturated ketones, nitriles, benzynes, hetarynes, and fullerenes to radial reactions and finally to concerted reactions of the Diels–Alder and 1,3 dipolar addition types.

a. Electrophilic Reactions. The study of the directing abilities of substituents in electrophilic substitutions on monosubstituted benzenes[203] were mentioned in the introduction to this section. Here, the reactivity descriptors for an electrophilic attack were used.

In Table 3, the values of the condensed Fukui function f_C^- and its σ and π components (based on the Mulliken population analysis) for the ortho, meta, and para positions of the above-mentioned systems are listed. These components still incorporate some spatial information, as they are only semicondensed. The overall positive values of $f_C^-(\pi)$ indicate high reactivity at the given atom for an electrophilic attack in the plane perpendicular to the molecular plane of the substituted benzenes. The negative values of $f_C^-(\sigma)$ indicate that it is very unlikely for an electrophilic attack to take place in the molecular plane of the substituted benzenes.

Focusing on $f_C^-(\pi)$, which is expected to be a better indicator of the reactivity in this case, as it refers to the π system, known to be of primary interest in S_E at aromatic systems, this descriptor gives rise to practically the same results as f_C^-. Only in the case of nitrobenzene is an actual improvement of the results observed. A fine example of the quality of the "condensed" Fukui function as a reactivity index is the ability to predict an increase of the ortho/para ratio when going from phenol to the phenoxide ion.

As an example of the local Fukui function, the contour plot of f^- for PhCHO is given in a plane perpendicular to the molecular plane. We will discuss this result in some detail to demonstrate the way these functions should be interpreted. According to f^-, it is very unlikely for an electrophilic attack to take place at the para position, due to the negative values in this area. For the ortho and meta positions, the positive values of f^- in these areas indicate a higher probability for an electrophilic attack. Here the meta position is favored, not only because contours of the same value are more extended at the meta site, but also because contours with higher values are present.

Here we also encounter a nice example of a case where the HOMO density is not a good approximation of the Fukui function f^-. This is easily seen when comparing the contour plots of the Fukui function (Figure 14) and the HOMO density (Figure 15), where the typical picture for a benzene substituted with a conjugated and electron-withdrawing group is obtained.[665] The reactivity at the para position is clearly overestimated, while the reactivity at the ortho position is underestimated. In general, it was found, as expected, that in all cases where the HOMO density correctly reproduces the reactivity sequence, the Fukui function f^- also does. Concentrating on those cases where the HOMO density fails, only for nitrobenzene was an improvement of the results obtained when considering the (HOMO − 1) density as well. It seems that the HOMO density is a relatively poor approximation to f^-, as opposed to earlier formulated arguments (ref 207 and section III.B.3).

Comparing the noncondensed Fukui function f^- with the MEP, both reactivity indices are found to

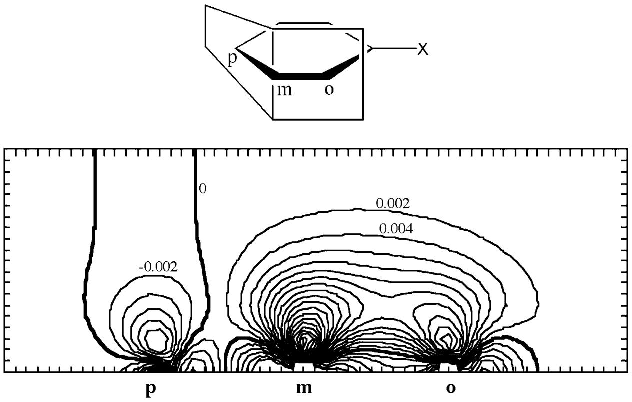

Figure 14. Contour plot of the Fukui function f^- for Ph−CHO in the plane shown at the top of the figure. Contour values (au): bold line, 0; negative values, decreasing from 0 with a contour interval of 0.002; positive values, increasing from 0 with a contour interval of 0.002. Reprinted with permission from ref 203. Copyright 1991 Elsevier Science.

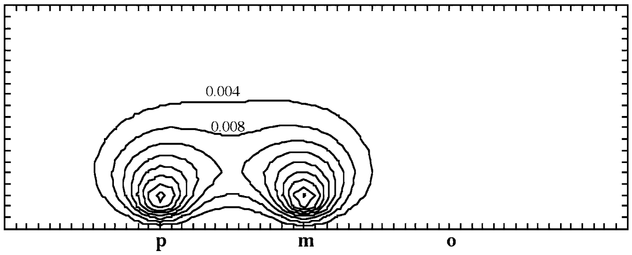

Figure 15. Contour plot of the HOMO density for Ph−CHO in the same plane as shown in Figure 14. Contour values (au): increasing from 0.004 with a contour interval of 0.004. Reprinted with permission from ref 203. Copyright 1991 Elsevier Science.

give satisfactory results in about six out of nine cases, of which only three are common. This is an indication of some complementarity, which could be explained within the framework of the HSAB theory, as was done in the Introduction: on one side the hard−hard interaction, which indicates that the reaction is primarily charge controlled, and on the other side the soft−soft interaction, which indicates that the reaction is primarily orbital controlled. The relationship between the MEP and a descriptor of especially the hard−hard interactions was investigated in a follow-up study,[285] concentrating on alternatives to local hardness (section III.B.4). Here, five different expressions for hardness-related descriptors were explored. All these descriptors contained the electronic part of the molecular electrostatic potential and were divided into two groups: two descriptors for the local hardness and three describing the hardness density. The local-hardness-type descriptors seem to generate a very poor intramolecular reactivity sequence, as the reactivity decreases in all cases with the distance to the substituent. The sequences generated by the other hardness-related quantities are in agreement with those obtained for the Fukui function and local softness, a result one could expect, as they all incorporate a factor describing the influence of the change of the electron density due to a change in the number of electrons. This, however, is not the result one would expect for a quantity that is the counterpart of the local softness.

In the context of the reaction of an electrophile with an aromatic system, in-depth studies of aniline were also reported.[256,270,666] They are concerned with the use of DFT-based reactivity descriptors in the study of basicity, i.e., the site of protonation. In solution, it has been well established that the protonation occurs on the nitrogen atom, since this protonated form is much better stabilized by solvatation than when the protonation occurs on one of the ring carbons.[667] In the gas phase, however, the favored site of protonation has been a matter of debate. Early experimental studies suggest that the most energetically feasible site for protonation is the ring carbon. On the basis of a correlation of the proton affinities of a series of substituted anilines with N 1s electron ionization energies, Pollack et al.,[668] however, concluded that the protonation occurs on N. This result was confirmed by mass spectroscopic studies involving collision-activated dissociation of partially deuterated aniline ions. Karpas, Berant, and Stimac,[669] using the ion mobility/mass spectroscopy technique, showed that the protonation at atmospheric pressure of aniline yields two isomers, the N and ring-protonated compounds. Smith et al.[670] showed, however, that the kinetically favored site for protonation is N. As can be seen from this short status report concerning experimental conclusions on the preferred site of protonation of aniline, the situation is less clear in the gas phase. This topic thus provides an ideal playground for theoretical studies. Minimal basis set Hartree−Fock and semiempirical calculations have shown that aniline is a nitrogen base, the energy difference between the N and ring-carbon-protonated forms being 1−3 kcal/mol. Sjoberg, Murray, Brinck, and Politzer[671] used the average local ionization energy (eq 296) to study this problem. They found that the para ring carbon is the site that is most reactive toward electrophiles. Ritchie,[672] however, showed that the absolute minimum in the molecular electrostatic potential of the molecule is found near the N atom. DFT-based reactivity criteria and descriptors were used for the first time in the problem by Roy, De Proft, and Geerlings.[270] In this work, aniline was investigated together with meta- and para-substituted anilines, the substituents being F, Cl, OCH_3, and CH_3. On the basis of the use of the quantity s^-/s^+, termed the relative nucleophilicity (cf. section III.B.3), they concluded that the preferred site of protonation is the N. These systems were revisited in two subsequent papers dealing with the nonnegativity of the Fukui function indices. Fuentealba, Perez, and Contreras[256] used an alternative method to calculate the condensed Fukui function and proved that the electrophilic Fukui function exhibits the correct selectivity for the site of protonation in aniline. Russo, Toscano, Grand, and Mineva[666] performed proton affinity calculations on aniline at the B3LYP, BP, MP4, and G2(MP2) levels of theory. They concluded that the nitrogen and para ring carbon are, indeed, the thermodynamically most favorable protonation sites. The DFT methods and MP4 all point to the para carbon as the most preferred protonation site, whereas, at the G2(MP2) level, protonation on N occurs, the energy difference from the protonation at the para carbon being only 0.7 kcal/mol. The orbital Fukui function indices, associated with the hardest orbitals, all point to the para carbon as the preferred site of protonation, and they do not unequivocally resolve the problem. However, the absolute hardness values of the protonated forms do not follow the principle of maximum hardness.

A study comparable to the aniline protonation problem was recently published by Nguyen and coworkers on the protonation of halogenated phenols and anisols.[673]

These authors also concentrated on the regioselectivity in the hydration reactions to carbon suboxide (O=C=C=C=O) and ketene (CH_2=C=O); the preferential reaction mechanism could be rationalized in terms of Fukui functions for both nucleophilic and electrophilic attack.[674,675]

Very recently, in a very promising approach by Clark, Ellis, and Snurr, the nature of the attacking electrophile has been introduced by considering the overlap integral of the Fukui functions of both reactants.[676] In the case study on the electrophilic substitution on toluene, aniline, anisole, phenol, chlorobenzene, and nitrobenzene, the integral

$$I_{AB}^{+,-} = \int f_A^-(\boldsymbol{r})\, f_B^+(\boldsymbol{r})\, d\boldsymbol{r} \tag{316}$$

(where A is an aromatic and B is an electrophile) was evaluated with B = methyl. (Note the difference with the corresponding overlap integral occurring in molecular similarity indices, where both Fukui functions are of the same type (+/+ or −/−).) Using isolated equilibrium geometry FF, the method makes it possible to look for configurations where high f_{aromatic}^- and high $f_{\text{electrophile}}^+$ regions overlap, giving rise to a strong tendency to transfer electrons from the nucleophile to the electrophile. In a second part of the same study, electrophiles of varying bulkiness (methyl, ethyl, isopropyl, *tert*-butyl) were investigated in their electrophilic attack on toluene. Not only inductive and mesomeric but also steric effects were thereby successfully probed. Maximum Fukui overlap configurations, moreover, can be viewed as a first approximation in the search for transition states.

b. Ambident Nucleophiles. The enolate ions are very important ambident nucleophiles.[677] They can undergo electrophilic reactions at two different yet connected sites: at the carbon atom in the α position and at the oxygen atom. The intramolecular reactivity sequence or site selectivity of this reaction depends on various factors,[678] such as the type of substituents, the electrophile, and the solvent. When considering these factors, which influence the site selectivity, the kinetic control of the reaction should be taken into account. Indeed, the ratio of the products is determined by the ratio of the reaction rates. This makes these reactions extremely well suited for a study with DFT-based reactivity descriptors (see also section IV.A). Enolate reactivity has, indeed, been the center of many studies employing DFT-based reactivity descriptors and principles. In these studies, the HSAB principle plays an important role. Reutov et al.[679] have stressed the importance of the softness of the alkylating agent in these reactions. Damoun, Van De Woude, Choho, and Geerlings[456] have investigated the influence of the alkylating reagent's softness on the regioselectivity of enolate alkylation using a local HSAB study. Moreover, the influence of the solvent was studied using the SCI−PCM model. The energy difference between the reaction energy for C and O alkylation, ΔE_C and ΔE_O, was derived to be

$$\Delta(\Delta E) = \Delta E_C - \Delta E_O = \frac{s_{A,C} - s_{A,O}}{(s_{A,C} + S_B)(s_{A,O} + S_B)}[-(\mu_A - \mu_B)^2 S_B^2 + \lambda) \tag{317}$$

where $s_{A,C}$ and $s_{A,O}$ are the local softness values of C and O in the enolate, S_B is the softness of the alkylating agent, and μ_A and μ_B are the chemical potentials of the two reacting molecules. The value of λ (eq 274) was set to 0.5, as suggested previously by Gazquez and Mendez.[443] For a given combination of $s_{A,C}$ and $s_{A,O}$, and with the knowledge that the carbon atom is always the softest atom in the enolate, the first term always favors C alkylation. The second term, however, favors a reaction at the oxygen atom. When the magnitude of both of the terms is investigated, however, it can be seen that the second term is predominant, essentially due to the smallness of the chemical potential difference.[456] However, upon increasing softness of the alkylating reagent S_B, C alkylation becomes less and less disfavored. This study is an example of a reactivity study conducted at the local−global level of the HSAB principle.

The influence of solvent effects (in this case, all the experiments were performed in HMPT) was studied using the self-consistent isodensity polarized continuum model (SCI−PM). This model was also used successfully in the study of solvent effects on group properties (section III.B.8). The results indicated a steady increase in the softness when passing from the gas phase to the solution phase, the effect being more pronounced for larger ϵ values. In the case of HMPT, with an ϵ value of 29.6, which is rather small compared to that of water (78.39), the effects were expected and were shown not to be large. Thus, the overall results for ΔE were found to be qualitatively the same for the gas phase and the solution phase.

Contreras et al.[371] used a slightly different approach in their study of the reactivity of the acetaldehyde enolate. They used a nonlocal (pair site) reactivity scheme in which a change of variables is introduced using the local softness and the derivative of the local softness with respect to N at fixed external potential. This leads to a variation of the Fukui function at site k which can be expressed in terms of a local contribution that is proportional to a change in the external potential due to the presence of the reaction partner, and a nonlocal term expressed in terms of a change in the electronic chemical potential that accounts for the charge transfer involved in the reaction. The first factor they considered in the alkylation reaction of the enolate was the nature of the electrophile. Two extreme cases were considered: an infinitely hard electrophile, modeled by means of a point charge, and a soft electrophile, simulated by means of a ghost atom carrying a fractional nuclear charge.

Incorporation of solvent effects in this framework, using a continuum approach to the surrounding medium, led to some very interesting results. In the gas phase, the reaction of enolate ions with methyl chloride is known to yield methyl vinyl ethers, the result of an O attack, in contrast to the reaction in a polar solvent, in which the main product corresponds with a C attack. Contreras et al.[373] used an ϵ value of 80 to simulate water polarity. They were able to demonstrate qualitatively that the reactivity of the O site decreases due to the presence of a solvent effect. In the case of a highly polar solvent, these effects can be rather large, probably large enough to change the intramolecular reactivity sequence.

c. Nucleophilic Additions. One of the first reactions studied systematically using DFT-based reactivity descriptors involved nucleophilic attack on α,β-unsaturated compounds (aldehydes, ketones, nitriles).[204] For acrolein, acrylonitrile, methylacrylate, and methyl methacrylate, the Fukui function f^+ was used in its condensed and noncondensed forms to examine the site selectivity for a nucleophilic attack on activated double bonds. In all cases, both types of the Fukui function predicted a higher reactivity at the β position than at the α position, in perfect agreement with experimental results[680] and ab initio transition-state calculations.[681] In the case of acrolein, the additional possibility of a carbonyl addition was investigated. Experimentally, the conjugate addition (β position) leads to a stabler product, whereas the carbonyl addition is much faster. As these reactivity descriptors are better suited for kinetically controlled reactions, one can expect the Fukui function to predict a higher reactivity at the carbonyl carbon. This was exactly the result of the reported study. Furthermore, the conformational dependence of the trend in the site selectivity in the case of acrolein (*s-cis*-acrolein compared to *s-trans*-acrolein) was reproduced.

A study by Nguyen and co-workers on the hydration of isocyanate (H—N═C═O) and ketene used similar techniques, f^+ pointing out that the nucleophilic attack is likely to happen at the central carbon atom, the N position being clearly favored for electrophilic attack.[682]

A second example of the quality of the Fukui function as a reactivity descriptor for regioselectivity in a nucleophilic reaction can be found in the study of a less common reaction mechanism involving more exotic reactants. We are referring to the benzyne mechanism for the aromatic nucleophilic substitution[205] (Figure 16). This is an elimination—addition reaction, which is much less common than the addition—elimination reaction.

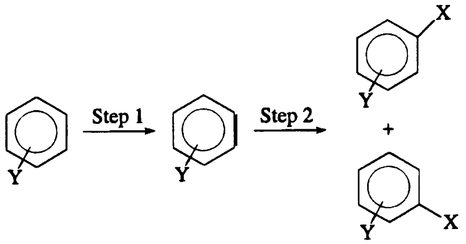

Figure 16. Elimination—addition or benzyne mechanism for the aromatic nucleophilic substitution. Reprinted with permission from ref 684. Copyright 1998 American Chemical Society.

Here, the attention was focused on the addition reaction in the second step of this mechanism, i.e., the reaction of a nucleophile with the triple bond in unsymmetrically substituted benzynes (e.g., *o*-didehydrobenzene or *o*-benzyne). The systems considered are 3- and 4-fluorobenzynes and 4,5-didehydropyrimidine. These reactive intermediates are interesting, as they form a real challenge for a reactivity study. The 4,5-didehydropyrimidine undergoes preferential nucleophilic attack at the 4- rather than the 5-position, as was experimentally found by Promel.[683] In comparison with the substituted benzynes, a higher regioselectivity was found (meta/ortho ratio varying from 16:1 to 100:1 for 3-fluorobenzyne, para/meta ratio varying from 1:1 to 2:1 for 4-fluorobenzyne, and the absence of a 5-substituted product for the hetarynes), yielding the general regioselectivity sequence shown in Figure 17.

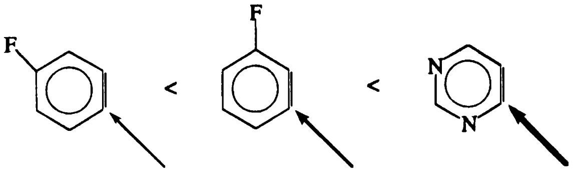

Figure 17. Regioselectivity for a nucleophilic attack in the 3- and 4-fluorobenzynes and 4,5-didehydropyrimidine. Reprinted with permission from ref 684. Copyright 1998 American Chemical Society.

The reactivity of the hetaryne was investigated using the Fukui function f^+ at the HF/3-21G* level, which was found to give a correct description of the intramolecular reactivity sequence. This result was confirmed at the DFT level by means of a B3LYP/cc-pVDZ calculation [$f^+_{C_4}$(tot) = 0.01902 and $f^+_{C_5}$(tot) = −0.08736].[684] Considering the σ and π components of the condensed Fukui function, it immediately becomes clear that the nucleophilic attack will take place in the σ plane (positive values for the σ component) and not perpendicular to this plane (negative values for the π component). Furthermore, the σ component was found to predict a reaction at the correct position in all cases. Moreover, the increase in regioselectivity when going from 4-fluorobenzyne to 3-fluorobenzyne was also described correctly.

The condensed local softness, s_k^+, or condensed Fukui function, f_k^+, was also used as a descriptor of the regioselectivity of a series of fullerenes (from C_{24} to C_{76}) toward a nucleophilic attack.[685] In general, the results, which are in agreement with experimental data, can be interpreted in terms of a pyramidalization angle effect, soft—hard alternations, and softness delocalization.

Until now (with the exception of ref 686), only those intramolecular reactivity studies were discussed, in which only the characteristics of one isolated molecule are considered. The next step in this kind of studies is the actual application of the HSAB principle, taking into account some characteristics of both reaction partners at various resolutions.

One example of this was, in fact, described in the section regarding the molecular properties. In the study reported by Zhang and Yang,[417] some form of local−global softness matching of isolated molecules was used in the study of maleic anhydride and β-propiolactone in interaction with different nucleophiles. In this study, an intuitive approach was used to check softness matching between two isolated reaction partners.

d. Radicalar Reactions. The softness-matching approach was also used in a study of free radical addition to olefins reported by Chandra and Nguyen.[253] They considered the addition of the CH_3 and CF_3 radicals to a series of olefins $H_2C{=}CHX$, where X determines the behavior of an attacking methyl radical in the reaction: for X = H, F, NH_2, CH_3, SiH_3, and OH, the methyl radical plays the role of an electron acceptor, and for X = NO_2, CN, and CHO, it acts as a weak donor.[686] In addition to these substituents, Cl and CF_3 were also considered. Generally, the radical attack will occur at the less substituted carbon of the olefin. There are, however, a few exceptions. One is found in the case of $F_2C{=}CHF$, where the CF_3 radical will follow this rule, whereas the methyl radical will attack on the difluorinated carbon. In all cases, the softness of the less substituted carbon was calculated to be higher, indicating a higher reactivity, in agreement with the experimental findings. Furthermore, it was found that, in all cases, the softness value of the less substituted carbon was closer to the softness of the carbon of the radical. The only failure of this approach was observed in the case of a radical reaction between the methyl radical and $F_2C{=}CHF$, where, in contrast with experimental observations, the less substituted carbon was also found to be more reactive. This failure was attributed to strong electronic reorganization in the supermolecule which is not accounted for in the isolated molecule approach.

The following studies actually use a more quantitative approach to investigate the compatibility of the partners.

e. Concerted Reactions. In the study of regioselectivity in Diels−Alder reactions, a local−local softness-matching approach was used.[446] The regioselectivity in this well-known reaction cannot be explained solely in terms of the electronic effect of different substituents; replacement of an electron-donating substituent by an electron-withdrawing one does not always alter the regioselectivity.[687]

So, knowledge of the inductive and mesomeric effects does not provide us with the necessary tools to explain the predominance of the ortho regioisomers over the meta regioisomers in the cycloaddition of 1-substituted dienes and asymmetrical dienophiles.[687]

Scheme 7. Regioselectivity in Diels−Alder Reactions

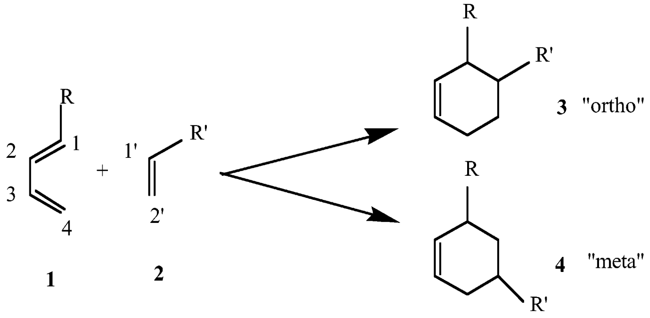

In the double local−local softness-matching approach, the resemblence of the termini combinations 1−1′ and 4−2′, yielding the ortho regioisomer, as compared to the 1−2′ and 4−1′ combinations, yielding the meta regioisomer, was considered (Scheme 7). Eight different substituents for the diene and six different substituents for the dienophile were considered. These R and R′ groups were chosen in such a way that, in most cases, a normal electronic demand reaction type was ensured, the dienophile being the electrophilic partner and the diene the nucleophilic one. To look for a simultaneous fulfillment of the local HSAB principle at both termini, the following local softness similarly indicators were evaluated:

$$\begin{aligned} S_{\text{ortho}} &= (s_1^- - s_{1'}^+)^2 + (s_4^- - s_{2'}^+)^2 \\ S_{\text{meta}} &= (s_1^- - s_{2'}^+)^2 + (s_4^- - s_{1'}^+)^2 \end{aligned} \tag{318}$$

In almost all of the 48 (=8 × 6) cases studied, corresponding to all R and R′ combinations, S_{ortho} is always smaller than S_{meta}. The presence of the CN substituent in the diene or the dienophile led to some discrepancies, which could be easily explained, as the DFT-related reactivity parameter for the CN group shows a high sensitivity to correlation effects (not taken into account in this study).

Furthermore, in almost all cases, the $s_4^- - s_{2'}^+$ term was the smallest of the four quadratic forms in eq 318. This result suggests that the $C_4{-}C_2$ bond forms faster than the $C_1{-}C_{1'}$ bond. The asynchronicity in the mechanism suggested on this basis is confirmed by Houk's transition-state calculations,[688] wherein all cases with R, R′ ≠ H asymmetric transition states were found with the $C_4{-}C_{2'}$ distance being invariably shorter than $C_1{-}C_{1'}$.

Ponti and Molteni[689] recently investigated the modest regioselectivity of 1,3 dipolar cycloadditions of nitrilimines to methyl propiolate. They directly confronted changes in the grand potential $\Delta\Omega$, and related differences in $\Delta\Omega$, $\delta\Delta\Omega$, for the two regioisomers successfully to experimentally determined activation energy differences (estimated from the regioisomer ratio). $\delta\Delta\Omega$ was found to be proportional to the difference in transition-state energies.

Nguyen, Chandra, and (partly) the present authors further explored regiochemical aspects of the cycloaddition of 1,3 dipoles and dipolarophiles in the case of phosphorus-containing dipolarophiles,[504,690] and in the case of thionitroso compounds ($R{-}N{=}S$) as dipolarophiles (on fulminic acid and $H{-}C{\equiv}N^+{-}O^-$ and azides),[503] with nitrous oxide (N_2O) as the 1,3 dipole, reacting with alkynes,[691] azides, and substituted ethylenes.[692]

A local−global approach to the interaction energy applied to the problem of regioselectivity of alkylation of enolate ambidents, is discussed in detail in the

Scheme 8. Regioselectivity in the Cycloadditions of Benzonitrile Oxide

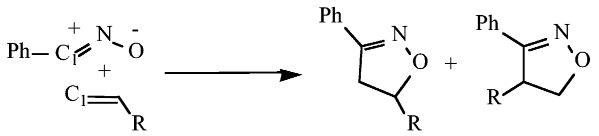

Table 4. Properties Needed in the Evaluation of the Energetics of the BNO + 1 Reaction[a]

property type		BNO		1	
global	μ (eV)		−3.022		−4.563
	η (eV)		4.339		4.647
	S (eV^{-1})		0.115		0.107
local Fukui function	f^{+}	C-1,	−0.0016	C-1,	0.0344
		O-3,	0.1690	C-2,	−0.0592
	f^{-}	C-1,	0.3292	C-1,	−0.0672
		O-3,	0.4093	C-2,	−0.0351

[a] Data from ref 457.

section on intermolecular reactivity (section IV.C.3-b). In the current section, we focus on a final type of application of the HSAB principle: the "double" local−global study of the interaction energy. The case presented here involves the cycloadditions of benzonitrile oxide (BNO) to obtain isoxazolines, as studied by Jimenez[693] (Scheme 8). It is an example of a 1,3 dipolar reaction involving the addition of 1,3 dipolar compounds to double bonds (dipolarophiles).

The regioselectivity of this type of reaction has not been satisfactorily rationalized by FMO theory. It turns out that, for the acetyl derivatives of vinyl *p*-nitrobenzoate **1** as dipolarophiles, exclusively the

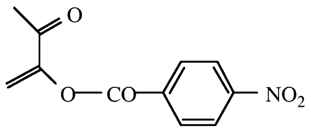

1

regioisomer involving C_1 of the dipolarophile and C_1 of the BNO is formed. A HSAB analysis of the reaction of **1** with BNO was performed at the HF 6-31G** level by Mendez, Tamariz, and Geerlings.[457]

Starting with a local viewpoint, concentrating on the carbon and oxygen atoms for BNO, and a global viewpoint for **1**, the local−global viewpoint was adopted first. Therefore, $f^{+}_{\text{C}-1}$ and $f^{+}_{\text{O}-3}$ (nucleophilic attack) were calculated.

Table 4 shows that the reaction is favored when **1** undertakes a nucleophilic attack at the C_1 atom, which is thus the electrophilic center in BNO. The nucleophilic center in **1** is not known at this time, as **1** is described using only global quantities in this approach.

Taking now the local viewpoint for **1** and the global viewpoint for BNO, the focus is on the C_1 and C_2 atoms of **1**. Table 5 shows that, again, ΔE_{μ} dominates and that the most important interaction occurs when BNO undertakes an electrophilic attack at C_1 of **1**. Even though the Fukui function for C_1 is negative, C_1 is the more reactive atom in the molecule. Note that the use of eq 262 yields the result sketched above, as long as $\lambda > 0.2$, which is largely fulfilled in view of the discussion in ref 456. Combining these results, we see that the maximum interaction will preferentially occur between C_1 from BNO and C_1 from **1**.

Table 5. Local−Global Analysis of the Energetics of the BNO + 1 Reaction[a]

		nucleophilic attack at atom		electrophilic attack at atom	
		C-1	O-3	C-1	O-3
BNO local/	ΔE_{ν}	0.02	−1.88	−3.20	−3.74
1 global	ΔE_{μ}	−451.64	−381.56	−333.03	−313.12
		C-1	C-2	C-1	C-2
BNO global/	ΔE_{ν}	−0.40	−0.76	0.87	0.44
1 local	ΔE_{μ}	−406.69	−443.95	−447.48	−433.66

[a] Data from ref 457. All values are in kJ mol^{-1}.

f. Medicinal Chemistry: An Outlook. To conclude this section, we mention an interesting study by Rice and co-workers which broadens the scope of the use of Fukui functions and local softness from organic and biomolecules to medicinal chemistry as such.[694] They studied, via $f^{-}(\boldsymbol{r})$ and $s^{-}(\boldsymbol{r})$, the regional reactivity (in contrast to the study of (global) activity discussed in section IV.B.1 and ref 188) of the two retroviral zinc fingers of the HIV-1 nucleocapsid p7 (NCp7) protein, representing antiviral targets.

By inspection of the Fukui function on the solvent-accessible surface of the Zn fingers, it is possible to discern a reactivity sequence between the two regions; in fact, the information considered is the sum of the thiolate Fukui indices.

The regions of both Zn fingers prove that the Cys thiolates are dominant in the reactivity profile of NCp7. The reactive sites of finger 2 form a more contiguous reactive surface in comparison with finger 1, where they appear more isolated. On the basis of the sum of the thiolate Fukui indices, the reactivity of finger 2 was predicted to be greater than that of finger 1. The thiolate of Cys 49 in the carboxyl terminal finger 2 turns out to be the most susceptible to electrophilic attack, providing a rationale for experimental evidence for antiviral agents that selectively target retroviral nucleocapsid protein Zn fingers.

3. Comparison of Intermolecular Reactivity Sequences

a. General Considerations. In this section, the use of DFT-based descriptors in the study of intermolecular reactivity sequences will be studied. In general, the observed trends will result from two principles: the hard and soft acids and bases principle, favoring the combination of a soft species with another soft species and of a hard species with another hard species, and the principle of maximum hardness.

Toro-Labbé investigated the consistency between the principle of maximum hardness and the Hammond postulate.[695] Both Hammond and anti-Hammond reactions were found to support the MHP. In the former case, the hardest species among the reactants and products are also the stablest ones.[490,696]

One type of reaction where DFT-based local and global descriptors and principles have been used exhaustively involves Brønsted acidity and basicity, which will be discussed in full detail in the next section. In a recent study,[460] Chattaraj, on the basis of ideas proposed previously by Klopman,[461] stated that soft–soft interactions are controlled by the frontier molecular orbitals and that they are predominantly covalent in nature. It then results that the preferred site of reaction will correspond with the maximum value of the Fukui function when intramolecular reactivity is concerned and local softness when the intermolecular reactivity sequences are discussed. Hard–hard interactions, on the other hand, are charge-controlled and thus are, for a large part, ionic in nature. The preferred site will thus be the site that bears the maximum net charge. This may or may not coincide with the site of a minimal Fukui function, since indeed, locally, the local hardness is not necessarily the inverse of the local softness (see section III.B.4). A lot of evidence has accumulated in recent years to support these conclusive statements.

b. Substitutions, Additions, Eliminations, etc. In a study on the electrophilic aromatic substitution of monosubstituted benzenes, Langenaeker, Demel, and Geerlings found that, although the Fukui function performs well in the description of the intramolecular reactivity sequences (i.e., the ortho, meta, and para orientation, described in more detail in section IV.C.2-a), the local softness performs poorly in the description of the intermolecular reactivity.[203] In a later contribution,[285] it was found that good results were obtained for the intermolecular reactivity sequences when the local hardenesses $\tilde{\eta}_{\mathrm{D}}^{\mathrm{TFD}}(\mathbf{r})$ (also put forward by Berkowitz, Ghosh, and Parr[288]) and $\eta'^{\mathrm{TFD}}_{\mathrm{D}}(\mathbf{r})$, given by eq 143 and

$$\eta'^{\mathrm{TFD}}_{\mathrm{D}}(\mathbf{r}) = \frac{1}{2N}\left[\frac{\partial V^{\mathrm{el}}(\mathbf{r})}{\partial N}\right]_{\nu}\rho(\mathbf{r}) \tag{319}$$

were used, all based on a Thomas–Fermi–Dirac density functional. The molecular electrostatic potential was also found to yield good intermolecular reactivity sequences. These quantities were, however, shown to perform not as well in the study of the intramolecular reactivity of these compounds. An explanation for these observations was provided using the mechanism of the electrophilic aromatic substitution, as shown in Figure 13. In a first step, which is nonspecific, a complex between the π system of the aromatic ring and the electrophile is formed. Since this complex is a donor–acceptor type of complex, its formation can be supposed to be charge controlled, so the formation should be described by the local hardness. In a second step, however, one forms a σ complex, the Wheland complex, where the position of substitution is determined. In this complex, a bond is formed, so it can be expected that orbital interactions are predominant, suggesting that importance should be given to the local softness. A last step is the dissociation of H$^+$ from the Wheland complex, which can be considered to be fast since the aromaticity is restored in this proces. As such, the first step—the formation of the π complex—can be considered to be slow, since the initial aromaticity of the system is lost. In this work, it was finally suggested, along the lines of the work of Chattaraj, that further attention be given to the construction of a global reactivity index $R(\mathbf{r})$, having the form

$$R(\mathbf{r}) = A(\mathbf{r})\eta(\mathbf{r}) + B(\mathbf{r})s(\mathbf{r}) \tag{320}$$

where $A(\mathbf{r})$ and $B(\mathbf{r})$ are distance-dependent factors.

Scheme 9. Formation of Enolate Intermediates upon Aldol Reaction on Unsymmetrical Ketones

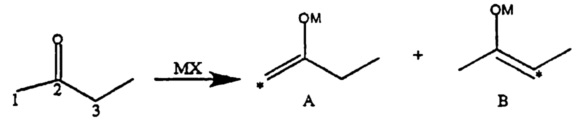

Roy, Krishnamurti, Geerlings and Pal used both the local softness and local hardness to probe both the intra- and intermolecular reactivity of a nucleophilic attack on carbonyl compounds.[269] From the local softness values and the newly introduced concepts of relative electrophilicity (s_k^+/s_k^-) and relative nucleophilicity (s_k^-/s_k^+) (cf. section III.B.3) calculated for these compounds, it was concluded that the nucleophilic attack occurs preferentially on the carbonyl carbon. For the intermolecular reactivity, the local hardness, as defined in eq 143, was found to perform the best, in accord with the previously mentioned results and statements made by Langenaeker et al.[285] To get discrete values for this quantity that can be compared between different molecules, use was made of the Felkin–Anh model for the nucleophilic attack on carbonyl compounds,[697–700] and values for this quantity were obtained along the so-called Bürgi–Dunitz trajectory;[701–703] here, the angle Nu$^-$–C$_{\mathrm{carb}}$–O is taken to be 109°, and the distance Nu$^-$–C$_{\mathrm{carb}}$ was set to 4 au, in accord with previous work. In a subsequent paper, Roy, Choho, De Proft, and Geerlings studied the reactivity of acetaldehyde and some aromatic aldehydes toward acid-catalyzed ^{18}O exchange, using the same set of reactivity descriptors.[636] Again, the intermolecular trends could be explained only by using the concept of local hardness. Moreover, the observed reactivity trends were also investigated using the concept of aromaticity, leading to the introduction of the intrinsic global hardness. To circumvent the intermolecular reactivity problem, and to be able to describe both intra- and intermolecular reactivity with the local softness, Roy et al. applied a new methodology in the study of the aldol reaction on unsymmetrical ketones, where two type of enolate intermediates are produced upon deprotonation, as can be seen in Scheme 9.[704]

The nature of the final aldol product will depend on which of the two enolate intermediates formed is the most reactive toward the incoming aldehyde. The authors then constructed a model system, simultaneously containing the two enolate intermediates, so that the intermolecular reactivity problem is reduced to an intramolecular one, permitting again the use of the local softness. It was shown that this approach was successful.

Intramolecular reaction sequences have also been studied in the case of reaction on fullerenes.

The relationship between fullerene reactivity toward a nucleophile and the curvature at the fullerene surface, which reflects the hybridization of the carbon

Scheme 10. Elimination−Substitution Competition in the Reaction of Para-Substituted Phenolates and *p*-Nitrophenyl Bromide

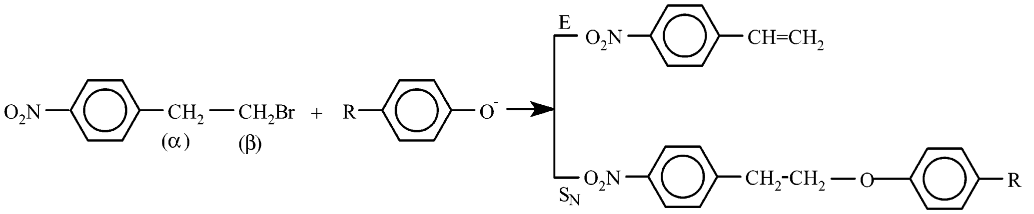

atoms, was investigated by Choho, Langenaeker, Van De Woude, and Geerlings.[685] It was shown, on the basis of calculations on distorted ethylene molecules, that the electronic part of the molecular electrostatic potential is a good descriptor for the reactivity of the double bond toward a nucleophile. For the molecules C_{60}, C_{70}, and C_{76}, this quantity, which is related to local hardness, reproduces both the intra- and intermolecular reactivity sequences. A fair correlation was encountered between the finite difference global hardnesses and the local hardness of these systems. In a subsequent paper,[705] both local softness and local hardness were used to describe the regioselectivity for a nucleophilic attack on the fullerenes C_{24}, C_{26}, C_{28}, C_{30}, C_{32}, C_{36}, C_{50}, C_{60}, C_{70}, and C_{76}. Also in these cases, the local hardness of the most reactive carbon was found to be a good indicator of intermolecular reactivity sequences. Moreover, the stability of a subset of these fullerenes (C_{50}, C_{60}, C_{70}, and C_{76}) was discussed using the maximum hardness principle. The absolute hardness, as approximated by the HOMO−LUMO gap, was found to be the largest for C_{60} and C_{70}, confirming that these molecules are the stablest fullerenes.

Mendez, de L. Romero, De Proft, and Geerlings investigated the elimination/substitution ratio in the reaction of para-substituted phenolates with *p*-nitrophenyl bromide (PNPB) (Scheme 10).[706] Nucleophilic substitution is one of the most fundamental and elementary reaction types in the interconversion of organic molecules.[707] When the nucleophile is a base, this proces usually cannot be completely disconnected from another fundamental reaction, elimination. Both reactions are often competing. The influence of the base on the substitution/elimination ratio is usually explained in terms of basicity (the affinity of the base toward the proton) and nucleophilicity (the affinity toward, in most cases, a carbon atom). Klopman has suggested that basicity should be directly related to the hardness of the base,[461] as will indeed be discussed in section IV.C.3-c. March,[356] however, stated that, since an alkyl substrate is much softer than the proton, it usually prefers soft nucleophiles. The correlation, as proposed by Klopman, was indeed shown to be true: the pK_a values of the para-substituted phenolates are, indeed, correlated with their global hardness. Also, the charge on the oxygen atom in the conjugate base increases with increasing basicity. The interaction with the *p*-nitrophenyl bromide can then be studied from both the local−local and global−local viewpoints (Scheme 10).

Suppose that P1 and P2 are two phenolates, which can attack the β hydrogens H_a and H_b and the carbon atom C_α. If $s_{O^-}(P1) > s_{O^-}(P2)$ and $s_H^+ > s_X^+$, then, from the local−local HSAB principle, it can be invoked that the most favorable interaction will occur with the β hydrogen (elimination). This is, indeed, observed: since both of the β hydrogen atoms in the PNPB are softer than the carbon atom, the phenolate with the highest condensed local softness on the oxygen atom will yield the highest E/S_N ratio. One can also explain the E/S_N ratio by using a local−global viewpoint. Since, as said, $s_H^+ > s_C^+$, the softer phenolate will give the higher E/S_N ratio. This is also observed. The softer phenolates are those that yield more elimination products.

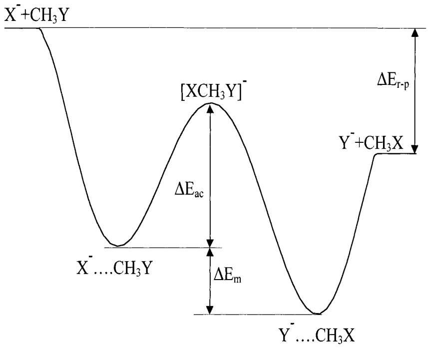

Figure 18. Reaction profile for a gas-phase S_N2 reaction. Reprinted with permission from ref 368. Copyright 2001 American Chemical Society.

Nucleophilic substitution has been central in other studies using the concepts of DFT. Safi, Choho, and Geerlings studied S_N2 reactions of the type[368]

$$X^- + CH_3Y \rightarrow Y^- + CH_3X$$

both in the gas phase and in solution using a polarizable continuum model. The cases studied were those for $X^- = F^-, H^-, OH^-, NH_2^-, HCC^-, CN^-, I^-, Cl^-, Br^-$, and SH^-, and $Y^- = F^-, Cl^-$, and Br^-. It is well known that, in solution, this reaction proceeds in one step, but in aprotic solvents and in the gas phase, three steps occur:[708,709]

$$X^- + CH_3Y \rightarrow X^- \cdots CH_3Y \rightarrow Y^- \cdots CH_3X \rightarrow Y^- + CH_3X$$

giving rise to the reaction profile shown in Figure 18.

Both the ab initio reaction energies and the activation barriers were compared with the same quantities calculated by using Gazquez's formula,[710] using polarizabilities instead of the usual softnesses:

$$\Delta E_{r-p} = \frac{1}{\sum S_r} - \frac{1}{\sum S_p} \qquad (321)$$

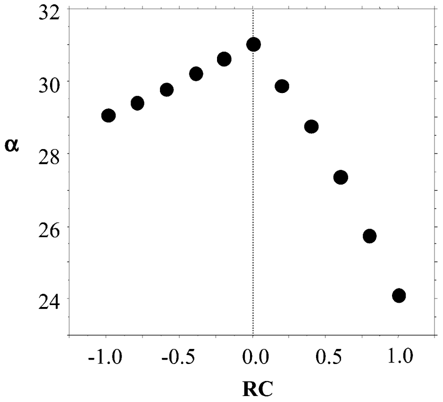

Figure 19. Polarizability (au) profile vs a generalized reaction coordinate for a model S_N2 gas-phase reaction. Reprinted with permission from ref 368. Copyright 2001 American Chemical Society.

and

$$\Delta E_{ac} \approx -\frac{1}{2}(\eta_{TS} - \eta_i) = -\frac{1}{2}\left(\frac{1}{S_{TS}} - \frac{1}{S_i}\right) \quad (322)$$

The agreement was quite good with these quantities. The trends in both the reaction energies and the reaction barriers could be explained by using the HSAB principle. The leaving group ability was found to correlate with its softness (polarizability): a softer leaving group is a better leaving group. Moreover, the charge on the leaving group Y in the complexes is a measure of the exothermicity of the reaction. Also, the exothermicity of the reaction is in the direction that forms the systems with the smallest polarizabilities, in accord with the principle of maximum hardness. The reaction barrier is also smaller with increasing hardness of X^-. For this reaction, a series of IRC paths were also obtained, and the polarizability was plotted along this path; an example is given in Figure 19, for the most exothermic reaction in this study,

$$H^- + CH_3F \rightarrow F^- + CH_4$$

As can be seen very clearly, the polarizability decreases much more sharply from the TS to the ion−product complex than to the ion−reactant complex, showing that, indeed, the hardest species is formed. The influence of the solvent on the kinetics of this reaction was studied using a polarizable continuum model.

Chandra, Uchimaru, Sugie, and Sekiya derived that the hardness values of a series of halomethane molecules correlate with the activation energies for the hydrogen abstraction of these molecules by the OH radical.[609]

Gazquez derived an expression relating reaction energies to differences in hardness of the reagents and products.[480] The derivation starts from the expression for the interaction energy of two species, A and B:

$$\Delta E_{int} = \Delta E_{\nu} + \Delta E_{\mu} + E_{AB}^{NN} \quad (323)$$

where the energy change associated with the first step corresponds to a charge-transfer process between the two species, due to the equalization of their chemical potentials, occurring at a fixed external potential ν. ΔE_{μ} corresponds to the reshuffling of the electron density, occurring after equalization of the chemical potential. Gazquez derived that the interaction energy may finally be expressed as

$$\Delta E_{int} \approx -\frac{1}{2}\frac{\mu_A^0 - \mu_B^0}{\eta_A^0 + \eta_B^0} - \frac{1}{2}N_{e,AB}^2\left(\eta_{AB} - \frac{\eta_A^0\eta_B^0}{\eta_A^0 + \eta_B^0}\right) \quad (324)$$

where N_e is the effective number of valence electrons. In a first application, eq 8 was used to calculate bond energies ($-\Delta E_{int}$). The interaction energy for molecular fragments, where atom i on A forms a bond with atom j on B, becomes

$$\Delta E_{int} \approx -\frac{1}{2}\frac{(\mu_A^0 - \mu_B^0)^2}{\eta_{A,i}^0 + \eta_{B,j}^0} - \frac{1}{2}N_{e,AB}^2\left(\eta_{AB} - \frac{\eta_{A,i}^0\eta_{B,j}^0}{\eta_{A,i}^0 + \eta_{B,j}^0}\right) \quad (325)$$

where, in Gazquez's, work,

$$\eta_{A,i}^0 = \eta_A^0/f_{A,i} \quad (326)$$

and

$$\eta_{B,j}^0 = \eta_B^0/f_{B,j} \quad (327)$$

In the calculation of bond energies, it was found that the contribution of the first term could be considered to be negligible with respect to the second term, except, of course, in those cases where the difference in chemical potentials between the interacting molecules is large. One can thus conclude that the bond energy is proportional to the difference in hardness at the equilibrium position and the hardness of the systems when they are far apart. These quantities were also applied to the computation of reaction energies. For the metathesis reaction

$$A{-}B + C{-}D \rightarrow A{-}C + B{-}D$$

one can derive that the reaction energy ΔE_r can be approximated as (where, among other approximations, $N_e \approx 1$)

$$\Delta E_r \approx -\frac{1}{2}(\eta_{AC} + \eta_{BD} - \eta_{AB} - \eta_{CD}) \quad (328)$$

which is in agreement with the experimental observations that these metathesis reactions go in the direction that produces the (on average) hardest molecules.

Chattaraj and Schleyer performed a quantitative study of the HSAB principle;[711] HF, MP2, and QCISD reaction energies were computed for complexes of the hard acid HF and soft acid Ag^+ with the bases HF, HCl, HBr, H_2O, H_2S, H_2Se, NH_3, PH_3, and AsH_3 using a 6-311+G** basis set and pseudopotentials for Br, Se, As, and Ag. For HF, the HSAB principle was found to be valid at all levels of theory. For the soft−soft interactions, inclusion of electron correlation was found to be absolutely necessary to correctly describe the ordering as predicted by the HSAB principle.

c. Acidity and Basicity. The acid–base equilibrium is one of the most fundamental reaction types in chemistry.[712] It also has been a particularly interesting reaction for the study of structure–reactivity relationships, leading to the development of substituent constants, derived classically in solvent.[713,714] The structure of a molecule can, indeed, affect its acidity or basicity in a large number of ways. Unfortunately, in most molecules, several effects are working simultaneously, and it becomes very complex and difficult to dissect the observed differences in acidity or basicity in terms of the various structural features. Moreover, one must also take into account the effect of the solvent or medium in which the structure–reactivity relationships are determined. It was realized quite early that DFT-based reactivity descriptors could provide valuable insight into acid–base sequences and structure–activity data, as can be noticed from the contributions in this section.

In the gas phase, a number of well-known solution-phase (in most cases, the solvent considered is water) acidity and basicity trends are reversed. The most classical examples are the acidities of carboxylic acids and alkyl-substituted alcohols and the basicities of amines.[707] In the case of the alkyl-substituted alcohols, it was shown that, in aqueous solution, the acidity follows the order $CH_3OH > CH_3CH_2OH > (CH_3)_2CHOH > (CH_3)_3COH$.[707] As can be seen, the acidity decreases with increasing substitution, in accord with the fact that alkyl groups are, in organic chemistry, generally considered to be electron releasing. In the gas phase, however, the sequence is reversed: $CH_3OH < CH_3CH_2OH < (CH_3)_2CHOH < (CH_3)_3COH$, so that alkyl groups can be considered to be electron-withdrawing[715] The first explanation for this apparently anomalous behavior of alkyl groups in the gas phase was provided by Huheey in the early 1970s,[171] just after the experimental gas-phase acidity scale was established.[716] The explanation was based upon the alkyl group electronegativity values that were reported by Huheey in a preceding paper,[587] together with the simple expression, also by Huheey, for the electronegativity of an atom in a molecule (eq 215). It was concluded that, when the inductive effect of a group was discussed, it was necessary to treat both the inherent electronegativity and the charge capacity.

De Proft, Langenaeker, and Geerlings calculated functional group electronegativities and hardnesses for the alkyl groups listed above using the methodology outlined in section IV.A.[717] The electronegativity of these groups was found to decrease with increasing alkyl group size, in accord with the traditional view of alkyl groups being electron releasing. The group hardness was found to decrease along with the group electronegativity, in accord with an increasing group polarizability (softness). The gas-phase acidity trends were rationalized by using a Huheey type of electronegativity equalization scheme using these functional group quantities. The charge transfer to OH and O^- in R–OH and R–O^-, ΔN_{R_I} and $\Delta N_{R_{II}}$, was calculated as

$$\Delta N_{R_I} = \frac{\chi_R^0 - \chi_{OH}^0}{2(\eta_R^0 + \eta_{OH}^0)} \tag{329}$$

and

$$\Delta N_{R_{II}} = \frac{\chi_R^0 - \chi_O^0}{2(\eta_R^0 + \eta_O^0)} + \frac{\eta_O^0}{\eta_R^0 + \eta_O^0} \tag{330}$$

The charge transfer upon deprotonation of the alcohol, $\Delta(\Delta N_R)$, can thus be calculated as

$$\Delta(\Delta N_R) = \Delta N_{R_{II}} - \Delta N_{R_I} \tag{331}$$

which reduces, when the approximation is used that $\chi_O^0 \approx \chi_{OH}^0$ and $\eta_O^0 \approx \eta_{OH}^0$ (i.e., the electronegativity or hardness of the group is mainly determined by the electronegativity and hardness of the central atom or group), to

$$\Delta N_R \approx \frac{\eta_O^0}{\eta_R^0 + \eta_O^0} \tag{332}$$

containing only the group hardness. This term, which can be considered as the ability of the alkyl groups to stabilize negative charge in the process of deprotonation, was shown to correlate well with the gas-phase acidities.

Safi, Choho, De Proft, and Geerlings also used substituent constants (electronegativity and hardness) that were determined in solution using a polarizable continuum model to study the alcohol acidity scale inversion.[366] Charge transfers according to eqs 329 and 330 were calculated with the use of these functional group properties. The charge transfer in these molecules was shown to increase with increasing dielectric constant of the medium. This charge transfer to the oxygen atom decreased, however, from methanol to 2-propanol, along with the stabilization of the conjugate base. In aqueous solution, however, an inversion in both of these quantities occurs. Moreover, the continuum method was used to calculate the relative acidities of the four alcohols. An inversion in the acidity scale was indeed observed, the most important parameter being the stabilization energy of the conjugate base in aqueous solution.

Perez et al. have published several papers on the irregular alkyl alcohol acidity sequences.[272,718,719] They put forward a HSAB rule for the gas-phase acidity: “within a family of related molecules, the greater the global softness value of the conjugate base RX^-, the higher the acidity of the corresponding RXH species”. Indeed, when the alcohol ROH becomes more acidic, the proton affinity of its conjugate base RO^- should decrease. As the proton is a very hard species, the harder the conjugate base, the better the interaction with the proton. It can, indeed, be derived that that, since hard likes hard and soft likes soft, soft conjugate bases correspond with more acidic conjugate acids. Moreover, Perez et al. also showed an inverse relationship between the conjugate bases’ polarizabilities and their proton affinities. It was also proposed to measure the inductive (electronegativity)

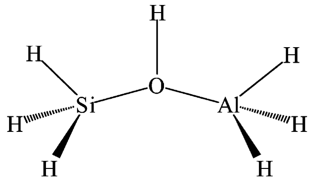

Figure 20. Model system for a bridging hydroxyl group in zeolites.

effect of the various alkyl substituents from the variations in the electronic population on the basic site (the oxygen atom in RO^-) or from the variations of the chemical potential $\Delta\mu^-$, defined as

$$\Delta\mu^- = \mu(RX^-) - \mu(RX'^-) \qquad (333)$$

reflecting the chemical potential differences between the conjugate base RX^- and a reference base RX'^-. In this manner, alkyl groups were shown to behave as electron-withdrawing groups, in accord with the work of Geerlings et al. The use of the electronic chemical potential to assess charge transfer associated with a proton-transfer process was rationalized on the basis of a simple scheme based on a classic ion transport model. Increasing the number of alkyl substituents thus leads to a decrease in electron population at the basic site, leading to an increase of the stabilization of the conjugate base. These concepts were also applied to the thioalkyl alcohols CH_3SH, CH_3CH_2SH, $(CH_3)_2CHSH$, and $(CH_3)_3CH_2SH$[272] and to a series of alkyl-substituted silanols SiH_3OH, $(CH_3)_2SiHOH$, and $(CH_3)_3SiOH$.[720] The polarization substituent effects were described as the variation of the local softness at the basic site. It was found that the basic site becomes softer, with increasing number of alkyl groups, in accord with the increasing polarizability of the substituents. For the silanols, it was concluded that the polarization substituent effect of the alkyl group, as measured from the global polarizability of the conjugate base, has the opposite effect.

The competition between electronegativity and hardness in determining the acidity of halogenated alcohols and silanols was also studied in detail by Damoun, Langenaeker, Van De Woude, and Geerlings, in view of the latter being the basic model systems for the description of zeolite acidity.[721] Zeolites are crystalline aluminosilicates with very distinct properties. (See also section IV.D on clusters and catalysis.) Their Brønsted acidity is due mainly to the presence of the so-called bridging hydroxyl groups, which can be, to a minimal extent, modeled by the system shown in Figure 20, which has been proven to be a minimal but good model system to investigate zeolite acidity.[722] Langenaeker, De Decker, Geerlings, and Raeymaekers modeled the variation of zeolite framework electronegativity by gradually substituting the hydrogen atoms by fluorine atoms.[202] It was found that, next to a series of more classical indicators of reactivity, such as the OH equilibrium distance, the IR frequency of the OH stretch, the OH bond ionicity, as measured by the quantity $|q_O q_H|$, and the dipole moment derivative $(\partial\mu/\partial R_{OH})$, a measure for the integrated IR intensity of the OH stretch, the Fukui function f^+, describing the acidic hydrogen, was a good descriptor for the acidity of these compounds. Corma, Sastre, Viruela, and Zicovich-Wilson calculated relative hardnesses for a series of zeolite model clusters.[723] The hardness of an acidic zeolite, as modeled by the energy of the LUMO, was found to increase with decreasing Si/Al ratio; the softness of the zeolite increases with increasing Si content. Moreover, these authors compared the hardness and the acid strength for a series of clusters, as modeled by the OH bond ionicity $|q_O q_H|$. They concluded that the acid strength determined in this way was dependent on both the zeolite's composition and the spatial arrangement of the different atoms surrounding the active site. The zeolite hardness, however, is mainly dependent on the chemical composition. In a subsequent paper, Corma, Llopin, Viruela, and Zicovich-Wilson studied the effect of changing the Si/Al ratio, in combination with substituting the Al atom by other trivalent atoms, such as Ga and B, using a series of cluster model systems.[724] Again, the hardness was approximated by the LUMO energy. The hardness was again found to decrease with increasing Si/Al ratio. Moreover, a relatively small increase in the hardness was observed by substitution of Al by Ga. The substitution of Al with B results in an even larger increase in the hardness. In an application, these theoretical results were confronted with the experimental para/ortho selectivity changes in the alkylation of toluene by methanol in HY types of zeolites with varying Si/Al content and in H-β zeolites with Al, Al + Ga, Ga, and B as trivalent framework elements. It was found that the para/ortho ratio increases with increasing Si/Al content of the zeolite Y. Since the para carbon in toluene possesses the highest softness, this result can be explained by the HSAB principle, since the zeolite softness also increases with increasing Si/Al ratio. Moreover, it was also found that the para/ortho ratio decreases in the order Si/Al > SiAlGa > SiGa > SiB, which is also in agreement with the calculated softness sequence. The influence of the so-called isomorphous substitution has also been studied in detail by Langenaeker, Coussement, De Proft, and Geerlings.[725] In this study, using model systems similar to those used in the 1990 study, the influence of the substitution of Al (by Ga and B) and Si (by Ge) was considered in detail, using the same range of reactivity descriptors, now also including the charge on the acidic hydrogen. The condensed local softness on the acidic hydrogen was found to be less suited for the description of the relative acidity of these model systems. This was explained by the fact that the experimental zeolite acidity is often determined using small amines and alcohols as reaction partners, which, upon inspection of Pearson's hardness data for molecules,[119,120] can be considered to be systems of intermediate hardness. It was therefore considered that, in view of the HSAB principle, it was not unlikely that the local hardness in the surroundings of the acidic hydrogen could be a good indicator of the relative acidity of these systems. Indeed, the charges on the acidic hydrogen were found to be in perfect agreement with the experimental acidity sequences. The charge, however, cannot be explained by the electronegativity of the groups on the OH group (as approximated by the electronegativity of the central atom). However, when the hardnesses of these groups are considered, the sequences can be explained; i.e., the acidity decreases with increasing hardness of the groups attached. This can be explained as follows: an increasing softness in the surroundings of the active site in the conjugate base or these acids leads to a large delocalization of the negative charge in the basic center, increasing the stabilization of this base, implying higher acidity. Moreover, in accord with the results reported by Perez et al., a softer conjugate base has a lower proton affinity, resulting in a higher acidity of the conjugate acid. The OH bond length and the OH bond ionicity were also found to be good indicators of the acidity, although they describe only one side of the acid−base equilibrium. The dipole moment derivative with respect to the OH bond length, however, failed. Deka, Vitrivel, and Pal revisited the use of the DFT-based descriptors in the study of the isomorphous substitution influence on the acidity of the simple model systems.[726] In their work, the failure of the local softness as an indicator of relative acidity was attributed to its dependence on the basis set, the model for the zeolite cluster, and the different population analysis schemes used to calculate the condensed Fukui function. They found that the relative electrophilicity, defined as the ratio of s^+/s^- on the acidic hydrogen, provided the correct acidity sequence, and they confirmed these results by using larger model systems.

Damoun, Langenaeker, and Geerlings also considered the effect of halogenation on the acidity of these model systems, including isomorphous substitution.[727]

Another example of a group of compounds of which the acidity is dependent on the medium are the alkyl-substituted carboxylic acids[728] and the halosubstituted acetic acids.[729] When considering the acids CH_3COOH, CH_3CH_2COOH, and $CH_3CH_2CH_2COOH$, it is found that the acidity in the gas phase increases from acetic to propionic to butyric acid, whereas in solution, it decreases from acetic to butyric acid. This can be explained by the increasing polarizability of the groups attached to the carboxyl groups. As a result, the negative charge in the conjugate base is more delocalized, thus stabilizing the base, resulting in an increased acidity. Moreover, as the base becomes more polarizable, its softness increases and, as a result, its proton affinity decreases, resulting in a higher acidity. In solution, however, the less polarizable system is the one that is hydrated the best, resulting in a reversal of the acidity sequence. For the halogenated acetic acids, a similar observation is encountered. When a hydrogen is substituted for a halogen in acetic acid, the acidity increases, in line with the higher electronegativity of a halogen with respect to hydrogen, thus increasing the stabilization of the negative charge in the conjugate base. When fluoro-, chloro-, and bromoacetic acids are considered, the acidity increases in the order $FCH_2COOH < ClCH_2COOH < BrCH_2COOH$; again, this is due to an increase in the polarizability of the functional groups attached to the acidic center. In aqueous solution, this sequence is reversed. De Proft, Amira, Choho, and Geerlings investigated the acidity of the substituted acetic acids $X{-}CH_2{-}COOH$, with $X = H$, F, CH_3, CH_2CH_3, $CH{=}CH_2$, CCH, OH, CN, OCH_3, CHO, CH_2F, CHF_2, CF_3, and NO_2, with DFT-based reactivity descriptors.[730] No correlation was found with the condensed local softness on the acidic hydrogen; the noncondensed local softness (the local softness in the surrounding of the acidic hydrogen) showed an inverse correlation with the experimental gas-phase acidities. Two parameters, intuitively found to give a qualitative description of the local hardness, the charge on the acidic hydrogen, and the molecular electrostatic potential, correlated well and positively with the experimental acidities. The softness of the group X was found to play a minor role in the description of the aqueous-phase acidities but becomes more important in the description of the gas-phase acidities, where it becomes a decisive parameter in the correct description of the relative acidities of the alkyl substituted and halogenated carboxylic acids. The relative acidity of the latter was also studied by Perez, Toro-Labbé, and Contreras for the molecules CH_2XCOOH, CHX_2COOH, and CX_3COOH, with X = F, Cl, and Br.[731] Use was made of the electronic chemical potential of transfer, $\Delta\mu_r = \mu(CH_3COO^-) - \mu(RCOO^-)$, which describes the amount and the direction of the charge transfer during the proton-transfer process,

$$\Delta\mu_r = \mu(CH_3COO^-) - \mu(RCOO^-) \qquad (334)$$

necessary to describe the electrostatic effects. For the whole series of acids considered, it was found that $\Delta\mu_r = \mu(CH_3COO^-) - \mu(RCOO^-) > 0$, pointing to a charge transfer consistently going from CH_3COO^- to $RCOO^-$, in the opposite sense of the proton transfer. Moreover, positive variations in energy associated with the proton transfer (as referenced to acetic acid) were found to be associated with negative variations in the global hardnesses of the system, which is in agreement with the maximum hardness principle. For the haloacetic acids, the increasing substitution results in an increase in both the global softness and the local softness at the basic center of the conjugate bases. Krishnamurti and Pal used the concept of group softness in the study of nucleophilic additions to carbonyl compounds and in a study of the relative acidity of acetic and propionic acid.[732] They also observed, in line with the conclusions of De Proft et al., that the local softness on the acidic hydrogen does not yield the correct ordering for those two acids. When the local softness of the adjacent oxygen atom was added to the acidic hydrogen local softness, mimicking the softness of the group OH, the incorrect trend, however, remained. When the next-neighbor atom's softness (i.e., the carbon atom) is finally added to that of the OH group, the correct trend results.

The present authors have also studied the acidity of first- and second-row hydrides CH_4, NH_3, H_2O, HF, SiH_4, PH_3, H_2S, and HCl with DFT-based global and local reactivity descriptors, calculated for the neutral acids and their conjugate bases.[733] A dual correlation between the experimental gas-phase acidities of HX on one hand and the group electronegativity and hardness of X on the other hand was set up, which revealed the importance of the group hardness in the determination of relative acidities, in line with previous findings. The acidity of a number of carbon acids CH_3X with X = NO_2, $CO\phi$, SO_2CH_3, CHO, COEt, COMe, COOMe, and CN was investigated by Rezende, using local and global DFT-based reactivity indices.[734] It was, in line with previous findings, also observed in this work that the local softness on the basic center in the conjugate base decreases with increasing acidity. Carbon acids were also at the center of a study by Choho, Van Lier, Van De Woude, and Geerlings, where the relative acidity of a series of hydrofullerenes was investigated.[735] This work was inspired by a proposition by Taylor and Walton, stating that hydrofullerenes could be real acids but that the acidity of these compounds decreased with increasing hydrogenation.[736] This was, indeed, confirmed by calculations presented in this work. Moreover, the importance of charge delocalization in the conjugate base was stressed. Finally, it was found that the softness of the conjugate base decreased upon hydrogenation; as a result, the proton affinity increases with increasing hydrogenation, resulting in a lower acidity, in line with the proposition by Taylor and Walton. In a subsequent paper, the influence of functional groups on the hydrofullerene acidity was investigated.[737]

This concludes a first subsection where DFT concepts and principles were applied to relative acidities both in the gas phase and in solution. Many basicity sequences have been studied as well. The well-known example, accompanying the acidity of alkyl-substituted alcohols, is the basicity of alkyl-substituted amines.[738] For the series NH_3, CH_3NH_2 $(CH_3)_2NH$, and $(CH_3)_3N$, the gas-phase basicity increases with increasing methyl substitution, whereas in solution, the dimethylamine is more basic than the trimethylamine. For the series NH_3, CH_3NH_2, $CH_3CH_2NH_2$, and $(CH_3)_2CHNH_2$, the gas-phase basicity increases with increasing alkyl group size, whereas in solution, the sequence is

$$NH_3 < CH_3NH_2 \sim CH_3CH_2NH_2 \sim (CH_3)_2CHNH_2$$

The first homologous series has, in fact, been the most studied. Many theoretical studies have been devoted to this irregular ordering of the alkylamine basicity. Yang and Mortier studied these gas-phase basicities using both global and local DFT-based molecular properties.[236] They set up correlations between the experimental gas-phase basicity and a local and a global parameter, the condensed Fukui function for electrophilic attack on the nitrogen atom and the Sanderson molecular electronegativity of the base (geometric average of the atomic electronegativities) on one hand, and the charge on the nitrogen atom and the molecular electronegativity as calculatated by the EEM method on the other hand.

Attention was already focused on the fact that properties of both sides of the acid–base equilibrium should be incorporated in the analysis to give a correct description of the basicity ordering. The alkylamine basicity ordering was revisited by Baeten, De Proft, Langenaeker, and Geerlings, who confirmed that the sole use of descriptors associated with the left-hand side of the acid–base equilibrium, such as the charge on the nitrogen atom, the condensed Fukui function for electrophilic attack on the N, or the molecular electrostatic potential minimum in its surroundings, is insufficient for the correct description of basicity ordering.[739] A dual correlation between the gas-phase basicity on one hand and the sum of the functional group electronegativities and softnesses of the substituents attached to N on the other hand revealed a high importance of the latter quantity: the basicity of the amines increases with increasing softness of the groups on N, in line with the better stabilization of the positive charge in the conjugate acid by groups with a larger polarizability. In a subsequent contribution, the group of compounds studied was extended, yielding the series XNH_2, with X = OH, OCH_3, F, Cl, CF_3, CHO, $C(CH_3)O$, $CH{=}CH_2$, NH_2, H, and CH_3.[740] In this case, however, the electronegativity and a resonance parameter were found to determine the basicity sequence. Perez and Contreras also studied the gas-phase protonation of hydroxylamine, its methylated derivatives, and the aliphatic amino acids glycine, alanine, and valine.[741] The gas-phase proton affinity of the amino acids was investigated along the same lines, where electronegativities and hardnesses were determined for artificially constructed amino acid groups, in both the α-helix and β-sheet conformations.[432] The proton affinity sequence of the amino acids was found to be almost uniquely defined by the group hardness.

Safi, Choho, De Proft, and Geerlings used the SCI–PCM methodology to calculate the relative basicity of NH_3, CH_3NH_2, $(CH_3)_2NH$, $(CH_3)_3N$, $CH_3CH_2NH_2$, and $(CH_3)_2CHNH_2$ in the gas phase and in different solvents.[367] An important parameter was the stabilization energy of the conjugate acid in solution, which was found to increase with increasing hardness of the functional groups on the basic center. This is in line with the findings of Perez, Contreras, and Aizman.[370] On the basis of an approximation of the softness kernel put forward by Vela and Gazquez[547] (treated in some detail in section IV.A), they derived a DFT-based expression for the solvatation energy. It reads

$$\Delta E_{\mathrm{solv}} = \frac{1}{2}\int \rho(\boldsymbol{r})\Phi_{\mathrm{R}}(\boldsymbol{r})\,\mathrm{d}\boldsymbol{r} - \frac{1}{2}S\left[\left(\int f(\boldsymbol{r})\Phi_{\mathrm{R}}(\boldsymbol{r})\,\mathrm{d}\boldsymbol{r}\right)^2 - \int f(\boldsymbol{r})|\Phi_{\mathrm{R}}(\boldsymbol{r})|^2\,\mathrm{d}\boldsymbol{r}\right] \quad (335)$$

where $\Phi_R(\boldsymbol{r})$ is the reaction field potential. This equation indeed bears a great analogy with eq 296. As can be seen, the solvatation energy correlates inversely with the softness of the solute, as was verified for a series of monatomic ions and alkylammonium ions. The alkylamine basicities were also studied using an empirical energy-density relationship for the analysis of substituent effects on chemical reactivity.[719] In this work, an equation was derived bearing close resemblance with the famous Hammett equation:

$$\log\left[\frac{K}{K_0}\right] = \rho\sigma \qquad (336)$$

where K and K^0 are the equilibrium constants (i.e., ionization energies of acids) for the substituted molecule and the reference, σ the substituent constant, and ρ the slope. Perez, Simón-Manso, Aizman, Fuentealba, and Contreras then derived approximately that

$$\ln\left[\frac{\mu}{\mu^0}\right] = \gamma\sum_{\mathrm{A}}\Delta f_{\mathrm{A}} \qquad (337)$$

For the alkylamine basicities, they wrote the following general energy-density expression:

$$\ln\left[\frac{\mathrm{PA(B)}}{\mathrm{PA(NH_3)}}\right] = \rho\Delta f_{\mathrm{N}}^{-} \qquad (338)$$

where PA(B) denotes the proton affinity of the base B and PA(NH_3) the proton affinity of NH_3, and Δf_N^- is equal to

$$\Delta f_{\mathrm{N}}^{-} = f_{\mathrm{N}}^{-}(\mathrm{NH_3}) - f_{\mathrm{N}}^{-}(\mathrm{B}) \qquad (339)$$

i.e., the difference between the condensed Fukui functions for electrophilic attack on the N in NH_3 and in the base B. A linear correlation was obtained, and similar findings were observed in the study of the acidity of alkyl alcohols and thiols. It is thus indeed possible, as also stated in the work of Kneisler and Zhou[598] (see section IV.A), to set up Hammett-type equations relating the variation in, e.g., the proton affinities of acidities with changes in local descriptors of reactivity.

From the whole of the studies reviewed in this section, however, it can be concluded that both DFT-based reactivity descriptors and principles are valuable tools in the correct description and analysis of acid−base equilibria, being an example of so-called “thermodynamic reactivity”. All of these studies also clearly point to the importance of including descriptors or parameters associated with the charged form of the acid−base equilibrium into the analysis. Next to the charge polarization of the initial state of the equilibrium (i.e., the acid or the base), which can be clearly described using the concept of electronegativity, much attention should be devoted to the stabilization of the conjugate base or acid, which is proportional to the polarizability of the groups attached to the acidic or basic center via the relationship[742]

$$E = -\frac{q^2\alpha}{\epsilon R^4} \qquad (340)$$

where q is the charge, α the polarizability, ϵ the relative dielectric constant of the medium, and R the distance. Since the global softness is proportional to the polarizability, the softer the groups attached to the charge in the conjugate base or acid, the stabler this form will become. However, since the solvatation energy is inversely proportional to the softness of the molecule, trends in solution could, and in some famous cases will, alter.

4. Excited States

Originally (cf. section II), density functional theory was introduced and developed for ground states of atoms and molecules. Moreover, all functionals currently available are designed for the ground state, and to the best of our knowledge, until now, no functionals have been explicitly designed for excited states. DFT has been generalized, however, for the lowest energy state of a given symmetry and for an ensemble of states. A current up-to-date status report on the treatment of excited states within DFT can be found in ref 743.

The study and calculation of DFT reactivity descriptors for excited states and the probing of the reactivity of these states using the concepts central in this review have, as a result, been relatively scarce. Chattaraj and Poddar computed the Fukui function, the local hardness and softness, and the polarizability for the ground state (^{1}S) and various excited states (^{1}P, ^{1}D, and ^{1}F) for He and a series of cations isoelectronic with He (i.e., Li^+, Be^{2+}, B^{3+}, and C^{4+}).[744] The relationship between the global softness and the cube root of the polarizability (see section IV.A) was found to hold also for the excited states. Moreover, as could be intuitively expected, the ground state was, in all cases, harder and less polarizable than any of the excited states. In a subsequent study, these authors calculated softnesses and polarizabilities for these systems, described by a two-state ensemble, and found that, when the excited-state contribution to the ensemble increased, an increase in softness and polarizability of the system occurred.[745] Molecular excited states have also been the subject of study. Chattaraj and Poddar performed calculations on the diatomics H_2, HF, N_2, BF, CO, and F_2 for the ground state and the first excited state, chosen to be the lowest energy of a given symmetry, different from the ground-state symmetry.[746] Again, it could be concluded that the hardness decreased upon going from the ground state to the excited state, implying an increase in reactivity. This was confirmed by a number of plots of the charge density, the laplacian of the electron density, the quantum and the molecular electrostatic potential, and the Fukui function, where it could be noticed that the molecular reactivity increases upon excitation. Fuentealba, Simón-Manso, and Chattaraj investigated a series of 12 diatomic molecules and also concluded that a molecule is less polarizable in its ground state than in an electronically excited state of the same spin multiplicity.[747]

Other studies involving excited states are those of Mendez and Garcia-Garibay, who studied the singlet−triplet gaps in carbenes and the addition of singlet carbenes to alkenes,[748] and Sengupta, Chandra, and Nguyen, who studied the regioselectivity of oxetane formation in the photocycloaddition of the lowest excited singlet and triplet states of carbonyl compounds.[749] In the latter study, it was concluded that the HSAB principle can be applied in the local resolution to predict the product formation in photochemical reactions.

D. Clusters and Catalysis

The study of reactivity trends, favorable arrangements, and preferred reaction paths involving extremely large systems such as clusters calls for a somewhat different approach. When considering catalytic activity, it is very important to gain some knowledge of the different electronic processes playing a role. A rather successful attempt in this field was based on a true two-reactant approach involving the analysis of the modes of electron redistribution of reactants within the framework of Nalewajski's charge sensitivity analysis (CSA; see also section III.A).[173,184,227−229] This technique is used mostly at an atomic resolution, using charge distributions from EEM or a semiempirical approach. Within the CSA, the local hardness data and corresponding nonlocal kernels and matrices have been shown to provide a basis for adequate new reactivity indices. These indices include the population normal modes,[226,227,750,751] minimum energy coordinates,[751] externally decoupled modes,[751] and mode contributions to the Fukui function distribution.[228] Important in this context is the establishment of the so-called mapping relations[328,751] between the atomic electron populations and the nuclear position modes. These relations describe the interaction or relation between geometrical and electronic factors associated with a given molecular structure.

The reactivity descriptors defined within the framework of CSA are based on the hardness matrix, $\boldsymbol{\eta}$, of the complete reactive system, say A + B, with two diagonal blocks reflecting the charge couplings within the two reactants (η^{AA} and η^{BB}) and two off-diagonal blocks (η^{AB} and η^{BA}) characterizing interreactant couplings:

$$\boldsymbol{\eta} = \begin{pmatrix} \eta^{AA} & \eta^{AB} \\ \eta^{BA} & \eta^{BB} \end{pmatrix} \tag{341}$$

Furthermore, a distinction is made between modes of charge transfer (CT), dealing with net in- or outflow of electrons, and modes of polarizability (P), dealing with purely internal redistributions of electron density.[226,751] These modes are the eigenvectors that diagonalize the hardness matrix.[228] The corresponding eigenvalues are called principal hardnesses and denote the resistance to charge redistribution. Nalewajski et al. studied the charge response by using this approach in a number of chemisorption systems,[750−758] including allyl-[MoO_3],[759] the study which we will describe in some detail as an example.

P and CT were examined separately as well as in combination (CT + P), to assess the relative importance of these effects in the chemisorption system considered. All the CSA-related quantities were calculated from a semiempirical hardness matrix, including the contributions of both the adsorbate and the substrate. The system itself was selected to study the catalytic reaction of the selective oxidation of the allyl radical to acrolein. On the basis of experimental findings, the [MoO_3] (010) surface was found to represent the active cut of the crystal and was thus selected for the current study.

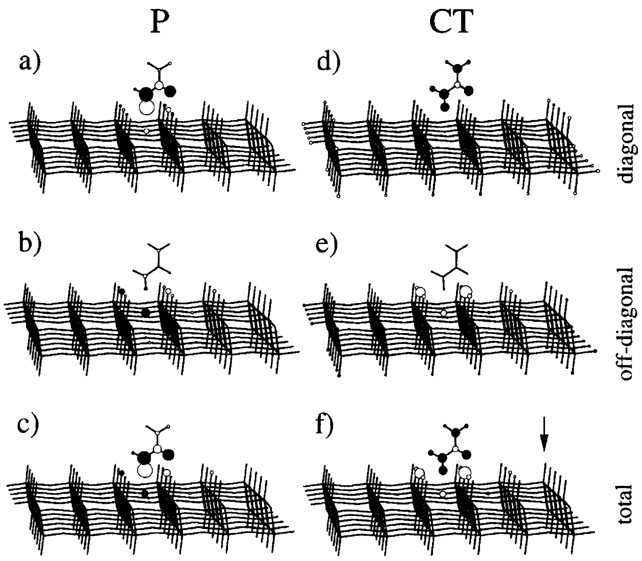

Figure 21. P and CT components for the allyl−MoO_3 interaction. Reprinted with permission from ref 759. Copyright 1996 American Chemical Society.

The relative importance of the P and CT effect in the considered chemisorption process is very interesting from the viewpoint of the "curly arrow" approach to describe reaction mechanisms.[760] In Figure 21, diagrams representing the different P and CT effects for a given arrangement of allyl on the molybdenum oxide surface are given. Similar to the findings of an earlier reported study involving the toluene-[V_2O_5] system,[757] it can be seen that the diagonal (intra-reactant) P and CT components are dominated by the adsorbate, whereas the cluster is mainly responsible for the off-diagonal (inter-reactant) components. In general, one can say that the total charge rearrangement is well approximated by the sum of the adsorbate diagonal contribution and the cluster off-diagonal contribution.

For different arrangements, involving different possibilities of bond formation between adsorbate and cluster, this method provides a tool to determine the type of electronic rearrangement involved in the chemical process. As a rule, it was found that, in all arrangements of the adsorbate with the surface, a CT from the allyl to the surface is predicted. Looking in detail at the P and CT for different arrangements, it was found from P, which can be linked to physisorption, that the allyl polarization is rather sensitive to the arrangement, thus leading to different trends of bond strengthening and weakening of particular bonds. The CT diagrams are, however, relatively insensitive to the adsorbate arrangement on the surface; moreover, they are dominant over the P effects and thus correspond with the overall (P + CT) effects, which is important in the case of chemisorption.

Other fine examples of the CSA can be found in the field of zeolite-catalyzed reactions.[294,328,404,761−764] As a highly representative example, the study of the H-exchange reaction of methane is discussed in some detail.[765] This reaction is characterized by the pres-

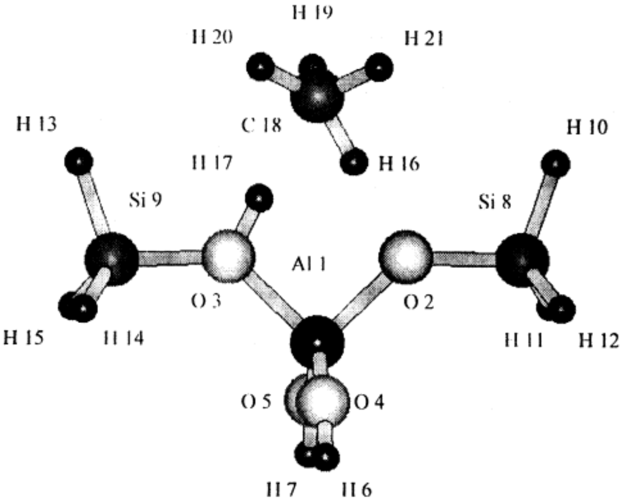

Figure 22. H-exchange reaction of methane over the Brønsted acid site of a zeolite cluster: initial situation. Reprinted with permission from ref 765. Copyright 1996 American Chemical Society.

ence of a "bifunctional" active site involving a Brønsted acid (the bridging hydroxyl (O3−H17)) and a neighboring Lewis base, the oxygen atom (O2).[766]

The zeolite has a direct influence on the activity as well as the selectivity of the reaction, as it is part of the reactive complex. The starting point of this study was an ab initio optimized structure[766] of the cluster shown in Figure 22. Because CSA at atomic resolution using the EEM is fast, the authors were able to study the influence of several characteristics of the model systems, such as the structure, the size, and the chemical composition (Al/Si ratio),[184,409] on the electronic processes involved in the reaction.

As a starting point, the different CSA-related descriptors were calculated for a series of small (cf. Figure 22) structures, modeling different stages of the H-exchange reaction following the reaction coordinate. Here, the two reactants were considered in a supermolecule approach, thus allowing for the treatment of all the charge transfers as internal charge redistribution or polarization. Therefore, only the P modes had to be considered. To identify the polarization modes that are critical for the reaction, their contributions, dQ, to the total charge redistribution (ref 229 and section II.B.1) at several points along the reaction coordinate were calculated. On the basis of this value, the energetical contribution of each mode to the exchange process could be calculated.[765] The softest interaction mode (shown in Figure 23) was found to grow rapidly along the reaction path, to reach a maximum contribution, at the transition state, of 80% to the energy. This mode exactly describes the electronic redistribution that one intuitively associates with the reaction coordinate. For example, the proton of the bridging hydroxyl (H17 in Figure 22) increases its positive charge, inducing a weakening of the O−H bond, while the neighboring bridging oxygen (O2 in Figure 22) decreases its negative charge, inducing an increase in the electron population on the methane hydrogen, thus weakening the C−H bond (C18−H16 in Figure 22).

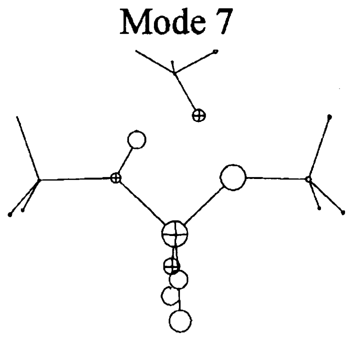

Figure 23. Schematic representation of the softest mode of the methane−cluster adsorption complex. White circles correspond to an electron outflow and white circles with a black cross to an electron inflow. The radii of the circles are proportional to the amount of the electron density displacement. Reprinted with permission from ref 765. Copyright 1996 American Chemical Society.

The effect of the Al distribution and content on the principal hardness of the reaction polarization mode was studied using a faujasite-type 12-ring cluster. When considering all possible positions of two Al atoms in this ring structure, i.e., different distances between two Al atoms for a fixed Si/Al ratio of 5, large distances between the Al atoms (Al atoms situated on opposite sides of the 12-ring) were found to have only a minor influence on the principal hardness, whereas small distances enhance the hardness substantially, thus making the H-exchange reaction much more difficult.

Finally, the cluster size used in this study was increased while keeping the geometry of the reaction center fixed. For relatively small clusters of less than 150 atoms, a drastic drop in the principal hardness value was observed with increasing cluster size. This implies that larger systems are more susceptible to charge polarization.

Finally, the work of Chatterjee and co-workers should be mentioned; they used DFT-based reactivity descriptors, such as the condensed Fukui functions and local softnesses, in a more conventional way to estimate and rationalize the interaction energy of several small molecules with a zeolitic framework, of utmost importance when studying adsorption properties of zeolites.[767−769] Moreover, they attemped to explain selective permeation of these molecules with this methodology.[768] A study was conducted on the choice of the best template for a particular zeolite synthesis by estimating the reactivity of the templating molecules,[769] and a reactivity index study was performed on 2:1 dioctahedral smectites as a selective sorbent for dioxins and furans.[770] Along the same lines, these authors obtained the best dioctahedral smectite for the interaction with some nitrogen heterocycles.[771] A similar approach was adopted earlier by Krishnamurti, Roy, Vitrivel, Iwata, and Pal, studying the interaction of CO, NH_3, and H_2O with a cluster model of faujasite X-type zeolite.[772] Pal and Chandrakumar used the local HSAB principle in the study of the interaction of N_2, CO_2, and CO with a series of zeolite A model clusters, and they proposed a procedure for evaluation of the λ parameter in eq 261, i.e., as the charge transfer at the reactive site.[458]

A. Vos et al. used a variety of DFT-based descriptors, such as activation hardness and the local HSAB principle, in a detailed study on the rate and mechanism of the elementary reaction steps for the methylation of benzene and toluene, as catalyzed by acidic zeolites. The activation hardness obtained via eq 287 by studies on a T_4 cluster (i.e., containing four Al or Si atoms) correlated well with the calculated activation energy, reflecting the reactivity sequence *o*-toluene < *p*-toluene < *m*-toluene < benzene.

When looking at the local level, softness matching (cf. section IV.C.2) did not give the right order for the methylation of benzene and *o*-, *m*-, and *p*-toluene, which is not unexpected, in view of the hardness of the electrophile (CH_3^+) reagent. If the local hardness values are simply approached by the charge on the C atom of the methyl group and the C atom of the aromatic nucleus undergoing the nucleophilic attack, then the indices $\Delta\eta_{CC}$ and $\Pi\eta_{CC}$, describing differences and products of these charges, respectively, correctly represent the reactivity sequence.[773]

To conclude this section, and to illustrate the diversity of problems in this field which were already treated within a conceptual DFT context, a remarkable application of the EEM method in the zeolite field by Guintini et al. should be mentioned. These authors performed thermally stimulated depolarization current (TSDC) measurements to evaluate the energy associated with the detrapping of exchangeable cations. This energy can be associated with the following process in the case of a monovalent exchangeable cation:

$$(\mathrm{Site}^{\delta-}\cdots\mathrm{M}^{\delta+}) \leftrightarrow \mathrm{Site}^- + \mathrm{M}^+$$

where $(\mathrm{Site}^{\delta-}\cdots\mathrm{M}^{\delta+})$ represents the chemical bond formed by the cation trapped in the zeolite site, showing a high degree of ionicity. EEM was used to interpret these data, reflecting cationic hopping processes in Na^+ and Li^+ mordenites.[774]

V. Conclusions

DFT-based concepts have proven to be of great use in the interpretation of a variety of experimental and theoretical results, either as such, or couched within three main principles: electronegativity equalization, the principle of the maximum hardness, and the hard and soft acids and bases principle.

The identification of electronegativity and hardness as the first and second derivatives of the energy vs the number of electrons paved the way to the introduction of many response functions of the system's energy with respect to perturbations with number of electrons or the external potential.

Although some fundamental problems remain (the discontinuity problem and the validity of a fractional particle number concept), and computational techniques still require some further upgrading and systematization (e.g., their implementation in standard quantum chemical packages), the number of papers treating applications of these descriptors is already impressive and continues to increase rapidly.

The general nature of the definition of the reactivity descriptors promotes them to useful tools in a wide variety of domains in chemistry: from regioselectivity in organic reactions, to interpreting the catalytic properties of zeolites or the role of amino acid residues in the catalytic activity of enzymes. Also in certain fields of spectroscopy, some of these concepts can be used to rationalize experimental or theoretical data.

In summary, conceptual DFT is a beautiful example of the way chemists look at molecules, and their properties, as isolated species interacting with either a reaction partner or solvent. Not (completely) satisfied with (let it be) excellent experimental data or (today sometimes amazing) computational accuracy, the chemist puts interpretation of the results on equal footing with their obtention. DFT well-defined atomic, group, or molecular descriptors provide parameter-free tools to continue this tradition, to which chemistry owes so much of its success, in years to come.

VI. Glossary of Most Important Symbols and Acronyms

α	polarizability tensor
$\alpha(\boldsymbol{r})$	local polarizability
A	electron affinity
ABEEM	atom−bond electronegativity equalization method
AhR	arylhydrocarbon receptor
AIM	atoms-in-molecules
APT	atomic polar tensor
$\mathbf{B}$	magnetic field
B	bulk modulus
B3LYP	Becke three-parameter Lee−Yang−Parr functional
B3PW91	Becke three-parameter Perdew−Wang '91 functional
BNO	benzonitrile oxide
BP	Becke−Perdew functional
χ, χ_α, χ_β	electronegativity and spin-polarized extensions
$\bar{\chi}$	average molecular electronegativity
χ_M	molecular electronegativity
$\chi_1(\boldsymbol{r},\boldsymbol{r}')$	linear response function
CISD	limited configuration interaction with all single and double excitations
CI	configuration interaction
CPHF	coupled perturbed Hartree−Fock
CSA	charge sensitivity analysis
CT	charge transfer
D^{at}	atomization energies
$D(r)$	radial density distribution function
DFT	density functional theory
$\Delta\eta^\ddagger$	activation hardness
E	elimination
E	energy
$E(N,\nu(\boldsymbol{r}))$	energy functional
ϵ_i	orbital energies
$E_{xc}[\rho]$	exchange correlation energy
EEM	electronegativity equalization method
ELF	electron localization function
F_B	binding function
$f(\boldsymbol{r})$, $f^+(\boldsymbol{r})$, $f^-(\boldsymbol{r})$	Fukui function
$f_{SN}(\boldsymbol{r})$, $f_{NN}(\boldsymbol{r})$, $f_{SS}(\boldsymbol{r})$	spin-polarized generalizations of the Fukui function
f_k^0, f_k^-, f_k^+	condensed Fukui function on atom *k*
$f^{CT}(\boldsymbol{r})$	charge-transfer Fukui function
$\boldsymbol{\Phi}_\alpha$	nuclear Fukui function
F_{HK}	Hohenberg−Kohn functional
FEOE	full equalization of orbital electronegativity

FF	Fukui function
FMO	frontier molecular orbital
$g(\epsilon_F)$	density of states at the Fermi level
$g(\epsilon_F,\boldsymbol{r})$	local density of states at the Fermi level
G	nuclear stiffness
G2(MP2)	MP2 variant of Gaussian-2 theory
GTO	Gaussian-type orbital
η, η_{NN}, η_{SN}, η_{SS}	global hardness and its spin-polarized generalizations
η_A^0	isolated atom hardness
η_{ij}	hardness tensor
η_M	molecular hardness
$\eta(\boldsymbol{r},\boldsymbol{r}')$	hardness kernel
$\eta(\boldsymbol{r})$	local hardness
$h(\boldsymbol{r})$	hardness density
H_{AB}^r, H_{AB}^s, etc.	Hodgkin–Richards index
H_{op}	molecular Hamiltonian
HF	Hartree –Fock
HIV	human immunodeficiency virus
HMPT	hexamethylphosphorous triamide
HOMA	harmonic oscillator model of aromaticity index
HOMO	highest occupied molecular orbital
HSAB	hard and soft acids and bases
I	ionization energy
$\bar{I}(\boldsymbol{r})$	average local ionization energy
$J(\rho)$	classical Coulombic interaction energy
κ	charge capacity
Λ	lability
LCAO	linear combination of atomic orbitals
LUMO	lowest unoccupied molecular orbital
μ, μ_S, μ_N	electronic chemical potential and spin-polarized generalizations
μ_B	Bohr magneton
MEP	molecular electrostatic potential
MHP	maximum hardness principle
MNDO	modified neglect of diatomic overlap
MO	molecular orbital
MP2	second-order Møller–Plesset
MP4	fourth-order Møller–Plesset
MPP	minimum polarizability principle
n	$= N - Z$
N	number of electrons
N_α	number of α-spin electrons
N_β	number of β-spin electrons
N_S	spin number
n_i	occupation number of the ith orbital
NFF	nuclear Fukui function
NICS	nucleus-independent chemical shift
NPA	natural population analysis
Qeq	charge equilibration method
P	pressure
P	polarization
PA	proton affinity
PAR	property–activity relationship
PCM	polarized continuum model
PEOE	partial equalization of orbital electronegativity
PNPB	*p*-nitrophenyl bromide
Q	total charge of the molecule
q_i	partial atomic charges
QCISD	quadratic configuration interaction with all single and double excitations
QMS	quantum molecular similarity
QSAR	quantitative structure–activity relationship
$\rho(\boldsymbol{r})$	electron density
$\rho_{HOMO}(\boldsymbol{r})$	density of the highest occupied molecular orbital
$\rho_{LUMO}(\boldsymbol{r})$	density of the lowest unoccupied molecular orbital
$s(\boldsymbol{r})$	local softness
$\sigma(\boldsymbol{r})$	shape function
$\boldsymbol{\sigma}_a$	nuclear softness
$s(\boldsymbol{r},\boldsymbol{r}')$	softness kernel
s_k, s_k^-	s_k^+condensed local softness on atom k
S	global softness
S_N	nucleophilic substitution reaction
SAR	structure–activity relationship
SCI–PCM	self-consistent isodensity polarized continuum model
STO	Slater-type orbital
T	temperature
$T(\boldsymbol{r})$	local temperature
$T[\rho]$	electronic kinetic energy functional
$T_S[\rho]$	electronic kinetic energy functional of the Kohn–Sham reference system
TDDFT	time-dependent density functional theory
TFD	Thomas–Fermi–Dirac theory
TS	transition state
TSDC	thermally stimulated depolarization current
UHF	unrestricted Hartree–Fock
ω	electrophilicity
ω_k	condensed local electrophilicity on atom k
Ω	grand potential
$\nu(\boldsymbol{r})$	external potential
$\nu_{eff}(\boldsymbol{r})$	effective potential
$\nu_{xc}(\boldsymbol{r})$	exchange correlation potential
$V(\boldsymbol{r})$	electrostatic potential
$V_{ee}[\rho]$	electron–electron interaction functional
$V_{el}(\boldsymbol{r})$	electronic part of the molecular electrostatic potential
V_o	molar volume
X_α	Slater's X_α method
Ξ	stability
Ψ	electronic wave function
Z	nuclear charge
Z_{AB}^ρ, Z_{AB}^s, etc.	Carbo index

VII. Acknowledgments

Besides his coauthors, P. Geerlings wishes to thank all his past and present collaborators of the Algemene Chemie/General Chemistry Group, figuring as authors or coauthors in the publications mentioned in this review. It has been a privilege to have so many excellent collaborators, with whom it has been a pleasure to work on a great diversity of DFT-related problems. This goal would not have been attainable without the intellectual support and the fruitful exchange of ideas of numerous colleagues, theoreticians as well as experimentalists, from the VUB, Belgium, as well as from numerous other countries. It has been a privilege to collaborate with R. Nalewajski (Cracow), L. Komorowski (Wroclaw), K. D. Sen (Hyderabad), W. Mortier and R. Schoonheydt (Leuven), F. Mendez (Mexico City), P. Fowler (Exeter), M. T. Nguyen (Leuven), and P. Schleyer (Erlangen). One person deserves our most sincere thanks: Professor R. G. Parr, who has supported our research for more than a decade and hosted two of the present authors as postdoctoral fellows. Continuous financial support by the Free University of

Brussels and the Fund for Scientific Research—Flanders is greatly appreciated.

F. De Proft wishes to acknowledge P. Geerlings for continuous support and encouragement throughout his scientific carreer. He also wishes to acknowledge W. Langenaeker for many years of fruitful collaborations and discussions. Moreover, it has been both an honor and a pleasure to interact and collaborate with all the leading scientists listed by P. Geerlings. He is also especially grateful to Professor R. G. Parr for his kind hospitality during his first visit to Prof. Parr's laboratory in the fall of 1996, and for the many encouraging and enlightening discussions.

W. Langenaeker would like to thank Prof. P. Geerlings for awakening his interest in theoretical chemistry and for continuing support throughout his career. Prof. Frank De Proft also deserves special attention for being a great colleague throughout the years and a dear friend. Furthermore, Prof. J. Tollenaere is gratefully acknowledged for giving W.L. the opportunity to work in an exciting industrial environment under his excellent mentorship.

The authors are extremely grateful to Mrs. G. Vandeperre, not only for her meticulous typing and styling of the manuscript but also for invaluable admnistrative assistance in the activities of the research group during the past 15 years. Dr. K. Choho also took care of an important part of this painstaking task. Finally, Mrs. D. Sorgeloos's help with the bibliographic search has been of extreme use. An anonymous reviewer is thanked for constructive remarks.

VIII. Note Added in Proof

A relatively large number of papers appeared in the field since the submission of this review. Below they are briefly presented, arranged in the context of this review following the order of the Table of Contents, however without going into an in-depth discussion. The references start at 775, the final reference of the original version of the text.

The information theoretical approach followed by Parr and Nalewajski[262] to analyze electron densities and to extract from it chemically relevant information, discussed in (II.B3), has further been developped by R. F. Nalewajski (for a comprehensive account, see ref 775). The local equalization of the subsystem information distance densities is discussed in ref 776 and illustrated for a series of di- and triatomic molecules (H_2, N_2, HF, LiF, HCN, HNC). Approximate relationships between information content diagrams and the familiar density difference $\Delta\rho(\boldsymbol{r})$ plots are explored. The analysis of the surprisal function $I(\boldsymbol{r})$,

$$I(\boldsymbol{r}) = \ln\frac{\rho(\boldsymbol{r})}{\rho^0(\boldsymbol{r})} \qquad (342)$$

$\rho^0(\boldsymbol{r})$ representing the reference density, is advocated as the entropic complement to the density difference diagram. A generalization of the formalism from a single electron density to many electron densities $\rho(\boldsymbol{r}_1,\boldsymbol{r}_2,\text{etc.})$ has been presented.[777]

Quite a number of interesting papers appeared on concepts and their calculation (section III.B).

Perez, Aizman, and Contreras[778] presented a comparative study between an experimental, relative scale of electrophilicity and a theoretical, absolute scale based on eq 84.

An important paper was published by Ayers, Morrison, and Roy,[779] presenting a systematic and mathematically rigorous approach to condensed reactivity indices, derived from the variational principle for the energy, thus complementing refs 197 and 342. The important open problem pertaining to the positivity of the condensed Fukui function is discussed in detail, leading to the conclusion that the Hirshfeld partitioning is optimal for obtaining non-negative Fukui functions, in line with the computational results by Roy, Hirao, and Pal[255] and very recent results by Thanikaivelan et al.[780] It is hypothesized that strong diagonal dominance of the condensed hardness matrix is sufficient for the non-negativity of the Fukui function. Errors in the atomic partitioning and inadequate treatment of correlations are pinpointed as the most likely causes of negative condensed Fukui functions. The authors also argue that condensed Fukui functions are, in some respect, more appropriate indicators for site selectivity than the Fukui function itself from a detailed consideration of the condition for maximization of the $\int\int f_A^+(\boldsymbol{r})f_B^-(\boldsymbol{r}')/|\boldsymbol{r} - \boldsymbol{r}'|\,d\boldsymbol{r}\,d\boldsymbol{r}'$ integral (Fukui function interaction integral between a nucleophilic partner B and an electrophilic partner A).

Polarization and charge-transfer components of general displacements of the equilibrium electron distribution in molecules have been treated by Nalewajski,[781] in line with his earlier work on charge sensitivity analysis (see sections III.A and IV.D).

Turning from Fukui functions and softness to the softness kernel (III.B.3), the work by Langenaeker and Liu[782] should be mentioned, in which they studied the response of the electron density to perturbations in external potential for atoms, concentrating on the linear response function $\chi(\boldsymbol{r},\boldsymbol{r}') = (\delta\rho(\boldsymbol{r})/\delta v(\boldsymbol{r}'))_N$ (cf. Scheme 4).

The change in $\rho(\boldsymbol{r})$, $\Delta\rho(\boldsymbol{r})$, upon the introduction of a small positive charge (0.01 au), mimicking some change in the external potential, has been investigated.

Correlations between characteristics of $\Delta\rho(\boldsymbol{r})$ and the polarizability α were investigated. Solà and coworkers[783] simplified the hardness kernel $\eta(\boldsymbol{r},\boldsymbol{r}')$ to $1/|\boldsymbol{r} - \boldsymbol{r}'|$ and $\delta(\boldsymbol{r} - \boldsymbol{r}')$ to calculate the global hardness via expressions such as eq 142. For a series of Lewis bases, the simplest model ($\delta(\boldsymbol{r} - \boldsymbol{r}')$), giving

$$\eta = \int f^2(\boldsymbol{r})\,d\boldsymbol{r} \qquad (343)$$

yields the best ordering of the systems when compared with "experimental" hardness (finite difference values, eq 54, combined with experimental I and A values). Correct esimates of the global hardness, however, are obtained only after empirical corrections, as the hardnesses in the simplified procedures are systematically underestimated (as opposed to the atomic calculations by Liu, De Proft, and Parr[301]).

In the context of their work on the nuclear Fukui function, the nuclear softness (cf. section III.B.6), Komorowski and Ordon studied the evolution of the molecular electronegativity and hardness upon bond elongation of diatomics.[784] The most important result is the "vibrational softening", indicating that diatomic molecules tend to be softer upon elongation, in line with earlier work by these authors.[339]

Coupling relations between the molecular electronic and geometrical degrees of freedom have been investigated in the context of the charge sensitivity analysis by Nalewajski.[785] Several mapping quantities and relations of both the electron-preceding and electron-following categories (cf. also Geerlings, Balawender, and De Proft[333,338]) have been identified, and the algorithms for their calculation have been derived within both local and atomic resolution. Electron-following mapping transformations allow one to predict qualitatively electron redistribution following a given displacement in the nuclear coordinates. The inverse electron-preceding transformations can be used to manipulate, e.g., atomic charges (reflected in their oxidation state) to achieve a desired change in the system geometry.

Within the context of spin-polarized generalizations (section III.B.7), Perez et al. extended the idea of electrophilicity[186,187] to spin-philicity (ω_s^+) and spin-donicity (ω_s^-) as global reactivity indices for molecular systems susceptible to undergo a change of their spin state as a result of a chemical reaction.[786a] They defined

$$\omega_s^{\pm} = \mu_s^{\pm}/2\eta_{ss}^0 \tag{344}$$

where μ_s and η_{ss}^0 are the spin potential and the general hardness of eqs 206 and 209. The phenomenon of spin catalysis[786b]—spin transformation of chemically reactive species induced by the interaction with external spin carriers—is discussed on the basis of an absolute scale for ω_s^+ and ω_s^-.

The influence of solvent on the hardness (cf. section III.B.8) has been studied by Russo and co-workers[787] in the case of a series of neutral and charged molecules. Combination of the PCM method[358] with different techniques for hardness evaluation shows that the internally resolved hardness tensor method (eq 78)[180] and the frontier orbital energy method (eq 68) yield much lower solvent dependences than the finite difference technique (eq 56). In general, Pearson's conclusion[365] that compounds seem to be much softer in water than in the gas phase is confirmed, as also in earlier work by Lipinski and Komorowski.[364]

Turning to principles (section III.C), Sengupta and Toro-Labbé[788] presented a new additivity scheme for both electronegativity and hardness, in line with earlier work by Sanderson,[113,378−391] Nalewajski,[384] Ghosh,[438] and Datta.[436,437] The chemical potential of a composite system is written as a weighted average of the constituents' chemicals potential, the weight factor being the Fukui function:

$$\frac{1}{\mu} = \sum_i \frac{f_i}{\mu_i} \tag{345}$$

which is a generalization of eq 223.

The corresponding hardness equation is obtained by differentiation with respect to N. In the resulting equations, generalizing eq 239, the Fukui function derivative $(\partial f_i/\partial N)_{v(r)}$ appears.

Numerical results for a large series of biradical-type fragments consistently show better results for the estimation of the aggregate chemical potential compared to those following Sanderson's scheme, highlighting the importance of the weighting of the constituent fragments via the Fukui function.

Bultinck et al.[789,790] presented an in-depth study on an extension of Mortier's[403] electronegativity equalization method, including the elements H, C, N, O, and F, aiming at fast calculation of the charge distributions of large molecules in large series of systems, which is needed in screening procedures in medicinal chemistry. A careful calibration of the effective electronegativity and hardness parameters (μ_A^*, η_A^*, eq 226) was performed using a large set of molecules, representing a large series of functional groups in medicinal chemistry.

EEM-derived Mulliken and NPA charges were in good agreement with the ab initio values; however, CHELPG, and, somewhat unexpectedly, Hirshfeld charges showed less agreement. Bultinck and Carbo-Dorca[791] presented a systematic and efficient procedure for computing various DFT-based reactivity descriptors with the EEM scheme, suitable for high-throughput screening.

Chandrakumar and Pal[792] extended the local HSAB principle, as discussed in section III.C.2-b, to the case of multiple-site interactions.

In line with the large series of studies mentioned in section III.C.3 by Toro-Labbé and co-workers, this group[793] studied the application of the maximum hardness/minimum polarizability principle to the imine−enamine tautomerism for a series of eight imine derivatives CH_3CXNH (X = H, F, Cl, Br, CH_3, OH, NH_2, $N(CH_3)_2$). The relative stability between reactants, transition states, and products follows an ordering that is consistent with both the MHP and the minimum polarizability principle.

Turning to the application section (section IV) on atoms and functional groups, the comprehensive study by Ghosh and Biswas[794] of the absolute radii of atoms and monatomic ions should be mentioned. They computed atomic hardness values, starting from the expression of the energy of charging a conducting sphere of radius R with charge q:

$$E = q^2/2R \tag{346}$$

Combining eq 346 with the hardness equation, eq 56, one easily arrives at (in cgs units)

$$\eta = e^2/2R \tag{347}$$

The values obtained via eq 347 were compared with Pearson's values[119] based on the use of experimental ionization energies and electron affinities in combination with eq 56. It was seen in a significant number of cases that the expected sequences of hardness and radius are inverted. In 26 cases, calculated and "experimental" $(I + A)/2$ values show deviations smaller than 1.0 eV. The radius/hardness relationship deserves further study, as it is one of the easiest ways to distinguish hardness patterns throughout the Periodic Table.

Geerlings and co-workers[795] used ab initio calculated functional group properties to interpret atomic dipoles determined within the Hirshfeld partitioning technique of the electron density (cf. refs 258−261) on the hydrogen and chlorine atoms of compounds of the type H−X and Cl−X. In the case of HX compounds, the atomic dipole moment of the X atom was found to be linearly correlated with the electronegativity of the group X. In the case of Cl−X compounds, group hardness enters the correlation if the group X carries a heteroatom as the central atom. The resulting correlation,

$$\mu(\mathrm{Cl}) = 0.036\chi_{\mathrm{x}} - 0.020\eta_{\mathrm{x}} - 0.0204 \quad (\mu \text{ in a.u.}; \chi \text{ and } \eta \text{ in eV}) \tag{348}$$

illustrates the opposite effect of χ and η, with the hardness effect being a factor of 2 smaller in the atomic dipole moment (largely caused by the nonbonding electron pairs on Cl).

Senthilkumar et al.[796] presented a detailed DFT and ab initio study on the evolution of the chemical hardness and electronic chemical potential with the internuclear distance.

As it has been previously shown that CBS-QB3 and G3B3 methods yield excellent results in the calculation of electron affinities of small diatomic molecules,[797a] Jalbout and co-workers used the same methodology to calculate ionization energies, absolute electronegativities, hardnesses, and softnesses of a series of homonuclear and heteronuclear diatomics, using the finite difference approximations, eqs 41 and 56.[797b] Correlations with experimental data for χ and η, when available, are very promising for the CBS-QB3 and G3B3 methodologies.

Several groups applied DFT-based descriptors and principles to various types of chemical reactions.

Aizman et al.[798] studied the Markovnikov regioselectivity rule in electrophilic additions of HCl to a series of asymmetrically substituted alkenes. A "static" local analysis, based on the electrophilic and nucleophilic condensed Fukui functions, shows that the attack of the proton to the Markovnikov center is preferred. The importance of the paper lies in the evaluation of the activation of the nucleophilic center in the carbocation in terms of the enhancement in local softness for nucleophilic attacks.

Local softness differences between TS and reactants, characterized by superscripts ‡ and °, respectively, were therefore evaluated as

$$\Delta s_k = s_k^{\ddagger} - s_k^{0} \tag{349}$$

where this difference may further be partitioned as

$$\Delta s_k = S^0 \Delta f_k + f_k^{\ddagger} \Delta S \quad \text{with} \quad \Delta f_k = f_k^{\ddagger} - f_k^{0} \quad \text{and} \quad \Delta S = S^{\ddagger} - S^{0} \tag{350}$$

The first term assesses the local activation at the site, and the second one takes into account the global activation of the whole system. The Markovnikov channel presents a transition state that is lower in energy and softer than the one corresponding to the anti-Markovnikov additions.

Mitnik and Lucero[799] used the standard static approach discussed in section IV.C.2-a to study the regioselectivity of electrophilic reactions on isomeric thiadiazolines. Korchowiec[800] used the radical charge-transfer Fukui function (cf. eq 108) in the AIM discretization to classify atoms of a given molecule into electrophilic and nucleophilic centers, taking pyridine and 2-aminopyridine as examples.

In line with earlier studies by our group on $\mathrm{SCN^-}$,[56,212] Tielens et al.[801] used condensed Fukui functions to interpret the results of interaction energy and IR frequency shift calculations of $\mathrm{SCN^-}$ with Ag clusters of various size, modeling a silver electrode. The most adequate representation seems to be a $\mathrm{Ag_{23}}$ cluster. The preferred interaction mode of $\mathrm{SCN^-}$ is via the sulfur atom on a hollow side of the silver electrode. At higher surface charge, adsorption via the nitrogen atom becomes more favorable as compared to adsorption via sulfur, in agreement with the HSAB principle.

In line with Mitnik and Lucero, Pilepic and Ursic[802] used the standard approach of the condensed Fukui functions (supplemented by the relative nucleophilicty indices f_k^+/f_k^-)[269,270] to study the nucleophilic reactivity of the nitroso group in nitrosobenzene and 2-methyl-2-nitrosopropropane. The O atom of the nitroso group was the most reactive nucleophilic center for softer reagents, its role being taken over by the harder N atom for harder reactants.

Finally, turning to regioselectivity in concerted reactions (section IV.C.2-e), the Diels−Alder reaction has been investigated independently by Cong et al., using the ABEEM $\sigma\pi$ model,[803a] and by Domingo using the local electrophilicity concept.[804]

In the former study, the softness-matching expression (eq 318) was used in combination with Yang and Wang's ABEEM method[413−418] to account successfully for the regioselectivity of Diels−Alder reactions of the type described in ref 446. Moreover, it has been shown that the MHP is obeyed in the exo/endo stereospecificity, the endo hardness being always larger than the exo hardness, in accordance with experiment.[803b] Endo isomers indeed constitute the main product of Diels−Alder reactions, where dienes and/or dienophiles carry carboxyl or fenyl groups as substituents.

Domingo et al.[804] extended the electrophilicity index ω introduced by Parr, Von Szentpaly, and Liu[186,187] (section III.B.2) to a local, condensed version, ω_k. Starting from eq 84, and using the additivity rule for global softness[226,438] (eq 241), the following expression was obtained (case of electrophilic attack):

$$\omega = \frac{\mu^2}{2\eta} = \frac{\mu^2}{2}S = \frac{\mu^2}{2}\sum_k s_{\mathrm{k}}^+ = \sum_k \omega_k^+ \qquad \text{with}$$
$$\omega_k = \frac{\mu^2}{2}s_k^+ \quad (\text{or } \omega_k = \omega f_k^+) \quad (351)$$

Whereas the polar character of the electrophile/nucleophile interaction is dictated by the global electrophilicity gap $\Delta\omega$ (see next section),[805] the selectivity at the electrophilic partner is described by eq 351. (Note that, within a given molecule, the sequence is parallel to the Fukui function sequence.)

Turning to intermolecular reactivity sequences, the same authors obtained information about the polarity of the transition-state structure for Diels–Alder reactions from the difference in electrophilicities of the diene/dienophile interaction pairs. The electrophilicity index comprises both the propensity of an electrophile to acquire an additional charge (driving force μ^2) and the resistance of a system to exchange electronic charge with the environment (described by η). High electrophilicity is therefore expected for a combination of high μ and low η values.

Small $\Delta\omega$ values might, therefore, favor nonpolar (pericyclic) mechanisms, and big $\Delta\omega$ values might favor polar (ionic) mechanisms. This result is confirmed by relating $\Delta\omega$ values to ΔN values obtained from transition-state calculations, the latter values characterizing the TS polarity: increasing $|\Delta\omega|$ is, in general, accompanied by increasing $\Delta\omega$.

Perez et al.[806a] investigated the global electrophilicity of benzhydryl cations as a function of the substituents in para position(s), calculated via eq 84 with an experimental scale recently proposed by Mayr.[806b] In ongoing research into the relationship between the toxicity of various dioxins, the electron acceptor or donor character of dioxins upon interaction with amino acids (histidine, phenylalanine, tryptophan) has been probed by Arulmozhiraja et al.,[807] using Huhey's formula (eq 217). The calculated ΔN values show that dioxins act as electron acceptors in the interactions considered. The nucleophilic centers of the amino acids were evaluated by considering f_k^- and s_k^- values.

Mignon et al.[808a] performed large-scale calculations on a nucleophilic activation dyad in ribonucleases. In a RNAse-catalyzed phosphodiester cleavage, a nucleophilic attack on the P atom of the phosphodiester bond by the 2′-hydroxyl group in RNA takes place. The nucleophilicty of the 2′-hydroxyl in the active site was mimicked by the charge on the oxygen, serving here as a crude model for the local hardness in view of the relatively hard character of the P atom in the phosphate group. On studying both "in vitro" and "in silico" mutations (both for single and double mutants), results were obtained that were entirely consistent with protein engineering and kinetic experiments.[808b]

Some interesting papers also recently appeared on clusters and catalysis (section IV.D).

A collaboration between theorists (Geerlings and co-workers) and NMR and tin chemists (Sanchez, Willem, and co-workers) led to the first large-scale ab initio DFT calculations on a Sn-containing nanocluster, $[(RSn)_{12}O_{14}(OH)_6]^{2+}$ ($R = CH_3$). Factors determining the exact nature of the interactions of the cluster with anions or neutral nucleophiles (F^-, Cl^-, OH^-, H_2O, acetone, DMSO) were studied with DFT-based reactivity descriptors.[809] The hexacoordinated tin atoms, situated at the poles of the Sn cage, are harder, while the pentacoordinated ones, situated at the equator, are softer. Combining these results with the local HSAB principle, theory is in line with ^{119}Sn NMR data, indicating that anions prefer to interact with the cage poles and neutral nucleophiles prefer to interact with the equatorial atoms.

In the zeolite field, Deka and Hira[810] used relative electrophilicity values s_k^+/s_k^- to probe the Lewis acidity of cation-exchanged faujasites (M-FAU), decreasing in the order (Li-FAU) > (Na-FAU) > (K-FAU). Both trends are in line with experiment. In an analogous way, the relative nucleophilicity s_k^-/s_k^+ of the framework oxygen atoms was investigated, showing an increasing Lewis basicity (Li-FAU) < (Na-FAU) < (K-FAU). As a sequel to the study on the acid zeolite catalysis of methylation of benzene and toluene,[773] Vos et al. performed an in-depth study on the use of reactivity descriptors for the acid zeolite-catalyzed ethylation and isopropylation of benzene.[811]

We finally mention the study by Jacque and Toro-Labbé on the characterization[812] of copper clusters Cu_n ($n = 2, 3, ..., 9$): descriptors such as electronic chemical potential μ and hardness η, combined with the minimum polarizability and maximum hardness principle, turn out to be operative for characterizing and rationalizing the electronic properties of copper clusters. It was found that the more stable the cluster, the less polarizable and the harder it is, in agreement with the MPP and MHP, respectively.

IX. References

(1) Hohenberg, P.; Kohn, W. *Phys. Rev. B* **1964**, *136*, 864. For a recent perspective, see: Ernzerhof, M.; Scuseria, G. E. *Theor. Chem. Acc.* **2000**, *103*, 259.
(2) Koch, W.; Holthausen, M. C. A *Chemist's Guide to Density Functional Theory*; Wiley-VCH: Weinheim, 2000.
(3) Pople, J. A. *Rev. Mod. Phys.* **1999**, *71*, 1267 (Nobel Lecture).
(4) Kohn, W. *Rev. Mod. Phys.* **1999**, *71*, 1253 (Nobel Lecture).
(5) Thomas, L. H. *Proc. Cambridge Philos Soc.* **1927**, *23*, 542.
(6) Fermi, E. *Z. Phys.* **1928**, *48*, 73.
(7) Dirac, P. A. M. *Proc. Cambridge Philos. Soc.* **1930**, *26*, 376.
(8) Von Weizsäcker, C. F. *Z. Phys.* **1935**, *96*, 431.
(9) Slater, J. C. *Phys. Rev.* **1951**, *81*, 385.
(10) Slater, J. C. *Adv. Quantum Chem.* **1972**, *6*, 1.
(11) Slater, J. C. *The Self-Consistent Field for Molecules and Solids*; Mc Graw Hill: New York, 1974.
(12) Kohn, W.; Sham, L. J. *Phys. Rev.* A **1965**, *140*, 1133.
(13) For a recent perspective, see: Baerends, E. J. *Theor. Chem. Acc.* **2000**, *103*, 265.
(14) Frisch, M. J.; Trucks, G. W.; Schlegel, H. B.; Scuseria, G. E.; Robb, M. A.; Cheeseman, J. R.; Zakrzewski, V. G.; Montgomery, J. A., Jr.; Stratmann, R. E.; Burant, J. C.; Dapprich, S.; Millam, J. M.; Daniels, A. D.; Kudin, K. N.; Strain, M. C.; Farkas, O.; Tomasi, J.; Barone, V.; Cossi, M.; Cammi, R.; Mennucci, B.; Pomelli, C.; Adamo, C.; Clifford, S.; Ochterski, J.; Petersson, G. A.; Ayala, P. Y.; Cui, Q.; Morokuma, K.; Malick, D. K.; Rabuck, A. D.; Raghavachari, K.; Foresman, J. B.; Cioslowski, J.; Ortiz, J. V.; Stefanov, B. B.; Liu, G.; Liashenko, A.; Piskorz, P.; Komaromi, I.; Gomperts, R.; Martin, R. L.; Fox, D. J.; Keith, T.; Al-Laham, M. A.; Peng, C. Y.; Nanayakkara, A.; Gonzalez, C.; Challacombe, M.; Gill, P. M. W.; Johnson, B. G.; Chen, W.; Wong, M. W.; Andres, J. L.; Head-Gordon, M.; Replogle, E. S.; Pople, J. A. *Gaussian 98*; Gaussian Inc.: Pittsburgh PA, 1998, and previous versions.
(15) Roothaan, C. C. J. *Rev. Mod. Phys.* **1951**, *23*, 69.
(16) Møller, C.; Plesset, M. S. *Phys. Rev.* **1934**, *46*, 618.

(17) Shavitt, I. The Method of Configuration Interaction. In *Methods of Electronic Structure Theory*; Schaefer, H. F., III, Ed.; Modern Theoretical Chemistry 3; Plenum Press: New York and London, 1977; p 189.

(18) Bartlett, R. J. *J. Phys. Chem.* **1989**, *93*, 1697.

(19) Hehre, W. J.; Radom, L.; Schleyer, P. v. R.; Pople, J. A. *Ab Initio Molecular Orbital Theory*; Wiley: New York, 1986.

(20) Jensen, F. *Introduction to Computational Chemistry*; Wiley: New York, 1999.

(21) Szabo, A.; Ostlund, N. S. *Modern Quantum Chemistry*; McMillan: New York, 1982.

(22) Helgaker, T.; Jørgenson, P.; Olsen, J. *Molecular Electronic Structure Theory*; John Wiley: New York, 2000.

(23) Parr, R. G.; Yang, W. *Annu. Rev. Phys. Chem.* **1995**, *46*, 701.

(24) Parr, R. G. *Annu. Rev. Phys. Chem.* **1983**, *34*, 631.

(25) *Theory of the Inhomogeneous Electron Gas*; Lundquist, S., March, N. H., Eds.; Plenum: New York, 1983.

(26) *Density Functional Methods in Physics*; Dreizler, R. M., de Providencia, J., Eds.; Plenum, New York, 1985.

(27) Parr, R. G.; Yang, W. *Density Functional Theory of Atoms and Molecules*; Oxford University Press and Clarendon Press: New York and Oxford, 1989.

(28) Jones, R. O.; Gunnarson, O. *Rev. Mod. Phys.* **1989**, *61*, 689.

(29) Kryachko, E. S.; Ludena, E. V. *Density Functional Theory of Many Electron Systems*; Kluwer: Dordrecht, The Netherlands, 1990.

(30) *Density Functional Theory: An Approach to the Quantum Many Body Problem*; Dreizler, R. M., Gross, E. K. U., Eds.; Springer-Verlag: Berlin, 1990.

(31) *Density Functional Theory of Many Fermion Systems*; Trickey, S. B., Ed.; Advances in Quantum Chemistry 21; Academic Press: San Diego, CA, 1990; pp 1−405.

(32) Ziegler, T. *Chem. Rev.* **1991**, *91*, 651.

(33) *Density Functional Methods in Chemistry*; Labanowski, J. K., Andzelm, J. W., Eds.; Springer-Verlag: New York, 1991.

(34) March, N. H. *Electron Density Theory of Atoms and Molecules*; Academic Press: London, 1992.

(35) Parr, R. G. *Philos. Mag. B* **1994**, *69*, 737.

(36) *Modern Density Functional Theory: A Tool for Chemistry, Theoretical and Computational Chemistry*; Politzer, P., Seminario, J. M., Eds.; Elsevier: Amsterdam, 1995; Vol. 2.

(37) Goursot, A., Mijoule, C., Russo, N., Eds. *Theor. Chim. Acta* **1995**, *91*, (3,4) (special issue).

(38) Chong, D. P. *Recent Advances in Density Functional Methods*; World Scientific: Singapore, 1995.

(39) Nalewajski, R. F., Guest Editor. Thirty years of DFT: Concepts and Applications. *Int. J. Quantum Chem.* **1995**, *56*, 197−875 (special issue).

(40) *Density Functional Theory*; Nalewajski, R. F., Ed.; Topics in Current Chemistry 179−182; Springer: Berlin, 1996.

(41) *Theoretical and Computational Chemistry*; Seminario, J., Ed.; Recent Developments and Applications of Modern Density Functional Theory 4; Elsevier: Amsterdam, 1996.

(42) *Metal−Ligand Interactions: Structure and Reactivity*; Russo, N., Salahub, D. R., Eds.; Kluwer: Dordrecht, The Netherlands, 1996.

(43) Springborg, M. *DFT Methods in Chemistry and Material Science*; Wiley: New York, 1997.

(44) Yang, W., Levy, M., Trickey, S., Guest Editors. Symposium on Density Functional Theory and Applications. *Int. J. Quantum Chem.* **1998**, *69*, 227−627.

(45) *DFT, a Bridge between Chemistry and Physics*; Geerlings, P., De Proft, F., Langenaeker, W., Eds.; VUB Press: Brussels, 1998.

(46) Nagy, A. *Phys. Rep.* **1998**, *298*, 1.

(47) Görling, A.; Trickey, S. B.; Gisdakis, P.; Rösch, N. In *Organometallic bonding and reactivity: fundamental studies*; Hofmann, P., Brown, J. M., Eds.; Topics in Organometallic Chemistry 4; Springer Verlag: Berlin, 1999; p 109.

(48) Dobson, J. F. *Int. J. Mod. Phys. B* **1999**, *13*, 511.

(49) Geerlings, P.; De Proft, F.; Langenaeker, W. *Adv. Quantum Chem.* **1999**, *33*, 303.

(50) Chermette, H. *J. Comput. Chem.* **1999**, *20*, 129.

(51) Frenking, G. *J. Comput. Chem.* **1999**, *20* (1) (Special Issue on Progress in Density Functional Theory).

(52) Mineva, T.; Neshev, N.; Russo, N. Sicilia, E.; Toscano, M. *Adv. Quantum Chem.* **1999**, *33*, 273.

(53) Argaman, N.; Makov, G. *Am. J. Phys.* **2000**, *68*, 69.

(54) *Density Functional Theory and its Application to Materials*; Van Doren, V., Van Alsenoy, C., Geerlings, P. Eds.; AIP Conference Proceedings 577; American Institute of Physics: New York, 2001.

(55) *Recent Advances in Density Functional Methods, Part III*; Barone, V., Bencini, A., Fantucci, P., Eds.; World Scientific: River Edge, NJ, 2002.

(56) Geerlings, P.; De Proft, F.; Martin, J. M. L. In *Recent Developments and Applications of Modern Density Functional Theory*; Seminario, J. M., Ed.; Theoretical and Computational Chemistry 4; Elsevier: Amsterdam, 1996; p 773.

(57) Geerlings, P.; De Proft, F.; Langenaeker, W. In *Density Functional Methods: Applications in Chemistry and Material Science*; Springborg, M., Ed.; John Wiley: New York, 1997; Chapter 2.

(58) Geerlings, P.; De Proft, F.; Langenaeker, W. In *Developments in the Theory of Chemical Reactivity and Heterogeneous Catalysis; Trends in Physical Chemistry*; Schoonheydt, R., Ed.; Transworld Research Network: Trivandrum, India, 1997; Chapter 1.

(59) De Proft, F.; Geerlings, P. *Chem. Rev.* **2001**, *101*, 1451.

(60) Geerlings, P.; De Proft, F. In *Reviews of Modern Quantum Chemistry, A Celebration to the Contributions of R. G. Parr*; Sen, K. D., Ed.; World Scientific: Singapore, 2002; p 1053.

(61) Chatterjee, A., Ed. Application of Density Functional Theory in Chemical Reactions. *Int. J. Mol. Sci.* **2002**, *3*, 234−444 (Special Issue).

(62) Geerlings, P.; De Proft, F. *Int. J. Mol. Sci.* **2002**, *3*, 276.

(63) Chandra, A. K.; Nguyen, M. T. *Int. J. Mol. Sci.* **2002**, *3*, 310.

(64) Chandrakumar, K. R. S.; Pal, S. *Int. J. Mol. Sci.* **2002**, *3*, 324.

(65) Wilson, E. B., quoted by Lowdin, P. O. *Int. J. Quantum Chem.* **1986**, *S19*, 19.

(66) Reference 27, p 51.

(67) Riess, J.; Münch, W. *Theor. Chim. Acta* **1981**, *58*, 295.

(68) Bader, R. F. W. *Atoms in Molecules: a Quantum Theory*; Clarendon Press: Oxford, 1990.

(69) Bader, R. F. W.; Becker, P. *Chem. Phys. Lett.* **1988**, *148*, 452.

(70) Mezey, P. G. *Mol. Phys.* **1999**, *96*, 169.

(71) Mezey, P. G. *J. Chem. Inf. Comput. Sci.* **1999**, *39*, 224.

(72) Hohenberg, P.; Kohn, W.; Sham, L. *Adv. Quantum Chem.* **1990**, *21*, 7.

(73) Harriman, J. E. *Phys. Rev. A* **1981**, *24*, 680.

(74) Kohn, W.; Becke, A. D.; Parr, R. G. *J. Phys. Chem.* **1996**, *100*, 12974.

(75) Perdew, J. P. In *Density Functional Theory and its Applications to Materials*, Van Doren, V., Van Alsenoy, C., Geerlings, P., Eds.; AIP Conference Proceedings 577; American Institute of Physics: New York, 2001; p 1.

(76) Becke, A. D. *J. Chem. Phys.* **1993**, *98*, 5648.

(77) Lee, C.; Yang, W.; Parr, R. G. *Phys. Rev. B* **1988**, *37*, 785.

(78) Hamprecht, F. A.; Cohen, A. J.; Tozer, D. J.; Handy, N. C. *J. Chem. Phys.* **1998**, *109*, 6264.

(79) Scott, A. P.; Radom, L. *J. Phys. Chem.* **1996**, *100*, 16502.

(80) De Proft, F.; Geerlings, P. *J. Chem. Phys.* **1997**, *106*, 3270.

(81) Curtiss, L. A.; Redfern, P. C.; Raghavachari, K.; Pople, J. A. *J. Chem. Phys.* **1998**, *109*, 42.

(82) De Oliveira, G.; Martin, J. M. L.; De Proft, F.; Geerlings, P. *Phys. Rev. A* **1999**, *60*, 1034.

(83) De Proft, F.; Martin, J. M. L.; Geerlings, P. *Chem. Phys. Lett.* **1996**, *250*, 393.

(84) De Proft, F.; Tielens, F.; Geerlings, P. *J. Mol. Struct.* (*THEOCHEM*) **2000**, *506*, 1.

(85) Rablen, P. R.; Pearlman, S. A.; Finkbiner, J. *J. Phys. Chem. A* **1999**, *103*, 7357.

(86) Parr, R. G.; Donnelly, R. A.; Levy, M.; Palke, W. E. *J. Chem. Phys.* **1978**, *68*, 3801.

(87) The authors thank Prof. P. Senet for a stimulating discussion on this topic.

(88) Iczkowski, R. P.; Margrave, J. L. *J. Am. Chem. Soc.* **1961**, *83*, 3547.

(89) Perdew, J. P.; Parr, R. G.; Levy, M.; Balduz, J. L., Jr. *Phys. Rev. Lett.* **1982**, *49*, 1691.

(90) Zhang, Y.; Yang, W. *Theor. Chem. Acc.* **2000**, *103*, 346.

(91) Mulliken, R. S. *J. Chem. Phys.* **1934**, *2*, 782.

(92) Gyftopoulos, E. P.; Hatsopoulos, G. N. *Proc. Natl. Acad. Sci. U.S.A.* **1965**, *60*, 786.

(93) Pauling, L. *J. Am. Chem. Soc.* **1932**, *54*, 3570.

(94) Pauling, L.; Sherman, J. *J. Am. Chem. Soc.* **1937**, *59*, 1450.

(95) Pauling, L. *The Nature of the Chemical Bond*, 3rd ed.; Cornell University Press: Ithaca, NY, 1960.

(96) Allred, A. L. *J. Inorg. Nucl. Chem.* **1961**, *17*, 215.

(97) Pritchard, H. O.; Skinner, H. A. *Chem. Rev.* **1955**, *55*, 745.

(98) Wells, P. R. *Prog. Phys. Org. Chem.* **1968**, *6*, 111.

(99) Batsnama, S. S. *Russ. Chem. Rev.* **1968**, *37*, 332.

(100) Ferreira, R. *Adv. Chem. Phys.* **1969**, *13*, 55.

(101) *Electronegativity*; Sen, K. D., Ed.; Structure and Bonding 66; Springer-Verlag: Berlin, 1987.

(102) Bergman, D.; Hinze, J. *Angew. Chem., Int. Ed. Engl.* **1996**, *35*, 150.

(103) See, for example: Atkins, P. W. *Physical Chemistry*, 6th ed.; Oxford University Press: Oxford, 1998; Chapters 5 and 7.

(104) Nguyen-Dang, T. T.; Bader, R. F. W.; Essén, H. *Int. J. Quantum Chem.* **1982**, *22*, 1049.

(105) Mermin, N. D. *Phys. Rev. A* **1965**, *137*, 1441.

(106) Callen, H. B. *Thermodynamics and an Introduction to Thermostatics*; Wiley: New York, 1985.

(107) Alberty, R. A. *J. Chem. Thermodyn.* **1997**, *29*, 501.

(108) Nalewajski, R. F.; Parr, R. G. *J. Chem. Phys.* **1982**, *77*, 399.

(109) Nalewajski, R. F. *J. Chem. Phys.* **1983**, *78*, 6112.

(110) De Proft, F.; Liu, S.; Geerlings, P. *J. Chem. Phys.* **1998**, *108*, 7549.

(111) Gordy, W. *Phys. Rev.* **1946**, *69*, 404.

(112) Allred, A. L.; Rochow, E. G. *J. Inorg. Nucl. Chem.* **1958**, *5*, 264.
(113) Sanderson, R. T. *Science* **1951**, *114*, 670.
(114) Mullay, J. In *Electronegativity*; Sen, K. D., Jørgenson, C. K., Eds.; Structure and Bonding 66; Springer-Verlag: Berlin, Heidelberg, 1987; p 1.
(115) Ghanty, T. K.; Ghosh, S. K. *J. Am. Chem. Soc.* **1994**, *116*, 3943.
(116) Lieb, E. H. *Int. J. Quantum Chem.* **1983**, *24*, 243.
(117) Janak, J. F. *Phys. Rev. B* **1978**, *18*, 7165.
(118) Casida, M. E. *Phys. Rev. B* **1999**, *59*, 4694.
(119) Pearson, R. G. *Inorg. Chem.* **1988**, *27*, 734.
(120) Pearson, R. G. *J. Org. Chem.* **1989**, *54*, 1423.
(121) Pearson, R. G. In *Theoretical Models of Chemical Bonding*; Maksic, Z. B., Ed.; Springer-Verlag: Berlin, 1990; Part 2, p 45.
(122) Pearson, R. G. *J. Mol. Struct.* (*THEOCHEM*) **1992**, *255*, 261.
(123) Koopmans, T. A. *Physica* **1933**, *1*, 104.
(124) Simons, J.; Jordan, K. D. *Chem. Rev.* **1987**, *87*, 535.
(125) Szarka, A. Z.; Curtiss, L. A.; Miller, J. R. *Chem. Phys.* **1999**, *246*, 147.
(126) Rösch, N.; Trickey, S. B. *J. Chem. Phys.* **1997**, *106*, 8940.
(127) (a) Hatti, S.; Datta, D. *J. Phys. Chem.* **1996**, *100*, 9828. (b) Dreuw, A.; Cederbaum, L. S. *Chem. Rev.* **2002**, *102*, 181.
(128) Slater, J. C.; Wood, J. H. *Int. J. Quantum Chem.* **1971**, *S4*, 3.
(129) Bartolotti, L. J. In *Electronegativity*; Sen, K. D., Jørgenson, C. K., Eds.; Structure and Bonding 66; Springer-Verlag: Berlin, Heidelberg, 1987; p 27.
(130) Alonso, J. A.; Balbas, L. C. In *Electronegativity*; Sen, K. D., Jørgenson, C. K., Eds.; Structure and Bonding 66; Springer-Verlag: Berlin, Heidelberg, 1987; p 41.
(131) Gazquez, J. L.; Vela, A. M.; Galvan, M. In *Electronegativity*; Sen, K. D., Jørgenson, C. K., Eds.; Structure and Bonding 66; Springer-Verlag: Berlin, Heidelberg, 1987; p 79.
(132) Sen, K. D.; Böhm, M. C.; Schmidt, P. C. In *Electronegativity*; Sen, K. D., Jørgenson, C. K., Eds.; Structure and Bonding 66; Springer-Verlag: Berlin, Heidelberg, 1987; p 99.
(133) Yamagouchi, Y.; Osamura, Y.; Goddard, J. D.; Schaefer, H. F., III. *A New Dimension to Quantum Chemistry*; Oxford University Press: New York, 1994.
(134) Komorowski, L.; Lipinski, J.; Pyka, M. J. *J. Phys. Chem.* **1993**, *97*, 3166.
(135) Allen, L. C. *J. Am. Chem. Soc.* **1989**, *111*, 9005.
(136) Allen, L. C. *Acc. Chem. Res.* **1990**, *23*, 175.
(137) Allen, L. C.; Knight, E. T. *J. Mol. Struct.* (*THEOCHEM*) **1992**, *261*, 313.
(138) Allen, L. C. *J. Am. Chem. Soc.* **1992**, *114*, 1510.
(139) Allen, L. C. *Int. J. Quantum Chem.* **1994**, *49*, 253.
(140) Liu, G. H.; Parr, R. G. *J. Am. Chem. Soc.* **1995**, *117*, 3179.
(141) Hinze, J.; Jaffé, H. H. *J. Am. Chem. Soc.* **1962**, *84*, 540.
(142) Pearson, R. G. *Acc. Chem. Res.* **1990**, *23*, 1.
(143) Hinze, J.; Whitehead, M. A.; Jaffé, H. H. *J. Am. Chem. Soc.* **1963**, *85*, 148.
(144) Hinze, J.; Jaffé, H. N. *Can. J. Chem.* **1963**, *41*, 1315.
(145) Hinze, J.; Jaffé, H. N. *J. Phys. Chem.* **1963**, *67*, 1501.
(146) Bergmann, D.; Hinze, J. In *Electronegativity*; Sen, K. D., Jørgenson, C. K., Eds.; Structure and Bonding 66; Springer-Verlag: Berlin, Heidelberg, 1987; p 145.
(147) Komorowski, L. *Chem. Phys. Lett.* **1983**, *103*, 201.
(148) Komorowski, L. *Chem. Phys. Lett.* **1987**, *134*, 536.
(149) Komorowski, L. *Chem. Phys.* **1987**, *114*, 55.
(150) Balawender, R.; Komorowski, L. *J. Chem. Phys.* **1998**, *109*, 5203.
(151) Balawender, R.; Komorowski, L.; Roszak, S. *Int. J. Quantum Chem.* **1997**, *61*, 499.
(152) Pearson, R. G. *J. Am. Chem. Soc.* **1963**, *85*, 3533.
(153) Pearson, R. G. *Science* **1966**, *151*, 172.
(154) Pearson, R. G.; Songstad, J. *J. Am. Chem. Soc.* **1967**, *89*, 1827.
(155) Pearson, R. G. *Hard and Soft Acids and Bases*; Dowden, Hutchinson & Ross: Stroudenbury, PA, 1973.
(156) Pearson, R. G. In *Chemical Hardness*; Sen, K. D., Ed.; Structure and Bonding 80; Springer-Verlag: Berlin, 1993; p 1.
(157) Pearson, R. G. *Chemical Hardness*; Wiley-VCH: Weinheim, 1997.
(158) Pearson, R. G. *J. Chem. Educ.* **1968**, *45*, 981.
(159) Pearson, R. G. *Current Contents*, 24 february 1986, p 18.
(160) Huheey, J. E. *Inorganic Chemistry*; 3rd ed.; Harper and Row: New York, 1983.
(161) Housecroft, C. E.; Sharpe, A. G. *Inorganic Chemistry*; Prentice Hall: Harlow, 2001.
(162) Shriver, D. F.; Atkins, P. W. *Inorganic Chemistry*, 3rd ed.; Oxford University Press: Oxford, 1999.
(163) Parr, R. G.; Pearson, R. G. *J. Am. Chem. Soc.* **1983**, *105*, 7512.
(164) Ford, P. C. *Coord. Chem. Rev.* **1999**, *187*, 3.
(165) Woodward, S. *Tetrahedron* **2002**, *58*, 1017.
(166) Reed, J. L. *J. Phys. Chem. A* **1997**, *101*, 7396.
(167) Reed, J. L. *J. Phys. Chem. A* **1997**, *101*, 7401.
(168) Politzer, P.; Huheey, J. E.; Murray, J. S.; Grodzicki, M. *J. Mol. Struct.* (*THEOCHEM*) **1992**, *259*, 99.
(169) Huheey, J. E. *J. Phys. Chem.* **1965**, *69*, 3284.
(170) Huheey, J. E.; Watts, J. C. *Inorg. Chem.* **1971**, *10*, 1553.
(171) Huheey, J. E. *J. Org. Chem.* **1971**, *36*, 204.
(172) Chattaraj, P. K.; Cedillo, A.; Parr, R. G. *J. Chem. Phys.* **1995**, *103*, 7645.
(173) Gazquez, J. L. In *Chemical Hardness*; Sen, K. D., Ed.; Structure and Bonding 80; Springer-Verlag: Berlin, 1993.
(174) Liu, S.; De Proft, F.; Parr, R. G. *J. Phys. Chem. A* **1997**, *101*, 6991.
(175) De Proft, F.; Geerlings, P.; Liu, S.; Parr, R. G. *Polish. J. Chem.* **1999**, *72*, 1737.
(176) Pariser, R. *J. Chem. Phys.* **1953**, *21*, 568.
(177) Giambiagi, M.; Segre de Giambiagi, M.; Pires, J. M. *Chem. Phys. Lett.* **1988**, *152*, 222.
(178) Segre de Giambiagi, M.; Giambiagi, M. *J. Mol. Struct.* (*THEOCHEM*) **1993**, *288*, 273.
(179) Julg, A. *J. Mol. Struct.* (*THEOCHEM*) **1993**, *280*, 129.
(180) Mineva, T.; Sicilia, E.; Russo, N. *J. Am. Chem. Soc.* **1998**, *120*, 9053.
(181) Nalewajski, R. F. In *Chemical Hardness*; Sen, K. D., Ed.; Structure and Bonding 80; Springer-Verlag: Berlin, 1993; p 194.
(182) For an authorative account, see, for example: Streiwieser, A. *Molecular Orbital Theory for Organic Chemists*; John Wiley: New York, 1961.
(183) Cioslowski, J.; Martinov, M. *J. Chem. Phys.* **1994**, *101*, 366.
(184) Baekelandt, B. G.; Mortier, W. J.; Schoonheydt, R. A. In *Chemical Hardness*; Sen, K. D., Ed.; Structure and Bonding 80; Springer-Verlag: Berlin, 1993; p 187.
(185) Toufar, H.; Nulens, K.; Janssens, G. O. A.; Mortier, W. J.; Schoonheydt, R. A.; De Proft, F.; Geerlings, P. *J. Phys. Chem.* **1996**, *100*, 15383.
(186) Parr, R. G.; Von Szentpaly, L.; Liu, S. *J. Am. Chem. Soc.* **1999**, *121*, 1922.
(187) Von Szentpaly, L. *Int. J. Quantum Chem.* **2000**, *76*, 222.
(188) Maynard, A. T.; Huang, M.; Rice, W. G.; Covell, D. G. *Proc. Natl. Acad. Sci. U.S.A.* **1998**, *95*, 11578.
(189) Parr, R. G.; Yang, W. *J. Am. Chem. Soc.* **1984**, *106*, 4049.
(190) For a perspective, see: Ayers, P. W.; Levy, M. *Theor. Chem. Acc.* **2000**, *103*, 353.
(191) Fukui, K.; Yonezawa, Y.; Shingu, H. *J. Chem. Phys.* **1952**, *20*, 722.
(192) Parr, R. G.; Parr, J. B. *Theor. Chem. Acc.* **1999**, *102*, 5.
(193) Kato, S. *Theor. Chem. Acc.* **2000**, *103*, 219.
(194) Li, Y.; Evans, J. N. S. *J. Am. Chem. Soc.* **1995**, *117*, 7756.
(195) Kato, T. *Comm. Pure Appl. Math.* **1957**, *10*, 151.
(196) Chattaraj, P. K.; Cedillo, A.; Parr, R. G. *J. Chem. Phys.* **1995**, *103*, 10621.
(197) Ayers, P. W.; Parr, R. G. *J. Am. Chem. Soc.* **2000**, *122*, 2010.
(198) Yang, W.; Parr, R. G.; Pucci, R. *J. Chem. Phys.* **1984**, *81*, 2862.
(199) Lee, C.; Yang, W.; Parr, R. G. *J. Mol. Struct.* (*THEOCHEM*) **1988**, *163*, 305.
(200) Mendez, F.; Galvan, M. In *Density Functional Methods in Chemistry*; Labanowski, J. K., Andzelm, J. W., Eds.; Springer-Verlag: New York, 1991; p 387.
(201) Mendez, F.; Galvan, M.; Garritz, A.; Vela, A.; Gazquez, J. *J. Mol. Struct.* (*THEOCHEM*) **1992**, *277*, 81.
(202) Langenaeker, W.; De Decker, M.; Raeymaekers, P.; Geerlings, P. *J. Mol. Struct.* (*THEOCHEM*) **1990**, *207*, 115.
(203) Langenaeker, W.; Demel, K.; Geerlings, P. *J. Mol. Struct.* (*THEOCHEM*) **1991**, *234*, 329.
(204) Langenaeker, W.; Demel, K.; Geerlings, P. *J. Mol. Struct.* (*THEOCHEM*) **1992**, *259*, 317.
(205) Tielemans, M.; Areschkha, V.; Colomer, J.; Promel, R.; Langenaeker, W.; Geerlings, P. *Tetrahedron* **1992**, *48*, 10575.
(206) Flurchick, K.; Bartolotti, L. *J. Mol. Graphics* **1995**, *13*, 10.
(207) Giambiagi, M.; Segre de Giambiagi, M. *Nuovo Cimento* **1990**, *12*, 139.
(208) Segre de Giambiagi, M.; Giambiagi, M. *Chem. Phys. Lett.* **1990**, *288*, 273.
(209) Bader, R. F. W.; Chang, C. *J. Phys. Chem.* **1989**, *93*, 2946.
(210) Bader, R. F. W.; Chang, C. *J. Phys. Chem.* **1989**, *93*, 5095.
(211) Langenaeker, W.; De Proft, F.; Geerlings, P. *J. Mol. Struct.* (*THEOCHEM*) **1996**, *362*, 175.
(212) De Proft, F.; Martin, J. M. L.; Geerlings, P. *Chem. Phys. Lett.* **1996**, *256*, 400.
(213) Dunning, T. H. *J. Chem. Phys.* **1989**, *90*, 1007.
(214) Kendall, R. A.; Dunning, T. H.; Harrison, R. J. *J. Chem. Phys.* **1992**, *96*, 6976.
(215) Pacios, L. F. *Chem. Phys. Lett.* **1997**, *276*, 381.
(216) Pacios, L. F.; Gomez, P. C. *J. Comput. Chem.* **1998**, *19*, 488.
(217) Gazquez, J. L.; Vela, A. M.; Galvan, M. In *Electronegativity*; Sen, K. D., Jørgenson, C. K., Eds.; Structure and Bonding 66; Springer-Verlag: Berlin, Heidelberg, 1987; p 87.
(218) Michalak, A.; De Proft, F.; Geerlings, P.; Nalewajski, R. F. *J. Phys. Chem. A* **1999**, *103*, 762.
(219) Mineva, T.; Parvanov, V.; Petrov, I.; Neshev, N.; Russo, N. *J. Phys. Chem. A* **2001**, *105*, 1959.
(220) Mayer, I. *Chem. Phys. Lett.* **1983**, *97*, 270.
(221) Mayer, I. *Chem. Phys. Lett.* **1985**, *117*, 396.
(222) Grigorov, M.; Weber, J.; Chermette, H.; Trouchet, J. M. J. *Int. J. Quantum Chem.* **1997**, *61*, 551.

(223) Grigorov, M.; Weber, J.; Vuillermet, N.; Chermette, H.; Troucher, J. M. J. *J. Chem. Phys.* **1998**, *108*, 8790.
(224) Liu, G. H. *J. Chem. Phys.* **1997**, *106*, 165.
(225) Nalewajski, R. F. *Z. Natürforsch.* **1988**, *43A*, 65.
(226) Nalewajski, R. F.; Korchowiec, J.; Zhou, Z. *Int. J. Quantum Chem.* **1988**, *S22*, 349.
(227) Nalewajski, R. F. In *Chemical Hardness*; Sen, K. D., Ed.; Structure and Bonding 80; Springer-Verlag: Berlin, 1993; p 117.
(228) Nalewajski, R. F. *Int. J. Quantum Chem.* **1995**, *56*, 453.
(229) Nalewajski, R. F.; Korchowiec, J.; Michalak, A. In *Density Functional Theory, IV*; Nalewajski, R. F., Ed.; Topics in Current Chemistry 183; Springer-Verlag: Berlin, 1996; p 25.
(230) Nalewajski, R. F.; Mrozek, J. *Int. J. Quantum Chem.* **1992**, *43*, 353.
(231) Nalewajski, R. F. *Int. J. Quantum Chem.* **1992**, *44*, 67.
(232) Ohno, K. *Theor. Chim. Acta* **1968**, *10*, 111.
(233) Ohno, K. *Adv. Quantum Chem.* **1967**, *3*, 39.
(234) Senet, P. *J. Chem. Phys.* **1996**, *105*, 6471.
(235) Senet, P. *J. Chem. Phys.* **1997**, *107*, 2516.
(236) Yang, W.; Mortier, W. J. *J. Am. Chem. Soc.* **1986**, *108*, 5708.
(237) For a review, see: Bachrach, S. M. In *Reviews in Computational Chemistry*, Vol. V; Lipkowitz, K. B., Boyd, D. B., Eds.; VCH: New York, 1995; p 171.
(238) Contreras, R.; Fuentealba, P.; Galvan, M.; Perez, P. *Chem. Phys. Lett.* **1994**, *304*, 405.
(239) Mulliken, R. S. *J. Chem. Phys.***1955**, *23*, 1833; 1841; 2338; 2343.
(240) Breneman, C. M.; Wiberg, K. B. *J. Comput. Chem.* **1990**, *11*, 361.
(241) Reed, A. E.; Curtiss, L. A.; Weinhold, F. *Chem. Rev.* **1988**, *88*, 899.
(242) Cioslowski, J. *J. Am. Chem. Soc.* **1984**, *111*, 8333.
(243) Cioslowski, J.; Martinov, M.; Mixon, S. T. *J. Phys. Chem.* **1993**, *97*, 10948.
(244) Cioslowski, J.; Hay, P. J.; Ritchie, J. P. *J. Phys. Chem.* **1990**, *94*, 148.
(245) De Proft, F. In *Density Functional Theory: A Bridge between Chemistry and Physics*; Geerlings, P., De Proft, F., Langenaeker, W., Eds.; VUB Press: Brussels, 1998; p 131.
(246) Gilardoni, F.; Weber, J.; Chermette, H.; Ward, T. R. *J. Phys. Chem. A* **1998**, *102*, 3607.
(247) Arulmozhiraja, S.; Kolandaivel, P. *Mol. Phys.* **1997**, *90*, 55.
(248) Pople, J. A.; Head Gordon, M.; Raghavachari, K. *J. Chem. Phys.* **1987**, *87*, 5968.
(249) Scuseria, G. E.; Schaefer, H. F., III. *J. Chem. Phys.* **1989**, *90*, 3700.
(250) Becke, A. *J. Chem. Phys.* **1988**, *88*, 2547.
(251) Misra, G. P.; Sannigrahi, A. B. *J. Mol. Struct.* (*THEOCHEM*) **1996**, *361*, 63.
(252) Kar, T.; Sannigrahi, A. B. *Indian J. Chem.* **2000**, *A39*, 68.
(253) Chandra, A. K.; Nguyen, M. T. *J. Chem. Soc., Perkin Trans. 2* **1997**, 1415.
(254) Roy, R. K.; Pal, S.; Hirao, K. *J. Chem. Phys.* **1999**, *110*, 8236.
(255) Roy, R. K.; Hirao, K.; Pal, S. *J. Chem. Phys.* **2000**, *113*, 1372.
(256) Fuentealba, P.; Perez, P.; Contreras, R. *J. Chem. Phys.* **2000**, *113*, 2544.
(257) Roy, R. K.; Hirao, K.; Krishnamurty, S.; Pal, S. *J. Chem. Phys.* **2001**, *115*, 2901.
(258) Hirshfeld, F. L. *Theor. Chim. Acta* **1977**, *44*, 129.
(259) Hirshfeld, F. L. *Isr. J. Chem.* **1977**, *16*, 198.
(260) Maslen, E. N.; Spackman, M. *Aust. J. Phys.* **1985**, *38*, 273.
(261) De Proft, F.; Van Alsenoy, C.; Peeters, A.; Langenaeker, W.; Geerlings, P. *J. Comput. Chem.* **2002**, *23*, 1198.
(262) (a) Nalewajski, R. F.; Parr, R. G. *Proc. Natl. Acad. Sci. U.S.A.* **2000**, *97*, 8879. (b) Nalewajski, R. F.; Parr, R. G. *J. Phys. Chem. A* **2001**, *105*, 7391.
(263) Ayers, P. W. *J. Chem. Phys.* **2000**, *113*, 10886.
(264) Korchowiec, J.; Uchimaru, T. *J. Phys. Chem. A* **1998**, *102*, 6682.
(265) Korchowiec, J.; Uchimaru, T. *J. Phys. Chem. A* **1998**, *102*, 10167.
(266) Korchowiec, J.; Chandra, A. K.; Uchimaru, T.; Kawahara, S.; Matsumura, K.; Tsuzuki, S.; Mikami, M. *Chem. Phys. Lett.* **1999**, *308*, 229.
(267) Yang, W.; Parr, R. G. *Proc. Natl. Acad. Sci. U.S.A.* **1985**, *82*, 6723.
(268) Brommer, K. D.; Galvàn, M.; Dal Pino, A.; Joannopoulos, J. D. *Surf. Sci.* **1994**, *314*, 57.
(269) Roy, R. K.; Krishnamurti, S.; Geerlings, P.; Pal, S. *J. Phys. Chem. A* **1998**, *102*, 3746.
(270) Roy, R. K.; De Proft, F.; Geerlings, P. *J. Phys. Chem. A* **1998**, *102*, 7035.
(271) Fuentealba, P.; Parr, R. G. *J. Chem. Phys.* **1991**, *94*, 5559.
(272) Perez, P.; Toro-Labbé, A.; Contreras, R. *J. Phys. Chem. A* **2000**, *104*, 11993.
(273) Fuentealba, P.; Cedillo, M. *J. Chem. Phys.* **1999**, *110*, 9807.
(274) Galvan, M.; Dal Pino, A.; Wang, J.; Joannopoulos, J. D. *J. Phys. Chem.* **1993**, *97*, 783.
(275) Hansma, P. K.; Tersoff, J. *J. Appl. Phys.* **1987**, *61*, R1−R23.
(276) Wu, X. L.; Lieber, Ch. M. *Prog. Inorg. Chem.* **1991**, *30*, 431.
(277) Berkowitz, M.; Parr, R. G. *J. Chem. Phys.* **1998**, *88*, 2554.
(278) Fuentealba, P. *J. Mol. Struct.* (*THEOCHEM*) **1998**, *433*, 113.
(279) Chamorro, E.; Contreras, R.; Fuentealba, P. *J. Chem. Phys.* **2000**, *113*, 10861.
(280) Gutierrez-Oliva, S.; Jaque, P.; Toro-Labbé, A. *J. Phys. Chem. A* **2000**, *104*, 8955.
(281) Liu, S. *Phys. Rev. A* **1996**, *54*, 1328.
(282) Liu, S.; Parr, R. G. *J. Chem. Phys.* **1997**, *106*, 5578.
(283) Ghosh, S. K.; Berkowitz, M. *J. Chem. Phys.* **1985**, *83*, 864.
(284) Harbola, M. K.; Chattaraj, P. K.; Parr, R. G. *Isr. J. Chem.* **1991**, *31*, 395.
(285) Langenaeker, W.; De Proft, F.; Geerlings, P. *J. Phys. Chem.* **1995**, *99*, 6424.
(286) Ghosh, S. K. *Chem. Phys. Lett.* **1990**, *172*, 77.
(287) Chattaraj, P. K.; Parr, R. G. In *Chemical Hardness*; Sen, K. D., Ed.; Structure and Bonding 80; Springer-Verlag: Berlin, 1993; p 11.
(288) Berkowitz, M.; Ghosh, S. K.; Parr, R. G. *J. Am. Chem. Soc.* **1985**, *107*, 6811.
(289) Bonaccorsi, R.; Scrocco, E.; Tomasi, J. *J. Chem. Phys.* **1970**, *52*, 5270.
(290) Parr, R. G.; Gazquez, J. L. *J. Phys. Chem.* **1993**, *97*, 3939.
(291) Nalewajski, R. F. *J. Phys. Chem.* **1984**, *93*, 2658.
(292) Nalewajski, R. F.; Korchowiec, J. *J. Mol. Catal.* **1989**, *54*, 324.
(293) Nalewajski, R. F.; Korchowiec, J. *J. Mol. Catal.* **1991**, *68*, 123.
(294) Baekelandt, B. G.; Mortier, W. J.; Lievens, J. L.; Schoonheydt, R. A. *J. Am. Chem. Soc.* **1991**, *113*, 6730.
(295) Kazansky, V. B.; Mortier, W. J.; Baekelandt, B. G.; Lievens, J. *J. Mol. Catal.* **1992**, *83*, 153.
(296) Parr, R. G.; Bartolotti, L. J. *J. Phys. Chem.* **1983**, *87*, 2810.
(297) Nalewajski, R. F. N.; Parr, R. G. *J. Chem. Phys.*, **1982**, *77*, 399.
(298) Ayers, P. W. *Proc. Natl. Acad. Sci. U.S.A.* **2000**, *97*, 1959.
(299) Baekelandt, B. G.; Cedillo, A.; Parr, R. G. *J. Chem. Phys.* **1995**, *103*, 8548.
(300) Cedillo, A. *Int. J. Quantum Chem.* **1994**, *S28*, 231.
(301) De Proft, F.; Liu, S.; Parr, R. G. *J. Chem. Phys.* **1997**, *107*, 3000.
(302) De Proft, F.; Geerlings, P. *J. Phys. Chem. A* **1997**, *101*, 5344.
(303) Fuentealba, P. *J. Phys. Chem. A* **1998**, *102*, 4747.
(304) Chan, G., K.-L.; Handy, N. C. *J. Chem. Phys.* **1998**, *109*, 6287.
(305) Gal, T. *Phys. Rev. A* **2001**, *63*, 2506; 9903.
(306) Carbo, R.; Colabuig, B.; Vera, L.; Besalu, E. *Adv. Quantum Chem.* **1994**, *25*, 253.
(307) Besalu, E.; Carbo, R.; Mestres, J., Solà, M. *Top. Curr. Chem.* **1995**, *173*, 31.
(308) Solà, M.; Mestres, J.; Oliva, J. M. *Int. J. Quantum Chem.* **1996**, *58*, 36.
(309) Carbo, R.; Besalu, E.; Girones, X. *Adv. Quantum Chem.* **2000**, *38*, 1.
(310) Carbo, R.; Arnau, M; Leyda, L. *Int. J. Quantum Chem.* **1980**, *17*, 1185.
(311) Hodgkin, E. E.; Richards, W. G. *Int. J. Quantum Chem., Quantum Biol. Symp.* **1987**, *295*, 122.
(312) Boon, G.; De Proft, F.; Langenaeker, W.; Geerlings, P. *Chem. Phys. Lett.* **1998**, *295*, 122.
(313) Boon, G.; Langenaeker, W.; De Proft, F.; De Winter, H.; Tollenaere, J. P.; Geerlings, P. *J. Phys. Chem. A* **2001**, *105*, 8805.
(314) Spatola, A. F. In *Chemistry and Biochemistry of Amino Acids, Peptides and Proteins*; Weinstein B., Ed.; Marcel Dekker: New York, 1983; Vol. 7, p 267.
(315) Dugham, L.; Burt, C.; Richards, W. G. *J. Mol. Struct.* (*THEOCHEM*) **1991**, *235*, 481.
(316) Allmendiger, T.; Felder, E.; Hungerbühler, A. *Tetrahedron Lett.* **1990**, 7301.
(317) Bartlett, P. A.; Otake, A. *J. Org. Chem.* **1995**, *60*, 3107.
(318) Cleff, A. D.; Ord, J. K. *Spatial Autocorrelation*; Pion Limited: London, 1973.
(319) Wagener, M.; Sadowski, J.; Gasteiger, J. *J. Am. Chem. Soc.* **1995**, *117*, 7769.
(320) Moreau, G.; Broto, P. *Nouv. J. Chem.* **1980**, *4*, 359.
(321) Moreau G.; Broto P. *Nouv. J. Chem.* **1980**, *4*, 757.
(322) Malinowski, E. R. *Factor Analysis in Chemistry*, 2nd ed.; John Wiley: New York, 1991.
(323) Eriksson, L.; Johansson, E.; Kettaneh-Wold, N.; Wold, S. *Introduction to Multi- and Megavariate Data Analysis using Projection Methods* (*PCA & PLS*); Umetrics AB: Umeå, Sweden, 1999.
(324) Nakatsuji, H. *J. Am. Chem. Soc.* **1973**, *95*, 345.
(325) Nakatsuji, H. *J. Am. Chem. Soc.* **1974**, *96*, 24.
(326) Nakatsuji, H. *J. Am. Chem. Soc.* **1974**, *96*, 30.
(327) Berlin, T. *J. Chem. Phys.* **1951**, *19*, 208.
(328) Baekelandt, B. G.; Janssens, G. O. A.; Toufar, H.; Mortier, W. J.; Schoonheydt, R. A.; Nalewajski, R. F. *J. Phys. Chem.* **1995**, *99*, 9784.
(329) Cohen, M. H.; Ganduglia-Pirovano, M. V.; Kudrnovsky, J. *J. Chem. Phys.* **1994**, *101*, 8988.
(330) Cohen, M. H.; Ganduglia-Pirovano, M. V.; Kudrnovsky, J. *J. Chem. Phys.* **1995**, *103*, 3543.
(331) Nalewajski, R. F. *Phys. Chem. Chem. Phys.* **1999**, *1*, 1037.
(332) Baekelandt, B. G. *J. Chem. Phys.* **1996**, *105*, 4664.
(333) Balawender, R.; Geerlings, P. *J. Chem. Phys.* **2001**, *114*, 682.
(334) Balawender, R.; De Proft, F.; Komorowski, L.; Geerlings, P. *J. Phys. Chem. A* **1998**, *102*, 9912.

(335) Hellman, H. *Einführung in die Quantenchemie*; Deuticke: Vienna, 1937; p 285.
(336) Feynman, R. P. *Phys. Rev.* **1939**, *56*, 340.
(337) Wang, X.; Peng, Z. *Int. J. Quantum Chem.* **1993**, *47*, 393.
(338) Balawender, R.; De Proft, F.; Geerlings, P. *J. Chem. Phys.* **2001**, *114*, 4441.
(339) Ordon, P.; Komorowski, L. *Chem. Phys. Lett.* **1998**, *292*, 22.
(340) Nalewajski, R. F.; Korchowiec, J. *Charge Sensitivity Approach to Electronic Structure and Chemical Reactivity*; Advanced Series in Physical Chemistry 8; World Scientific: Singapore, 1997.
(341) Chamorro, E.; Contreras, R.; Fuentealba, P. *J. Chem. Phys.* **2001**, *115*, 6822.
(342) Ayers, P. W.; Parr, R. G. *J. Am. Chem. Soc.* **2001**, *123*, 2007.
(343) Ayers, P. W. *Theor. Chem. Acc.* **2001**, *106*, 271.
(344) Grochala, W.; Albrecht, A. C.; Hoffmann, R. *J. Phys. Chem. A* **2000**, *104*, 2195.
(345) Ayers, P. W.; Parr, R. G. *J. Phys. Chem. A* **2000**, *104*, 2211.
(346) Von Barth, U.; Hedin, L. *J. Phys. Chem.* **1972**, *5*, 1629.
(347) Pant, M. M.; Rajagopal, A. K. *Solid State Commun.* **1972**, *10*, 1157.
(348) See ref 27, Chapter 8.
(349) Capelle, K.; Vignale, G. *Phys. Rev. Lett.* **2001**, *86*, 5546.
(350) Galvan, M.; Gazquez, J. L.; Vela, A. *J. Chem. Phys.* **1986**, *85*, 2337.
(351) Galvan, M.; Vela, A.; Gazquez, J. L. *J. Phys. Chem.* **1988**, *92*, 6470.
(352) (a) Vargas, R.; Galvan, M. *J. Phys. Chem.* **1996**, *100*, 14561. (b) Vargas, R.; Galvan, M.; Vela, A. *J. Phys. Chem. A* **1998**, *102*, 3134.
(353) Galvan, M.; Vargas, R. *J. Phys. Chem.* **1992**, *96*, 1625.
(354) Garza, J.; Robles, J. *Int. J. Quantum Chem.* **1994**, *49*, 159.
(355) Cioslowski, J.; Martinov, M. *J. Chem. Phys.* **1995**, *102*, 7499.
(356) Smith, B. M.; March, J. *March's Advanced Organic Chemistry*, 5th ed.; Wiley: New York, 2001.
(357) Isaacs, N. *Physical Organic Chemistry*; Longman Scientific and Technical: Singapore, 1995.
(358) Tomasi, J.; Perisco, M. *Chem. Rev.* **1994**, *94*, 2027.
(359) Onsager, L. *J. Am. Chem. Soc.* **1936**, *58*, 1486.
(360) Miertus, S.; Scrocco, E.; Tomasi, J. *J. Chem. Phys.* **1981**, *55*, 117.
(361) Tomasi, J.; Bonaccorsi, R.; Cammi, F.; Valle, F. O. *J. Mol. Struct.* (*THEOCHEM*) **1991**, *234*, 401.
(362) Wiberg, K. B.; Keith, T. A.; Frisch, M. J.; Murcko, M. *J. Phys. Chem.* **1995**, *99*, 9072.
(363) Foresman, J. B.; Keith, T. A.; Wiberg, K. B.; Snoonian, J.; Frisch, M. J. *J. Phys. Chem.* **1996**, *100*, 16096.
(364) Lipinski, J.; Komorowski, L. *Chem. Phys. Lett.* **1996**, *262*, 449.
(365) Pearson, R. G. *J. Am. Chem. Soc.* **1986**, *108*, 6109.
(366) Safi, B.; Choho, K.; De Proft, F.; Geerlings, P. *J. Phys. Chem. A* **1998**, *102*, 5253.
(367) Safi, B.; Choho, K.; De Proft, F.; Geerlings, P. *Chem. Phys. Lett.* **1999**, *300*, 85.
(368) Safi, B.; Choho, K.; Geerlings, P. *J. Phys. Chem. A* **2001**, *105*, 591.
(369) Sivanesan, D.; Amutha, R.; Subramanian, V.; Nair, B. U.; Ramasami, T. *Chem. Phys. Lett.* **1999**, *308*, 223.
(370) Perez, P.; Contreras, R.; Aizman, A. *J. Mol. Struct.* (*THEOCHEM)* **1997**, *390*, 169.
(371) Perez, P.; Contreras, R.; Aizman, A. *Chem. Phys. Lett.* **1996**, *260*, 236.
(372) Contreras, R; Safont, V. S.; Perez, P.; Andres, J.; Moliner, V.; Tapia, O. *J. Mol. Struct. (THEOCHEM)* **1998**, *426*, 277.
(373) Contreras, R.; Domingo, L. R.; Andres, J.; Perez, P.; Tapia, O. *J. Phys. Chem. A* **1999**, *103*, 1367.
(374) Perez, P.; Toro-Labbé, A.; Contreras, R. *J. Am. Chem. Soc.* **2001**, *123*, 5527.
(375) Balawender, R.; Safi, B.; Geerlings, P. *J. Phys. Chem. A* **2001**, *105*, 6703.
(376) Safi, B.; Balawender, R.; Geerlings, P. *J. Phys. Chem. A* **2001**, *105*, 11102.
(377) Day, P. N.; Jensen, J. H.; Gordon, M. S.; Webb, P.; Stevens, W. J.; Krauss, M.; Garnes, D. R.; Basch, H.; Cohen, D. *J. Chem. Phys.* **1996**, *105*, 1968.
(378) Freitag, M. A.; Gordon, M. S.; Jensen, J. H.; Stevens, W. J. *J. Chem. Phys.* **2000**, *112*, 7300.
(379) Chattaraj, P. K. *Int. J. Quantum Chem.* **1992**, *41*, 845.
(380) Chattaraj, P. K.; Nath, S. *Int. J. Quantum Chem.* **1994**, *49*, 705.
(381) Chattaraj, P. K.; Nath, S. *Chem. Phys. Lett.* **1994**, *217*, 342.
(382) Chattaraj, P. K.; Sengupta, S. *J. Phys. Chem.* **1996**, *100*, 16126.
(383) Chattaraj, P. K.; Sengupta, S. *J. Phys. Chem. A* **1997**, *101*, 7893.
(384) Chattaraj, P. K.; Maiti, B. *J. Phys. Chem. A* **2001**, *105*, 169.
(385) Vuilleumier, R.; Sprik, M. *J. Chem. Phys.* **2001**, *115*, 3454.
(386) Car, R.; Parinello, M. *Phys. Rev. Lett.* **1985**, *55*, 2471.
(387) Sanderson, R. T. *Science* **1952**, *116*, 41.
(388) Sanderson, R. T. *J. Chem. Educ.* **1952**, *29*, 539.
(389) Sanderson, R. T. *Science* **1955**, *121*, 207.
(390) Sanderson, R. T. *Chemical Bonds and Bond Energy*; Academic Press: New York, 1976.
(391) Sanderson, R. T. *Polar Covalence*; Academic Press: New York, 1983.
(392) Pauling, L.; Herman, Z. S. J. In *Chemical bonding models*; Liebman, J. F., Greenberg, A., Eds.; Molecular Structure and Energetics 1; VCH Publishers: Deerfield Beach, FL, 1986; p 1.
(393) Donnelly, R. A.; Parr, R. G. *J. Chem. Phys.* **1978**, *69*, 4431.
(394) Politzer, P.; Weinstein, H. *J. Chem. Phys.* **1979**, *71*, 4218.
(395) Parr, R. G.; Bartolotti, L. J. *J. Am. Chem. Soc.* **1982**, *104*, 3801.
(396) Nalewajski, R. F. *J. Am. Chem. Soc.* **1984**, *106*, 944.
(397) Ohwada, K. *J. Phys. Chem.* **1993**, *97*, 1832.
(398) Wilson, M. S.; Ichikawa, S. *J. Phys. Chem.* **1989**, *93*, 3087.
(399) Nalewajski, R. F. *J. Phys. Chem.* **1985**, *89*, 2831.
(400) Gasteiger, J.; Marsili, M. *Tetrahedron* **1980**, *36*, 3219.
(401) Gasteiger, J.; Marsili, M. *Org. Magn. Reson.* **1981**, *15*, 353.
(402) Nalewajski, R. F.; Koninski, M. *J. Phys. Chem.* **1984**, *88*, 6234.
(403) Mortier, W. J. In *Electronegativity*; Sen, K. D., Jørgenson, C. K., Eds.; Structure and Bonding 66; Springer-Verlag: Berlin, 1987; p 125.
(404) Janssens, G. O. A.; Mortier, W. J.; Schoonheydt, R. A. *Developments in the Theory of Chemical Reactivity and Heterogeneous Catalysis*; Research Signpost: Trivandrum, India, 1997; Chapter II.
(405) Mortier, W. J.; Van Genechten, K.; Gasteiger, J. *J. Am. Chem. Soc.* **1985**, *107*, 829.
(406) Mortier, W. J.; Ghosh, S. K.; Shankar, S. *J. Am. Chem. Soc.* **1986**, *108*, 4315.
(407) Van Genechten, K. A.; Mortier, W. J.; Geerlings, P. *Chem. Commun.* **1986**, 1278.
(408) Van Genechten, K. A.; Mortier, W. J.; Geerlings, P. *J. Chem. Phys.* **1987**, *86*, 5063.
(409) Uytterhoeven, L.; Mortier, W. J.; Geerlings, P. *J. Phys. Chem. Solids* **1989**, *50*, 479.
(410) Cioslowski, J.; Mixton, S. T. *J. Am. Chem. Soc.* **1993**, *115*, 1084.
(411) Cioslowski, J.; Stefanov, B. B. *J. Chem. Phys.* **1993**, *99*, 5151.
(412) Rappé, A. K.; Goddard, W. A. *J. Phys. Chem.* **1991**, *95*, 3358.
(413) Yang, Z. Z.; Wang, C. S. *J. Phys. Chem. A* **1997**, *101*, 6315.
(414) Wang, C. S.; Li, S. M.; Yang, Z. Z. *J. Mol. Struct.* (*THEOCHEM*) **1998**, *430*, 191.
(415) Wang, C. S.; Yang, Z. Z. *J. Chem. Phys.* **1999**, *110*, 6189.
(416) Wang, C. S.; Yang, Z. Z. *Chem. Phys. Lett.* **2000**, *330*, 132.
(417) Zhang, Y. L.; Yang, Z. Z. *J. Mol. Struct.* (THEOCHEM) **2000**, *496*, 139.
(418) Cong, Y.; Yang, Z. Z. *Chem. Phys. Lett.* **2000**, *316*, 324.
(419) York, D. M. *Int. J. Quantum Chem.* **1995**, *S29*, 385.
(420) York, D. M.; Yang, W. *J. Chem. Phys.* **1996**, *104*, 159.
(421) Itzkowitz, P.; Berkowitz, M. L. *J. Phys. Chem. A* **1997**, *101*, 5687.
(422) No, K. T.; Grant, J. A.; Sheraga, H. A. *J. Phys. Chem.* **1990**, *94*, 4732.
(423) No, K. T.; Grant, J. A.; Shik, M. S.; Sheraga, H. A. *J. Phys. Chem.* **1990**, *94*, 4740.
(424) Park, J. M.; No, K. T.; Jhon, M. S.; Sheraga, H. A. *J. Comput. Chem.* **1993**, *14*, 1482.
(425) Ghosh, S. K.; Parr, R. G. *Theor. Chim. Acta* **1987**, *72*, 379.
(426) Ghanty, T. K.; Ghosh, S. K. *J. Phys. Chem.* **1991**, *95*, 6512.
(427) Ghanty, T. K.; Ghosh, S. K. *J. Mol. Struct.* (*THEOCHEM*) **1992**, *276*, 83.
(428) Ghanty, T. K.; Ghosh, S. K. *J. Phys. Chem.* **1996**, *100*, 1840.
(429) Von Szentpaly, L. *J. Mol. Struct.* (*THEOCHEM*) **1991**, *233*, 71.
(430) De Proft, F.; Langenaeker, W.; Geerlings, P. *J. Mol. Struct.* (*THEOCHEM*) **1995**, *339*, 45.
(431) Berkowitz, M. *J. Am. Chem. Soc.* **1987**, *109*, 4823.
(432) Baeten, A.; De Proft, F.; Geerlings, P. *Int. J. Quantum Chem.* **1996**, *60*, 931.
(433) De Proft, F.; Langenaeker, W.; Geerlings, P. *J. Phys. Chem.* **1993**, *97*, 1826.
(434) Baeten, A.; Geerlings, P. *J. Mol. Struct.* (*THEOCHEM*) **1999**, *465*, 203.
(435) Datta, D.; Singh, S. *J. Chem. Soc., Dalton Trans.* **1991**, 1541.
(436) Datta, D. *J. Phys. Chem.* **1986**, *90*, 4217.
(437) Patra, G. K.; Hati, S.; Datta, D. *Indian J. Chem.* **1999**, *38A*, 1.
(438) Yang, W.; Lee, C.; Ghosh, S. K. *J. Phys. Chem.* **1985**, *89*, 5412.
(439) Chattaraj, P. K.; Lee, H.; Parr, R. G. *J. Am. Chem. Soc.* **1991**, *113*, 1855.
(440) Parr, R. G.; Chattaraj, P. K. *J. Am. Chem. Soc.* **1991**, *113*, 1854.
(441) Cedillo, A.; Chattaraj, P. K.; Parr, R. G. *Int. J. Quantum Chem.* **2000**, *77*, 403.
(442) Gazquez, J. L. *J. Phys. Chem. A* **1997**, *101*, 4657.
(443) Mendez, F.; Gazquez, J. L. *J. Am. Chem. Soc.* **1994**, *116*, 9298.
(444) Gazquez, J. L.; Mendez, F. *J. Phys. Chem.* **1994**, *98*, 4591.
(445) Geerlings, P.; De Proft, F. *Int. J. Quantum Chem.* **2000**, *80*, 227.
(446) Damoun, S.; Van de Woude, G.; Mendez, F.; Geerlings, P. *J. Phys. Chem. A* **1997**, *101*, 886.
(447) Chandra, A. K.; Geerlings, P.; Nguyen, M. T. *J. Org. Chem.* **1997**, *62*, 6417.
(448) Nguyen, L. T.; Le, T. N.; De Proft, F.; Chandra, A. K.; Langenaeker, W.; Nguyen, M. T.; Geerlings, P. *J. Am. Chem. Soc.* **1999**, *121*, 5992.
(449) Ponti, A. *J. Phys. Chem. A* **2000**, *104*, 8843.
(450) Li, Y.; Evans, J. N. S. *Proc. Natl. Acad. Sci. U.S.A.* **1996**, *93*, 4612.

(451) Ireta, J.; Galvan, M.; Kyeonjgae, C.; Joannopoulos, J. D. *J. Am. Chem. Soc.* **1998**, *120*, 9771.
(452) Payne, M. C.; Teter, M. P.; Allan, D. C.; Arias, T. A.; Joannopoulos, J. D. *Rev. Mod. Phys.* **1992**, *64*, 1045.
(453) Galvan, M.; Dal Pino, A.; Joannopoulos, J. D. *Phys. Rev. Lett.* **1993**, *70*, 21.
(454) Dal Pino A.; Galvan, M.; Arias, T. A.; Joannopoulos, J. D. *J. Chem. Phys.* **1993**, *98*, 1606.
(455) Chandra, A. K.; Michalak, A.; Nguyen, M. T.; Nalewajski, R. F. *J. Phys. Chem. A* **1998**, *102*, 10182.
(456) Damoun, S.; Van de Woude, G.; Choho, K.; Geerlings, P. *J. Phys. Chem. A* **1999**, *103*, 7861.
(457) Mendez, F.; Tamariz, J.; Geerlings, P. *J. Phys. Chem. A* **1998**, *102*, 6292.
(458) Pal, S.; Chandrakumar, K. R. S. *J. Am. Chem. Soc.* **2000**, *122*, 4145.
(459) Chandrakumar, K. R. S.; Pal, S. *J. Phys. Chem. B* **2001**, *105*, 4541.
(460) Chattaraj, P. K. *J. Phys. Chem. A* **2001**, *105*, 511.
(461) Klopman, G. In *Chemical Reactivity and Reaction Paths*; Klopman, G., Ed.; Wiley: New York, 1974; p 1.
(462) Koslyk, R. J.; Whitehead, M. A. *J. Mol. Struct.* (*THEOCHEM*) **1991**, *230*, 83.
(463) Chattaraj, P. K.; Gomez, B.; Chamorro, E.; Santos, J.; Fuentealba, P. *J. Phys. Chem. A* **2001**, *105*, 8815.
(464) Pearson, R. G. *Acc. Chem. Res.* **1993**, *26*, 250.
(465) Pearson, R. G. *J. Chem. Educ.* **1999**, *76*, 267.
(466) Parr, R. G.; Zhou, Z. *Acc. Chem. Res.* **1992**, *26*, 256.
(467) Zhou, Z.; Parr, R. G.; Garst, J. F. *Tetrahedron Lett.* **1988**, *29*, 4843.
(468) Zhou, Z.; Parr, R. G. *J. Am. Chem. Soc.* **1989**, *111*, 7371.
(469) Zhou, Z.; Navangul, H. V. *J. Phys. Org.Chem.* **1990**, *3*, 784.
(470) Zhou, Z. *J. Phys. Org.Chem.* **1995**, *8*, 103.
(471) (a) Sebastian, K. L. *Chem. Phys. Lett.* **1994**, *231*, 40. (b) Sebastian, K. L. *Chem. Phys. Lett.* **1995**, *236*, 621.
(472) Pearson, R. G.; Palke, W. E. *J. Phys. Chem.* **1992**, *96*, 3283.
(473) Chattaraj, P. K.; Nath, S.; Sannigrahi, A. B. *Chem. Phys. Lett.* **1993**, *212*, 223.
(474) Chattaraj, P. K.; Nath, S.; Sannigrahi, A. B. *J. Phys. Chem.* **1994**, *98*, 9143.
(475) Datta, D. *Inorg. Chem.* **1992**, *31*, 2797.
(476) Harbola, M. K. *Proc. Natl. Acad. Sci. U.S.A.* **1992**, *89*, 1036.
(477) Chandra, A. K., *J. Mol. Struct.* (*THEOCHEM*) **1994**, *312*, 297.
(478) Hati, S.; Datta, D. *J. Org. Chem.* **1992**, *57*, 6056.
(479) Ghanty, T. K.; Ghosh, S. K. *J. Phys. Chem.* **1996**, *100*, 12295.
(480) Gazquez, J. L. *J. Phys. Chem. A* **1997**, *101*, 9464.
(481) Hohm, U. *J. Phys. Chem. A* **2000**, *104*, 8418.
(482) Datta, D. *J. Phys. Chem.* **1992**, *96*, 2409.
(483) Gazquez, J. L.; Martinez, A.; Mendez, F. *J. Phys. Chem.* **1993**, *97*, 4059.
(484) Cárdenas-Jirón, G. I.; Lahsen, J.; Toro-Labbé, A. *J. Phys. Chem.* **1995**, *99*, 5325.
(485) Gutiérrez-Oliva, S.; Letelier, J. R.; Toro-Labbé, A. *Mol. Phys.* **1999**, *96*, 61.
(486) Chattaraj, P. K.; Fuentealba, P.; Jaque, P.; Toro-Labbé, A. *J. Phys. Chem. A* **1999**, *103*, 9307.
(487) Cárdenas-Jirón, G. I.; Toro-Labbé, A. *J. Phys. Chem.* **1995**, *99*, 12730.
(488) Cárdenas-Jirón, G. I.; Letelier, J. R.; Toro-Labbé, A. *J. Phys. Chem. A* **1998**, *102*, 7864.
(489) (a) Cárdenas-Jirón, G. I.; Gutierrez-Oliva, S.; Melin, J.; Toro-Labbé, A. *J. Phys. Chem. A* **1997**, *101*, 4621. (b) Chattaraj, P. K.; Perez, P.; Zevallos, J.; Toro-Labbé, A. *J. Phys. Chem. A* **2001**, *105*, 4272.
(490) Solà, M.; Toro-Labbé, A. *J. Phys. Chem. A* **1999**, *103*, 8847.
(491) Jaque, P.; Toro-Labbé, A. *J. Phys. Chem. A* **2000**, *104*, 995.
(492) Perez, P.; Toro-Labbé, A. *J. Phys. Chem. A* **2000**, *104*, 1557.
(493) Kar, T.; Scheiner, S. *J. Phys. Chem.* **1995**, *99*, 8121.
(494) Kar, T.; Scheiner, S.; Sannigrahi, A. B. *J. Phys. Chem. A* **1998**, *102*, 5967.
(495) Mineva, T.; Russo, N.; Sicilia, E.; Toscano, M. *Theor. Chem. Acc.* **1999**, *101*, 388.
(496) Sicilia, E.; Russo, N.; Mineva, T. *J. Phys. Chem. A* **2001**, *105*, 442.
(497) Arulmozhiraja, S.; Kolandaivel, P. *Int. J. Quantum Chem.* **1997**, *64*, 231.
(498) Jayakumar, N.; Kolandaivel, P. *Int. J. Quantum Chem.* **2000**, *76*, 648.
(499) Ghanty, T. K.; Ghosh, S. K. *Int. J. Quantum Chem.* **1997**, *63*, 917.
(500) Ghanty, T. K.; Ghosh, S. K. *J. Phys. Chem. A* **2000**, *104*, 2975.
(501) Nguyen, L. T.; De Proft, F.; Nguyen, M. T.; Geerlings, P. *J. Org. Chem.* **2001**, *66*, 4316.
(502) Nguyen, L. T.; De Proft, F.; Nguyen, M. T.; Geerlings, P. *J. Chem. Soc., Perkin Trans. 2* **2001**, 898.
(503) Le, T. N.; De Proft, F.; Geerlings, P.; Nguyen, M. T. *J. Chem. Soc., Perkin Trans. 2* **1999**, 1249.
(504) Chandra, A. K.; Nguyen, M. T. *J. Phys. Chem. A* **1998**, *102*, 6181.
(505) Chandra, A. K. *J. Mol. Struct.* (*THEOCHEM*) **1994**, *118*, 297.
(506) Uchimaru, T.; Chandra, A. K.; Kawahara, S.; Matsumura, K.; Tsuzuki, S.; Mikami, M. *J. Phys. Chem. A* **2001**, *105*, 1343.
(507) Nguyen, M. T.; Chandra, A. K.; Sakai, S.; Morokuma, K. *J. Org. Chem.* **1999**, *64*, 65.
(508) Cohen, H. D.; Roothaan, C. C. J. *J. Chem. Phys.* **1965**, *43*, S34.
(509) Torrent-Sucarrat, M.; Luis, J. M.; Duran, M.; Solà, M. *J. Am. Chem. Soc.* **2001**, *123*, 7951.
(510) Chandra, A. K.; Uchimaru, T. *J. Phys. Chem. A* **2001**, *105*, 3578.
(511) Makov, G. *J. Phys. Chem.* **1995**, *99*, 9337.
(512) Nalewajski, R. F. Personal communication to the authors.
(513) Chattaraj, P. K.; Fuentealba, P.; Gómez, B.; Contreras, R. *J. Am. Chem. Soc.* **2000**, *122*, 348.
(514) Woodward, R. B.; Hoffmann, R. *The Conservation of Orbital Symmetry*; Academic Press: New York, 1970.
(515) Zhou, Z.; Parr, R. G. *J. Am. Chem. Soc.* **1990**, *112*, 5720.
(516) For a comprehensive account of this type of reaction, see: Taylor, R. *Electrophilic Aromatic Substitution*; John Wiley: New York, 1990.
(517) Amic, D.; Trinajstic, N. *Bull. Soc. Chim. Belg.* **1991**, *100*, 527.
(518) Ray, N. K.; Rastogi, R. C. *Int. J. Quantum Chem.* **1994**, *51*, 99.
(519) Ray, N. K.; Rastogi, R. C. *Indian J. Chem. A* **1993**, *32*, 927.
(520) Pearson, R. G. *J. Phys. Chem.* **1994**, *98*, 1989.
(521) Pearson, R. G. *Int. J. Quantum Chem.* **1995**, *56*, 211.
(522) Pearson, R. G. *Chemical Hardness*; Wiley-VCH: Weinheim, 1997; Chapter 6.
(523) Gilman, J. J. *Mater. Res. Innovations* **1997**, *1*, 71.
(524) Yang, W.; Parr, R. G.; Uytterhoeven, L. *Phys. Chem. Miner.* **1987**, *15*, 191.
(525) See, for example: Dana, E. S. *Textbook of Mineralogy*; 4th ed.; Wiley: New York, 1932; p 214.
(526) Grossman, J. C.; Mizel, A.; Cote, M.; Cohen, M. L.; Louie, S. G. *Phys. Rev. B* **1999**, *60*, 6343.
(527) Jhi, S. H.; Ihm, J.; Louie, S. G.; Cohen, M. L. *Nature* **1999**, *399*, 132.
(528) Murphy, L. R.; Meek, T. L.; Allred, L. A.; Allen, L. C. *J. Phys. Chem. A* **2000**, *104*, 5867.
(529) Bartolotti, L. J.; Gadre, S. R.; Parr, R. G. *J. Am. Chem. Soc.* **1980**, *102*, 2945.
(530) Sen, K. D.; Schmidt, P. C.; Weiss, A. *Theor. Chim. Acta* **1980**, *16*, L69.
(531) Robles, J.; Bartolotti, L. J. *J. Am. Chem. Soc.* **1984**, *106*, 3723.
(532) Gunnarsson, O.; Jonson, M.; Lundqvist, B. I. *Phys. Rev. B* **1979**, *20*, 3136.
(533) Gazquez, J. L.; Ortiz, E. *J. Chem. Phys.* **1984**, *81*, 2741.
(534) Larson, E. G.; Smith, D. W. *Int. J. Quantum Chem.* **1971**, *S4*, 87.
(535) Ray, N. K.; Samuels, L.; Parr, R. G. *J. Chem. Phys.* **1979**, *70*, 3680.
(536) Teller, E. *Rev. Mod. Phys.* **1962**, *34*, 627.
(537) Balazs, N. L. *Phys. Rev.* **1967**, *156*, 42.
(538) Sen, K. D. *J. Phys. B* **1983**, *16*, L149.
(539) Pearson, R. G. *J. Am. Chem. Soc.* **1988**, *110*, 7864.
(540) Politzer, P.; Parr, R. G.; Murphy, D. R. *J. Chem. Phys.* **1983**, *79*, 3859.
(541) Deb, B. M.; Singh, R.; Sukumar, N. *J. Mol. Struct.* (*THEOCHEM*) **1992**, *91*, 121.
(542) Harbola, M. K.; Parr, R. G.; Lee, C. T. *J. Chem. Phys.* **1991**, *94*, 6055.
(543) Pasternak, A. *Chem. Phys.* **1977**, *26*, 101.
(544) Komorowski, L. In *Chemical Hardness*; Sen, K. D., Ed.; Structure and Bonding 80; Springer-Verlag: Berlin, 1993; p 45.
(545) Politzer, P.; Murray, S. J.; Grice, M. E. In *Chemical Hardness*; Sen, K. D., Ed.; Structure and Bonding 80; Springer-Verlag: Berlin, 1993; p 102.
(546) Politzer, P. *J. Chem. Phys.* **1987**, *86*, 1072.
(547) Vela, A.; Gazquez, J. L. *J. Am. Chem. Soc.* **1990**, *112*, 1490.
(548) Stott, M. J.; Zaremba, E. *Phys. Rev. A* **1980**, *21*, 12.
(549) Langenaeker, W.; De Proft, F.; Tielens, F.; Geerlings, P. *Chem. Phys. Lett.* **1998**, *288*, 628.
(550) Nagle, J. K. *J. Am. Chem. Soc.* **1990**, *112*, 4741.
(551) Ghanty, T. K.; Ghosh, S. K. *J. Phys. Chem.* **1993**, *97*, 4951.
(552) Fuentealba, P.; Reyes, O. *J. Mol. Struct.* (*THEOCHEM*) **1993**, *282*, 65.
(553) Hati, S.; Datta, D. *J. Phys. Chem.* **1994**, *98*, 10451.
(554) Simón-Manso, Y.; Fuentealba, P. *J. Phys. Chem. A* **1998**, *102*, 2029.
(555) Ghanty, T. K.; Ghosh, S. K. *J. Am. Chem. Soc.* **1994**, *116*, 8801.
(556) Ghanty, T. K.; Ghosh, S. K. *J. Phys. Chem.* **1994**, *98*, 9197.
(557) Ghanty, T. K.; Ghosh, S. K. *J. Phys. Chem.* **1996**, *100*, 17429.
(558) Ghanty, T. K.; Ghosh, S. K. *J. Mol. Struct.* (*THEOCHEM*) **1996**, *366*, 139.
(559) Fricke, B. *J. Chem. Phys.* **1986**, *84*, 862.
(560) Politzer, P.; Murray, J. S.; Grice, M. E.; Brinck, T.; Ranganathan, S. *J. Chem. Phys.* **1991**, *95*, 6699.
(561) Ghosh, S. K.; Berkowitz, M.; Parr, R. G. *Proc. Natl. Acad. Sci. U.S.A.* **1984**, *81*, 8028.
(562) Nagy, A.; Parr, R. G.; Liu, S. *Phys. Rev. A* **1996**, *53*, 3117.
(563) Gal, T.; Nagy, A. *Mol. Phys.* **1997**, *91*, 873.
(564) Senet, P. *Chem. Phys. Lett.* **1997**, *275*, 527.

(565) Boyd, R. J. *J. Phys. B* **1976**, *9*, L69.
(566) Bader, R. W. F.; MacDougall, P. J.; Lau, C. D. H. *J. Am. Chem. Soc.* **1984**, *106*, 1549.
(567) Bader, R. W. F.; Essén, H. *J. Chem. Phys.* **1984**, *80*, 1943.
(568) Hunter, G. *Int. J. Quantum Chem.* **1986**, *XXIX*, 197.
(569) Sagar, R. P.; Ku, A. C. T.; Smith, V. H., Jr.; Simas, A. M. *J. Chem. Phys.* **1988**, *88*, 4367.
(570) Shi, Z.; Boyd, R. J. *J. Chem. Phys.* **1988**, *88*, 4375.
(571) Sagar, R. P.; Ku, A. C. T.; Smith, V. H., Jr.; Simas, A. M. *Can. J. Chem.* **1988**, *66*, 1005.
(572) Simas, A. M.; Sagar, R. P.; Ku, A. C. T.; Smith, V. H., Jr. *Can. J. Chem.* **1988**, *66*, 1923.
(573) Becke, A. D.; Edgecombe, K. E. *J. Chem. Phys.* **1990**, *92*, 5397.
(574) Kohout, M.; Savin, A.; Preuss, H. *J. Chem. Phys.* **1991**, *95*, 1928.
(575) Politzer, P. *J. Chem. Phys.* **1980**, *72*, 3027.
(576) Politzer, P. *J. Chem. Phys.* **1980**, *73*, 3264.
(577) Sen, K. D.; Gayatri, T. V.; Krishnaveni, R.; Kakkar, M.; Toufar, H.; Janssens, G. O. A.; Baekelandt, B. G.; Schoonheydt, R. A.; Mortier, W. J. *Int. J. Quantum Chem.* **1995**, *56*, 399.
(578) Weinstein, H.; Politzer, P.; Srebrenik, S. *Theor. Chim. Acta* **1975**, *38*, 159.
(579) Politzer, P.; Parr, R. G. *J. Chem. Phys.* **1976**, *64*, 4634.
(580) De Proft, F.; Geerlings, P. *Chem. Phys. Lett.* **1994**, *220*, 405.
(581) Chattaraj, P. K.; Sengupta, S. *J. Phys. Chem. A* **1999**, *103*, 6122.
(582) Wells, P. R. *Prog. Phys. Org. Chem* **1986**, *6*, 11.
(583) Inamoto, N.; Masuda, S. *Tetrahedron Lett.* **1977**, 3287.
(584) Inamoto, N.; Masuda, S.; Tori, K.; Yoshimura, Y. *Tetrahedron Lett.* **1978**, 4547.
(585) Inamoto, N.; Masuda, S. *Chem. Lett.* **1982**, 1003.
(586) Inamoto, N.; Masuda, S. *Chem. Lett.* **1982**, 1007.
(587) Huheey, J. E. *J. Phys. Chem.* **1966**, *70*, 2086.
(588) Mullay, J. *J. Am. Chem. Soc.* **1985**, *107*, 7271.
(589) Bratsch, S. G. *J. Chem. Educ.* **1985**, *62*, 101.
(590) Marriott, S.; Reynolds, W. F.; Taft, R. W.; Topsom, R. D. *J. Org. Chem.* **1984**, *49*, 959.
(591) Boyd, R. J.; Edgecombe, K. E. *J. Am. Chem. Soc.* **1988**, *110*, 4182.
(592) Boyd, R. J.; Boyd, S. L. *J. Am. Chem. Soc.* **1992**, *114*, 1652.
(593) Suresh, C. H.; Koga, N. *J. Am. Chem. Soc.* **2002**, *114*, 1790.
(594) Reed, L. H.; Allen, L. C. *J. Phys. Chem.* **1992**, *96*, 157.
(595) Korchowiec, J.; Nalewajski, R. F. *Int. J. Quantum Chem.* **1992**, *XLIV*, 1027.
(596) Vivas-Reyes, R.; De Proft, F.; Biesemans, M.; Willem, R.; Geerlings, P. *J. Phys. Chem. A* **2002**, *106*, 2753.
(597) Roy, R. K.; Pal, S. *J. Phys. Chem.* **1995**, *99*, 17822.
(598) Kneisler, J.; Zhou, Z. *Int. J. Quantum Chem.* **1994**, *49*, 309.
(599) BABEL: Walters, P.; Stahl, M. *Babel*, version 1.6; 1992−1996 (babel@mercury.aichem.arizona.edu).
(600) Gasteiger, J. PETRA: Parameter Estimation for the Treatment of Reactivity Applications. Empirical Methods for the Calculation of Physicochemical Data of Organic Compounds. In *Physical Property Prediction in Organic Chemistry*; Jochum, C., Hicks, M. G., Sunkel, J., Eds.; Springer-Verlag: Heidelberg, 1988; pp 119−138.
(601) Dinur, U. *J. Mol. Struct.* (*THEOCHEM*) **1994**, *303*, 227.
(602) van Duin, A. C. T.; Baas, J. M. A.; van de Graaf, B. *J. Chem. Soc. Faraday Trans.* **1994**, *90*, 2881.
(603) Castro, R.; Barardi, M. J.; Córdova, E.; Ochoa de Olza, M.; Kaifer, A. E.; Evanseck, J. D. *J. Am. Chem. Soc.* **1996**, *118*, 10257.
(604) Hayashi, M.; Nakamura, Y.; Higashi, K.; Kato, H.; Kishida, F.; Kaneko, H. *Toxicol. in Vitro* **1999**, *13*, 915.
(605) Thanikaivelan, P.; Subramanian, V.; Raghava Rao, J.; Nair, B. U. *Chem. Phys. Lett.* **2000**, *323*, 59.
(606) Sullivan, J. J.; Jones, A. D.; Tanji, K. K. *J. Chem. Inf. Comput. Sci.* **2000**, *40*, 1113.
(607) Kobayashi, S.; Hameshima, K.; Ishii, Y.; Tanaka, A. *Chem. Pharm. Bull.* **1995**, *43*, 1780.
(608) Baeten, A.; Tafazoli, M.; Kirsch-Volders, M.; Geerlings, P. *Int. J. Quantum Chem.* **1999**, *74*, 351.
(609) Chandra, A. K.; Uchimaru, T.; Sugie, M.; Sekiya, A. *Chem. Phys. Lett.* **2000**, *318*, 69.
(610) Kobayashi, S.; Hamashima, H.; Kurihara, M.; Miyata N.; Tanaka, A. *Chem. Pharm. Bull.* **1998**, *46*, 1108.
(611) Ma, Q.; Dong, L.; Whitlock, J. P. *J. Biol. Chem.* **1995**, *270*, 12697.
(612) Shen, L. L.; Kohlbrenner, W. E.; Weigl, D.; Baranowski, J. *J. Biol. Chem.* **1989**, *264*, 2973.
(613) Staudenbauer, W. L.; Orr, E. *Nucleic Acids Res.* **1981**, *9*, 3589.
(614) Garrat, P. J. *Aromaticity*; Wiley: New York, 1986.
(615) Minkin, V. J.; Glukhovtsev, M. N.; Simkin, B. Y. *Aromaticity and Antiaromaticity: Electronic and Structural Aspects*; Wiley: New York, 1984.
(616) Schleyer, P. v. R.; Jiao, H. *Pure Appl. Chem.* **1996**, *68*, 209.
(617) Krygowski, T. M.; Cyranski, M. K.; Czarnocki, Z.; Häfelinger, G; Katritzky, A. R. *Tetrahedron* **2000**, *56*, 1783.
(618) Schleyer, P. v. R., Guest Editor. *Chem. Rev.* **2001**, *101* (5) (special issue on Aromaticity).
(619) Cava, M. P.; Mitchell, M. J. *Cyclobutadiene and Related Compounds*; Academic Press: New York, 1967.
(620) Dewar, M. J. S. *Angew. Chem., Int. Ed. Engl.* **1971**, *10*, 761.
(621) Dewar, M. J. S. *Angew. Chem.* **1971**, *83*, 859.
(622) Vollhardt, K. P. C.; Yee, L. S. *J. Am. Chem. Soc.* **1977**, *99*, 2010.
(623) Willner, I.; Rabinovitz, M. *J. Org. Chem.* **1980**, *45*, 1628.
(624) Minsky, A.; Meyer, A. Y.; Rabinovitz, M. *Tetrahedron* **1985**, *41*, 785.
(625) Cohen, Y.; Klein, J.; Rabinovitz, M. *J. Chem. Soc., Chem. Commun.* **1986**, 1071.
(626) Cohen, Y.; Roelofs, N. H.; Reinhardt, G.; Scott, L. T.; Rabinovitz, M. *J. Org. Chem.* **1987**, *52*, 4207.
(627) Budzelaar, P. H. M.; Cremer, D.; Wallasch, M.; Wurthwein, E. U.; Schleyer, P. v. R. *J. Am. Chem. Soc.* **1987**, *109*, 6290.
(628) Fowler, P. *Nature* (*London*) **1991**, *350*, 20.
(629) Aihara, J. *Phys. Chem. Chem. Phys.* **1999**, 1, 3193.
(630) Aihara, J. *Theor. Chem. Acc.* **1999**, *102*, 134.
(631) Yoshida, M.; Aihara, J. *Phys. Chem. Chem. Phys.* **1999**, 1, 227.
(632) Aihara, J. *Phys. Chem. Chem. Phys.* **2000**, 2, 3121.
(633) Zhou, Z.; Navangul, H. V. *J. Phys. Org. Chem.* **1990**, *3*, 784.
(634) Chamizo, J. A.; Morgado, J.; Sosa, O. *Organometallics* **1993**, *12*, 5005.
(635) Bird, C. W. *Tetrahedron* **1997**, *53*, 3319.
(636) Roy, R. K.; Choho, K.; De Proft, F.; Geerlings, P. *J. Phys. Org. Chem.* **1999**, *12*, 503.
(637) Lazeretti, P. Tossell, J. A. *J. Mol. Struct.* (*THEOCHEM*) **1991**, *236*, 403.
(638) Bulgarevich, S. B.; Yusman, T. A.; Osipov, O. A. *J. Gen. Chem. USSR* **1984**, *54*, 1427.
(639) Archibong, E. F.; Thakkar, A. J. *Mol. Phys.* **1994**, *81*, 557.
(640) El-Bakali, N.; Doerksen, R. J.; Thakkar, A. J. *J. Phys. Chem.* **1995**, *99*, 12790.
(641) Millifiori, S.; Alparone, A. *J. Mol. Struct.* (*THEOCHEM*) **1998**, *431*, 59.
(642) Katritzky, A. R.; Barczynski, P.; Musumarra, G.; Pisano, D.; Szafran, M. *J. Am. Chem. Soc.* **1989**, *111*, 7.
(643) Howard, S. T.; Krygowski, T. M. *Can. J. Chem.* **1997**, *75*, 1174.
(644) Kruszewski, J.; Krygowski, T. M. *Tetrahedron Lett.* **1972**, 3839.
(645) Krygowski, T. M. *J. Chem. Inf. Comput. Sci.* **1993**, *33*, 70.
(646) Krygowski, T. M.; Cyranski, M. K. *Tetrahedron* **1996**, *52*, 1713.
(647) Schleyer, P. v. R.; Maerker, C.; Dransfeld, A.; Jiao, H.; van Eikema Hommes, N. J. R. *J. Am. Chem. Soc.* **1996**, *118*, 6317.
(648) Van Lier, G.; Fowler, P.; De Proft, F.; Geerlings, P. *J. Phys. Chem. A* **2002**, *106*, 5128.
(649) Murray, J. S.; Seminario, J. M.; Politzer, P. *Int. J. Quantum Chem.* **1994**, *94*, 575.
(650) Murray, J. S.; Abu-Awwad, F.; Politzer, P. *J. Mol. Struct.* (*THEOCHEM*) **2000**, *501*, 241.
(651) Chesnut, D. B.; Bartolotti, L. J. *Chem. Phys.* **2000**, *253*, 1.
(652) Becke, A. D.; Edgecombe, K. E. *J. Chem. Phys.* **1990**, *92*, 5397.
(653) Silvi, B.; Savin, A. *Nature* **1994**, *371*, 683.
(654) Fuster, F.; Silvi, B. *J. Phys. Chem. A* **2000**, *104*, 947 and references therein.
(655) Suresh, C. H.; Gadre, S. R. *J. Org. Chem.* **1999**, *64*, 2505.
(656) Clar, E. *Polycyclic Hydrocarbons*; Academic Press: London, 1964; Vols. 1 & 2.
(657) Clar, E. *The Aromatic Sextet*; John Wiley and Sons: London, 1972.
(658) Li, S.; Jiang, Y. *J. Am. Chem. Soc.* **1995**, *117*, 8401.
(659) Carey; F. A.; Sundberg, R. J. *Advanced Organic Chemistry*, 3rd ed.; Plenum Press: New York, 1990; Part A, Chapter 4.
(660) Isaacs, N. S. *Physical Organic Chemistry*, 2nd ed.; Longmans: Essex, England, 1995; Chapter 2.
(661) Klopman, G.; Moriishi, H.; Kokuchi, O.; Suzuki, K. *Tetrahedron Lett.* **1983**, *23*, 1027.
(662) See ref 516, Preface.
(663) Ma, J. C.; Dougherty, D. A. *Chem. Rev.* **1997**, *97*, 1303.
(664) See ref 356, Chapter 11.
(665) Fleming, I. *Frontier Orbitals and Organic Chemical Reactions*; Wiley: London, 1976; p 55.
(666) Russo, N.; Toscano, M.; Grand, A.; Mineva, T. *J. Phys. Chem.* **2000**, *104*, 4017.
(667) Mc Murry, J. *Organic Chemistry*, 4th ed.; Brook/Cale: Pacific Grove, CA, 1996.
(668) Pollack, S. K.; Devlin, J. L.; Summerhays, K. D.; Taft, R. W.; Hehre W. J. *J. Am. Chem. Soc.* **1977**, *99*, 4583.
(669) Karpas, Z.; Berant, Z.; Stimac, R. *Struct. Chem. Soc.* **1990**, *1*, 201.
(670) Smith, R. L.; Chyall, L. J.; Beasly, B. J.; Kenttänaa, H. I. *J. Am. Chem. Soc.* **1995**, *117*, 7971.
(671) Sjoberg, P.; Murray, J. S.; Brinck, T.; Politzer, P. *Can. J. Chem.* **1990**, *68*, 1440.
(672) Ritchie, J. P. *J. Mol. Struct.* (*THEOCHEM*) **1992**, *225*, 297.
(673) Tishchenko, O.; Pham-Tran, N. N.; Kryachko, E. S.; Nguyen, M. T. *J. Phys. Chem.* **2001**, *105*, 8709.
(674) Nguyen, M. T.; Raspoet, G. *Can. J. Chem.* **1999**, *77*, 817.
(675) Nguyen, M. T.; Raspoet, G.; Vanquickenborne, L. G. *J. Phys. Org. Chem.* **2000**, *13*, 46.
(676) Clark, L. A.; Ellis, D. E.; Snurr, R. Q. *J. Chem. Phys.* **2001**, *114*, 2580.
(677) Reference 356, p 458.
(678) le Noble, W. J. *Highlights of Organic Chemistry, An Advanced Textbook*; Dekker; New York, 1974; p 822.

(679) Reutov, O. A.; Beletskaya, I. P.; Kuts, A. L. In *Ambident Anions (Translation from Russian)*; Michael J. P., Ed.; Plenum: New York, 1983.
(680) Patai, S.; Rappoport, Z. In *The Chemistry of alkenes*; Patai, S., Ed.; Interscience Publishers: London, 1964; p 468.
(681) Wong, S. S.; Paddon-Row, M. N.; Li, Y.; Houk, K. N. *J. Am. Chem. Soc.* **1990**, *112*, 8679.
(682) Raspoet, G.; Nguyen, M. T.; McGanaghy, M.; Hegarty, A. F. *J. Org. Chem.* **1998**, *63*, 6807.
(683) Tielemans, M.; Promel, R.; Geerlings, P. *Tetrahedron Lett.* **1988**, 1687.
(684) Langenaeker, W.; De Proft, F.; Geerlings, P. *J. Phys. Chem. A* **1998**, *102*, 5944.
(685) Choho, K.; Langenaeker, W.; Van de Woude, G.; Geerlings, P. *J. Mol. Struct.* (*THEOCHEM*) **1995**, *338*, 293.
(686) Wong, M. W.; Pross, A.; Radom, L. *J. Am. Chem. Soc.* **1993**, *115*, 11050.
(687) Eisenstein, O.; Lefour, J. M.; Anh, N. T.; Hudson, R. F. *Tetrahedron* **1977**, *33*, 523.
(688) Houk, K. N.; Li, Y.; Evanseck, J. T. *Angew. Chem., Int. Ed. Engl.* **1992**, *31*, 682.
(689) Ponti, A.; Molteni, G. *J. Org. Chem.* **2001**, *66*, 5252.
(690) Chandra, A. K.; Nguyen, M. T. *J. Comput. Chem.* **1998**, *19*, 195.
(691) Nguyen, L. T.; De Proft, F.; Chandra, A. K.; Uchimari, T.; Nguyen, M. T.; Geerlings, P. *J. Org. Chem.* **2001**, *66*, 6091.
(692) Chandra, A. K.; Uchimari, T.; Nguyen, M. T. *J. Chem. Soc., Perkin Trans. 2* **1999**, 2117.
(693) Jimenez, R.; Perez, L.; Tamariz, J.; Salgado, H. *Heterocycles* **1993**, *35*, 591.
(694) Huang, M.; Maynard, A.; Turpin, J. A.; Graham, L.; Janihi, G. M.; Lovell, D. G.; Rice, W. G. *J. Med. Chem.* **1998**, *41*, 1371.
(695) Hammond, G. S. *J. Am. Chem. Soc.* **1955**, *77*, 334.
(696) Toro-Labbé, A. *J. Phys. Chem. A* **1999**, *103*, 4398.
(697) Cherest, M.; Felkin, H. *Tetrahedron Lett.* **1968**, 2205.
(698) Cherest, M.; Felkin, H.; Prudent, N. *Tetrahedron Lett.* **1968**, 2199.
(699) Cherest, M.; Felkin, H.; Tacheau, P.; Jacques, J.; Varech, D. *J. Chem. Soc., Chem. Commun.* **1977**, 372.
(700) Anh, N. T. *Top. Curr. Chem.* **1980**, *88*, 145.
(701) Bürgi, H. B.; Dunitz, J. D.; Lehn, J. M. Wipff, G. *Tetrahedron* **1974**, *30*, 1563.
(702) Bürgi, H. B.; Dunitz, J. D.; Schefter, E. J. *J. Am. Chem. Soc.* **1973**, *95*, 5063.
(703) Bürgi, H. B.; Lehn, J. M.; Wipff, G. *J. Am. Chem. Soc.* **1974**, *96*, 1956.
(704) Roy, R. K.; Tajima, N.; Hirao, K. *J. Phys. Chem. A* **2001**, *105*, 2117.
(705) Choho, K.; Langenaeker, W.; Van De Woude, G.; Geerlings, P. *J. Mol. Struct.* (*THEOCHEM*) **1996**, *362*, 305.
(706) Mendez, F.; de L. Romero, M.; De Proft, F.; Geerlings, P. *J. Org. Chem.* **1998**, *63*, 5774.
(707) Reference 356, Chapter 10.
(708) Pross, A. *Theoretical and Physical Principles of Organic Reactivity*; Wiley: New York, 1995; Part C.
(709) Su, T.; Wang, H.; Hase, W. L. *J. Phys. Chem. A* **1998**, *102*, 9819.
(710) Gazquez, J. L. *J. Phys. Chem. A* **1997**, *101*, 8967.
(711) Chattaraj, P. K.; Schleyer, P. v. R. *J. Am. Chem. Soc.* **1994**, *116*, 1067.
(712) Reference 356, Chapter 8.
(713) Taft, R. W.; Topsom, R. D. *Prog. Phys. Org. Chem.* **1987**, *16*, 1.
(714) Hansch, C.; Leo, A.; Taft, R. W. *Chem. Rev.* **1991**, *91*, 165.
(715) Brauman, J. I.; Blair, L. K. *J. Am. Chem. Soc.* **1970**, *92*, 5986.
(716) Lias, S. G.; Bartmess, J. E.; Holmes, J. L.; Levin, R. D.; Mallard, W. G. J. *Phys. Chem. Ref. Data* **1988**, *17*, Suppl. 1.
(717) De Proft, F.; Langenaeker, W.; Geerlings, P. *Tetrahedron* **1995**, *51*, 4012.
(718) Perez, P.; Toro-Labbé, A.; Contreras, R. *J. Phys. Chem. A* **1999**, *103*, 11246.
(719) Perez, P.; Simón-Manso, Y.; Aizman, A.; Fuentealba, P.; Contrereas, R. *J. Am. Chem. Soc.* **2000**, *122*, 4756.
(720) Perez, P. *J. Phys. Chem. A* **2001**, *105*, 6182.
(721) Damoun, S.; Langenaeker, W.; Van De Woude, G.; Geerlings, P. *J. Phys. Chem.* **1995**, *99*, 12151.
(722) Sauer, J. *Chem. Rev.* **1989**, *89*, 199.
(723) Corma, A.; Sastre, G.; Viruela, R.; Zicovich-Wilson, C. *J. Catal.* **1992**, *136*, 521.
(724) Corma, A.; Llopis, R.; Viruela, R.; Zicovich-Wilson, C. *J. Am. Chem. Soc.* **1994**, *116*, 134.
(725) Langenaeker, W.; Coussement, N.; De Proft, F.; Geerlings, P. *J. Phys. Chem.* **1994**, *98*, 3010.
(726) Deka, R.; Vitrivel, R.; Pal, S. *J. Phys. Chem. A* **1999**, *103*, 5978.
(727) Damoun, S.; Langenaeker, W.; Geerlings, P. *J. Phys. Chem. A* **1997**, *101*, 6951.
(728) Yamdagni, R.; Kebarle, P. *J. Am. Chem. Soc.* **1973**, *95*, 4050.
(729) Hiraoka, K.; Yamdagni, R.; Kebarle, P. *J. Am. Chem. Soc.* **1973**, *95*, 6833.
(730) De Proft, F.; Amira, S.; Choho, K.; Geerlings, P. *J. Phys. Chem.* **1994**, *98*, 5227.
(731) Pérez, P.; Toro-Labbé, A.; Contreras, R. *J. Phys. Chem. A* **2000**, *104*, 5882.
(732) Krishnamurti, S.; Pal, S. *J. Phys. Chem. A* **2000**, *104*, 7639.
(733) De Proft, F.; Langenaeker, W.; Geerlings, P. *Int. J. Quantum Chem.* **1995**, *55*, 459.
(734) Rezende, M. C. *J. Braz. Chem. Soc.* **2001**, *12*, 73.
(735) Choho, K.; Van Lier, G.; Van De Woude, G.; Geerlings, P. *J. Chem. Soc., Perkin Trans. 2* **1996**, 1723.
(736) Taylor, R.; Walton, D. *Nature* **1993**, *363*, 685.
(737) Van Lier, G.; Safi, B.; Geerlings, P. *J. Chem. Soc., Perkin Trans. 2* **1998**, 349.
(738) Aue, D. H.; Webb, H. M.; Bowers, M. T. *J. Am. Chem. Soc.* **1976**, *98*, 318.
(739) Baeten, A.; De Proft, F.; Langenaeker, W.; Geerlings, P. *J. Mol. Struct.* (*THEOCHEM*) **1994**, *112*, 203.
(740) Baeten, A.; De Proft, F.; Geerlings, P. *Chem. Phys. Lett.* **1995**, *235*, 17.
(741) Perez, P.; Contreras, A. *Chem. Phys. Lett.* **1998**, *293*, 239.
(742) Buckingham, A. D. In *Intermolecular Interactions: from Diatomics to Biopolymers*; Pullman, B., Ed.; John Wiley: New York, 1978; Chapter 1.
(743) Nagy, A. *Int. J. Quantum Chem.* **1998**, *70*, 681.
(744) Chattaraj, P. K.; Poddar, A. *J. Phys. Chem. A* **1998**, *102*, 9944.
(745) Chattaraj, P. K.; Poddar, A. *J. Phys. Chem. A* **1999**, *103*, 1274.
(746) Chattaraj, P. K.; Poddar, A. *J. Phys. Chem. A* **1999**, *103*, 8691.
(747) Fuentealba, P.; Simón-Manso, Y.; Chattaraj, P. K. *J. Phys. Chem. A* **2000**, *104*, 3185.
(748) Mendez, F.; Garcia-Garibay, M. A. *J. Org. Chem.* **1999**, *64*, 7061.
(749) Sengupta, D.; Chandra, A. K.; Nguyen, M. T. *J. Org. Chem.* **1997**, *62*, 6404.
(750) Nalewajski, R. F.; Korchowiec, J.; Michalak A. *Proc. Indian Acad. Sci. (Chem. Sci.)* **1994**, *106*, 353.
(751) Nalewajski, R. F. In *Proceedings of the NATO ASI on Density Functional Theory*, Il Ciocco, August 1993; Dreizler, R. M., Gross, E. K. U., Eds.; Plenum: New York, 1995; p 339.
(752) Nalewajski, R. F. *Int. J. Quantum Chem.* **1991**, *40*, 265.
(753) Nalewajski, R. F.; Korchowiec, J.; Tokarz, R.; Broclawik, E.; Witko, M. *J. Mol. Catal.* **1992**, *77*, 165.
(754) Nalewajski, R. F.; Korchowiec, J. J. *Mol. Catal.* **1993**, *82*, 383.
(755) Nalewajski, R. F.; Köster, A. M.; Bredow, T.; Jug, K. *J. Mol. Catal.* **1993**, *82*, 407.
(756) Nalewajski, R. F.; Michalak A. *Int. J. Quantum Chem.* **1995**, *56*, 603.
(757) Nalewajski, R. F.; Korchowiec, J. *J. Mol. Catal.* **1996**, *112*, 167.
(758) Nalewajski, R. F.; Korchowiec, *J. Comput. Chem.* **1995**, *19*, 217.
(759) Nalewajski, R. F.; Michalak A. *J. Phys. Chem.* **1996**, *100*, 20076.
(760) See, for example: Clayden, J.; Greeves, N.; Warren, S.; Woxthers, P. *Organic Chemistry*; Oxford University Press: Oxford, 2000; p 123.
(761) Baekelandt, B. G.; Janssens, G. O. A.; Toufar, H.; Mortier, W. J.; Schoonheydt, R. A. In *Acidity and Basicity of Solids*; Fraissard, J., Petrakis, L., Eds.; NATO ASI Series C444; Kluwer Academic Publishers: Dordrecht, The Netherlands, 1994; p 95.
(762) Toufar, H.; Baekelandt, B. G.; Janssens, G. O. A.; Mortier, W. J.; Schoonheydt, R. A. *J. Phys. Chem.* **1995**, *99*, 13876.
(763) Janssens, G. O. A.; Baekelandt, B. G.; Toufar, H.; Mortier, W. J.; Schoonheydt, R. A. *J. Phys. Chem.* **1995**, *99*, 3251.
(764) Heidler, R.; Janssens, G. O. A.; Mortier, W. J.; Schoonheydt, R. A. *J. Phys. Chem.* **1996**, *100*, 19728.
(765) Janssens, G. O. A.; Toufar, H.; Baekelandt, B. G.; Mortier, W. J.; Schoonheydt, R. A. *J. Phys. Chem.* **1996**, *100*, 14443.
(766) Kramer, G. J.; van Santen, R. A.; Emeis, C. A.; Nowak, A. K. *Nature* **1993**, *363*, 529.
(767) Chatterjee, A.; Iwasaki, T.; Ebina, E. *J. Phys. Chem. A* **1999**, *103*, 2489.
(768) Chatterjee, A.; Iwasaki, T. *J. Phys. Chem. A* **1999**, *103*, 9857.
(769) Chatterjee, A.; Iwasaki, T. *J. Phys. Chem. A* **2001**, *105*, 6187.
(770) Chattarjee, A.; Iwasaki, T.; Ebina, T. *J. Phys. Chem. A* **2002**, *106*, 641.
(771) Chattarjee, A.; Ebina, T.; Iwasaki, T. *J. Phys. Chem. A* **2001**, *105*, 10694.
(772) Krishnamurti, S.; Roy, R. K.; Vitrivel, R.; Iwata, S.; Pal, S. *J. Phys. Chem. A* **1997**, *101*, 7253.
(773) Vos, A.; Nulens, K.; Schoonheydt, R. A.; De Proft, F.; Geerlings, P. *J. Phys. Chem. B* **2002**, *106*, 2026.
(774) Devautour, S.; Guintini, J. C.; Henn, F.; Douillard, J. M.; Zanchetta, J. V.; Vanderschueren, J. *J. Phys. Chem. B* **1999**, 103, 3275.
(775) Nalewajski, R. F. *Int. J. Mol. Sci.* **2002**, *3*, 237.
(776) Nalewajski, R. F.; Switka, E. *Phys. Chem. Chem. Phys.* **2002**, *4*, 4952.
(777) Nalewajski, R. F. *Phys. Chem. Chem. Phys.* **2002**, *4*, 1710.
(778) Perez, P.; Aizman, A.; Contreras, R. *J. Phys. Chem. A* **2002**, *106*, 3964.
(779) Ayers, P. W.; Morrison, R. C.; Roy, R. K. *J. Chem. Phys.* **2002**, *116*, 8731.
(780) Thanikaivelan, P.; Padmanabhan, J.; Subramanian, V.; Ramasami, T. *Theor. Chem. Acc.* **2002**, *107*, 326.
(781) Nalewajski, R. F. *Chem. Phys. Lett.* **2002**, *353*, 143.

(782) Langenaeker, W.; Liu, S. *J. Mol. Struct.* (*THEOCHEM.*) **2001**, *535*, 279.
(783) (a) Torrent-Sucarrat, M.; Duran, M.; Solà, M. *J. Phys. Chem. A* **2002**, *106*, 4632. (b) Solà, M.; Mestres, J.; Oliva, J. M.; Duran, M.; Carbo, R. *Int. J. Quantum Chem.* **1996**, *58*, 361.
(784) Komorowski, L.; Ordon, P. *Theor. Chem. Acc.* **2001**, *105*, 338.
(785) Nalewajski, R. F. *Comput. Chem.* **2000**, *24*, 243.
(786) (a) Perez, P.; Andrés, J.; Safont, V. S.; Tapia, O.; Contreras, R. *J. Phys. Chem. A* **2002**, *106*, 5353. (b) Plachkevytch, O.; Minaev, B.; Agren, H. *J. Phys. Chem.* **1996**, *100*, 8308.
(787) De Luca, G.; Sicilia, E.; Russo, N.; Mineva, T. *J. Am. Chem. Soc.* **2002**, *124*, 1494.
(788) Sengupta, S.; Toro-Labbé, A. *J. Phys. Chem. A* **2002**, *106*, 4443.
(789) Bultinck, P.; Langenaeker, W.; Lahorte, P.; De Proft, F.; Geerlings, P.; Waroquier, M.; Tollenaere, J. P. *J. Phys. Chem. A* **2002**, *106*, 7887.
(790) Bultinck, P.; Langenaeker, W.; Lahorte, P.; De Proft, F.; Geerlings, P.; Van Alsenoy, C.; Tollenaere, J. P. *J. Phys. Chem. A* **2002**, *106*, 7895.
(791) Bultinck, P.; Carbo-Dorca, R. *Chem. Phys. Lett.* **2002**, *364*, 357.
(792) Chandrakumar, K. R. S.; Pal, S. *J. Phys. Chem. A* **2002**, *106*, 5737.
(793) Perez, P.; Toro-Labbé, A. *Theor. Chem. Acc.* **2001**, *105*, 422.
(794) Ghosh, D. C.; Biswas, R. *Int. J. Mol. Sci.* **2002**, *3*, 87.
(795) De Proft, F.; Vivas-Reyes, R.; Peeters, A.; Van Alsenoy, C.; Geerlings, P. *J. Comput. Chem.* **2003**, *24*, 463.
(796) Senthilkumar, K.; Ramaswamy, M.; Kolandaivel, P. *Int. J. Quantum Chem.* **2001**, *81*, 4.
(797) (a) Jalbout, A. F.; Jalbout, F. N.; Alkahby, H. Y. *J. Mol. Struct.* (*THEOCHEM*) **2001**, *574*, 141. (b) Jalbout, A. F.; Darwish, A. M.; Alkahby, H. Y. *J. Mol. Struct.* (*THEOCHEM*) **2002**, *585*, 205.
(798) Aizman, A.; Contreras, R.; Galvan, M.; Cedillo, A.; Santos, J. C.; Chamorro, E. *J. Phys. Chem. A* **2002**, *106*, 7844.
(799) Mitnik, D. G., Lucero, A. M. *J. Mol. Struct.* (*THEOCHEM*) **2001**, *535*, 39.
(800) Korchowiec, J. *J. Comput. Chem.* **2000**, *24*, 259.
(801) Tielens, F.; Saeys, M.; Tourwé, E.; Marin, G. B.; Hubin, A.; Geerlings, P. *J. Phys. Chem. A* **2002**, *106*, 1450.
(802) Pilepic, V.; Ursic, S. *J. Mol. Struct.* (*THEOCHEM*) **2001**, *583*, 41.
(803) (a) Cong, Y.; Yang, Z. Z.; Wang, C. S.; Liu, X. C.; Zao, X. H. *Chem. Phys. Lett.* **2002**, *357*, 59. (b) See, for example: Smith, M. B.; March, J. *March's Advanced Organic Chemistry*, 5th ed.; Wiley Interscience: New York, 2001; p 1064.
(804) Domingo, L. R.; Aurell, M. J.; Perez, P.; Contreras, R. *Tetrahedron* **2002**, *58*, 4417.
(805) Domingo, L. R.; Aurell, M. J.; Perez, P.; Contreras, R. *J. Phys. Chem. A* **2002**, *106*, 6871.
(806) (a) Perez, P.; Toro-Labbé, A.; Aizman, A.; Contreras, R. *J. Org. Chem.* **2002**, *67*, 4747. (b) Mayr, H.; Bug, T.; Gotta, M. F.; Hering, N.; Irrgang, B.; Janker, B.; Kempf, B.; Loos, R.; Ofial, A. R.; Remennikov, G.; Schimmel, H. *J. Am. Chem. Soc.* **2001**, *123*, 9500.
(807) Arulmozhiraja, S.; Fujii, T.; Sato, G. *Mol. Phys.* **2002**, *100*, 423.
(808) (a) Mignon, P.; Steyaert, J.; Loris, R.; Geerlings, P.; Loverix, S. *J. Biol. Chem.* **2002**, *277*, 36770. (b) Steyaert, J.; Wyns, L. *J. Mol. Biol.* **1993**, *229*, 770.
(809) Vivas-Reyes, R.; De Proft, F.; Geerlings, P.; Biesemans, M.; Willem, R.; Ribot, F.; Sanchez, C. *New J. Chem.* **2002**, *26*, 1108.
(810) Deka, R. Ch.; Hirao, K. *J. Mol. Catal. A* **2002**, *181*, 275.
(811) Vos, A. M.; Schoonheydt, R. A.; De Proft, F.; Geerlings, P. *J. Phys. Chem. B* **2003**, *107*, 2001.
(812) Jaque, P.; Toro-Labbé, A. *J. Chem. Phys.* **2002**, *117*, 3208.

CR990029P